This electronic thesis or dissertation has been downloaded from the King's Research Portal at https://kclpure.kcl.ac.uk/portal/

The phenotype, functions and cytokine properties of 5-azacytidine induced Treg-like FOXP3+ CD4+T cells

Benfatto, Cinzia

Awarding institution:
King's College London

The copyright of this thesis rests with the author and no quotation from it or information derived from it may be published without proper acknowledgement.

END USER LICENCE AGREEMENT

Unless another licence is stated on the immediately following page this work is licensed

under a Creative Commons Attribution-NonCommercial-NoDerivatives 4.0 International

licence. https://creativecommons.org/licenses/by-nc-nd/4.0/

You are free to copy, distribute and transmit the work

Under the following conditions:

- Attribution: You must attribute the work in the manner specified by the author (but not in any way that suggests that they endorse you or your use of the work).
- Non Commercial: You may not use this work for commercial purposes.
- No Derivative Works - You may not alter, transform, or build upon this work.

Any of these conditions can be waived if you receive permission from the author. Your fair dealings and other rights are in no way affected by the above.

Take down policy

If you believe that this document breaches copyright please contact librarypure@kcl.ac.uk providing details, and we will remove access to the work immediately and investigate your claim.

Download date: 08. Oct. 2023

The phenotype, functions and cytokine properties of 5-Azacytidine (5AzaC) induced Treg-like FOXP3^{+} CD4^{+} T cells

A thesis presented for the degree of Doctor of Philosophy (Ph.D.) in Cancer Studies, King's College London

By
Cinzia Benfatto
Department of Haematological Medicine
London, 2017

"Salimmo sù, el primo e io secondo,
tanto ch'i' vidi de le cose belle
che porta 'l ciel, per un pertugio tondo.
E quindi uscimmo a riveder le stelle."

[Dante Alighieri
Inferno- Canto XXXIV, vv 136-139]

“All that I am or hope to be, I owe to my angel mother” A. Lincoln

I would like to dedicate my work to my beloved mum, who inspire me everyday and to my caring grandparents. You are in my heart and in my mind.

Table of Contents

1. ABBREVIATIONS 13

2. INTRODUCTION 15

2.1. BACKGROUND 15

2.1.1. The Immune System 15

2.1.2. Regulatory T cells (Tregs) 21

2.2. THE ROLE OF TREGS IN CANCERS 28

2.2.1. Myelodysplastic syndromes (MDS) 30

2.2.2. 5-Azacytidine 35

2.2.3. Tregs in MDS 35

2.3. RESEARCH PLAN 38

3. MATERIALS AND METHODS 39

3.1. GENERAL MATERIALS AND METHODS 39

3.2. CELLS ISOLATION 39

3.2.1. Gradient cell separation 40

3.2.2. Trypan blue counting 40

3.2.3. Red blood cell Lysis 41

3.2.4. Bead separation 41

3.3. CRYOPRESERVATION AND THAWING OF PBMCS 43

3.3.1. PBMCs Cryopreservation 43

3.3.2. PBMCs thawing 43

3.4. FLUORESCENCE-ACTIVATED CELL SORTING (FACS) 44

3.5. STAINING 46

3.5.1. Surface staining 48

3.5.2. Intracellular staining 48

3.5.3. Purity analysis 48

3.6. COMPENSATION AND DATA ANALYSIS 50

3.7. CELL SURFACE PROTEIN ISOLATION 52

3.8. GEL ELECTROPHORESIS 55

3.9. MASS SPECTROMETRY 57

3.10. SINGLE CELL MASS CYTOMETRY 58

3.11. GENOMIC DNA EXTRACTION 61

3.11.1. Genomic DNA isolation 61

3.11.2. Determination of DNA concentration 61

3.11.3. Bisulfite modification of DNA 62

3.12. POLYMERASE CHAIN REACTION (PCR) AND QUANTITATIVE REAL TIME PCR (QPCR) 66

3.12.1. Polymerase chain reaction (PCR) 66

3.12.2. Quantitative real time PCR (qPCR) 67

3.12.3. Oligodeoxynucleotides 68

3.13. PLASMID 70

3.13.1. Transformation of Competent ECO k12 70

3.13.2. Miniprep extraction 70

3.13.3. Restriction digests 71

3.13.4. Agarose gel analysis 71

3.13.5. Fragment recovery 72

3.14. CYTOKINE MEASUREMENT 73

3.14.1. Enzyme-linked immunosorbent assay (ELISA) 73

3.14.2. Cytokine Human 30-Plex Panel for the Luminex platform 73

3.14.3. Cytometric Bead Array (CBA) 75

3.15. METHYLOME 450K ARRAY 78

3.16. STATISTICAL ANALYSIS 80

4. FUNCTION AND CYTOKINE PROFILE OF 5AZAC TREATED T_{CON} 81

4.1. INTRODUCTION 81
4.2. MATERIALS AND METHODS 82
4.2.1. Cell Culture and Proliferation assay 82
4.2.2. Staining for surface and intracellular protein markers 88
4.2.3. Cytokine measurement 89
4.2.4. Statistical analysis 89
4.3. RESULTS 91
4.3.1. Function and FOXP3 expression by 5AzaC treated T_{con} cells 91
4.3.2. Functional analysis of T_{con} after 5AzaC treatment 95
4.3.3. Cytokine concentration analysis 97
4.3.4. Tregs: polarisation and functional analysis 100
4.4. DISCUSSION 107

5. PROTEOME AND SINGLE-CELL MASS CYTOMETRY, CYTOMETRY BY TIME OF FLIGHT (CYTOF) ANALYSIS 108
5.1. SUMMARY 108
5.2. INTRODUCTION 109
5.2.1. Identification of novel components of the cell surface proteome 109
5.2.2. Identification of the TrLC phenotype by multi-parameter analysis of known proteins. 109
5.3. MATERIALS AND METHODS 111
5.3.1. Cell surface protein isolation by Biotinylation 111
5.3.2. Phenol-based DNA extraction 112
5.3.3. Single cell mass cytometry or cytometry by time-of-flight (CyTOF) 113
5.3.4. Statistical analysis 124
5.4. RESULTS 125
5.4.1. Cell surface protein identification 125
5.4.2. TrLC phenotype characterisation 136
5.5. DISCUSSION 150

6. QUANTIFICATION OF METHYLATED AND DEMETHYLATED*FOXP3 TSDR* AND DNA METHYLOME ANALYSIS 153
6.1. SUMMARY 153
6.2. INTRODUCTION 154
6.2.1. TSDR analysis 154
6.2.2. Genome-wide DNA methylation analysis 155
6.3. MATERIALS AND METHODS 157
6.3.1. TSDR analysis 157
6.3.2. Phenol-based DNA extraction 163
6.4. RESULTS 164
6.4.1. Quantification of methylated and demethylated TSDR and the GAPDH promoter in gDNA from CD3+ T cells, Treg and CD4+ T_{con}. 164
6.4.2. Percentage of unmethylated CpGs of the TSDR intron in TrLCs, Tregs and in Tcon from HD 174
6.4.3. Human Methylation450 BeadChip (Illumina Infinium) array 176
6.5. DISCUSSION 189

7. GENERAL DISCUSSION AND FURTHER DIRECTIONS 191
7.1. BACKGROUND 191
7.2. FINDINGS 196
7.2.1. The effects of 5AzaC on phenotype, cytokine profile and function of T_{con}. 196
7.2.2. Phenotypic characterisation of TrLCs 197
7.2.3. Methylation statues of Treg related genes in TrLCs 198
7.3. CONCLUSIONS AND FUTURE DIRECTIONS 199

9. REFERENCES 201

10. APPENDIX..... 213

List of Figures

Figure 1. Innate and adaptive immunity. 15
Figure 2. Function of different antigen presenting cells. 19
Figure 3. T cell recognition of a peptide MHC complex. 20
Figure 4. Thymus derived and peripheral derived regulatory T cells. 23
Figure 5. CNS2 or TSDR sequence. 24
Figure 6. Basic mechanisms used by Treg cell to suppress the immune system. 26
Figure 7. Mechanisms of tumor immune tolerance. 29
Figure 8. Structure of cytidine and methylation inhibitors 5AzaC and Decitabine. 35
Figure 9 Leukocyte cone pre and post centrifugation. 40
Figure 10 Flow cytometer chamber. 45
Figure 11. Gating strategy for flow cytometry analysis. 51
Figure 12. Cell surface isolation protocol. 52
Figure 13. CyTOF workflow. 58
Figure 14 Overview of the bisulfite conversion. 63
Figure 15. Conversion of cytosine. 63
Figure 16 PCR method. 66
Figure 17 Preparing the standard curve. 74
Figure 18. Broader Coverage Using Infinium I and II Assay Designs. 79
Figure 19. 5AzaC culture workflow. 83
Figure 20. IL-1β, IL-6, IL-2 culture workflow. 85
Figure 21. Proliferation assay workflow. 87
Figure 22. Gating strategy workflow. 89
Figure 23. FOXP3+ cells in T_{CON}. 93
Figure 24. Percentage of $FOXP3^+$ cells. 94
Figure 25. Percentage of $FOXP3^+IL\text{-}17^+$ cells. 95
Figure 26. Proliferation assay 5AzaC treated T_{CON}. 96
Figure 27. Proliferation assay 5AzaC treated T_{CON}. 97
Figure 28. INF- γ measurement. 99
Figure 29. TNF-α measurement. 100
Figure 30. $FOXP3^+IL\text{-}17^+$ cells. 101
Figure 31. Percentage of $FOXP3^+$ $IL\text{-}17^+$ cells. 102
Figure 32. Proliferation assay of Tregs secreting IL-17 cells. 103
Figure 33. Proliferation assay of IL-17 secreting Tregs. 104
Figure 34. Comparing proliferation assay from Tregs, 5AzaC treated T_{CON} and IL-17 secreting Tregs. 106
Figure 35. CyTOF workflow. 114
Figure 36. Gating strategy. 120
Figure 37. Stochastic Neighbor Embedding (SNE) – Machine Learning to Reduce Dimensionality. 121
Figure 38. Visualisation of initial populations on viSNE map. 122
Figure 39. Cell subsets using SPADE analysis. 123
Figure 40. Flow cytometry analysis using Streptavidin-eFluor450. 127
Figure 41. Western blot analysis. 128
Figure 42. Biotin compound. 129
Figure 43. Summary of identified proteins. 130
Figure 44. Location of labelled proteins (Bio condition). 132
Figure 45. Analysis of PBMCs expressing FOXP3 from HDs treated with 5AzaC. 138
Figure 46. Analysis of PBMCs expressing FOXP3 from HDs treated with DMSO. 139
Figure 47. Analysis of PBMCs expressing FOXP3 from MDS patients treated with DMSO. 140
Figure 48. Analysis of PBMCs expressing FOXP3 from MDS patients treated with 5AzaC. 141
Figure 49. $CD4^+$ cells from HDs and MDS patients: marker analysis. 142
Figure 50. $CD4^+$ T cells expressing high FOXP3 from PBMCs isolated from MDS patients. 143
Figure 51. $CD4^+$ T cells expressing high FOXP3 from PBMCs isolated from HDs. 144
Figure 52. T_{CON} from HDs treated with DMSO. 145
Figure 53. T_{CON} from HDs treated with 5AzaC. 146
Figure 54. FOXP3 expression clusters of 5AzaC treated T_{CON}. 147
Figure 55. FOXP3 expression clusters of DMSO treated T_{CON}. 148
Figure 56. $CD4^+$ T cells expressing high FOXP3 from T_{CON} isolated from HDs. 149

FIGURE 57. *TSDR* SEQUENCE WITHIN THE *FOXP3* GENE. THE FIGURE SHOWS THE PERCENTAGE OF 155
FIGURE 58. QPCR ANALYSIS TO IDENTIFY THE MOST SUITABLE ANNEALING TEMPERATURE. 158
FIGURE 59. HUMAN METHYLATION450 BEADCHIP ARRAY. 162
FIGURE 60. COPY NUMBER CALCULATOR WEBSITE. 165
FIGURE 61. TSDR UNMETHYLATED STANDARD CURVE. 166
FIGURE 62. TSDR METHYLATED STANDARD CURVE. 167
FIGURE 63. CD3G/CD3D UNMETHYLATED STANDARD CURVE. 167
FIGURE 64. CD3G/CD3D METHYLATED STANDARD CURVE. 168
FIGURE 65. GAPDH METHYLATED STANDARD CURVE. 169
FIGURE 66. TSDR METHYLATED QPCR. 170
FIGURE 67. TSDR UNMETHYLATED QPCR. 171
FIGURE 68. STANDARD CURVE REPETITION. 174
FIGURE 69. LIST OF METHYLOME ARRAY CONDITIONS. 178
FIGURE 70. METHYLOME DATA WORKFLOW. 179
FIGURE 71. FOXP3⁺ CELLS BACKGATING ANALYSIS. 183
FIGURE 72. DNA INTEGRITY ANALYSIS. 185
FIGURE 73. CREB1 AND TIGIT PRIMERS. 186
FIGURE 74. TIGIT AND CREB1 PCR. 187
FIGURE 75. IMMUNE RESPONSE IN MDS. 192
FIGURE 76. TREGS POLARISATION INTO T INFLAMMATORY SUBSETS. 194
FIGURE 77. PLASTICITY OF T INFLAMMATORY CELLS VERSUS TREGS. 195
FIGURE 78. CREB1 PRIMERS. 217
FIGURE 79. TIGIT PRIMERS. 218

List of Tables

Table 1. Cell-associated pattern recognition receptors. 17
Table 2. Soluble recognition receptors.. 18
Table 3. WHO 2008 classification. 31
Table 4. IPSS score classification. 32
Table 5. IPSS-R scoring system. 33
Table 6. Role of the immune response in low and high- risk MDS. 36
Table 7 List of antibodies and dyes used 47
Table 8 Bisulfite conversion thermal cycle condition 64
Table 9. List of Primers used. 69
Table 10 Enzyme and buffer digestion 71
Table 11 Standard's serial dilutions 76
Table 12. Selected antibody markers for membrane and intracellular staining. 117
Table 13. Workflow for semi-supervised high dimensional single cell data analysis (Diggins et al[126]). 119
Table 14. List (Location order) of the 55 proteins identified in the Bio condition. 133
Table 15. *TSDR* primers used. 160
Table 16. Calculation 172
Table 17. Percentage of methylation. 176
Table 18. Methylation level T_{CON} HD. 181
Table 19. Unmethylated genes in 5AzaC condition. 182
Table 20. Zhang et al list of FOXP3 binding sites and interesting genes 213

Abstract

Myelodysplatic Syndrome (MDS) is a group of premalignant diseases characterised by ineffective erythropoiesis and categorised into risk groups ranging from low/intermediate to high-risk, based on the risk of disease progression toward acute myeloid leukaemia (AML)[1]. Expansion of $CD4^+CD25^{hi}CD127^{low}FOXP3^+$ (Tregs) is a characteristic feature of high-risk MDS[2]. Although the only curative treatment for high-risk MDS is bone marrow transplantation, this is not always available due to age or lack of a compatibile donor. Nevertheless, treatment with the hypomethylating agent 5-Azacytidine (5AzaC) can improve quality of life and enhance life expectancy[3, 4]. Although the hypomethylating activity of 5AzaC is well established, its mechanism of action remains unclear. It has been shown by our group that following treatment with 5AzaC, the absolute number of Tregs is reduced, they became non-suppressive and secrete IL-17 and IFN-γ. We have also shown increased FOXP3 expression in the conventional $CD4^+$ T cells (T_{con}) of healthy donors following *in-vitro* culture with 5AzaC, without significant immunosuppressive properties. This subpopulation is so-called "Treg-like" cells. The focus of the study was on the $FOXP3^+$ "Treg-like" cells derived from 5AzaC treated T_{con} ($CD4^+CD25^-$). Our data demonstrate: 1) "Treg-like" cells show an increase in secretion of IL-17 and expression of FOXP3 and have no significant immunosuppressive properties; 2) the Treg-specific-demethylated region (*TSDR*) within the *FOXP3* gene in "Treg-like" cells is fully methylated compared with Tregs; 3) analyses of cell surface and intracellular protein expression by CyTOF strongly suggeste that cells with high FOXP3 expression following 5AzaC treatment are not-stable Tregs, therefore the FOXP3 marker is not an indication of Tregs. Also, 5AzaC polarised T_{con} towards a T inflammatory profile and PBMCs towards a T helper profile rather then Tregs. The phenotype and the CyTOF analyses gave an improvement in understanding how these "Treg-like" cells develop, behave and their potential use in therapy.

1. Abbreviations

5AzaC	5-Azacytidine
5q syndrome	Myelodysplastic syndrome with isolated del5q
AML	Acute Myeloid Leukaemia
APCs	Antigen-presenting cells
BM	Bone marrow
cAMP	Cyclic adenosine monophosphate
CNS	Conserved non-coding sequence
CTLA4	Cytotoxic T-Lymphocyte Antigen 4
CTLs	Cytotoxic T cells
DAMPs	Damage-associated molecular patterns
DC	Dendritic cells
DNA	Deoxyribonucleic acid
DNMT	DNA methyltransferase
FAB-1982	French-American-British classification
FOXP3	Forkhead box 3
G-CSF	Granulocyte colony-stimulating factor
HDs	Healthy donors
HL	Hodgkin's lymphoma
IDO	Indoleamine 2,3-dioxygenase
IFN-γ	Interferon-γ
IL-1	Interleukin 1
IL-12	Interleukin 12
IL-2	Interleukin 2
IL-23	Interleukin 23
IL10	Interleukin 10
IPEX syndrome	Immune disregulation, polyendocrinopaty, enteropaty, X-linked
IPSS	International Prognostic Scoring System
IPSS-R	Revised IPSS classification
iTreg	*In vitro* induced Treg
MDS	Myelodysplastic Syndrome
MHC	Major histocompatibility complex
NK	Natural killer
PAMPs	Pathogen associated molecular patterns
pTreg	Peripherally derived Treg
RA	Refractory cytopenia
RAEB1 and RAEB2	Refractory anaemia with excess blasts
RARS	Refractory anaemia with ringed sideroblasts
RCMD	Refractory cytopenia with multilineage dysplasia

RNA	Ribonucleic acid
T_{con}	Conventional T cells
TGF-β	Transforming growth factor–β
Th-17	Pro-inflammatory IL-17 producing CD4+ T cells
TLRs	Toll-like receptors
TNF-α	Tumour necrosis factor alpha
Tregs	Regulatory T cells
TrLCs	Treg-like cells
TSDR	Treg specific demethylation region
tTreg	Thymus derived Treg
VEGF	Vascular endothelial growth factor
WHO	World Health Organization

2. Introduction

2.1. Background

2.1.1. *The Immune System*

The immune system has the role to protect the host against pathogenic microbes through elimination of allergenic and toxic substances. The community of microbes includes both obligate pathogens and beneficial commensal organisms, which are important for the host. The immune system is balanced between the capacity to eliminate pathologic microbes and toxic or allergenic proteins and prevents responses that could produce damage to self-tissues or defeat beneficial commensal microorganisms. The immune system can discriminate between exogenous pathogens and the cells of the host through structural features. This distinction is crucial for the elimination of pathogens without damaging self-tissues (host cells).

The immune system consists of innate and adaptive immunity[5, 6].

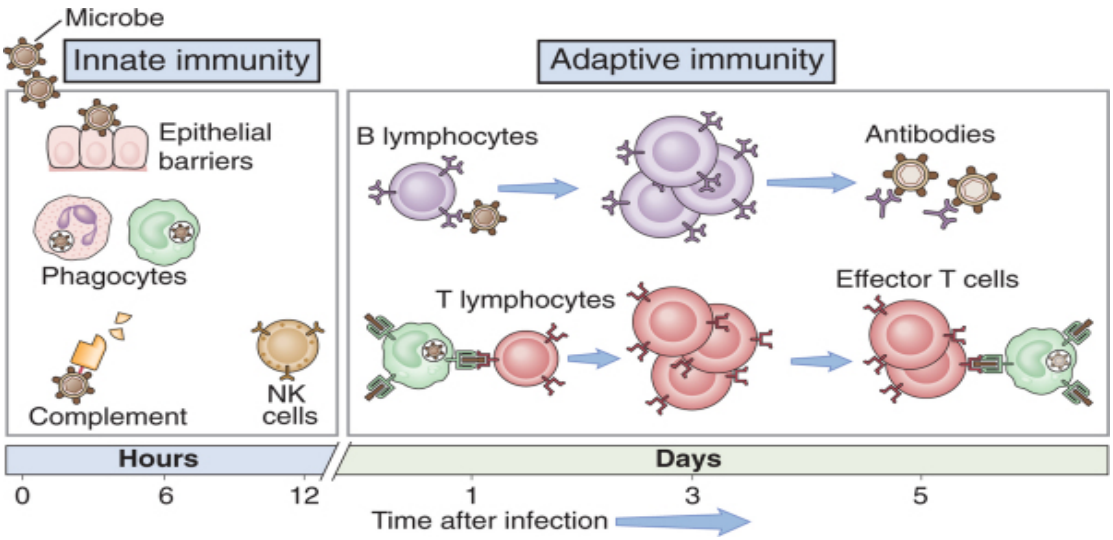
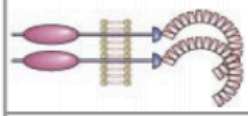
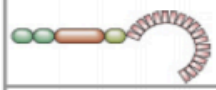


Figure 1. Innate and adaptive immunity. Innate immune responses are activated within hours by pathogens and defend all multicellular organisms against infection. The adaptive immunity comes later and presents a specific defence of the host. *From: Cellular and Molecular Immunology A. Abbas et al, 7th edition* [7]

The early line of defence against infections that triggers a rapid and non-specific response usually within twelve hours is innate immunity (Figure 1). It consists of several components, called physical barriers, such as epithelial cell layers, the mucus layer that overlays the epithelium in the respiratory, gastrointestinal and genitourinary tracts and the epithelial cilia. Phagocytic cells, dendritic cells (DC), natural killer cells (NK), members of the complement system and cytokines are also components of innate immunity[8, 9]. The way the innate immune system can recognise microbes and toxins is through their "molecular patterns", which are not present in the mammalian host. The microbial substances that stimulate innate immunity are called pathogen associated molecular patterns (PAMPs). Gram negative bacteria, gram positive bacteria, viruses and fungi express different PAMPs, for example double strand RNA from viruses and unmethylated CpG DNA sequences from bacteria. Innate immunity also recognises endogenous molecules released by dying and damaged cells, so-called damage-associate molecular patterns (DAMPs). These structures are released because of cell damage caused by infection.

PAMPs and DAMPs are recognised by cellular receptors such as cell-associated pattern recognition receptors (Table 1) and soluble recognition receptors (Table 2), expressed by DC, epithelial cells and phagocytes. When PAMPs or DAMPs bind cell-associated pattern recognition receptors, there is an activation of intracellular pathways that trigger different cellular responses like inflammation. PAMP and DAMP ligands are recognised by toll-like receptors (TLRs). The functional molecules work as dimers. TLRs can recognise PAMPs through activation of transcription factors, such as nuclear factor κB, (NF-κB) and activation protein 1 (AP-1). This activation stimulates the expression of genes encoding inflammatory cytokines (Tumor necrosis factor alpha (TNF-α), Interleukin 12 (IL-12), Interleukin 23 (IL-23), Inteleukin 1 (IL-1)) and chemokines (*CCL2*)[8, 10].

Table 1. Cell-associated pattern recognition receptors.

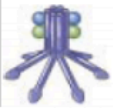
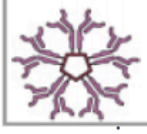
Cell-Associated Pattern Recognition Receptors	Location	Specific Examples	PAMP/DAMP Ligands
Toll-like receptors (TLRs) 	Plasma membrane and endosomal membranes of dendritic cells, phagocytes, B cells endothelial cells, and many other cell types	TLRs 1-9	Various microbial molecules including bacterial LPS and peptidoglycans, viral nucleic acids
NOD-like receptors (NLRs) 	Cytoplasm of phagocytes epithelial cells, and other cells	NOD1/2 NALP family (inflammasomes)	Bacterial cell wall peptidoglycans Flagellin, muramyl dipeptide, LPS; urate crystals; products of damaged cells
RIG-like receptors (RLRs) 	Cytoplasm of phagocytes and other cells	RIG-1, MDA-5	Viral RNA
C-type lectin-like receptors 	Plasma membranes of phagocytes	Mannose receptor	Microbial surface carbohydrates with terminal mannose and fructose
		Dectin	Glucans present in fungal cell walls
Scavenger receptors 	Plasma membranes of phagocytes	CD36	Microbial diacylglycerides
N-Formyl met-leu-phe receptors 	Plasma membranes of phagocytes	FPR and FPRL1	Peptides containing *N*-formylmethionyl residues

These cellular receptors are linked to intracellular pathways that activate different cellular responses (*e.g.* inflammation) *From: Cellular and Molecular Immunology A. Abbas et al, 7th edition*[7]

Soluble recognition receptors (Table 2) are present on the membrane of the host cell and they function in two major ways:

1. They enhance the ability of neutrophilis, macrophages and DC to phagocytose microbes.
2. They promote inflammatory responses and then they recruite phagocytes to directly kill microbes[11].

Table 2. Soluble recognition receptors.

Soluble Recognition Molecules	Location	Specific Examples	PAMP Ligands
Pentraxins 	Plasma	C-reactive protein	Microbial phosphorylcholine and phosphatidylethanolamine
Collectins 	Plasma	Mannose-binding lectin	Carbohydrates with terminal mannose and fructose
	Alveoli	Surfactant proteins SP-A and SP-D	Various microbial structures
Ficolins 	Plasma	Ficolin	*N*-Acetylglucosamine and lipoteichoic acid components of the cell walls of gram-positive bacteria
Complement 	Plasma	C3	Microbial surfaces
Natural antibodies 	Plasma	IgM	Phosphorylcholine on bacterial membranes and apoptotic cell membranes

The major components are natural antibodies, the complement system, collectins, pentraxins and ficolins. *Cellular and Molecular Immunology A. Abbas et al, 7th edition*[7]

The adaptive immune system can recognize all pathogens and to enhance protection against re-infection. Usually it occurs within days after the infection. This unique feature of adaptive immunity is based on clonal selection of lymphocytes (B cells, T cells and NK cells). Each lymphocyte displays cell-surface receptors unique for a single antigen. When lymphocytes encounter their specific antigens, they are induced to proliferate. Their progeny then differentiates into conventional T cells (T_{con}) or effector T cells, able to eradicate the infectious agent and into memory cells or antigen-experienced T cells. The memory T cells have already come across and responded to their antigen, so they are ready to respond if they encounter the same pathogen again[12, 13].

As described previously, innate immunity is the first defence against pathogens, but when it fails the initiation of adaptive immunity occurs. An

activated antigen-presenting cell (APC) (Figure 2) can capture and digest the antigen. Then, the antigen peptide is presented to T cells, through specialised proteins called major histocompatibility complex (MHC) molecules (Figure 3), expressed on the surface of APCs. There are two different MHC: MHC I recognised by CD8+ cytotoxic T cells (CTLs), which destroy tumour or infected cells (Figure 2) and MHC II recognised by CD4+ T cells[14, 15].

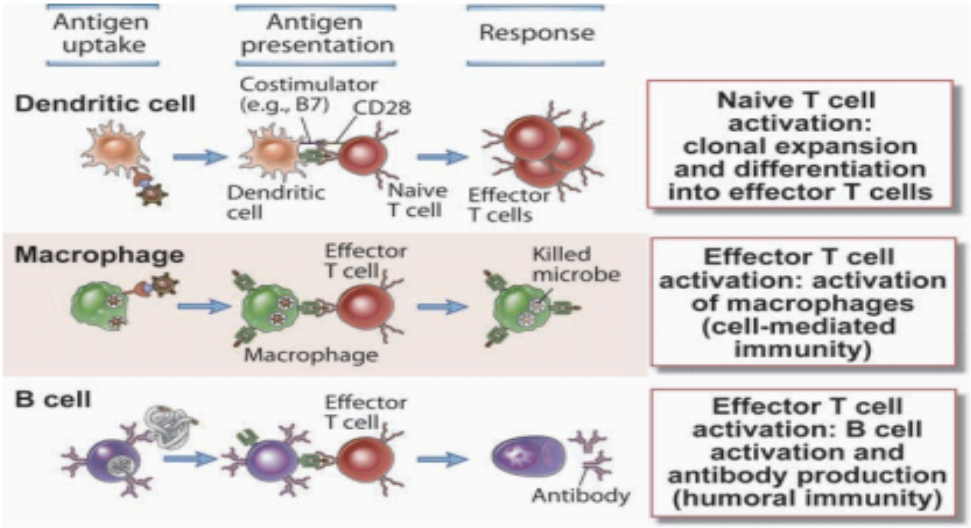


Figure 2. Function of different antigen presenting cells. DC, macrophages and B cells are called specialised APCs for CD4+ helper T cells. Effector T cells activate macrophages and B cells because of the activation by recognition of specific antigens. *From Cellular and Molecular Immunology A. Abbas et al, 7th edition*[7]

The MHC II antigens are taken by DC, macrophages and B lymphocytes, processed and presented to helper T cells[16]. Next, either cell-mediated immunity (helper cells assist phagocytes to destroy microbes) or humoral immunity (B cells can produce immunoglobulins) can occur to inactivate viruses and microbial toxins.

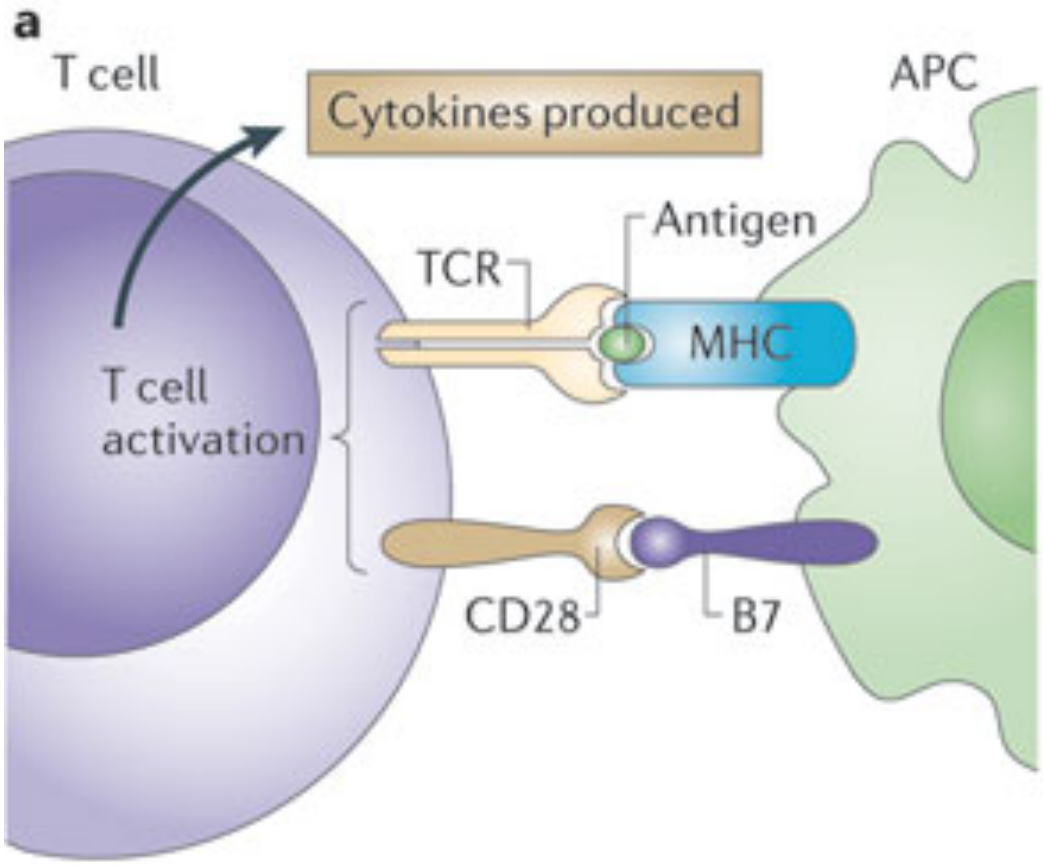


Figure 3. T cell recognition of a peptide MHC complex. The interaction between T cell receptor (TCR) and an MHC-bound to an antigen in an APC leads to the activation of the T cell (also called signal 1). Additional signals, such as the interaction between CD28 and B7 (signal 2) complete T cell activation. *Adapted from Sharma P et al. Novel cancer immunotherapy agents with survival benefit: recent successes and next steps. Nature reviews Cancer 2011,* ***11****(11):* *805-812*.[17]

The synergy between the innate and adaptive immune systems is critical for a functional immune response.

2.1.2. *Regulatory T cells (Tregs)*

2.1.2.1. History of "suppressive T cells"

Treg is a specialised subpopulation of T cells that has a pivotal role in maintaining homeostasis within the immune system and they are generated primarily in the thymus, but also in the peripheral lymphoid tissues (see later in the Chapter). From the late 1960s to the 1980s the concept of "suppressor cells" attracted much interest among the scientific community. In fact during this period studies from Francis Alber Pierre Millers described that thymectomised mice had a severe lymphocyte deficiency both in the circulation and in the lymphoid tissues[18 19]. Later, studies were carried out to investigate how infusions of lymphocytes could restore immune function in thymectomised animals[19, 20, 21]. Tregs were first observed and described as "suppressor cells" by Gershon and Kondo in 1971[22]. In their work, they identified a T cell population that is different from T helper cells, which could mediate the downregulation of the immune response. From this time to 1995, many investigations were conducted on these "suppressive cells". A major milestone was achieved by Sakaguchi *et al*. in 1995[23] who identified the alpha chain of the inteleukin 2 (IL-2) receptor (CD25) as a surface marker for suppressive T cells (in a murine model), later called regulatory T cells[23, 24]. In 2001, the forkhead box 3 (*FOXP3)* gene was identified[25] in mice as the gene responsible for the Scurfy mice, which are characterised by severe autoimmunity. Mutation of the human *FOXP3* was also found to occur in patients with IPEX syndrome (immune disregulation, polyendocrinopaty, enteropaty, X-linked) which is also characterised by severe autoimmunity[26]. The similarities between these autoimmunity diseases prompted severeal reaserch groups to investigate the role of *FOXP3* in Tregs. In 2003 Sakaguchi and others indeed reported that *FOXP3* is essencial for Treg function and development[27, 28, 29, 30]. At the same time another factor was shown to be crucial for Tregs: Trasforming growth factor beta (TGF-β). Horowitz *et al*. described in 2001[31] how TGF-β is able to induce naïve CD4+ T cell from humans to develop a suppressor activity in a cell-contact dependent manner[31]. During the years following and still now, many research groups

have focused on different aspects of the biology of Treg cells, their phenotype and the cytokines they secrete.

2.1.2.2. Treg classification

Tregs are a subpopulation of T cells which express CD25 and *FOXP3*. As I mentioned in the previous section, the *FOXP3* gene plays a crucial role in Tregs as it encodes a lineage-specific transcriptor factor. It has been shown by many groups that the major population of *FOXP3*$^{+}$ Tregs is generated in the thymus and they have been called natural or preferably thymus derived Tregs (tTreg)[32, 33]. It has been demonstrated that *FOXP3*$^{+}$ Tregs can be generated also from CD4+ or CD8+ CD25^{-}*FOXP3*$^{-}$ T cells in peripheral sites through the action of cytokines, such as IL-10, IFN-γ and TGF-β and a low number of antigens. They have been called inducible or preferably peripherally derived Tregs (pTreg)[34, 35]. These pTregs include T regulatory 1 cells or T_R1, which secrete high levels of IL-10 and no IL-4; T helper 3 or T_H3, which secrete high levels of TGF- β and CD8+ regulatory T cells, which can secrete IL-10[36] (Figure 4). In addition, it is suggested that the term iTregs[37] could be used for "*in vitro* induced Tregs" generated from *FOXP3*$^{-}$ Tcells using TGF-β [34].

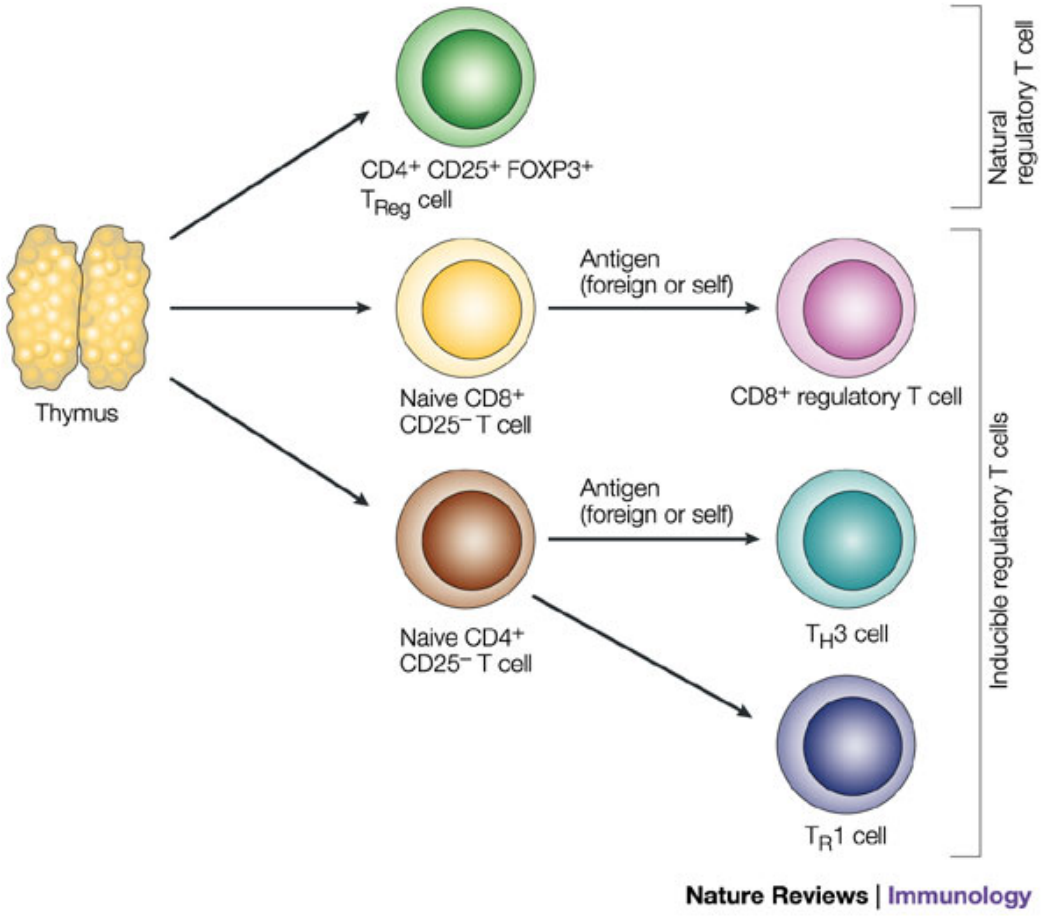


Figure 4. Thymus derived and peripheral derived regulatory T cells. Regulatory T cells classification. From Mills KH. Regulatory T cells: friend or foe in immunity to infection? Nature reviews Immunology 2004, **4**(11)**:** 841-855.[36]

tTregs originate *de novo* in the thymus through the recognition of self-antigen[38]. They express high levels of CD25 together with the transcription factor and lineage marker *FOXP3*. The phenotype of Tregs in normal circumstances is stable and the cells are long-lived due to the epigenetic modification of the conserved non-coding sequences (CNS) in the *FOXP3* locus[35, 39]. In particular, CNS1, 2 and 3 are crucial for *FOXP3* expression. CNS1 contains a TGF-β -NFAT response element and has a pivotal role for iTreg cell generation. In the CNS2 (also known as *TSDR* Treg specific demethylation region_ Amp 5 Figure 5)[40] *FOXP3* binds to *CNS2* itself in a CpG DNA methylation dependent manner, that leads to demethylated CpG dinucleotides in stable Tregs but methylated CpGs in naive and T_{con} cells. CNS3 appears to control *de novo FOXP3* expression[40, 41].

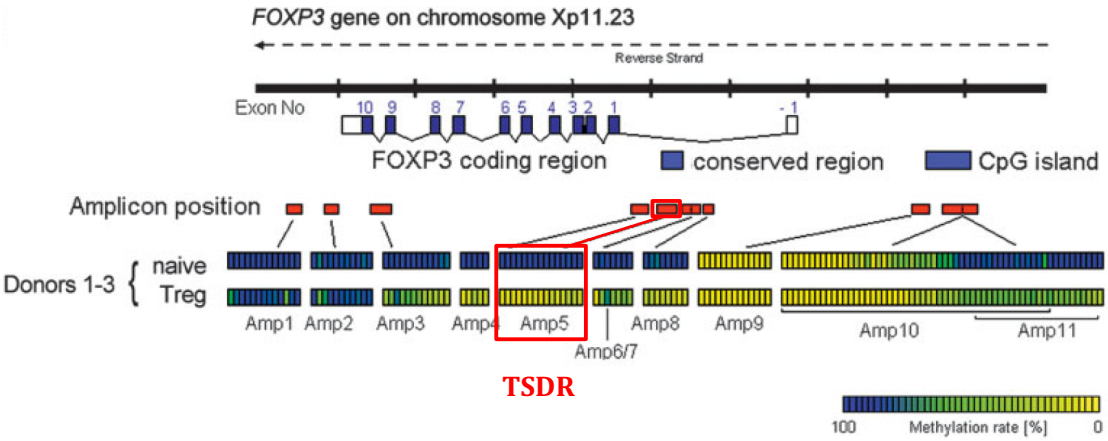


Figure 5. CNS2 or TSDR sequence. *FOXP3* amplicons in Tregs *versus* naive T cells. Each box represents methylation of a single CpG according to the colour (yellow=0%, blue=100% methylation). The *TSDR* (Amp 5) from Tregs is less methylated compared with the same region in naive T cells. *Figure adapted from Baron et al 2007*[40]

Furthermore, according to Sakaguchi's paper of 2009, tTregs can be classified into 3 additional subsets, based on their CD45RA and *FOXP3* expression: activated Treg (aTreg), resting Treg (rTreg) and non-treg. Both aTreg CD45RA^{-}*FOXP3*^{hi} and rTreg CD45RA^{+}*FOXP3*^{low} are immunosuppressive *in vitro*, but not the non-Treg subpopulation[42].

Even though CD25^{hi} and CpG demethylation of the *FOXP3 TSDR* is a prerequisite to define a stable population of nTregs[7,43,44,40,45,46,47] other markers such as the "quintet" of transcription factors (Interferon regulatory factor 4 (IRF4), Eos, Lymphoid enhancer-binding factor 1 (Lef1), Globin transcriptor factor 1 (Gata1) and special AT-rich sequence-binding protein-1 (Satb1)) contribute to the gene signature of Tregs[48]. tTregs represent approximately 5–10% of the total CD4^{+} T cell population[35, 49] and are detectable in the peripheral blood, lymph nodes and spleen[49, 50]. Their main function is to prevent the autoreactivity of T_{con} [34].

The presence of IL-2, CD28 and transforming growth factor–β (TGF-β) is crucial for the development and survival of Tregs.

Tregs are characterised by:

1. Strong suppressive function that affects a very broad range of cells (Tcon, B cells and APCs). Tregs modulate immune responses and maintain self – tolerance[38].

2. *FOXP3* is the master regulator of Tregs. The demethylation of the *TSDR* within the *FOXP3* is required for their stability[44].
3. The presence of CD25 and Cytotoxic T-Lymphocyte Antigen 4 (CTLA4). High expression of CD25 is required for Tregs survival[35]. CTLA4 is also important for the suppressive function through downregulation of CD80 and CD86 expression on APCs[35] and therefore inhibits the capacity of APCs, for example DC, to activate naïve T cells.

Although the expression of CD25 and *FOXP3* is a reliable and specific marker to identify Tregs in mice, in humans CD25 and *FOXP3* are not considered as specific markers [38, 51]. On the contrary, CD127 low expression, has been seen in Tregs compared with non Treg $CD4^+$ T cells[38, 52]. In addition, Liu *et al* demonstrated that there is a 90% correlation between *FOXP3* expression and $CD4^+CD25^+CD127^{low}$ T cells[53].

Tregs use the following mechanism in order to suppress T_{con}[38] :

1. Inhibitory cytokines (Interleukin 10 (IL-10), TGF-β and Interleukin 35 (IL-35)),
2. Cytolysis through Granzyme A and B,
3. Metabolic disruption (consumption of IL-2 and presence of cyclic adenosine monophosphate (cAMP)),
4. Modulation of DC maturation or function. (Figure 6)

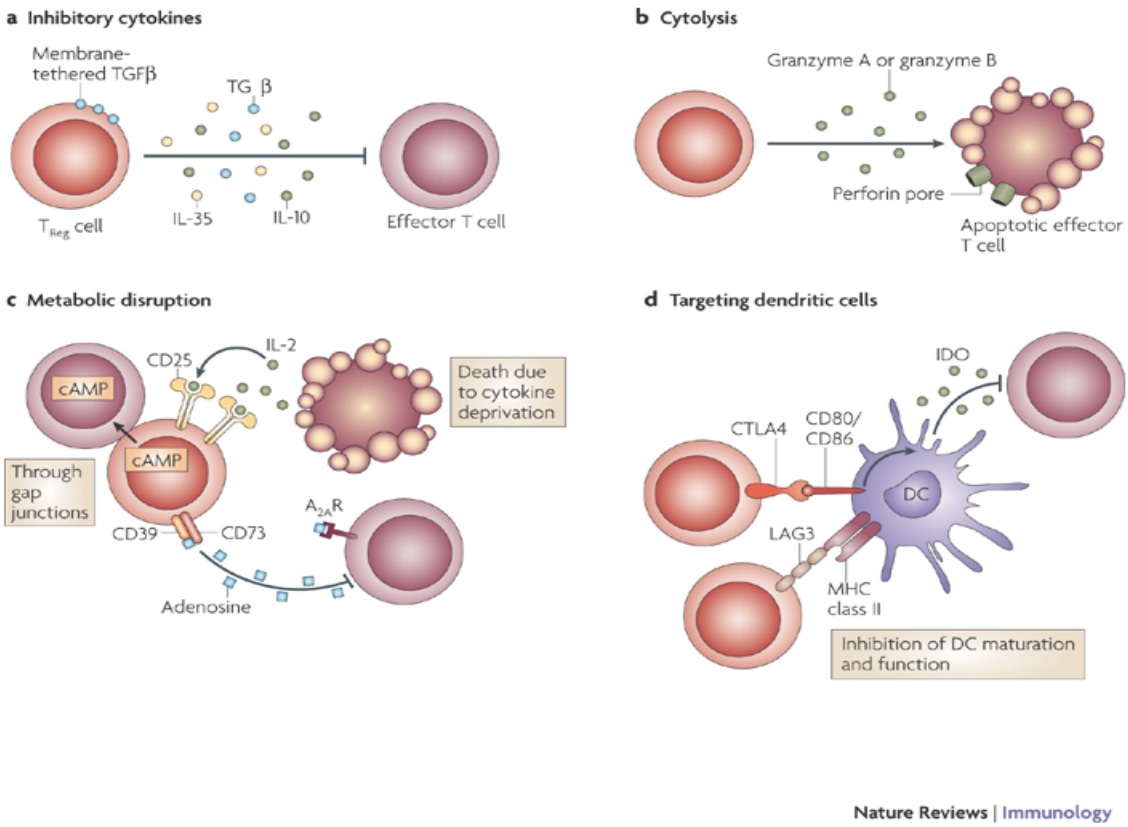


Figure 6. Basic mechanisms used by Treg cell to suppress the immune system. Inhibitory cytokine production: IL-10, IL-35 and TGF-β and granzyme B dependent and perforin dependent. C) Metabolic disruption. D) Targeting DC includes mechanisms that modulate DC maturation and function. *From Nature Reviews Immunology 8, 523-532 (July 2008) Dario A. A. Vignali et al*[38].

Suppression by inhibitory cytokines: Tregs induce immunosuppression through cytokine production, such as IL-10, IL-35 and TGF-β. IL-10 leads to the inhibition of IL-12 production that is crucial for IFN-γ secretion. IFN-γ plays an important role in the innate and the adaptive cell mediated immune reactions against intracellular microbes[38]. In addition, IL-10 prevents the expression of co-stimulators and class MHCII molecules on DCs and macrophages[54]. Another important cytokine is TGF-β that prevents the proliferation and effector function of T cells. In addition, IL-35 is an interleukin which enhances the inhibitory effect of Tregs on Teffector cells[38].

Suppression by cytolysis: Tregs have been shown to express the protease Granzyme A. It enters target cells through perforin induced pores in order to cleave and activate intracellular caspases and induce apoptosis[38]. Noelle *et al* have shown that Tregs are capable of suppressing NKs and CTLs by inducing apoptosis through a Granzyme-B-dependent pathway[55].

Suppression by metabolic disruption: Tregs can consume IL-2 in the microenvironment through high expression of CD25, effectively depriving Teffector cells of IL-2[56]. In addition, Tregs can transfer the inhibitory second messenger cAMP into the T_{con} cells, through membrane gap junctions and the cAMP suppresses Teffector cell functions[56].

Suppression by modulation of DC maturation or function: Tregs may also modulate maturation and/or function of DCs[57, 58]. DCs can be forced to express a pro-apoptotic metabolite called indoleamine 2,3-dioxygenase (IDO)[57] through the interaction of CTLA4 with CD80/CD86 that leads to the suppression of Teffector cells[58]. The down-regulation of the expression of co-stimulatory proteins CD80 and CD86[58] by Tregs is another way to down-modulate the capacity of DCs to activate Teffector cells. In addition, lymphocyte activation gene 3 (LAG3) that is present on Tregs also mediates the suppression of DC maturation[59].

2.1.2.3. Reprogrammed Tregs: origin of pro-inflammatory cytokine IL-17 producing FOXP3+ regulatory T cells

It has been proposed that, under specific conditions such as inflammation, Treg can switch their lineage fate to T_{con}, during which *FOXP3* expression is maintained or suppressed [60, 61]. The canonical cytokines produced by Tregs are anti-inflammatory markers, such as IL-10, TGF-β and IL-35. However accumulating evidence indicate the ability of Tregs to reprogramme into T helper like cells, producing pro-inflammatory cytokines such as IL-17[62].

Even though Tregs and Th-17 are distinct populations, they are both promoted to differentiate by TGF-β. Moreover Th-17 cells can co-express *RORγt* with *FOXP3*[63] and secrete IL-17A with IL-10[64].

2.2. The role of Tregs in cancers

In the last few years the importance of the roles of Treg in the development of human cancer has been shown. Increased numbers of Treg cells have been reported in different tumours, such as ovarian carcinoma[65], breast cancer[66], colorectal cancer[67], squamous-cell carcinoma[68], melanoma[69], pancreatic cancer[70], hepatocellular carcinoma[71], lymphoma[72], B cell-derived non-Hodgkin lymphomas [73] and AML[54]. Chemokines can facilitate the recruitment of Tregs *in-situ* acting *via* their cognate receptors expressed by Treg cells[74]. However the frequency and functions of Tregs can lead to a different prognosis depending on the type of malignancies[75]. The expansion of Tregs is generally correlated with poor prognosis, even though in certain cancers such as Hodgkin's lymphoma (HL) the presence of Tregs seems to have a positive influence, which could be due to their anti-inflammatory effect[67, 76].

In cancer, several mechanisms can boost the expansion of Tregs[77], such as the production of tumour-derived factors like vascular endothelial growth factor (VEGF), IL-10, prostaglandin E2 (PGE), SDF-1 and TGFβ[78, 79, 80]. TGFβ could play a crucial role in the tumour microenvironment, inducing the differentiation of naïve $CD4^+CD25^-$*FOXP3*$^-$ T cells into *FOXP3*$^-$ expressing Tregs. It has also been shown that IDO, that is able to enhance the differentiation of Tregs[81], is secreted by various tumour cell types. In addition, non-soluble factors such as tumour-driven hypoxia inducible factor (HIF1) have been shown to induce the differentiation of Tregs[82]. (Figure 7)

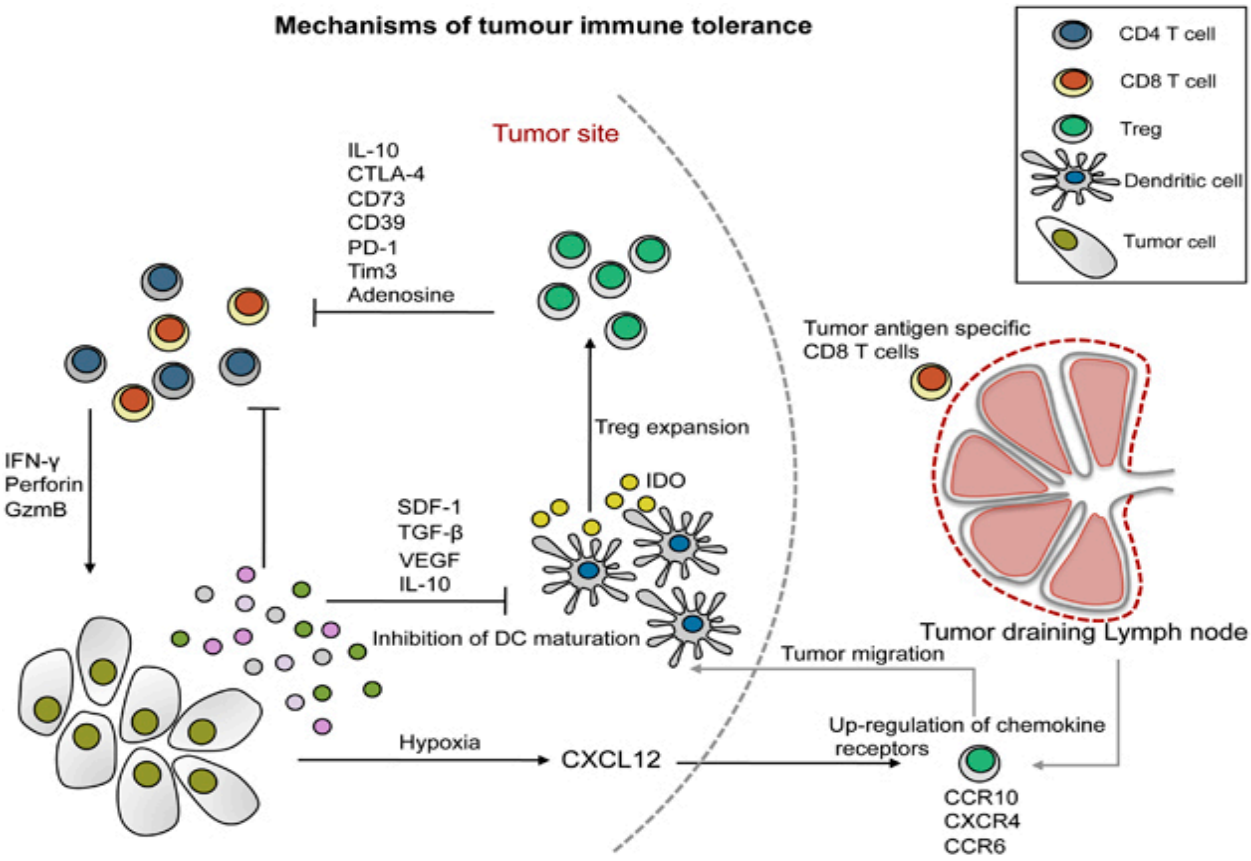


Figure 7. Mechanisms of tumor immune tolerance. In a normal situation CD4 and CD8 T cells are able to kill tumour cells through effector molecules *e.g.* IFN-γ. Tumour cells mediate recruitment, activation and proliferation of Tregs employing soluble and non-soluble factors like SDF-1, TGF-β and hypoxia. In addition, IL-2, CTLA-4 and CD73 are used by tumour-associated Tregs to inhibit effector T-cell function, which could possibly lead to tumour progression. *From Ashish Banerjee, et al Modulating T regulatory cells in cancer: how close are we? Immunology and Cell Biology (2013) 91, 340–349*[74]*;*

It is becoming clear that intra-tumoural Tregs play a significant and active role in tumour development and progression[65, 67, 72, 73, 74]. Hence, depletion of Tregs in tumours was shown to enhance and restore anti-tumoural immunity[67, 78]. Therefore manipulation of Tregs can lead to strategies for tumour immunotherapy, including vaccination and CTLA-4 blockade[79].

2.2.1. *Myelodysplastic syndromes (MDS)*

Primary MDS are heterogeneous clonal haematopoietic stem-cell disorders, characterised by ineffective and dysplastic haematopoiesis with varying degrees of peripheral cytopenias and an increased risk of transformation to AML[80, 83]. Erythrocytic, granulocytic, and megakaryocytic progenitor cells are affected in MDS. According to the French-American-British (FAB-1982) classification, MDS can be divided into five categories based on morphology and bone marrow blast count. In 2001, the World Health Organization (WHO) classification modified the FAB system, adding cytogenetic and molecular biology characteristics[84, 85].

The latest classification (WHO-2008) is based on:

1. The number of peripheral cytopenias,
2. The percentage of blasts in the peripheral blood and bone marrow,
3. The percentage of ringed sideroblasts,
4. The possible presence of Auer Rods (clumps of fused lysosomes, neutrophilic granules and lysosomal enzymes),
5. The detection of a cytogenetic abnormality (*e.g.* Chromosome 5q deletion).

WHO-2008 classification divided MDS disease into refractory cytopenia (RA), refractory anaemia with ringed sideroblasts (RARS), refractory cytopenia with multilineage dysplasia (RCMD), refractory anaemia with excess blasts (RAEB1 and RAEB2), myelodysplastic syndrome unclassifiable and myelodysplastic syndrome with isolated del5q (5q syndrome)[85]. (Table 3)

Table 3. WHO 2008 classification.

Disease	Marrow Blast	Clinical Presentation	Cytogenetic abnormalities
Refractory Anaemia (RA)	< 5%	Anaemia	25%
RA with ring sideroblast (RARS)	< 5%	Anaemia, > 15% ringed sideroblast	5 - 20%
MDS with isolated del(5q) (5q- syndrome)	< 5%	Anaemia, normal platelets	100%
Refractory Cytopenia with Multilineage Dysplasia (RCMD)	< 5%	Bicytopenia/pancytopenia ± 15% ringed sideroblast	50%
RA with Excess Blast-1 (RAEB-1)	5 - 9%	Cytopenia with peripheral blast	30 - 50%
RA with Excess Blast-2 (RAEB-2)	10 - 19%	Cytopenia with peripheral blast	50 - 70%
Myelodysplastic syndrome, unclassified	< 5%		50%

It is based on clinical features, peripheral blood and BM findings and cytogenetic analysis. Revised International Prognostic Scoring System (IPSS) Predicts Survival and Leukemic Evolution of Myelodysplastic Syndromes Significantly Better Than IPSS and WHO. *From Vardiman JW et al. The 2008 revision of the World Health Organization (WHO) classification of myeloid neoplasms and acute leukemia: rationale and important changes. Blood 2009,* ***114****(5): 937-951*[85]

Although MDS can affect people of all ages, it is primarily a disease of the elderly and the median age is 70[86]. MDS is a pre-malignant condition and about 30% of patients develop AML. The International Prognostic Scoring System (IPSS) provides an improved method for evaluating the severity of MDS. It was first introduced based on survival analysis and the risk of progression to AML in 816 patients with *de novo* MDS. The IPSS score is based on cytogenetic abnormalities, percentage of BM myeloblasts, number of cytopenias, age and gender. It provides an estimation for the overall and disease-free survival. Cytogenetic subgroups which defined a "good" prognosis category were normal, -Y alone, del(5q) alone, del(20q) alone. A "poor" prognosis category was defined as patients with complex (*i.e.,* ≥3 abnormalities) or chromosome 7 anomalies and the "intermediate" prognosis category contained cells with other abnormalities. Combined analysis of cytogenetic subgroups, percentage of BM blasts and number of cytopenias allows the generation of a prognostic model that divides MDS patients who progress to AML into three groups: low (31% of patients), 9.4 years;

intermediate-1 (INT-1; 39%), 3.3 years; INT-2 (22%), 1.1 years; and high (8%), 0.2 year. (Table 4)

Table 4. IPSS score classification.

Factors for Determining IPSS Score					
	Score Value				
Prognostic variable	0	0.5	1	1.5	2
Blasts in marrow (%)[a]	<5	5-10	—	11-20	21-30
Karyotype[b]	Good	Intermediate	Poor	—	—
Cytopenias[c]	0/1	2/3	—	—	—

Risk of Transformation and Median Survival			
Risk	Total Score	Progression to AML Without Therapy for 25% (y)	Median Survival Without Therapy (y)
Low	0	9.4	5.7
Int-1	0.5-1.0	3.3	3.5
Int-2	1.5-2.0	1.1	1.2
High	≥2.5	0.2	0.4

[a] Scoring system developed prior to WHO classification, which lowered blast percentage to ≥20% for diagnosis of AML.
[b] Good: normal, -Y, del(5q) alone, del(20q); poor: complex (≥3 abnormalities) or chromosome 7 abnormalities; intermediate: other abnormalities.
[c] Neutrophil count <1,500/mcL, platelets <100,000/mcL, hemoglobin <10 g/dL.
AML: acute myeloid leukemia; Int: intermediate; IPSS: International Prognostic Scoring System; WHO: World Health Organization.
Source: References 4, 5.

The IPSS score classification identifies four risk classes based on cytopenias, cytogenetics (karyotype) and bone-marrow blasts and aids in treatment decisions. *From Greenberg P et al. International scoring system for evaluating prognosis in myelodysplastic syndromes. Blood 1997,* ***89****(6)****:*** *2079-2088*[1, 87]

A revised version of the IPSS classification (IPSS-R) was introduced to have a more precise prognostic value than the original IPSS. The cohort of patients was increased to 7012 (instead of 816 for the original IPSS)[87] and the classification includes IPSS factors as well as ferritin and lactate dehydrogenase. Compared to IPSS, IPSS-R is characterised by five disease features, which are used to generate five prognostic categories[1]. (Table 5)

Table 5. IPSS-R scoring system.

IPSS-R Cytogenetic risk groups*, **

Cytogenetic prognostic subgroups	Cytogenetic abnormalities
Very good	-Y, del(11q)
Good	Normal, del(5q), del(12p), del(20q), double including del(5q)
Intermediate	del(7q), +8, +19, i(17q), any other single or double independent clones
Poor	-7, inv(3)/t(3q)/del(3q), double including -7/del(7q), Complex: 3 abnormalities
Very poor	Complex: >3 abnormalities

IPSS-R Prognostic Score Values*

Prognostic variable	0	0.5	1	1.5	2	3	4
Cytogenetics	Very Good		Good		Intermediate	Poor	Very Poor
BM Blast %	<=2		>2-<5%		5-10%	>10%	
Hemoglobin	=>10		8-<10	<8			
Platelets	=>100	50-<100	<50				
ANC	=>0.8	<0.8					

IPSS-R Prognostic Risk Categories/Scores*

RISK CATEGORY	RISK SCORE
Very Low	<=1.5
Low	>1.5 - 3
Intermediate	>3 - 4.5
High	>4.5 - 6
Very High	>6

IPSS-R: Prognostic Risk Category Clinical Outcomes*

	No. pts	Very Low	Low	Intermediate	High	Very High
Patients (%)	7012	19%	38%	20%	13%	10%
Survival***		8.8	5.3	3.0	1.6	0.8
AML/25%***, ^		NR	10.8	3.2	1.4	0.7

***Medians, years ^Median time to 25% AML evolution

*Greenberg, Tuechler, Schanz et al, Revised International Prognostic Scoring System (IPSS-R) for Myelodysplastic Syndrome, Blood 120: 2454, 2012.

**Schanz J et al, J Clin Oncology 2012; 30:820

IPSS-R is characterised by five disease features that are used to generate five prognostic categories to define the disease more precisely. *From http://www.mds-foundation.org*

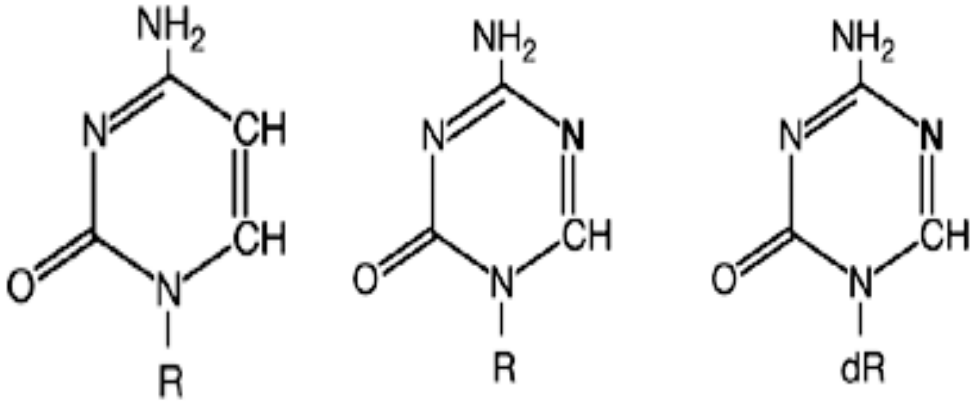
Age, performance status, co-morbidities, donor availability, WHO classification, IPSS-R score and cytogenetics are critical to design an effective treatment plan for MDS patients.

There are a few treatments available to MDS patients:

1. Bone marrow transplant is usually considered as the only curative option for patients with MDS and is the treatment of choice for younger patients when a matched donor is available[87].
2. Supportive care: red blood cell transfusions are routinely used to alleviate symptoms related to anaemia, in combination with antibiotics and haematopoietic growth factors such as erythropoietin and granulocyte colony-stimulating factor (G-CSF). G-CSF stimulates the survival, proliferation, differentiation and function of neutrophil precursors and mature neutrophilis. Patients with low risk disease are usually treated with G-CSF[1].
3. Immunosuppressive treatments: Antithymocyte globulin (ATG) depletes T-cells and restores haematopoiesis, cyclosporin A (CSA) blocks IL-2 production and suppresses apoptotic cytokines like TNF-α[88] . This type of treatment is usually helpful in patients with low risk disease.[89]
4. Epigenetic modifying drugs[90]: 5AzaC and Decitabine are two hypomethylating agents with anti-neoplastic activity which are in clinical use for MDS treatment. 5AzaC causes DNA hypomethylation by inhibiting DNA methyltransferase enzymes. Patients with high-risk disease are usually treated with 5AzaC which reduces transfusion dependence and on average postpones the progression to AML by ten months[4]. Histone deacetylase inhibitors, such as Vorinostat and Valproic acid are able to reverse some of the aberrant gene repression in MDS and increase the time to progression to AML[1].
5. Immunomodulatory agents: Lenalidomide is the main treatment for low risk disease, in particular the 5q- subset of MDS and improves the transfusion dependence of these patients. However, the exact mechanism of action is yet to be identified[91, 92].

2.2.2. *5-Azacytidine*

5-Azacytidine (5AzaC) ($C_8H_{12}N_4O_5$) and 5-Aza-2-deoxycytidine (Decitabine) ($C_8H_{12}N_4O_4$) were first synthesised by Piskala and Sorm (1964)[93] as substitute for cytidine specific for AML (Figure 8). 5AzaC is able to be incorporated into both RNA and DNA, whereas 5-Aza-2-deoxycytidine is incorporated only into DNA[94]. In this reaserch project I choose to focus on the effects of 5AzaC because it has already been studed by our group. The capacity of 5AzaC to cause DNA demethylatinon was discovered by Jones and Taylor in 1980[95]. DNA methyltransferase (DNMT) is a family of enzymes able to catalyse the transfer of a methyl group to DNA[96, 97, 98]. Aza-nucleotides can be incorporated into DNA during DNA replication and recognized by DNMT. The Aza-nucleotide acts as suicide substrate for DNMT, leading to its inactivation. The DNMT is first trapped then degraded through an intermediate formed *via* the sulfhydrylic side chain of the catalytic cysteine residue[99]. 5AzaC has been largely used in heamatological malignancies, however it has been shown to have an effect in *in vitro* culture of human breast cancer cells[100] and in a murine breast cancer model[101].



Cytidine 5-Aza-cytidine 5-Aza- 2' deoxycytidine

Figure 8. Structure of cytidine and methylation inhibitors 5AzaC and Decitabine. Figure adapted from *Fenaux P (2005) Inhibitors of DNA methylation: beyond myelodysplastic syndromes Nat Clin Pract Oncol* ***2:*** *S36–S44 doi:10.1038/ncponc0351*[94]

2.2.3. *Tregs in MDS*

There are differences between low and high risk MDS in terms of bone marrow (BM) blasts, cytopenias, cytogenetic abnormalities and immune profiles[1, 102]. (Table 6)

Table 6. Role of the immune response in low and high- risk MDS.

Immune cells	*Low-risk MDS*	*High-risk MDS*	*Role in MDS*
NK cells	↑	↓	Mediation of cytotoxicity of BM precursor cells in Low-risk MDS
Macrophages	↑	↓	IFN-γ producing cells. They are cytotoxic for BM precursor cells in low-risk MDS
Dendritic cells	↓	↓	Low number of myeloid and lymphoid circulating. Precursor DCs clonal evolution has been documented
B cells	↓	↓	MDS-HSC loses potential to differentiate into B cells progenitor
Tregs	↓	↑	Activation of auto-reactive T cell clones (in low-risk MDS), suppression of immune response against dysplastic clones (in high-risk MDs)
$Th^{-}17$ cells	↑	↓	Mediation of cytotoxicity of BM precursor cells in low-risk MDS
Cytotoxic $CD8^{+}$ cells	↑	↓	Contradictory role in MDS pathology
↓ Decrease in number		↑ Decrease in number	

The role of the immune response in low and high- risk MDS leads to the idea that the two conditions are different. *Table adapted from Aggarwal S et al. Role of immune responses in the pathogenesis of low-risk MDS and high-risk MDS: implications for immunotherapy. Br J Haematol 2011,* ***153****(5):* *568-581*[102]

One of the important features of low risk MDS is an increase in the number of pro-inflammatory IL-17 producing CD4+ T cells (Th-17), increasing levels of apoptosis in BM and increasing pro-inflammatory cytokines[103]. In high–risk MDS however, the increased number of Tregs leads to immunesupression and the immunosuppressive BM microenvironment favours expansion of the dysplastic clone, which leads to disease progression toward AML[2].

The role of Tregs in both low and high-risk MDS is crucial:

- In low-risk MDS, the number of Tregs tends to be lower andthis is consistent with facilitating the emergence of autoimmune responses, including autoreactive T cell clones and secondary BM hypoplasia[2, 103].

- In high-risk MDS, Tregs are expanded (predominantly from the naïve subset) and could contribute to disease progression. The increase in the number of polyclonal Tregs is likely to affect the immune response against the dysplastic clone, thus facilitating the progression of the disease.[2]

The numbers of Tregs are less in high risk MDS following treatment with 5AzaC, however after nine months of therapy the number of Tregs increased in patients who responded to 5AzaC. *In-vitro* experiments demonstrated that after 5AzaC treatment, Tregs lose their suppressive function, although maintaining their phenotype. Following *in-vitro* culture of peripheral blood mononucleocite cells (PBMCs) from healthy donors in the presence of 5AzaC the number of *FOXP3*$^{+}$ IL-17 secreting "Treg like" cells were increased. These cells mainly originated from T_{con} cells rather than Tregs.[4] The role of these cells in MDS immune-surveillance is not fully understood and is one of the main objectives of this PhD project.

2.3. Research plan

It has been shown by our group that following treatment with 5AzaC, the absolute number of Tregs is reduced and they not only became non-suppressive but also secrete pro-inflammatory cytokines, such as IL-17 and IFN-γ. There is also increased *FOXP3* expression in the T_{con} of healthy donors (HDs) following *in-vitro* culture with 5AzaC, without significant immunosuppressive properties. This subpopulation is known as "Treg-like" cells[104].

Due to these promising data, we wanted to investigate further the difference between Tregs, T_{con} and Treg-like cells from HD and MDS patients in terms of phenotype, cytokine secretion and DNA methylation profile.

Furthermore, we wanted to assess the difference between Tregs, T_{con} and Treg-like cells from MDS patients. Therefore, in order to address these main topics, the following points were investigated:

- The percentage of *FOXP3*$^+$ cells in T_{con} after 5AzaC trearment
- The percentage of *FOXP3*$^+$ cells in T_{con} after cytokine induced environment (Il-1β, IL-6, IL-2)
- The suppressive property of "Treg-like" cells coming from 5AzaC or cytokines induced
- The methylation profile of the *TSDR* intron within the "Treg-like" cells
- The phenotype signature of "Treg-like" cells compared with Tregs

3. Materials and Methods

3.1. General Materials and Methods

In this Chapter, general methods which have been used in this project are discussed. Any specific method or deviation from standard methods related to a specific Chapter will be discussed at the beginning of that Chapter.

3.2. Cells isolation

Blood samples were obtained from leukocyte cones provided by the NHS Blood and Transplant (Tooting, UK) The cones contain the anticoagulant Citrate Dextrose. The cones are used as filters for leukodepletion during the component donation process and they contain a high concentration of leukocytes. The number of leukocytes obtained was determined by manual counting in the presence of Trypan Blue after the Ficoll separation (described in section 3.2.2 of this current Chapter).

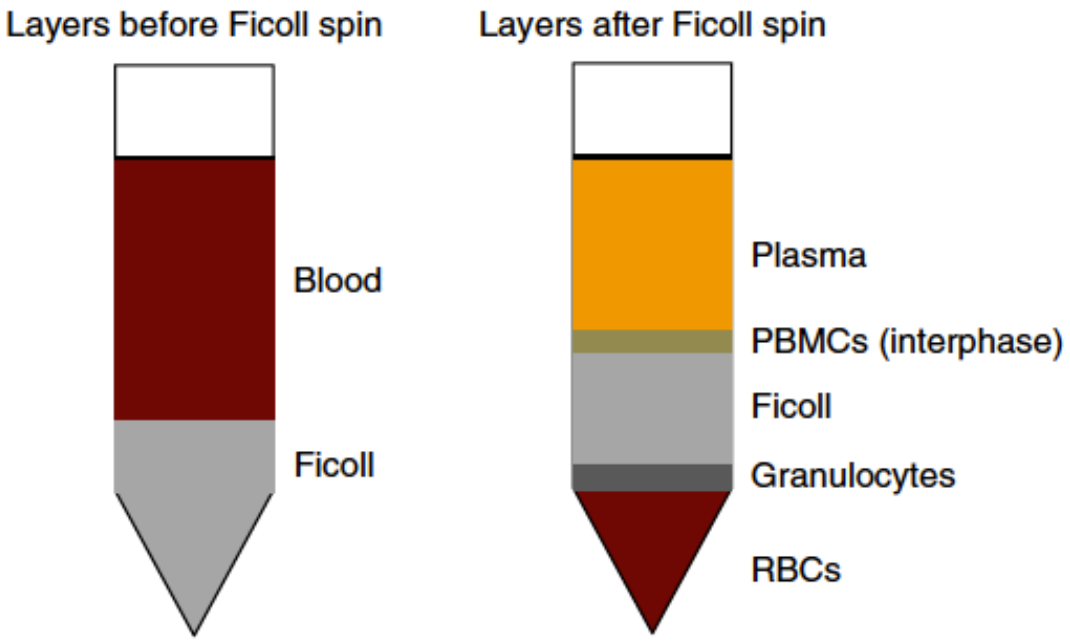


Figure 9 Leukocyte cone pre and post centrifugation. After centrifugation cells are separated based on their density. From the top layer, we have platelets that are the least dense cells compare with the Ficoll. Followed by PBMCs which are placed in the interface, are also not dense enough to cross the Ficoll whereas red blood cells and other white blood cells are dense enough to cross the Ficoll. Imagine adapted from Lin *et al*[105]

3.2.1. *Gradient cell separation*

Lympocytes were isolated by Ficoll-Paque[105] (LSM 1077 Lymphocyte PAA Laboratories GmbH) gradient centrifugation at 1000 x G_{max} for 20 minutes. Due to their different densities, three layers occur: a plasma layer, the interphase consisting of Peripheral Blood Mononuclear Cells (PBMCs) and a Ficoll-Paque layer (Figure 9). The PBMCs layer was removed and centrifuged at 300 x G_{max} for 10 minutes. The supernatant was decanted and the pellet was resuspended in 20 ml of Hank's balanced salt solution (HBSS, PAA). PBMCs was then centrifuged twice at 220 x G_{max} for 10 minutes, the supernatant was decanted and the pellet resuspended with HBSS. The pellet was finally resuspended in Hematopoietic Media (X-Vivo 15, Lonza).

3.2.2. *Trypan blue counting*

The number of leukocytes obtained was determined by manual counting using a haemocytometer (Bio Rad) in the presence of Trypan Blue. The method is

based on the function of the dye to selectively colour dead cells in blue since the plasma membrane is disruptured. Live cells, which have an intact plasma membrane are not coloured. 10 μl of the cell suspension was transferred into the counting chamber and all the cells in the central large square of haemocytometer were counted. The total number of cells was calculated (cells/ml) as follows:

cells counted (25 sq grid) x dilution factor $x10^4$ x volume of the cell suspension. Trypan blue was used in a ratio of 1:1 and the total calculated cell number was multiplied by 2.

3.2.3. *Red blood cell Lysis*

The Red Blood Cell Lysis Buffer 10X (BioLegend; components not realised by the manufacturer) is designed for the lysis of red blood cells from PBMCs, yielding intact white blood cells (free of red blood cells) for further applications. This method was applied after the gradient cell separation step. The 10X buffer was diluted to 1X working concentration with deionised water before use it. 2 ml of 1X buffer was added to each tube containing up to $10x10^7$ PBMCs and gently vortexed immediatly after adding the lysing solution. The tube was incubated at room temperature, protected from light due to the light sensitivity of the components, for 10 minutes and then centrifuged at 300 x G_{max} for 10 minutes. The supernatant was aspirated and the cell pellet was resuspended in the appropriate buffer for further procedures.

3.2.4. *Bead separation*

This method was used to separate different subtypes of T cells for either functional or molecular assays.

3.2.4.1. $CD4^+$ T helper cell isolation

The human $CD4^+$ T helper cell population was isolated from PBMCs by depletion of non-$CD4^+$ cells, using the $CD4^+$ T cell negative isolation kit (MACS) and Magnetic-activated cell sorting (MACS) column magnetic separation system (all from Miltenyi Biotec Ltd.). After collecting the PBMCs

by centrifugation at 220 x G_{max} for 10 minutes, the media was removed and the cell pellet resuspended in MACS Buffer (1xPBS, 2mM EDTA, 0.5% (w/v) BSA) (40μl per 10^7 cells). To isolate CD4+ T cells, a cocktail of Biotin-conjugated monoclonal antibodies against non-CD4+ T cells (10μl per 10^7 cells) was added to the cell pellet and incubated for 10 minutes at 4°C (the antibodies bind to all cells other than $CD4^+$ T cells). Microbeads conjugated to a monoclonal anti-Biotin antibody and monoclonal anti-CD16 (NK cell and macrophage marker) antibody (20μl per 10^7 cells) provided with the kit, were then added and incubated for 10 minutes at 4°C. After washing the cells with 2 ml MACS buffer and centrifugation at 220 x G_{max} for 10 minutes, the pellet was resuspended in 500 μl of MACS buffer and then placed in a MACS column. The column magnetically retains the non-$CD4^+$ cells, while the $CD4^+$ cells in the flow-through were collected (negative selection). Cells were then centrifuged at 220 x G_{max} for 10 minutes and the pellet was resuspended in 10 ml of X-Vivo 15 media.

3.2.4.2. $CD4^+CD25^+$ regulatory T cells isolation

Tregs were isolated from PBMCs using the $CD4^+CD25^+$ regulatory T cell isolation kit (Milteny Biotec) in a two-step protocol. The first step was the isolation of $CD4^+$ T cells as described above. In the second step, the flow-through fraction, containing $CD4^+$ cells were labelled with CD25 Microbeads provided with the kit (10μl per 10^7 cells) for 15 minutes, then resuspended in 500μl of MACS buffer and placed in the MACS column. Tregs were retained in the column (positive selection) and Tcon were the flow-through fraction. The column was removed from the magnet, placed in a 15ml tube and a total of 500μl of MACS buffer was added to the column. Using a specific plunger provided from the manifacturer, the Tregs and the 500μl of MACS buffer were flushed out in the tube. Cells were then centrifuged at 220 x G_{max} for 10 minutes and the pellet was resuspended in X-Vivo 15 (2 x 10^5 cells /ml).

3.3. Cryopreservation and thawing of PBMCs

3.3.1. *PBMCs Cryopreservation*

Live cells are preserved at cryogenic temperature (below 150°C) in liquid nitrogen to be stored in a way that their normal metabolic activity is suspended. Cells can be thaw and used as needed[106].

After isolation of PBMCs, 1 ml of PBS were added and cells were centrifuged at 220 x G_{max} for 10 minutes. Supernatant was removed by aspiration and pellett was resuspended in 1 ml of Cryomaxx (1 ml /50x10^6 cells) (PAA Laboratories GmbH).

3.3.2. *PBMCs thawing*

Frozen cells were thawed at 37°C in a waterbath till the Cryomaxx became liquid.

The 1 ml Cryomaxx and the cells suspended were transfered in a 15 ml tube.

A total of 5 ml of X-Vivo (Lonza) were added and then centrifudged at 220 x G_{max} for 10 minutes (2X). Cells were then resuspened in 1 ml of X-Vivo and counted to assess the post-thaw viability. Cells were then ready to use.

3.4. Fluorescence-activated cell sorting (FACS)

FACS or flow cytometry techniques are employed for the characterisation and quantification of different populations of cells. This technique involves hydrodynamic focusing to ensure the cells pass through the laser beams in single file (about 500 cells per second). Once the lasers hit the cells, forward scatter (in line with the laser beam), side scatter (perpendicular to laser beam) and fluorescent emissions are recorded. Certain cell surface proteins are only present on specific cell types and so can be used as markers to identify these cells. Different fluorochromes conjugated to antibodies specific for the target markers are attached to the cells, absorbing light and then emitting a specific wavelength depending on the type of fluorochrome. The filters direct the light emitted by the fluorochromes to the colour detectors that collect the different data and these informations are sent directly to the computer processor for processing and display. The relative size of each particle (in this case, cells), relative granularity or internal complexity can be assessed by using flow cytometry analyses[107]. (Figure 10).

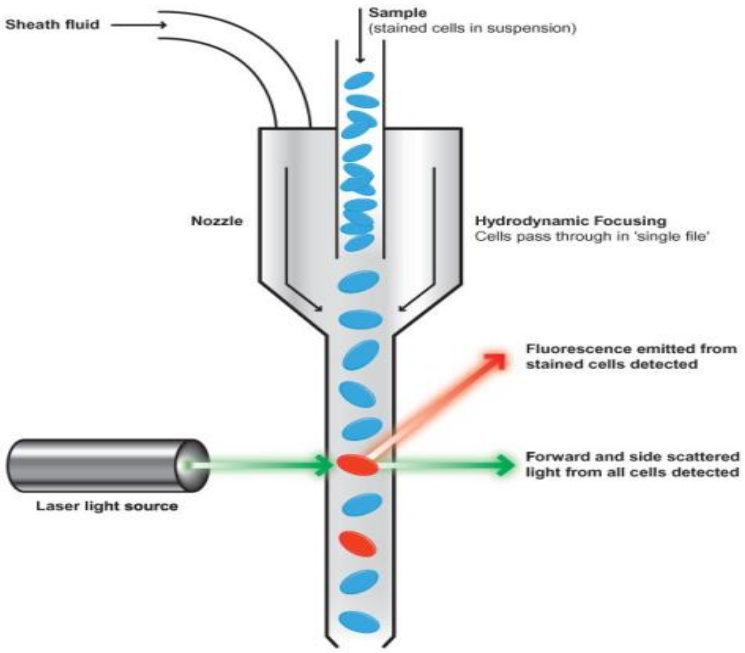


Figure 10 Flow cytometer chamber. A single wavelength is directed into a focused stream of liquid. Several detectors point where the stream passes through the light beam: one in line with the light beam (forward scatter FSC) and several perpendicular to it (Side Scatter or SSC) and one or more fluorescence detectors. *From www.abcam.com*

For this project, the following flow cytometers were used: FacsCanto II (3 lasers), LSRFortessa (4 lasers) as cell analysers and FACSAria II (5 lasers) for cell sorting. FacsDiva software was used to analyse the raw data (BD Bioscience).

3.5. Staining

Two cell staining methods were used to analyse Tcells markers; one for surface markers (*e.g.* CD3 or CD4) and the other for intracellular proteins such as FOXP3 or intracellular cytokines (*e.g.* IL-17). The antibodies used are shown in Table 7.

Table 7 List of antibodies and dyes used

Antibody	Supplier	Clone	μl per 1 x10^6 cells	Cat no.
Surface Antibody				
CD3 Viogreen	Miltenyi Biotech	BW264/56	1	130-096-910
CD4 eFluor 450	eBioscience	RPA-T4	1	48-0049-42
CD127nPerCP Cy5.5	eBioscience	eBioRDR5	1	45-1278-42
CD25 PE	BD Bioscience	M-A251	3	555432
CD45RA Alexa Fluor 700	Biolegend	HI100	1	304120
Fixable Viability Dye eFluor 780	eBioscience		0.5	65-0865
CD8 eF450	eBioscience	RPA-T8	2.5	48-0088-42
CD3 APC	Biolegend	OKT3	2	317318
Intracellular Antibody				
FOXP3 FITC	eBioscience	PCH101	1.5	11-4776-42
IL-17 PerCP Cy5.5	eBioscience	eBio64DEC17	1.5	45-7179-42
TNF-α PE-Cy7	eBioscience	MAb11	5	557647
IFN-γ	eBioscience	LS.B3	1.5	17-7319-82
Cell trace violet proliferation dye				
VPD	Invitrogen		1	C34557

In this list, the antibodies and dyes used in this thesis are listed. The antibodies are divided into 2 groups: Surface and Intracellular, depending on the target marker.

3.5.1. *Surface staining*

The separated PBMCs, Tregs and T_{con} cells were washed with 1 ml of PBS, then centrifuged at 270 x G_{max} for 10 minutes. The appropriate antibodies (Table 1) were added and the samples were incubated for 20 minutes at room temperature. A total of 1ml of FACS Buffer was added to the cells and then were centrifuged at 270 x G_{max} for 10 minutes. Supernatant was decanted and cell pellet was resouspended up to 10^7 cells in 100µl of Fluorescence Activated Cell Sorter (FACS) Buffer (2.5% (v/v) Fetal Calf Serum FCS (invitrogen), 0.1% (w/v) NaN_3) for FACS based analysis or cell sorting. Protein contained in FCS was used to reduce non-specific antibody binding.

3.5.2. *Intracellular staining*

After surface staining the intracellular Fixation buffer (containing 4% Para-formaldehyde, eBioscience) was used in order to fix the cells, together with a Permeabilisation buffer (eBioscience) used to create holes in the cell surface thereby allowing the entrance of the intracellular staining antibodies.1 ml of Fixation/Permeabilisation (1:3) buffer per 10^6 cells was added. Cells were incubated at 4°C for 40 minutes. 2 ml of Permeabilisation Diluent 1X (eBioscience) were added and the cell suspension was centrifuged at 270 x G_{max} for 10 minutes. Intracellular antibodies (Table 7) were then added and incubated for 30 minutes at 4°C. A total of 1 ml of Permeabilisation Diluent 1X (eBioscience) was added to the cells and centrifuged at 270 x G_{max} for 10 minutes. A total of 200µl of PBS was added to the cells and analysed using flow cytometry.

3.5.3. *Purity analysis*

On average, the purity of the cells isolated by magnetic beads was 95% ± 0.52 (n=6 independent experiments) for T_{con}, 96.35% ± 0.71 (n=4 independent experiments) for Tregs. To determine the purity of T_{con}, 0.25 x 10^6 $CD4^+$ T cells were stained for 30 minutes in the dark with anti-human CD4 eFluor V450 (eBioscience) and anti-human CD3 APC (eBioscience), then centrifuged at 270 x G_{max} for 10 minutes with 1 ml of FACS Buffer. The

samples were then analysed by flow cytometry. To determine the purity of Tregs, 0.25 x 10^6 $CD4^+CD25^+$ T cells were stained for 30 minutes in the dark with 2 μl of anti-human CD4 eFluor V450 (eBioscience) and 4 μl of anti-human CD25 APC (eBioscience). Cells were then centrifuged at 270 x G_{max} for 10 minutes with 1 ml of FACS Buffer. The samples were then analysed by flow cytometry.

3.6. Compensation and data analysis

Before running the samples a compensation adjustment was carried out to counterbalance the spectra overlap, using BD CompBeads (BD Biosciences). The proper laser voltages were verified by running the setup beads (BD biosciences), using FACSDiva software (BD biosciences). These procedures ensured the consistency of lasers during the entire project. The compensation beads with the antibody that we want to use in the actual experiment were run on the FACS machine after initial checks and compensation. Compensation beads were acquired and recorded for 5000 events to identify the target population. Raw files from the recorded experiments were used for data analysis by FACSDiva software (BD Biosciences). FlowJo software v 9.8.4 (Tristar) was used to produce FACS plots for the thesis. The workflow to gate flow cytometry data is described in figure 11.

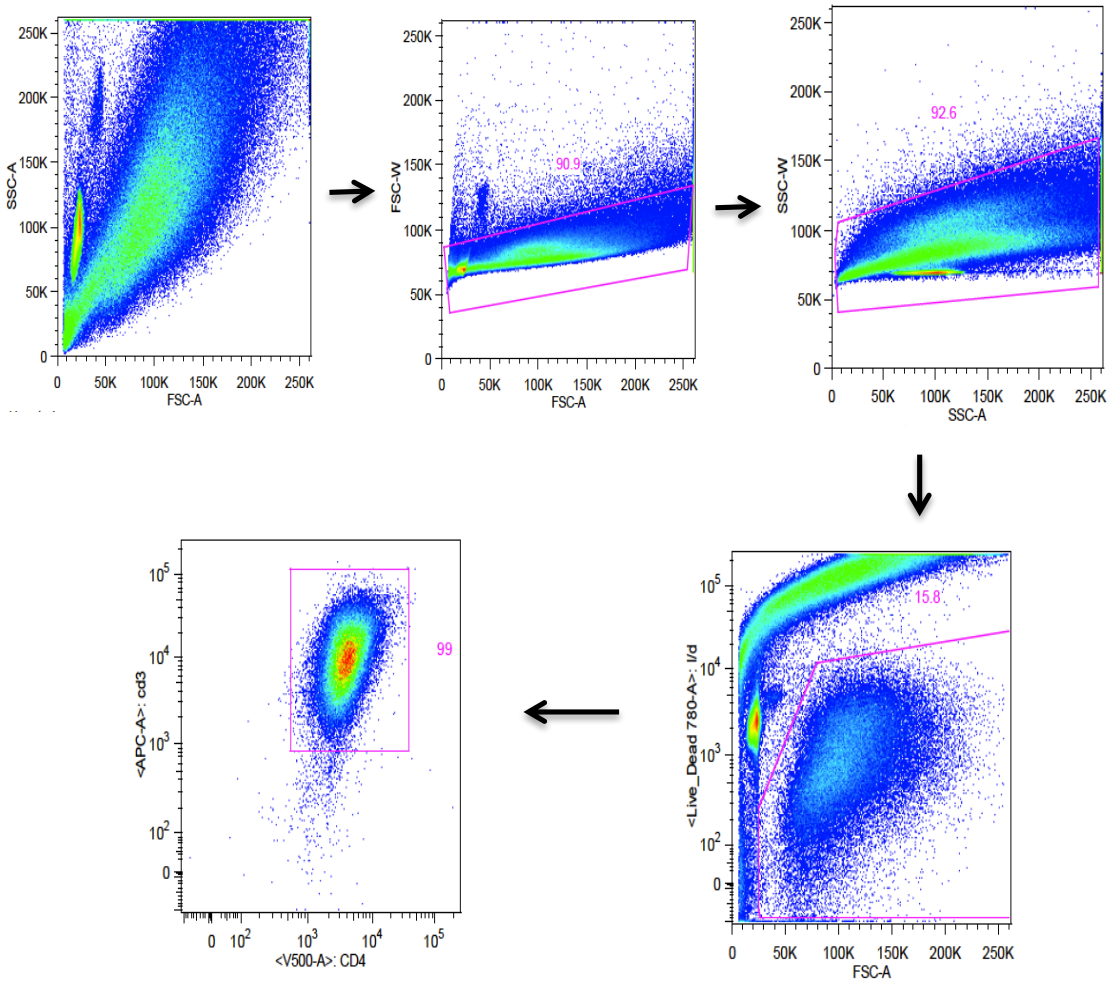


Figure 11. Gating strategy for flow cytometry analysis. In this T cells sample, cells were first gated based on the physical parameters such as cell granularity or internal complexity (Side Scatter SSC) and cell surface area or size (Forward Scatter FSC). Correlated measurements of SSC and FSC (FSC-W vs FSC-A and SSC-W vs SSC-A) can allow for differentiation of single cell types and to exclude debris, clumps and doublets in a heterogeneous cell population. The lymphocyte gate is then analysed based on Live/Dead staining dye to determined live versus dead cells (Live_Dead 780 vs FSC-A). Gating the live cells, T cells population is determined with surface expression of CD3+CD4+ (CD3 APC vs CD4 V500). The CD4+CD3+ population is now ready to be further analysed depending on the experiment.

3.7. Cell surface protein isolation

The Pierce cell surface protein isolation kit (Thermo Scientific) was used to isolate cell surface proteins[108]. Purified $CD4^+$ cells were centrifuged with 5 ml ice-cold PBS at 220 x G_{max} for 10 minutes, then 60 x 10^6 cells were divided into three conditions (20 x 10^6 cells for each condition) (Figure 12): total cell lysate, Biotinylated cells and control, PBS-treated cells.

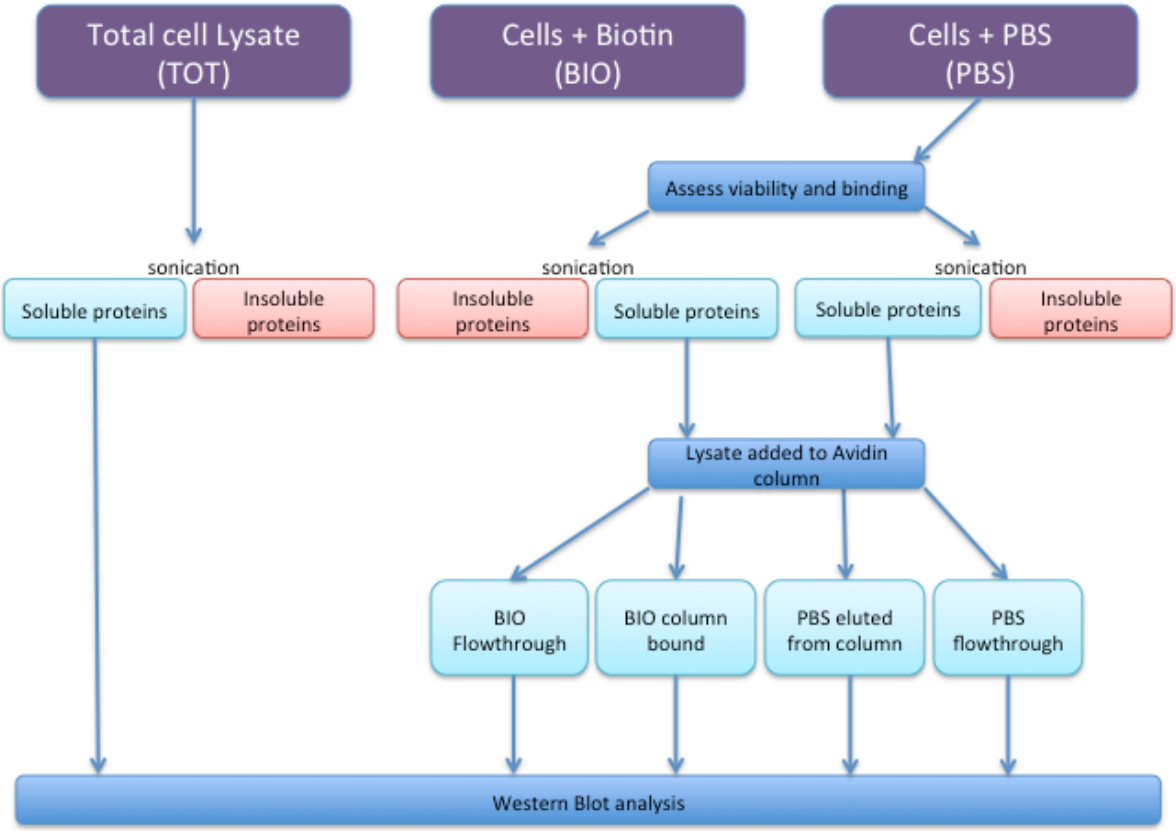


Figure 12. Cell surface isolation protocol. Cells were divided into three conditions (20 x 10^6 cells for each condition): total cell lysate (TOT), Biotinylated cells (Bio) and PBS-treated cells (PBS) (see *Biotinylation* section). Cells were lysed by sonication (cell lysis). Cell lysate was divided into the clarified supernatant (soluble protein) and the pellet (insoluble protein). The soluble proteins from Bio and PBS were then added to the Avidin matrix column (isolation of labelled proteins). Both columns flow through and the elution after using DTT at 95°C (protein elution) were analysed using gel electrophoresis (Western Blot method).

The steps of the protocol (Figure 13) are: Biotinylation, cell lysis, isolation of labelled proteins and Biotinylated protein elution from NeutrAvidin columns.

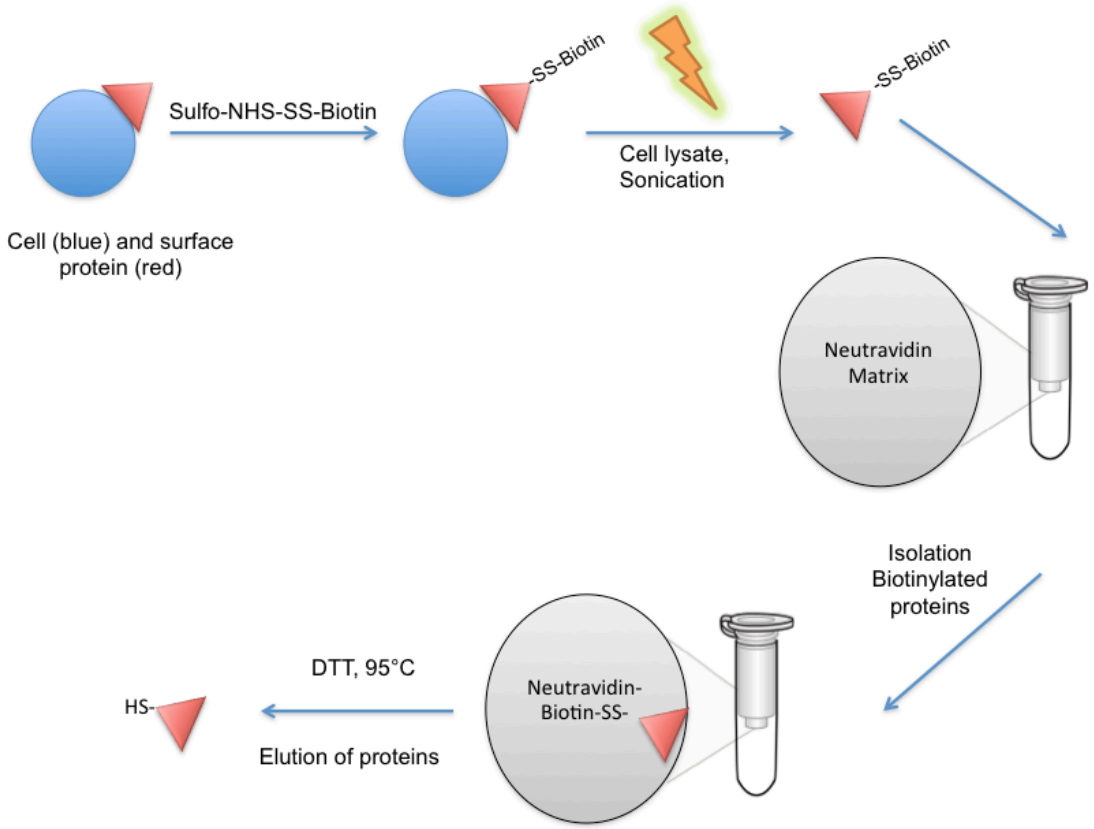


Figure 13. Isolation of surface protein using biotinylation method. Surface proteins were first bound to a Sulfo-NHS-SS-Biotin compound (biotinylation). The cells were then disrupted by sonication (cell lysis). Proteins with the Sulfo-NHS-SS-Biotin residue were bound to an Avidin matrix (isolation of labelled proteins) and then eluted using DTT at 95°C (protein elution).

Biotinylation: The sorted $CD4^+$ T cells were treated using 3 different conditions. The first condition (PBS) was a diluent control for the Biotinylation step, the second condition (Bio) was treated with the Sulfo-NHS-SS-Biotin compound and the third condition (Total cell lysate) was used as a control for the Biotinylation steps. $60x10^6$ $CD4^+$ T cells were used for the assay, which were divided into three microcentrifuge tubes ($20x10^6$ $CD4^+$ T cells each), one for each of the three different conditions. Cells were centrifuge at 220 x G_{max} for 10 minutes and the pellets were treated in different ways:

3. The pellet of the Total cell lysate (Tot) condition was kept on ice.
4. In the Bio condition 1.5 x 10^4 µg of Sulfo-NHS-SS-Biotin in 1 ml of PBS (Thermo Scientific) was added to the pellet.
5. The PBS condition pellet was resuspended with 1 ml PBS only.

The Bio condition with Sulfo-NHS-SS-Biotin and the PBS condition were placed in an orbital shaker for 30 minutes at 4°C. To stop the reaction, 50µl of

Quenching solution (Thermo Scientific: components not divulged by the manufacturer) was added. After 3 washes with Tris buffered saline (TBS Thermo Scientific) at 300 x G_{max} for 10 minutes I took 0.50 x 10^6 of $CD4^+$ T cells from Bio and PBS condition to check the viability by counting cells in the presence of Trypan blue. In addition, a flow cytometry method (Material and Methods 3.3) using Streptavidin e-FluorV450 was implied to check whether the biotin compound bound the surface proteins. Cells treated using theBio and PBS conditions were centrifuged at 270 x G_{max} for 10 minutes and the pellets were kept on ice.

Cell lysis: The pellets from the three conditions (TOT, BIO and PBS) were lysed with 50µl of Lysis Buffer (Thermo Scientific: conponents not divulged by the manufacturer) and placed on ice for 30 minutes. They were sonicated 2 x 10 minutes on medium power in a Bioruptor water bath (Diagenode) and vortexed for 5 seconds. Cells treated according to the three conditions were centrifuged at 300 x G_{max} for 2 minutes at 4°C. The clarified supernatant was the soluble fraction, the pellet the insoluble fraction.

Isolation of labelled proteins: The clarified supernatants of the BIO and PBS conditions were added to two different columns containing an Avidin matrix (previously washed with 100µl of Neutravidin Agarose and centrifuged at 270 x G_{max} for 10 minutes) and incubated with rolling for 60 minutes at room temperature to let the Biotin bind to Avidin, then centrifuged at 270 x G_{max} for 10 minutes to eliminate unbound proteins as flow thorugh.

Protein elution: Columns were incubated for 5 minutes at 95°C with 50µl of 4x Sample Buffer (1 M Tris-HCl (pH 6.8), 400 mM DTT, 8% (w/v) SDS, 0.4% (w/v) bromophenol blue, 40% (v/v) glycerol) and then centrifuged to elute the proteins bound to Avidin. The samples were then ready to be analyse by gel electrophoresis.

3.8. Gel electrophoresis

We used the Western blot in order to identify a specific protein based on its known size (measure in Kilodaltons kDa). The method consists of gel electrophoresis, electroblotting, blocking, detection and analysis.

1. *Gel electrophoresis:* An aliquot corresponding to 10% of each sample (see 3.6 Cell surface protein isolation) is loaded into wells in the gel (4-12% (w/v) polyacrylamide, Bis-Tris gels, NuPAGE, Novex). One lane was reserved for a pre-stained coloured marker mix of proteins of defined molecular weights. Separation of proteins occurred by electrophoresis for 45 minutes at a constant voltage of 120 V in running buffer (NuPAGE Life Technologies: 50mM MES, 50mM Tris, 1mM EDTA, 0.1% (w/v) SDS, pH 7.3).
2. *Electroblotting:* Proteins were transferred from the gel to the nitrocellulose membrane (HybondC Extra, GE healthcare) for 1 hour at a constant voltage of 200 V in transfer buffer (NuPAGE Life technology 25mM Bis-Tris, 25mM bicine, 1mM EDTA, pH 7.2) and 20 % (v/v) methanol.
3. *Blocking:* This step prevents non-specific binding of the primary or secondary antibody to the membrane. The membrane was incubated in PBST (PBS, 0.1% (v/v) Tween 20 in 1x TBS) with 5% (w/v) of non-fat dried milk (commercially available skimmed milk powder, Marvel) for 1 hour at room temperature.
4. *Detection:* The membrane is washed once with 10 ml of PBST prior to antibody probing. Primary antibodies were used at dilution of 1:2000 in PBST with 3% (w/v) BSA and 0.01% (w/v) NaN_3. Blots were incubated in primary antibodies with gentle agitation over night at 4^oC, then washed 3 x 5 minutes in PBST and incubated in secondary antibody for 30 minutes. Horse radish peroxidase (HRP) conjugated secondary antibodies (Dako) were used at the dilution on 1:2000 in PBST with 5% (w/v) of non-fat dried milk and added to the membrane for 1 hour at room temperature.
5. *Chemiluminescent analysis*: After the membrane was washed with 25 ml of 1 x TBS and 0.1% (v/v) Tween 20 for 3 x 10 minutes, protein

bands were detected using 2 ml of Enhanced Chemiluminescence reagent (Amersham ECL Prime Western Blotting Detection Reagent, GE Healthcare) and exposed to X-ray film (Hyperfilm-ECL, GE Healthcare) for various periods of time. Primary antibodies used were: CD44 (eBioscience, Anti-Human-Mouse) and Histone H3 (D1H2 Cell Signaling Technology).

3.9. Mass spectrometry

Samples from the Cell Surface Isolation experiment were prepared for Mass Spectrometry analysis, which was carried out at the King's College London Mass Spectrometry Core Facility. Samples were first alkylated using iodoacetamide (IAM) to prevent peptides from forming disulfide bonds and then digested with Trypsin in order to cleave the protein at the carboxyl side of the amino acid lysine or arginine, except when followed by proline[109] After digestion, the peptides were separated using high pressure liquid chromatography (HPLC) and then analysed using an in-line Orbitrap Velos Pro mass spectrometer[110] (Thermo-Fisher). Peptides were identified based on their spectra (mass-to-charge ratio). All the three sets of data were processed with Mascot software (Matrix Sciences) and they were searched against the sequences of all proteins encoded by genes in the human genome. In addition, a Mascot search was carried out with variable modifications on Lysine due to Biotin residue.

3.10. Single cell mass cytometry

The purpouse of this method is to analyse the cellular phenotype, signalling state, cytokine/chemokine expression and viability at a single cell level in frozen PBMCs or fresh bone marrow or peripheral blood samples using mass cytometry: Cytometry by Time-of-Flight (CyTOF) technology[111] (Figure 13).

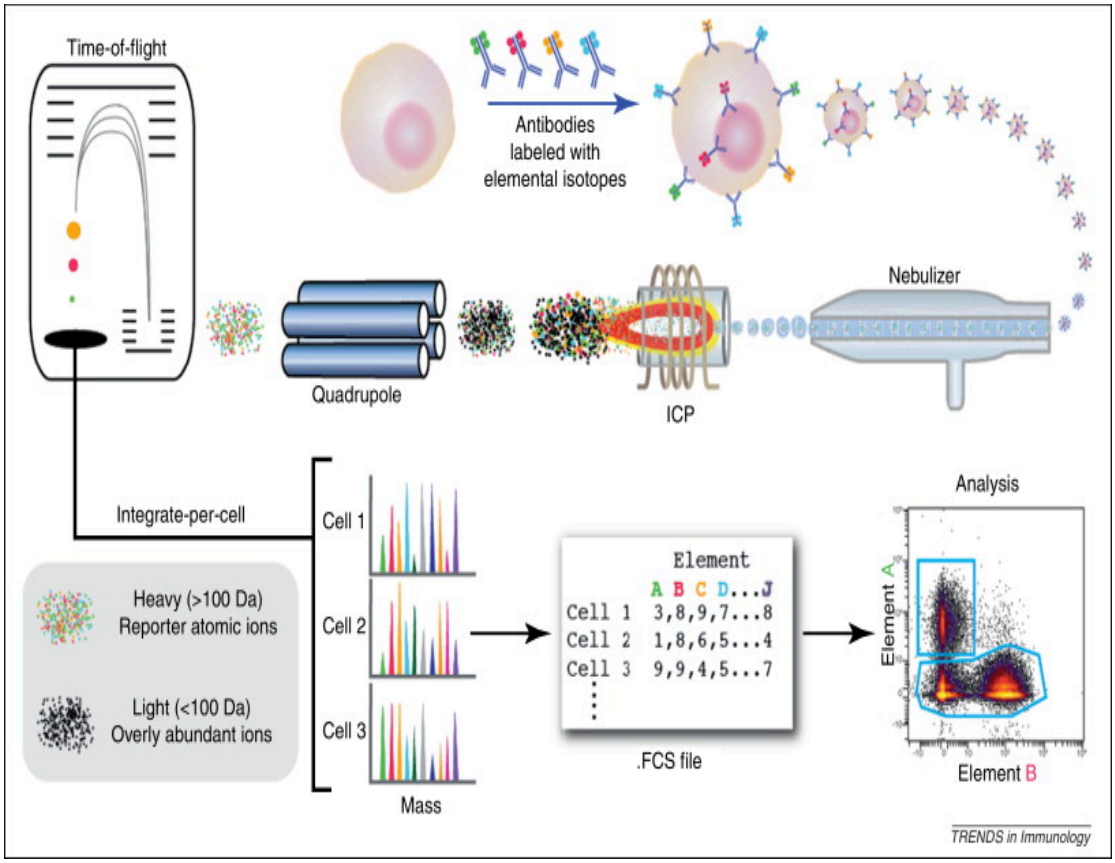


Figure 13. CyTOF workflow. CyTOF machine workflow: *a heavy metal isotope is conjugated to the antibody of interest. A panel of up to 40 chosen antibodies are assembled for membrane and intracellular staining. Cells are stained and then passed through a nebulizer. Cells are sprayed into an ICP TOF mass spectrometer. The individual ions are counted and then the raw data are collected into a flow cytometry file format.* Image adapted from Bendall, et al 2011 [111]

Antibodies targeting the cellular markers of interest are labelled with antibody metal isotope-conjugate probes. Labelled cells are then introduced in an Inductively Coupled Plasma (ICP) where they are atomized and ionized. The cloud of atomic ions for each single cell moves across a magnetic field towards a detector at a speed proportional to the size of the particle: the

lighter the particle, the faster it moves and the lesser the time-of-flight. Compared to fluorescence-based flow cytometry, CyTOF overcomes spectral overlap and cellular auto-fluorescence issues, the latter since the rare earth metal isotopes used in CyTOF are not naturally found in biological systems.

Cells were prepared adding a total of 2 µL of Leukocyte Activation Cocktail, with BD GolgiPlug stimulation (LAC) (BD, 550583) per 1ml of cell suspension and incubated for 4 hours at 37^{o}C, 5% CO_2. The Leukocyte Activation Cocktail is a polyclonal cell activation mixture containing a calcium ionophore (Ionomycin), the phorbol ester, the protein transport inhibitor BD GolgiPlug™ (Brefeldin A) and the PMA (Phorbol 12-Myristate 13-Acetate).

This cocktail is able to elicit a primary cytokine response from T cells. Cytokines are produced and then localised in the rough endoplasmic reticulum of the cells due to the Brefeldin A (a protein transport inhibitor component) that blocks intracellular protein transport processes. The accumulation of cytokine protein levels enhances the detectability of cytokine-producing cells by immunofluorescent staining and flow cytometric analysis. During this incubation, the Cell Staining Media (CSM) was prepared using 500 ml low barium PBS (no Ca^{2+}/Mg^{2+}) (Sigma, D8537) plus 2.5% foetal calf serum (FCS) and 0.02% sodium azide. In addition, the antibody cocktail was prepared using protein Low Bind tubes to avoid loss of antibodies by adsorption to the plastic walls of the tubes. Antibodies were kept cold during cocktail preparation. The exact amount of each Ab was added as indicated in the staining panel table (see Table 12) for each particular experiment. These volumes have been determined by previous titration of the antibodies. Once the cocktails were ready, tubes were placed in a box at 4 ^{o}C until needed. The Viability Stain (Rhodium) was prepared from the stock rhodium-intercalator solution that was provided from Dr Richard Ellis NIHR GSTFT/ KCL Biomedical Research and kept at -20 ^{o}C.

The (1x) rhodium working solution was 1:500 in PBS (no Ca^{2+}/Mg^{2+}). 500 µL of rhodium working solution was needed per test.

The Fc block working solution was 1:20 in CSM from the stock solution (Kiovig; Baxter, Human Ig, 100 mg/ml bottle). 10 µL of the working solution was added per test. After the 4 hours' incubations, cells were harvested and put into FACS tubes.

Tubes were centrifuged at 300 x G_{max} for 10 minutes to pellet cells at the bottom of the tube. Tubes were washed 1x with 2 ml PBS (no Ca^{2+}/Mg^{2+}), centrifuged at 300 x G_{max} for 10 minutes. Supernatant was discarded.

Cell pellet was resuspended in 500 µL (1x) Rhodium-intercalator working solution and incubated for 15 minutes at room temperature (RT).

Tubes were washed 2x with 2 ml PBS (no Ca^{2+}/Mg^{2+}), centrifuged at 300 x G_{max} for 10 minutes. Supernatant was discarded. A total of 10 µL of diluted Fc blocking reagent was added to the cells and incubated for 10 minute at RT.

Straight after the fc blocking the surface staining Ab cocktail was centrifuged at >10000 g for 5 minutes at 4 ^{o}C to bring the contents at the bottom of the tube and the appropriate volume of the cocktail was added to the cells (Table 12) and cells were incubated for 30 minutes at RT.

Cells were centrifuged twice with 2 ml of CSM at 300 x G_{max} for 10 minutes. Supernatant was discarded. Cell pellet was re-suspended in 1 ml of (1x) Fix/Perm solution (eBioscience freshly prepared, 1:3 dilution) and incubated for 45 minutes at 4° C. A total of 2 ml of (1x) Permeabilisation wash buffer was added to a final volume of 3 ml. Cell pellet was centrifuged at 400 x G_{max} for 8 minutes. Supernatant was discarded.

The appropriate volume of the cocktail was added to the cells (Table 12) and cells were incubated for 30 minutes at RT. Cells were centrifuged 2x with 2 ml of CSM at 300 x G_{max} for 10 minutes. Supernatant was discarded.

Cells were fixed with 500 µL 4% Paraformaldehyde (PFA) solution per test

Cell suspensions were transferred into eppendorf tubes and ready to be analysed using CyTOF machine.

CyTOF data were output as. fcs file format. The datasets generated on each experiment were high-dimensional (up to 40 markers analysed in millions of single cells) and should be analysed using a special tool kit (Cytobank) that include histograms, bivariate plots, SPADE clustering algorithm and heat maps. This tool facilitated the analysis and visualization of the data

3.11. Genomic DNA extraction

3.11.1. *Genomic DNA isolation*

Genomic DNA from human CD4+CD25+ Tregs and CD4+ T cells were isolated using the DNeasy blood and tissue kit (Qiagen). This method was performed following the manifacturer's guidelines. The components of the Buffers used (AL, AW1, AW2, AE) were not released by the manufacturer. A total of $0.5x10^6$ CD4+CD25+ Tregs and $5x10^6$ CD4+ T cells were centrifuged separately for 5 minutes at 300 x G_{max} and pellets were resuspended with 200µl PBS and 20µl of Proteinase K was added (manufacturer did not release the number of units of the enzyme). 200µl of buffer AL was added and samples were kept at 56°C for 10 minutes. 200 µl 100% ethanol was added while vortexing. The two extracts (from CD4+CD25+ Treg cells and CD4+ T cells) were placed into two separate DNeasy Mini columns, placed into two collection tubes and centrifuged for 1 minute at 300 x G_{max}. After discarding the flow-through, 500µl of AW1 (wash buffer) was added into the spin columns and centrifuged for 1 minute at 300 x G_{max}. After discarding the flow-through, 500µl of AW2 (wash buffer) was then added into the spin columns and centrifuged for 3 minute at 500 x G_{max}. After discarding the flow-through the spin columns were placed into two DNALoBind tubes (Eppendorf 022431021), DNA was eluted by adding AE buffer to the column, incubated for 1 minute at room temperature, then centrifuged to recover genomic DNA (gDNA), which was kept at 4°C.

3.11.2. *Determination of DNA concentration*

3.11.2.1. Quant-iT picogreen dsDNA

DNA concentration was determined by using the Rotor-Gene 6000 and Quant-iT pico-green dsDNA Assay kit. Quant-iT Picogreen dsDNA reagent (Life Science Technologies) is an ultra-sensitive fluorescent nucleic acid stain for quantifying the amount of double-stranded DNA (dsDNA) present in a solution.

DNA was diluted in 1x TE (1:10 and 1:15). 6 DNA standards 2ng/µl; 1ng/µl 0.5ng/µl; 0.25ng/µl and 0.125ng/µl were made from a standard stock of 10ng/ul. 5 µl of diluted DNA was added to 5 µl of 1x florescent dye Pico-green (Life Science Technologies). Tubes were loaded into the Corbett Rotor-gene RG300A alongside the 6 dsDNA standards. The unknown DNA will evantually fall within the standard's range curve, giving us the amount of DNA. In the case the unknown DNA samples won't fall in the standard curve range, the samples were diluted again or diluted less from the original sample.

3.11.2.2. Nanodrop

DNA concentration was determined by Nanodrop (ND-1000; Nanodrop) spectrophotometry, measuring the absorbance of the DNA solution at 260nm. Typically, 1 µl of DNA in TE was placed on the Nanodrop optical fibre and the absorbance was measured against a blank of dH_2O. The 260nm/280nm ratio of absorbancies is a good indicator of protein contamination and a value of 1.5 or higher indicates reasonable purity of DNA. The Beer-Lambert equation is used to correlate absorbance with concentration ($A=\varepsilon*b*c$), where A is the measured absorbance, ε is the dependant molar absorbitivity coefficient with units of M^{-1} cm^{-1} , b is the path lenght and c is the analyte concentration[112].

3.11.3. *Bisulfite modification of DNA*

A bisulfite conversion reaction is required to investigate methylation patterns of gDNA. The method is based on the property of sodium bisulfite to selectively deaminate cytosine residues to uracil (Figure 14).

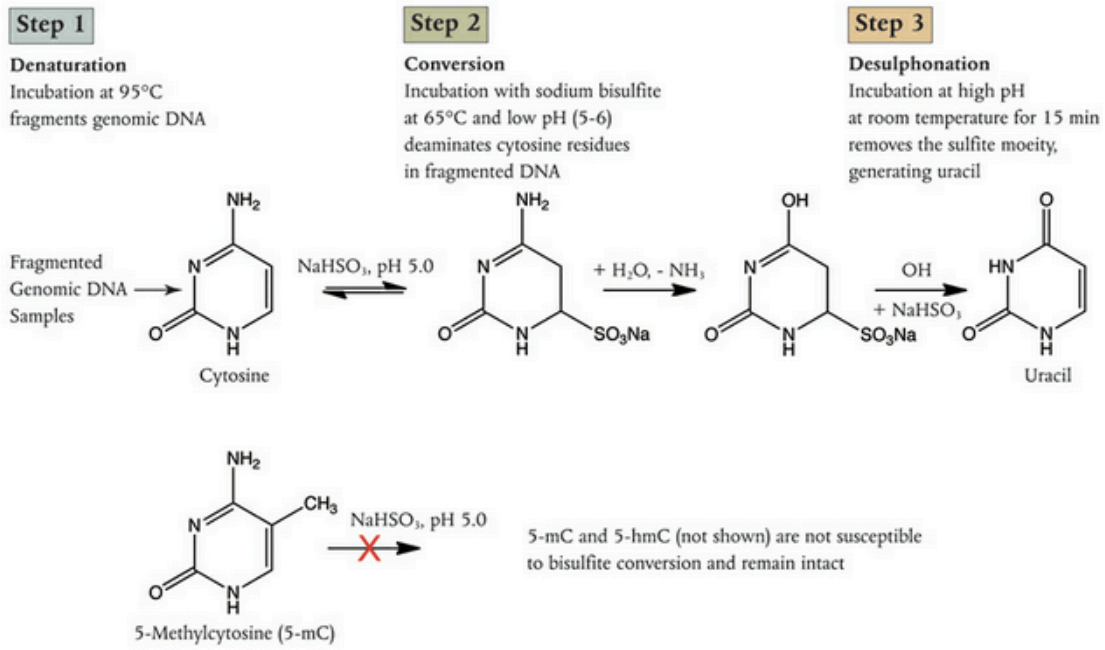


Figure 14 Overview of the bisulfite conversion. This figure displays the step to accomplish a bisulfite convertion. Step 1 – Denaturation, involves a reaction between cytosine and bisulfite, that leads to deamination (Step 2 – Conversion) at acid pH. Therefore, desulfonation at alkaline pH produces uracil (Step 3- Desulphonation). Figure adapted from *www.neb.com*

Because 5-methylcytosine (5-MeC) is not converted under these conditions, it is possible to distinguish between methylated and unmethylated cytosines[113] (Figure 15).

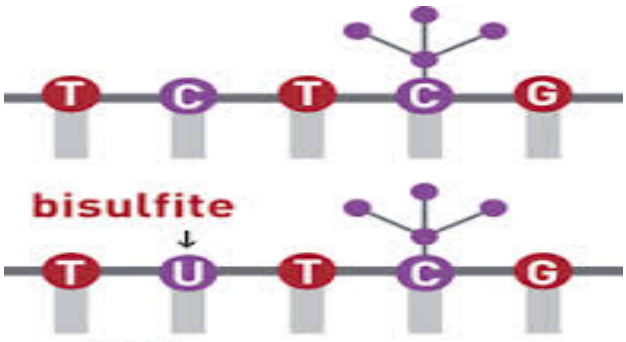


Figure 15. Conversion of cytosine. Bisulfite treatment converts cytosine residues to uracil, but leaves 5-methylcytosine residues unaffected. The 4 bubbles represent C and 3 H. Imagine adapted from https://www.diagenode.com/applications/dna-bisulfite-conversion.

The gDNA from T_{con}, Tregs and $CD3^+$ T cells was bisulfite converted using the EpiTect Bisulfite Kit (Qiagen). The samples were prepared by adding the Bisulfite mix and incubated in a PCR machine using the Bisulfite conversion program (Table 8).

Table 8 Bisulfite conversion thermal cycle condition

Step	Time	Temperature
Denaturation	5 min	95°C
Incubation	25 min	60°C
Denaturation	5 min	95°C
Incubation	85 min (1 h 25 min)	60°C
Denaturation	5 min	95°C
Incubation	175 min (2 h 55 min)	60°C
Hold	Indefinite*	20°C

Once the conversion was completed, samples were transferred into two separate 1.5 ml microcentrifuge tubes. A total of 310 µl of Buffer BL (Qiagen) containing 10µg/ml carrier RNA (Qiagen) was added to each sample. Samples were mixed by vortexing for 10 seconds. 250 µl of Ethanol (Sigma-Aldrich 100%) was added to each sample and mixed by vortexing for 15 seconds. The entire mixture from each tube was transferred into two separate MinElute DNA spin columns (Qiagen) placed in a collection tube. The two spin columns were centrifuged at maximum speed for 1 minute and the flow-through was discarded. A total of 500µl Buffer BW (Qiagen) was added to each spin column and centrifuged for 1 minute at 300 x G_{max} and the flowthrough was discarded. A total of 500 μ l Buffer BD (Qiagen) wad added to each spin column and left to incubate for 30 minutes at 37°C. Spin columns were centrifuged at 300 x G_{max} for 1 minute and the flow-through was discarded. A total of 550µl of Buffer BW was added to each spin column and centrifuged for 1 minute at 300 x G_{max} and the flow-through was discarded. A total of 250 µl of Ethanol (100%) was added to each sample and then centrifuged for 1 minute at 300 x G_{max}. Spin columns were placed into two new clean tubes and centrifuged for 1 minute at 300 x G_{max} to remove any residual liquid. Spin columns were placed into two DNALoBind tubes (Eppendorf). The gDNA was eluted by adding 20µl Buffer EB (Qiagen), incubated for 1 minutes at room temperature and centrifuged for 1 minute at 400 x G_{max}. The gDNA was kept at 4°C.

3.12. Polymerase chain reaction (PCR) and Quantitative Real Time PCR (qPCR)

3.12.1. *Polymerase chain reaction (PCR)*

3.12.1.1. Protocol

PCR with specific primers was conducted on converted gDNA to amplify specific regions using AccuPrime™ Taq DNA Polymerase High Fidelity (Invitrogen). Samples were prepared by adding 5 μl from the kit mentioned above (600 mM Tris-SO_4 (pH 8.9), 180 mM $(NH_4)_2SO_4$, 20 mM $MgSO_4$, 2 mM dGTP, 2 mM dATP, 2 mM dTTP, 2 mM dCTP, thermostable AccuPrime protein, 10% v/v glycerol), 10mM of primers (See table 3), 10 ng gDNA, 0.2μl Taq polymerase, HyClone molecular biology grade water (GE Healthcare) up to 50μl. PCR cycles consisted of denaturation, annealing and extension/elongation steps (Figure 16).

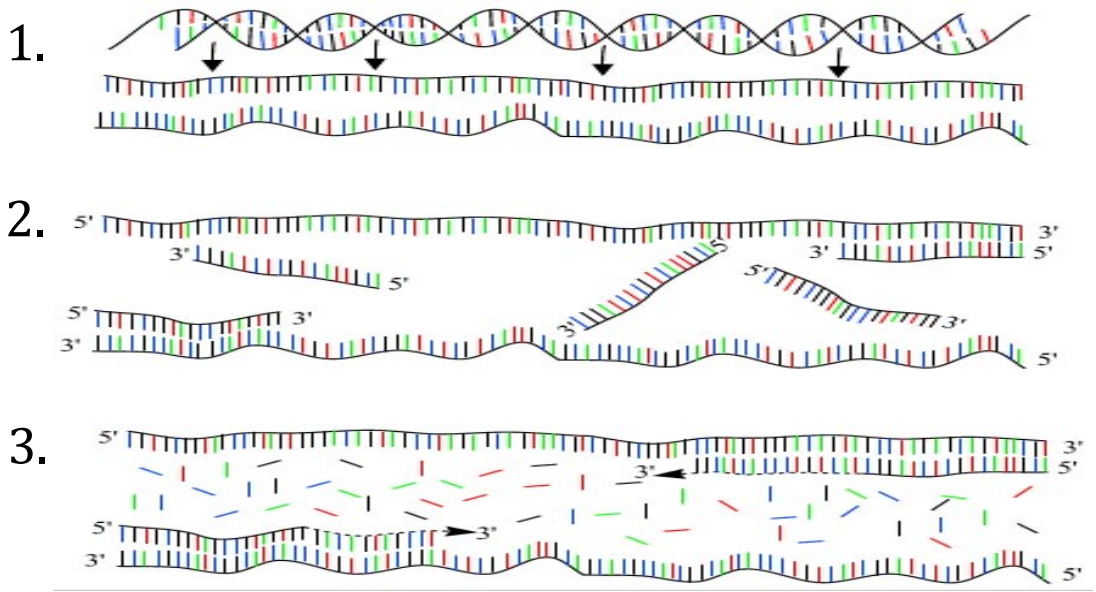


Figure 16 PCR method.1.Denaturation step: allow DNA to melt by disrupting hydrogen bonds between complementary bases.2. Annealing step: primers anneal to single strand DNA template; the polymerase binds to the primerstemplate and begins the DNA formation. 3.Extension/elongation step: DNA polymerase synthesized a new DNA strand complementary to the DNA template. From http://users.ugent.be/~avierstr/principles/pcr.html

The initial denaturation step was at 94ºC for 2 minutes. In addition, 40 cycles of denaturation step at 94ºC for 20 seconds, annealing step at 58°C for 40 seconds and elongation step at 68ºC for 1 minute were applied, according to the manifacturer. Samples were then kept at 4ºC.

3.12.2. *Quantitative real time PCR (qPCR)*

3.12.2.1. Overview

Quantitative real time PCR (qPCR) uses sequence detection methods to quantify amplification products after each cycle of the PCR. DNA binding dyes (SYBR green) can be used that only fluoresce when intercalated with double stranded DNA *i.e.* amplified PCR products. The fluorescence generated is directly proportional to the amount of amplified products and is measured after each cycle allowing product accumulation to be quantified. Quantification is achieved by reference to a standard curve generated using data from samples in which the copy number is already known (absolute quantification)[114].To control for variations in sample loading values are normalised to that of an endogenous control that is also quantified. In this study *GAPDH* was employed as control for normalisation.

Five different plasmids with *TSDR, CD3* bisulfite converted and unconverted sequences as insert and *GAPDH* unconverted sequence as insert (see 3.13 Plasmid) were used as standard curve samples. The plasmids were serially diluted in 0.1% (v/v) TE (Life Technologies) + tRNA (Life Technologies) to generate a 5 point standard curve, comprised of $12.5x10^3$, $2.5x10^3$, $0.5x10^3$, 100 and 20 copies/5μl.

qPCR was performed using a Rotor Gene 6000 (Corbett Lifescience). HotStarTaq Master Mix (Qiagen), which contains HotStarTaq DNA Polymerase, SYBR Green dye, PCR Buffer with 3 mM $MgCl_2$, and 400 μM of each dNTP was used for qPCR. qPCR was performed in a final volume of 10μl using HotStarTaq Master Mix (Qiagen); 1μM (final concentration) of bisulfite converted or non-converted *TSDR, CD3* and *GAPDH* specific forward and reverse primers (Table 4), 25 ng of bisulphite converted or non-converted genomic DNA and HyClone molecular biology grade water (GE Healthcare).

3.12.2.2. Protocol

Genomic DNA (bisulfite converted and non-converted) isolated from Tregs, T_{con} and CD3 cells, primers HotStarTaq Master Mix and water were thawed on ice for 2 hours. Assays (*CD3, GAPDH, TSDR* methylated, non methylated and non converted primers) and templates (Tregs, T_{con}, CD3 cells bisulfite converted and non converted, and water) were prepared using a metal rack in order not to activate the HotStarTaq DNA Polymerase.

qPCR conditions consisted of a 95°C pre-heating step for 1 minute and 40 cycles of 95° for 15 seconds and 61°C for 1 minute according to the manifacturer's instructions. Data were displayed using Rotor-Q Gene Software V2.0 (Qiagen).

3.12.3. *Oligodeoxynucleotides*

The following oligodeoxynucleotides [forward (fp), reverse (rp) primers] (IDT) were used to perform qPCR. They are indicated by chromosomal positions of human genome assembly GRCh37 (Ensemble Genome Browser release 56; September 2009) (Table 9).

Table 9. List of Primers used.

CD3G(ENSG00000160654)/CD3D(ENSG00000167286)		
CpG-specific	forward	5'-CTAAACACTACCACATCTCGA-3'
	reverse	5'AAATTTAGTTGTTACGGTTTGC-3'
TpG-specific	forward	5'-CCTAAACACTACCACATCTCAA-3'
	reverse	5'-AGAAATTTAGTTGTTATGGTTTGT-3'
non-converted	forward	5'-TGAACTTTAGCGTCCCTATTGAC -3'
	reverse	5'-TGAGAAAGATCAGCCTCCATG-3'
FOXP3(ENSG00000049768)		
CpG-specific	forward	5'-GTTTTCGATTTGTTTAGATTTTTTCGTT-3'
	reverse	5'-CCTCTTCTCTTCCTCCGTAATATCG-3'
TpG-specific	forward	5'-GTTTTTGATTTGTTTAGATTTTTTTGTT-3'
	reverse	5'-CCTCCTTCTCTTCCTCCATAATATCA-3'
non-converted	forward	5'-TTCAGAGCTAGGGGCTTGTC-3'
	reverse	5'-GGACACTTGGCCAGAGCTAA-3'
GAPDH(ENSG00000111640)		
TpG-specific	forward	5'-GGTTTTTGGTATTGTAGGTTTT-3'
	reverse	5'-CCAATTACAACATAACAACCA-3'
non-coverted	forward	5'-TTCTTTCCTTTCGCGTCTG-3'
	reverse	5'-AACGGCTGCCCATTCATTTC-3'

In this list, the primers to amplify FOXP3, CD3G/CD3D and GAPDH sequences are listed[45, 115].

3.13. Plasmid

A total of 2 plasmids, *TSDR* bisulfite converted and unconverted sequences cloned into 2.1-TOPO vector[115], used for this part of the project were provided by Prof C. Anisetti Department of Blood and Marrow Transplantation, Moffitt Cancer Center, Tampa, FL, United States. 3 additional plasmids (pUC57-Amp with GAPDH unconverted, CD3 unconverted and CD3 bisulfite converted sequences as insert) were provided by Genewiz.

3.13.1. *Transformation of Competent ECO k12*

Transformations were performed using ECO k12 competent cells (kindly given by Dr. Kevin Ford). 25μl of the cells was mixed with 10ng of plasmid and incubated on ice for 30 min. Reactions were then heat shocked at 37°C for 30 seconds and returned to the ice for further 5 min before adding 1ml of Luria-Bertani broth (LB) (Sigma) and incubating at 37°C in a waterbath for 1h, shaking every 10 mins. After centrifugation at 300 x G_{max} for 1 minute, the bacteria were decanted and the pellet was resuspended in 300μl of LB and streaked on LB (Sigma) agar plates containing carbenicillin (Sigma) at 50μl/ml and incubated at 37°C overnight.

3.13.2. *Miniprep extraction*

A single colony was picked from the plate and inoculated in 3ml LB plus 2μl of carbenicillin and cultured overnight at 37°C with shaking. Bacteria from a single colony were then pelleted at 400 x G_{max} for 10 minutes and plasmids were extracted using the QIAprep Spin Miniprep kit (Qiagen)

According to the manifacturer's protocol. Cells were resuspended in 250μl of Buffer P1 (Qiagen) before lysing with 250μl of Buffer P2 (Qiagen), after 5 mins the lysis reaction was stopped with 350μl of Buffer N3 (Qiagen). Protein precipitate was pelleted at 400 x G_{max} for 10 minutes and the supernatant was applied to the DNA binding columns and centrifuged at 400 x G_{max} for 1 minute. Columns were subsequently washed through with 750μl of Buffer PE (Qiagen) and centrifuged at 400 x G_{max} for 10 minutes to remove any residual

buffer. The plasmid DNA was eluted from the column with 50μl of Buffer EB (Qiagen). Plasmids were stored at -20°C.

3.13.3. *Restriction digests*

All restriction digests were performed in a total volume of 30 µl. The restriction reaction contained 3μl of 10X restriction enzyme buffer, 1μl of restriction enzyme (2000 units), 200 to 500ng of gDNA and distilled water to reach 30 µl final volume. All digestions were incubated for 2 hours at 37°C. The following table (Table 10) shows the combinations of enzymes and buffers used.

Table 10 Enzyme and buffer digestion

Enzyme	Buffer
TaqI	NEB 4
AseI	NEB 3
EcoR1	Cutsmart
MmeI	NEB 4
ClaI	NEB 4
SalI	NEB 3
XmaI	Cutsmart
SmaI	Cutsmart

This table displays the list of enzymes and buffers used to cleave target sequences.

Digested DNA was then separated by electrophoresis through an agarose gel.

3.13.4. *Agarose gel analysis*

DNA analysis was performed using agarose gel.1.5% to 2% (w/v) agarose (Sigma) was dissolved in 0.5x Tris-Acetate-EDTA buffer (TAE) buffer (Applichem) by boiling in a microwave oven. The intercalating agent Ethidium Bromide (Sigma) was added to a final concentration of 0.5 μg/ml after the agarose solution had cooled. The solution was then cast on a plastic tray that

contains a removable comb and allowed to cool down to room temperature. Usually 5 to 10 nanograms of DNA samples were loaded in the gel wells with a 6X Loading dye (Life Technology) and elecrophoresis was carried out at 95V (current <70mA). A UV transilluminator (GeneFlash, Syngene Bio Imaging) was used to visualise the DNA. The size of the DNA was determined by comparing with DNA markers (GeneRuler Life Technology) with known sizes as separated in the same gel.

3.13.5. *Fragment recovery*

DNA fragments that has been separeted by agarose gel electrophoresis and visualised using the UV transilluminator were isolated by cutting a slice of the gel with a scalpel. A gel extraction kit (QIAquick Gel Extracton Kit, Qiagen Cat Num 20704) was used to extract and purify the DNA. The manufacturer's instructions were used throughout. The gel extracted agarose fragment that contains the DNA of interest was mixed with 3 volumes of Buffer PBI, then incubated at 50^{o}C for 10 mins. Once the agarose slice was dissolved, the solution wa applied to a QIAquick spin column and centrifuged at 400 x G_{max} for 10 minutes. A total of 750μl of Buffer PE was added to the QIAquick column and then centrifuged 400 x G_{max} for 10 minutes. A total of 20μl of Buffer EB was applied to the column and incubated for 5 minutes at room temperature. The column was centrifuged 400 x G_{max} for 1 minute to recover the DNA fragment. DNA was then stored at -20^{o}C in a DNALoBind tube (Eppendorf).

3.14. Cytokine measurement

3.14.1. *Enzyme-linked immunosorbent assay (ELISA)*

Sandwich ELISA for different cytokines in Tcell supernatants was carried out in duplicate, regarding standard curves derived from known controls, using kits purchased from R&D systems. Optical density was measured with a Bio-tek EL800 automatic plate reader (Wolf Laboratories). The 96-well ELISA plates (brand) were coated with 100 µl/well of the appropriate capture antibody (4ug/ml) and incubated overnight at room temperature. Each well was washed three times with 400 µl/well of wash buffer (0.05% (v/v) Tween 20 in PBS, pH 7.2-7.4) at 300 x G_{max} for 10 minutes and blocked by 300 µl/well of blocking buffer (1% BSA in PBS with 0.05% NaN3) and incubated for an hour followed by three more washes, as described above. 100 µl of samples or standards were added to each well and incubated for 2 hours at room temperature followd by another three washes. The appropriate detection antibody (50ng/ml) was then added to the wells and incubated for another 2 hours. After three washes 100 µl of the working dilution of Streptavidin-Horseradish peroxidase (HRP) (R&D system) were added to each well, for labeling biotinylated-secondary antibodies, incubated for further 20 minutes in the dark, followed by three more washes. This step was repeated with 100 µl/well of Substrate Solution (1:1 mixture of Colour Reagent A (H_2O_2) and Colour Reagent B (Tetramethylbenzidine) R&D System). Then 50 µl/well of Stop Solution (2 NH_2SO_4 R&D System) were added to each well. The optical density of each well was immediately measured, using a microplate reader set to 450 nm.

3.14.2. *Cytokine Human 30-Plex Panel for the Luminex platform*

Multiple cytokine analysis of Tcell supernatants was carried out with a Cytokine 30-plex antibody kit (Invitrogen) and Luminex 100™ machine (Luminex Corporation). Invitrogen's Multiplex Bead Immunoassay is a solid phase protein assay which uses spectrally encoded antibody-conjugated

beads as the solid support. The assay was performed in a 96-well plate format and analysed with Luminex 100™ instrument which monitors the spectral properties of the associated fluorophore. A standard curve was prepared according to the protocol provided by Invitrogen by serial dilutions from the original stock (Figure 17).

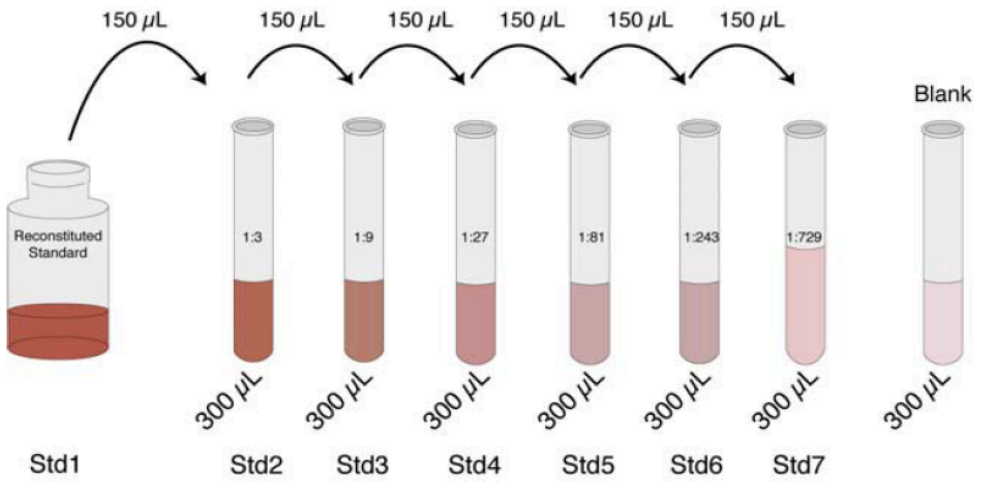


Figure 17 Preparing the standard curve. This figure shows the serial dilutions in order to have a standard curve.

Polystyrene beads were specific for:

1. Growth factor: HGF (Hepatocyte growth factor), FGF-Basic (Basic fibroblast growth factor), VEGF (Vascular endothelial growth factor) and EGF (Epidermal growth factor);
2. Chemokines: CCL11 (Eotaxin), IP-10 (Interferon gamma-induced protein 10), MCP-1 (Monocyte chemoattractant protein-1), MIG or CXCL9 (Monokine induced by gamma interferon), MIP-1α (macrophage inflammatory protein 1 alpha), MIP-1β (macrophage inflammatory protein 1 beta), RANTES (regulated on activation, normal T cell expressed and secreted);
3. Cytokines: IL-8 (Interleukin 8), IL-6 (Interleukin 6), IL-12 (p40/p70) (Interleukin 12 etherodimer 40 and 70), IL-13 (Interleukin 13), IL-2R (Interleukin 2 receptor), IFN-α (interferon alpha domain), IL-15 (Interleukin 15), IL-7 (Interleukin 7), G-CSF (Granulocyte-colony stimulating factor), IFN-γ (interferon gamma domain), GMCSF (Granulocyte-macrophage colony-stimulating factor), TNF-α (Tumor

necrosis factor alpha), IL-1β (Interleukin 1 beta), IL-2 (Interleukin 2), IL-4 (Interleukin 4), IL-5 (Interleukin 5), IL-1RA (Interleukin-1 receptor antagonist), IL-10 (Interleukin 10), IL-17 (Interleukin 17).

The 96-well plate was pre-wet by adding 150ul of washing solution (0.05% Tween 20 in PBS, pH 7.2- 7.4) and removed by aspiration through a filtered bottom microplate (Seahorse Bioscience). The aspiration was performed using a controlled vacuum. For the standards, a total of 25μl of the 30-Plex beads, 50μl of Assay diluent (Invitrogen) and, 100μl of appropriate standard dilution designated for the standard curve were added in the design well. For the samples assay diluent (Invitrogen) (50μl) and samples (50μl) were added to the designated wells. The plate was incubated for 2 hours at room temperature on an orbital shaker, covered by aluminium foil to protect it from the light. After incubation the wells were aspirated, followed by 2 washes with 200μl of wash buffer. 100μl of 1X Biotinylated Detector Antibody was added to each well and incubated for 1 hour at room temperature. After the incubation, the plate was again washed twice with 200μl of washing solution and then aspirated. 100μl of 1X Streptavidin-RPE (Invitrogen) was added to each well and incubated for 30 minutes and then washed 3 times as before. 100μl of working wash solution was added to the well and gently agitated for 3 minutes. The samples were analysed using the Luminex 200 machine. Raw data were investigated through Luminex xPONENT software in order to measure the amount of cytokines.

3.14.3. *Cytometric Bead Array (CBA)*

The BD CBA[116] assay was intended for the simultaneous quantification of multiple soluble analytes (multiplex) from a single serum, plasma or tissue culture supernatant sample. After flow cytometry acquisition, the data were analysed in the BD FCAP array analysis software.

Lyophilized standard spheres from each flex set that will be tested was pooled in one 15ml tube. 400μl of Assay Diluent to a final concentration of 25.000.000 fg/ml was reconstituted, mixed with the pipette and left for 15 minutes at room temperature. 8 FACS tubes were prepared and labeled starting from Std08 to

Std01. We then prepared standards by serial dilutions (Table 11) of the top standard (dilution 1:3) mixing thoroughly by pipetting gently up and down and using a new tip each time.

Table 11 Standard's serial dilutions

Std	08	07	06	05	04	03	02	01
Dilution	Top standard	1/3	1/9	1/27	1/81	1/243	1/729	none
Microliters	4 (stock Std) + 496 (assay diluent)	50 + 100	50 + 100	50 + 100	50 + 100	50 + 100	50 + 100	100 (assay diluent only)
Fg/ml	200000	66667	22222	7407	2469	823	274	0

The table above shows the serial dilutions to have standards.

The number of flex sets to be used in the experiment was determined and this was the number of analytes to be quantified. The number of tests in the experiment: 8 standards + number of test samples + 2 extra (for pipetting losses) was determined.

The volume of diluted beads required for the experiment was determined. The stock bottles of capture beads were 20x concentrated and were diluted for the assay. Each test required 15µl of diluted beads. 0.25 µl of each stock capture bead per test was used.

For 11 tests and 2 analytes to be measured:

- 11 tests x 15 µl diluted beads per test= 165 µl total volume of diluted beads
- 165 – (11 x 0.25 µl beads) x 2 = 165 – (2.75 µl beads) x 2 = 159.5 µl capture beads diluent.
- 2.75 µl of each capture bead

New FACS tubes (enough for 8 standards plus the test samples) were prepared.

15 µl of the ‘capture beads mixture’ was added to all tubes then 15 µl of the standards and test samples were added to each tube as it corresponds and then incubated for 2 hours at room temperature in the dark.

The exact same calculations made for the capture beads mixture was applied for the detection reagent (part A) preparation. Therefore, for example for 11 tests and 2 analytes to be measured the detection reagent (part A) will consist of:

- 159.5 µl detection reagent diluent.
- 2.75 µl of each detection reagent stock bottle

Detection reagent (part A) was mixed in bottle by pipetting up and down right before adding them to the mixture. The detection reagent (part A) was added first followed by the detection reagent diluent into a polypropylene FACS tube labeled as 'Detection reagent (part A)' and stored at 4°C until it was required. Then, the lyophilized enhanced sensitivity detection reagent (part B) was reconstituted with 550µl of detection reagent diluent, mixed by pipetting and incubated for 15 min at room temperature. A total 4.5ml of detection reagent diluent was added to a new 15-ml conical tube. A total of 500µl of the reconstituted enhanced sensitivity 'Detection reagent (part B)' was transferred to the conical tube and vortexed. Once the first incubation (2 hours) has been completed, 15 µl of the 'Detection reagent (part A)' was added to all tubes and incubated for 2 hours at RT. Once the second incubation (2 hours) has been completed, 250µl of Wash Buffer was added to each tube and centrifuged at 200 x G_{max} for 5 minutes. Supernatant was aspirated. A total of 25µl of enhanced sensitivity 'Detection reagent (part B)' was added to each tube and incubated for 1 hour at RT. 250µl of Wash Buffer was added to each tube and centrifuged at 200 x G_{max} for 5 minutes. Supernatant was aspirated. A total of 200µl of Wash Buffer was added to each tube and vortexd. Samples were ready for flow cytometry analysis. Raw data were then analysed using FACS capture array analysis software (FCAP). The software is able to report fluorescence with the known concentrations of the standards to enable quantitative analysis of the analytes in our unknown samples.

3.15. Methylome 450k array

The Human Methylome of the samples was studied using the HumanMethylation450 BeadChip (Illumina Infinium) (Figure 18) which was carried out in the Department of Respiratory Medicine and Allergy, Division of Asthma, Allergy and Lung Biology, King's College London. The Infinium methylation assay uses beads displaying target specific probes designed to interrogate individual CpG sites within a DNA sample. This technique employs two types of assay: Infinium I and Infinium II to enhance the extent of coverage. In the Infinium I assay two bead types per CpG locus were used. Each probe is designed to match either the protected cytosine (methylated) or the thymine base (unmethylated). In the Infinium II assay only one bead that was designed for the methylated state was used, in this case the probe complements the base directly upstream of the query site given a G or A base complementary to either the "methylated" C or "unmethylated" T[117].

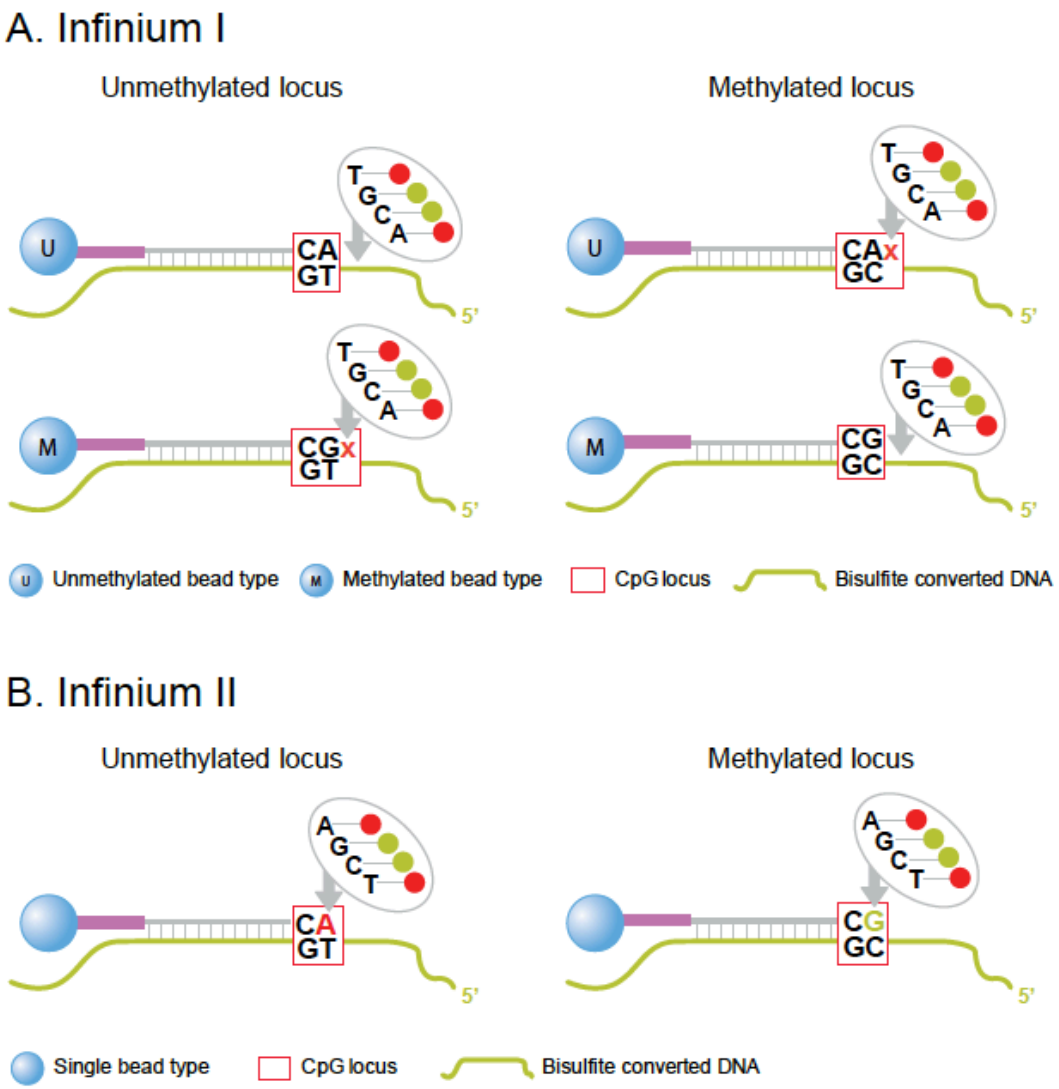


Figure 18. Broader Coverage Using Infinium I and II Assay Designs. The Figure above shows the workflow of the HumanMethylation450 BeadChip, that consists of 2 sections: Infinium I and Infinium II. Figure adapted from *www.Illumina.com*

A total of 150ng of gDNA from the samples were bisulfite converted as described in section 3.9.3. Samples were then processed through HumanMethylation450 BeadChip assay. Raw data were investigated using R software.

3.16. Statistical analysis

Statistical analysis was performed using Prims GraphPad software version 6 or SPSS version 22. The mean value and the standard error of the mean (SEM) were used as statistical analyses of the experiments where the $CD4^+$ T cell population was employed. The purpose was to have an estimation of the population mean and to provide the interval in which the population mean was likely to fall, respectively. If needed data were first tested to determine whether or not they are normally distributed (based on their mean, mode and median). One-way Anova followed by Bonferroni's multiple comparison tests were used to compare more than 2 sets of non-parametric data. T test followed by Mann Whitney's multiple comparison test were used to compare 2 sets of non-parametric data. Error bars are standard error of the mean. Significance was set at $p < 0.05$.

Legend for data p values: **** $p<0.0001$, *** $p<0.001$, ** $p<0.01$, * $p<0.05$.

4. Function and cytokine profile of 5AzaC treated T_{con}

4.1. Introduction

The focus of this Chapter is to investigate the function and cytokine profile of "Treg-like" cells (TrLCs) which are polarised by culturing T_{con} (CD4+CD25-) with 5AzaC, as described in Chapter 4 section 2.1.1. We wanted to investigate whether this subpopulation was still T_{con} or whether it polarised into another population (*e.g.* Tregs or Tregs secreting IL-17). To do so we studied their cell surface protein phenotype, cytokine secretion and function and compared these TrLCs with untouched Tregs and T_{con}. In addition, we wanted to determine whether we could polarise Tregs into IL-17 secreting Tregs by culturing Tregs *in-vitro* with IL-1β, IL-6 and IL-2 (see section 2.1.2) as shown before[118, 119]. Then, we wanted to compare the differences in terms of function between TrLCs and the polarised IL-17 secreting Tregs.

This Chapter addresses the following questions:

1. Are T_{con} after 5AzaC treatment still T_{con} or are they similar to Tregs?
2. Is *FOXP3* expressed by TrLCs?
3. Are TrLCs functional and can they suppress T_{con} cells?
4. How different are TrLCs and Tregs from those IL-17 secreting Tregsthat polarised *in-vitro* by IL-1β, IL-6 and IL-2, in terms of function and cytokine secretion?

4.2. Materials and Methods

This section provides a description of the variation of the materials and methods described in Chapter 3. For canonical protocols, reagents and materials see Chapter 3.

4.2.1. Cell Culture and Proliferation assay

4.2.1.1. 5AzaC culture

Culture with 5-Aza-2-deoxycytidine (2 μM 5AzaC Celgene) or Dimethyl sulfoxide as vehicle (2 μL/ml DMSO, Sigma) was carried out in a 48-well cell culture plate (Cellstar) ($1x10^6$ cells each well) with 1ml/well X-Vivo media (Lonza) or a 96-well cell culture plate (Cellstar) ($0.5x10^6$ to $0.25x10^6$ cells each well) with 500μL/well X-Vivo. 5AzaC was dissolved in DMSO, therefore the same volume of DMSO was added to separate wells as a control. T_{con} and Tregs were isolated using magnetic beads (material and methods, Chapter 3). Culture conditions were as follows: control (no stimulation, no drugs), with 2μM 5AzaC, with μL/ml DMSO, Tregs:T_{con} (1:1 ratio) with 2μM 5AzaC, Tregs:T_{con} (1:1 ratio) with μL/ml DMSO. In all the conditions, except for the controls, cells were stimulated with 10 μL/$1x10^6$ cells anti-CD3/CD28 expander beads (Dynabeads Human T-activator, Invitrogen ratio 1:15). Cultured cells were initially stimulated for 24 hours. 5AzaC or DMSO were added to the culture on days 2 to 5 and cells were harvested for further analysis on day 6. Because of the abundant stimulation induced by the beads, at day 8 magnetic beads were removed using a magnetic plate and cells were left in culture overnight to rest. At day 9, 2μL /ml Leukocyte Activation Cocktail with BD Golgi Plug (BD Pharmingen) was added and incubated for 4 hours according to the manufacturer's instructions at 37°C in the 5% CO_2 Incubator (240i HERACell ThermoScientific) (Figure 19). Cells were harvested as follows: the X-Vivo media containing the cells was transferred to a 15ml tube, then centrifuged at 270 x G_{max} for 10 minutes and the media was removed. The centrifugation step and removal of media was repeated twice. The cell pellet was finally resuspended in 100 μl of PBS. Cells were then ready to be

stained for intracellular and surface proteins and analysed using flow cytometry.

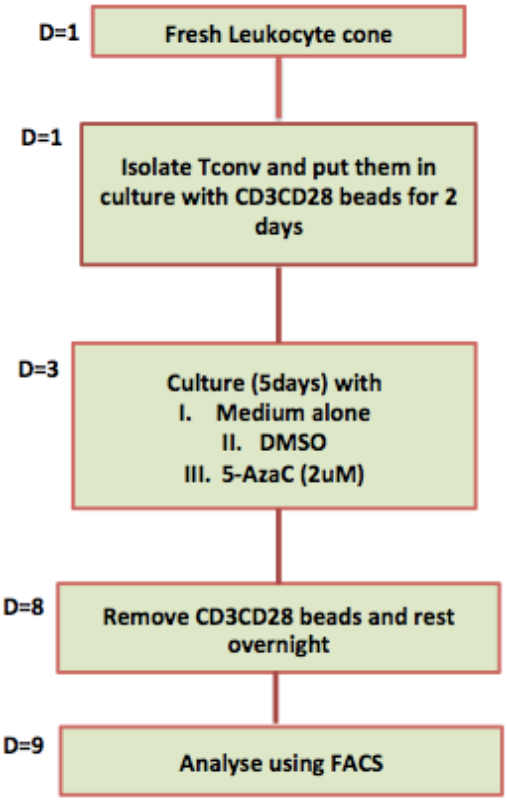


Figure 19. 5AzaC culture workflow. This diagram explains the timing of cell culture. On the first day (D=1) Tregs and T_{con} were isolated from PB of HDs, then usually 0.25 x 10^6 were cultured *in vitro* for 2 days with or without (+/-) stimulation using anti-CD3/CD28 expander beads (ratio 1:15). On day 3 (D=3) 5AzaC or DMSO were added every day for 5 days. On day 8 (D=8) anti-CD3/CD28 expander beads were removed from the culture. Cells were rested overnight and the day after (D=9) were analysed by flow cytometry using surface and intracellular protein's antibodies (Table 7).

4.2.1.2. Treg polarisation

Culture with IL-1β, IL-6 and IL-2 cytokines was carried out in a 48-well cell culture plate (Cellstar) (1x10^6 cells each well) with 1ml/well X-Vivo or a 96-well cell culture plate (Cellstar) (0.5x10^6 to 0.25x10^6 cells each well) with 500ul/well X-Vivo. Tregs were isolated using magnetic beads (see Chapter 3 section 2.4.2.). Cells were treated as follows: stimulated (CD3/CD28 beads ratio 1:15) + IL-1β 10ng/ml + IL-6 25ng/ml + IL-2 10 IU/ml. All the conditions, except for the controls, were stimulated with 4 μL/1x10^6 cells anti-CD3/CD28 expander beads (Dynabeads Human T-activator, Invitrogen ratio 1:15).

Experiments were set up for 7 days. After the 6th day anti-CD3/CD28 expander beads were removed with a magnetic plate and cells were given rest overnight at 37°C in the 5% CO_2 incubator. On the 7th day, cells were prepared by adding a total of 2μL /ml of Leukocyte Activation Cocktail, with BD GolgiPlug inhibitor (LAC) (BD, 550583) per 1ml of cell suspension and incubated for 4 hours at 37^{o}C, 5% CO_2 incubator. This cocktail was able to elicit a primary cytokine response from T cells. Cytokines were produced and then localised in the rough endoplasmic reticulum of the cells due to the Brefeldin A (a protein transport inhibitor component) that blocks intracellular protein transport processes. The accumulation of cytokine proteins enhanced the detectability of cytokine-producing cells.

Cells were harvested and analysed at day 7 (Figure 20).

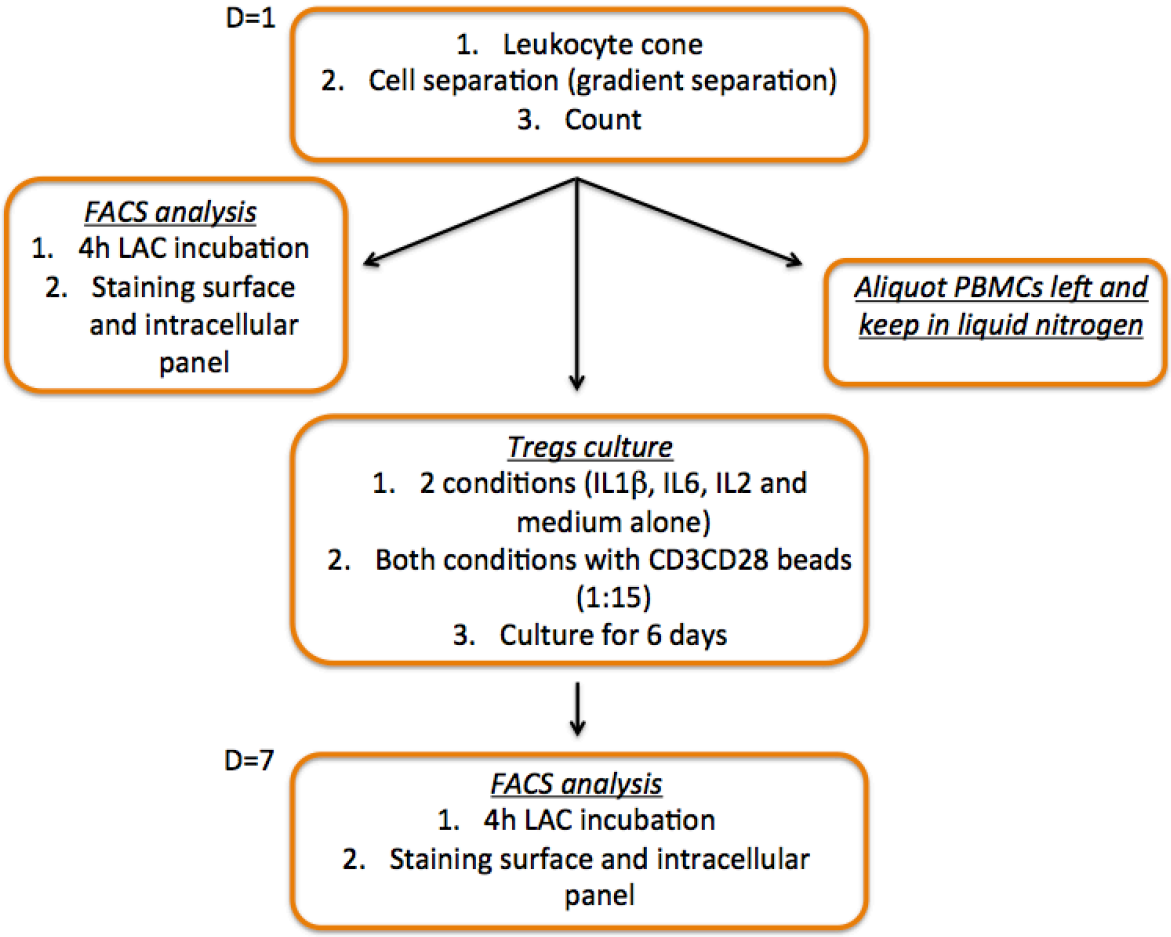


Figure 20. IL-1β, IL-6, IL-2 culture workflow. This diagram shows the timing of cell culture. On the first day (D=1) cells inside the leukocyte cone were gradient separated using "Ficol-Paque" solution (See Chapter 3 section 2.1). PBMC were counted. Aliquots of the PBMC were cryopreserved in liquid nitrogen for further any use (See "Aliquot" in Figure 2). Tregs were isolated from PBMCs of HDs, then usually 0.12 x 10^6 were cultured with or without (+/-) stimulation using anti-CD3/CD28 expander beads and (+/-) IL-1β 10ng/ml + IL-6 25ng/ml + IL-2 10 IU/ml for 6 days. On day 7 (D=7) cells were incubated with leukocyte activation complex (LAC) then cells were stained for cytokines, cellular and intracellular proteins and analysed using FACS.

4.2.1.3. Cell Proliferation assay

Proliferation assays were carried out after the culture with 5AzaC explained above. In this assay 300x10^6 PBMCs from the same donor were kept in liquid nitrogen until day 8. T_{con} isolated from PBMCs were cultured under the following conditions: CD3/CD8 proliferation beads with 2μM 5AzaC, CD3/CD8 proliferation beads with 2 μL/ml DMSO. At day 8 the proliferation beads were removed from the culture using a magnetic washer (Bio Plex, Handheld magnetic washer, BioRad) and cells were kept at 37°C over night in the 5%

CO_2 incubator. At day 9, PBMCs kept in liquid nitrogen from the same donor were thawed. T_{con} and Tregs were isolated from the PBMCs as described in Chapter 3. T_{con} were stained with the Cell Trace Proliferation Dye (Violet Proliferation Dye, VPD, Invitrogen) and co-cultured with the T_{con} (ratio 1:1) (+/- 5AzaC) from the 5AzaC culture assay (Figure 21).

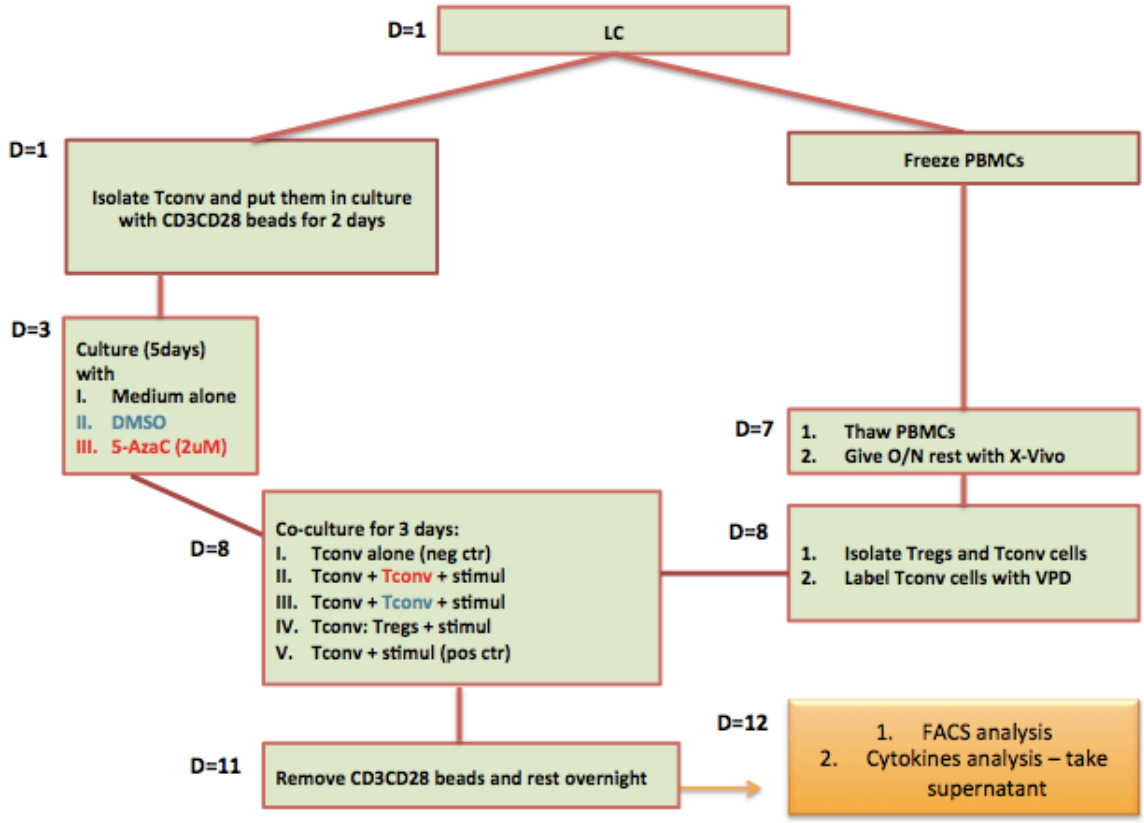


Figure 21. Proliferation assay workflow. This diagram explains the timing of the proliferation assay. On the first day (D=1) T_{con} were isolated from a leukocyte cone (LC) of PB of HDs, then usually 1 x 10^6 were put in culture with or without (+/-) stimulation using anti-CD3/CD28 expander beads for 2 days. On day 3 (D=3) 5AzaC or DMSO were added every day for 5 days. On day 8 (D=8) anti-CD3/CD28 expander beads were removed from the culture in the early morning. In the meanwhile, Tregs and T_{con} were isolated from PBMCs previously isolated from the same LC and stored in liquid nitrogen. Isolated T_{con} were stained with proliferating dye (Violet Proliferating Dye- VPD) and put in co-culture with the T_{con} treated with DMSO or 5AzaC and with Tregs. In the evening, anti-CD3/CD28 expander beads ("stimul" in the figure) were added to the culture. Cells were cultured for 3 days under the following conditions: T_{con} alone ("neg ctr" stands for negative control), stained VPD T_{con} co-cultured with 5AzaC treated T_{con}, stained VPD T_{con} co-cultured with DMSO treated T_{con}, stained VPD T_{con} co-cultured with Tregs, T_{con} stimulated with CD3CD28 ("pos ctr" stands for positive control). On day 11 (D=11) anti-CD3/CD28 expander beads were removed using a magnetic plate and cells were cultured overnight at 37°C. The next morning supernatants were kept being investigated and cells were stained and analysed using FACS.

Cells were cultured for an additional 3 days, harvested at day 12 and analysed by FACS in order to analyse the relative abundance of surface and intracellular proteins and cytokines (Table 7).

The same protocol was applied to Tregs cultured *in vitro* with IL-1β, IL-6 and IL-2.

4.2.2. Staining for surface and intracellular protein markers

The antibodies previously described (see Chapter 3 section 5.1 and 5.2) were used for cellular and intracellular staining (Table 7) according to the manufacturer's instructions, following 4 hours of incubation with LAC.

Data from cells were acquired and analysed using a FACS Canto II or FACS Fortessa flow cytometer running the FACSDiva software (BD Bioscience). The gating strategy was based first on the physical parameters such as cell granularity or internal complexity (Side Scatter SSC) and cell surface area or size (Forward Scatter FSC). Correlated measurements of SSC and FSC can allow for differentiation of single cell types and to exclude debris, clumps and doublets in a heterogeneous cell population. Discrimination between viable and non-viable cells was determined using Live/Dead dye (L/D dye) (See Chapter 3 section 4) (Figure 22).

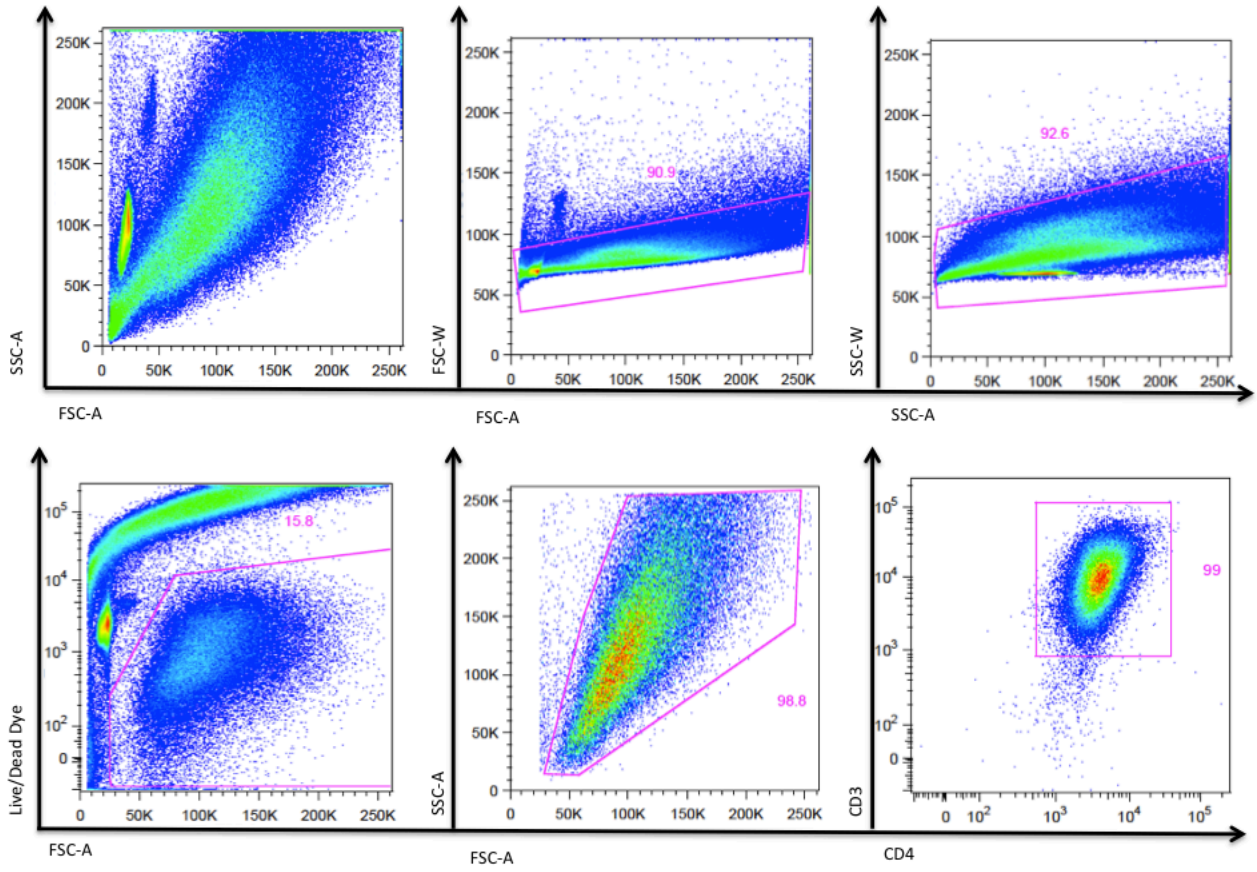


Figure 22. Gating strategy workflow. In this example, cells were first gated based on physical parameters (Forward Scatter Width FSC-W vs Forward Scatter Area FSC-A and Side Scatter Width SSC-W vs Side Scatter Area SSC-A) in order to exclude doublets. The lymphocyte gate is then analysed based on Live/Dead staining dye to determine viable versus non-viable cells (Live_Dead 780 vs FSC-A). CD3+CD4+ cells were then determined from the viable cells using $CD3^{+}CD4^{+}$ markers (CD3 APC vs CD4 V500).

4.2.3. Cytokine measurement

Cytokine measurements were carried out using a Cytokine 30-plex antibody kit or a CBA assay according to the manufacturer's instructions (See Chapter 3 section 14).

4.2.4. Statistical analysis

Statistical analysis was performed using Prims GraphPad software version 6 or SPSS version 22. Data were first tested to determine whether they are normally distributed (based on their mean, mode and median). One-way Anova followed by Bonferroni's multiple comparison tests were used to

compare more than 2 sets of non-parametric data. T test followed by Mann Whitney's multiple comparison test were used to compare 2 sets of non-parametric data. Error bars are standard error of the mean. Significance was set at $p < 0.05$.

Legend for data p values: **** $p<0.0001$, *** $p<0.001$, ** $p<0.01$, * $p<0.05$

4.3. Results

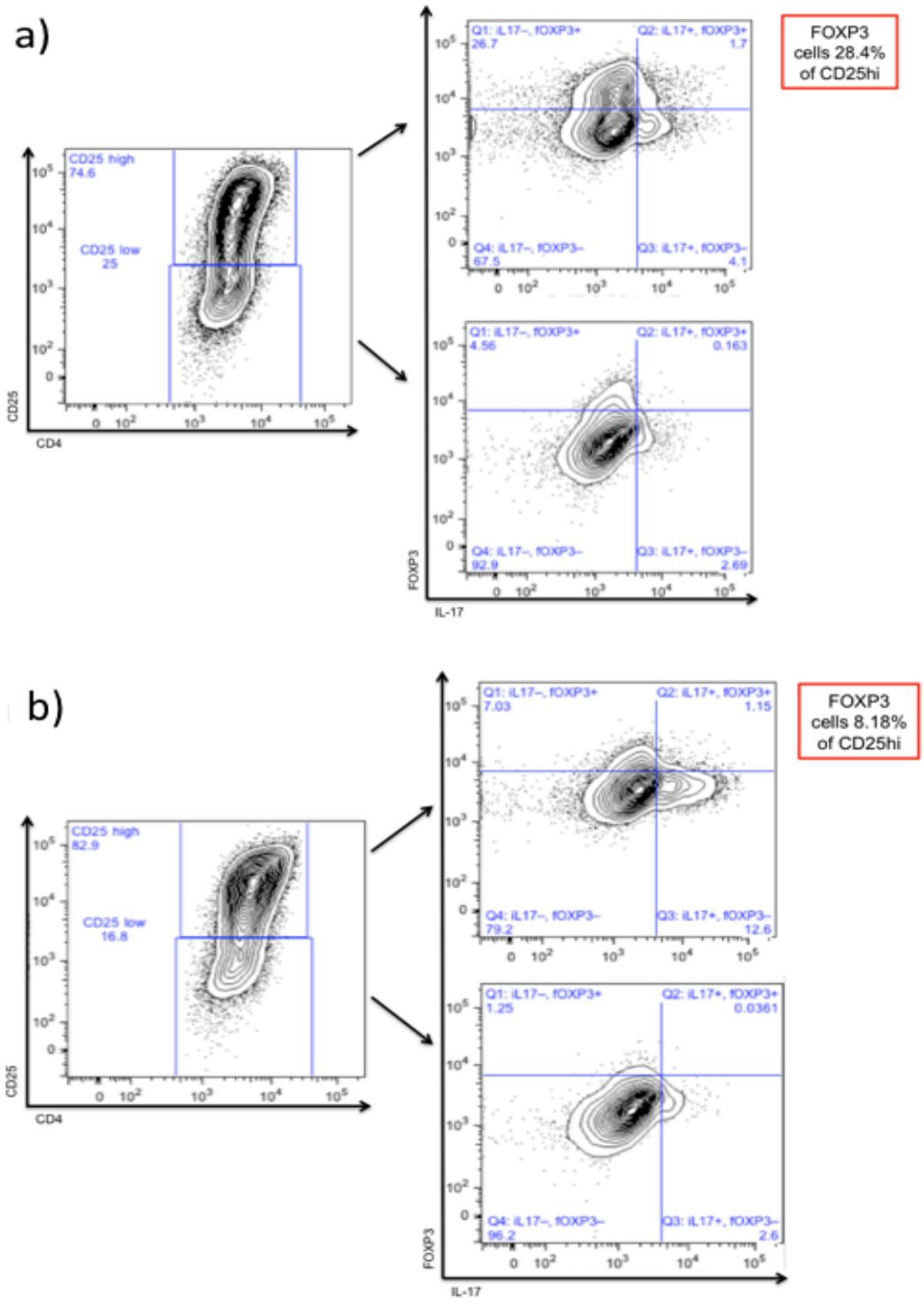
4.3.1. Function and FOXP3 expression by 5AzaC treated T_{con} cells

The following questions were investigated in this section:

1. Are T_{con} after 5AzaC treatment still T_{con} or are they similar to Tregs ?
2. *FOXP3* expression by TrLCs?

Through this section, we wanted to confirm whether T_{con} cultured with 5AzaC, so called TrLCs, expressing Tregs profile markers or they were close to another CD4+ population. In order to characterise the "Treg-like" cells, flow cytometry was used to identify cellular and intracellular proteins and the expression of cytokines.

We cultured T_{con} with 5AzaC, with DMSO and in medium alone (See section 2.1.1 of this current Chapter and Figure 19) and then we analysed the expression of the targeted markers using flow cytometry. A clear increase of FOXP3 expression occurred in T_{con} stimulated with anti-CD3/CD28 expander beads and treated with 5AzaC from HDs (28.4 % $FOXP3^+$ cells) (Figure 23, a), as compared with T_{con} stimulated with anti-CD3/CD28 expander beads and treated with DMSO (8.1% $FOXP3^+$ cells) (Figure 23, b). Figure 23 is a representative example of 10 independent experiments using cells isolated from 10 different donors.


a)
CD25 high
74.6
CD25 low
25
CD25
CD4
Q1: iL17−, fOXP3+
26.7
Q2: iL17+, fOXP3+
1.7
Q4: iL17−, fOXP3−
67.5
Q3: iL17+, fOXP3−
4.1
Q1: iL17−, fOXP3+
4.56
Q2: iL17+, fOXP3+
0.163
Q4: iL17−, fOXP3−
92.9
Q3: iL17+, fOXP3−
2.69
FOXP3
IL-17
FOXP3 cells 28.4% of CD25hi
b)
CD25 high
82.9
CD25 low
16.8
CD25
CD4
Q1: iL17−, fOXP3+
7.03
Q2: iL17+, fOXP3+
1.15
Q4: iL17−, fOXP3−
79.2
Q3: iL17+, fOXP3−
12.6
Q1: iL17−, fOXP3+
1.25
Q2: iL17+, fOXP3+
0.0361
Q4: iL17−, fOXP3−
96.2
Q3: iL17+, fOXP3−
2.6
FOXP3
IL-17
FOXP3 cells 8.18% of CD25hi

c)

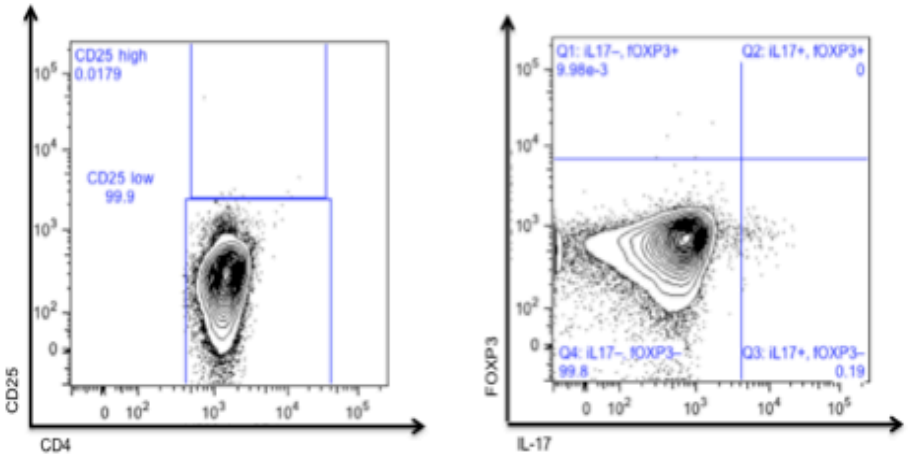


Figure 23. FOXP3+ cells in T_{con}. The figure above shows the flow cytometry plots from T_{con} from HDs following the $CD3^+CD4^+$ gating step (Chapter 4 section 3.2) to detect % of $FOXP3^+$ cells. Figure a) T_{con} treated with 5AzaC and stimulated with CD3/CD28 beads. 28.4% of FOXP3+ cells were detected in cells that expressed a high level of CD25 (from CD25hi). Figure b) T_{con} stimulated with anti-CD3/CD28 expander beads and treated with DMSO. 8.18% of FOXP3+ cells in CD25hi. Figure c) T_{con} not stimulated with low CD25 expression. 0% of FOXP3+ cells in CD25hi. This figure is a representative example of 10 independent experiments using cells isolated from 10 different donors.

The overall percentage of $FOXP3^+$ cells was higher in T_{con} after 5AzaC treatment as compared with both T_{con} after DMSO and T_{con} not stimulated (n=10) (18.9 % ±12 *vs* 8.1 % ±3.8 & 0.1 % ±1.5, $p<0.0001$) (Figure 24).

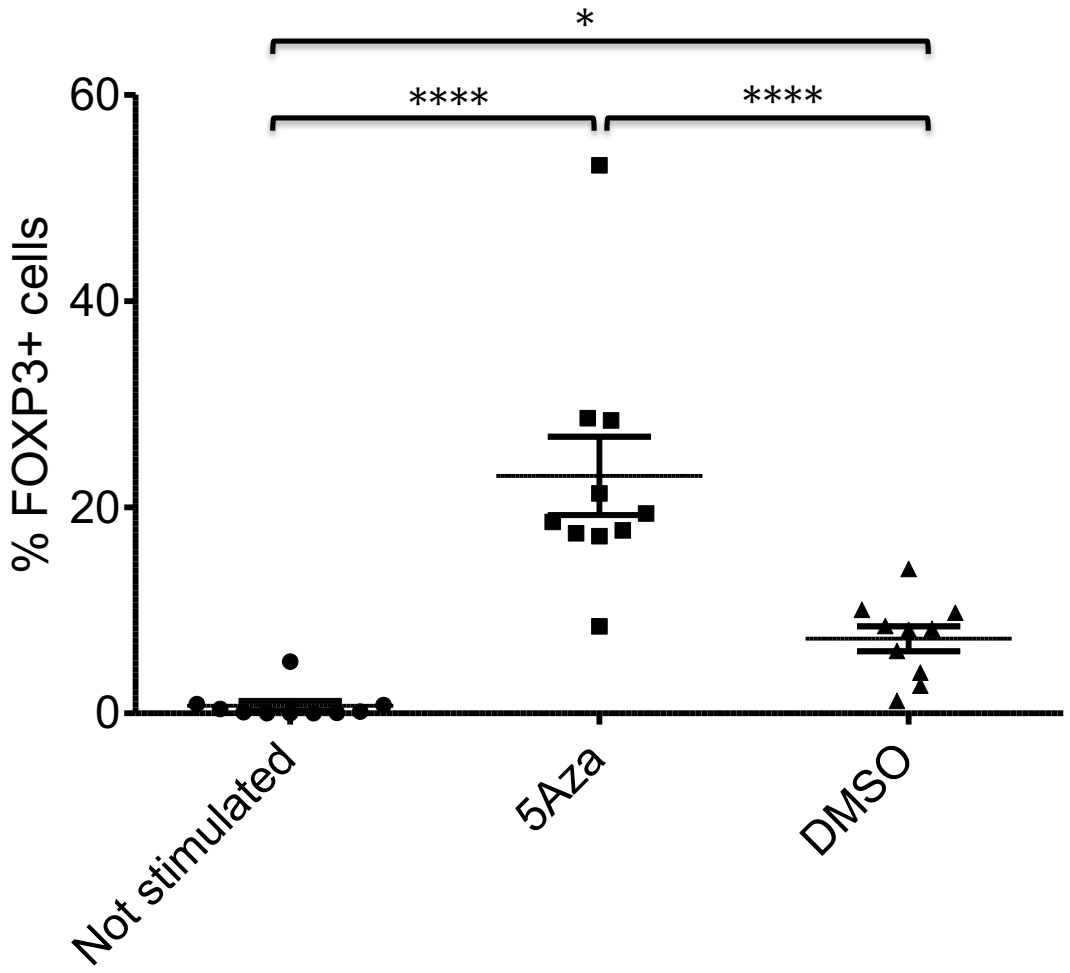


Figure 24. Percentage of FOXP3$^+$ cells. This figure represents the median of 10 experiments from 10 different donors. The percentage of *FOXP3*+ cells was higher in "5Aza" treated cells compared with "DMSO" treated cells and "Not stimulated" cells. Data were analysed using one-way ANOVA followed by Bonferroni's multiple comparison test. Error bars are standard error of the mean. Significance was set at $p < 0.05$. Legend for data *p* values: **** $p<0.0001$, *** $p<0.001$, ** $p<0.01$, * $p<0.05$

In addition to the percentage of FOXP3 expression, we have also determined whether there was an increase in the percentage of IL-17 secreting cells after 5AzaC treatment as compared with T_{con} after DMSO treatment. The percentage of FOXP3+IL-17+ cells was investigated after 5AzaC treatment and there was an increased expression of IL-17 in 5AzaC treated T_{con} as compared with T_{con} treated with DMSO (n=10) (1.5 % ±1 versus 0.1 % ±0.3, *p<0.0001*) (Figure 25).

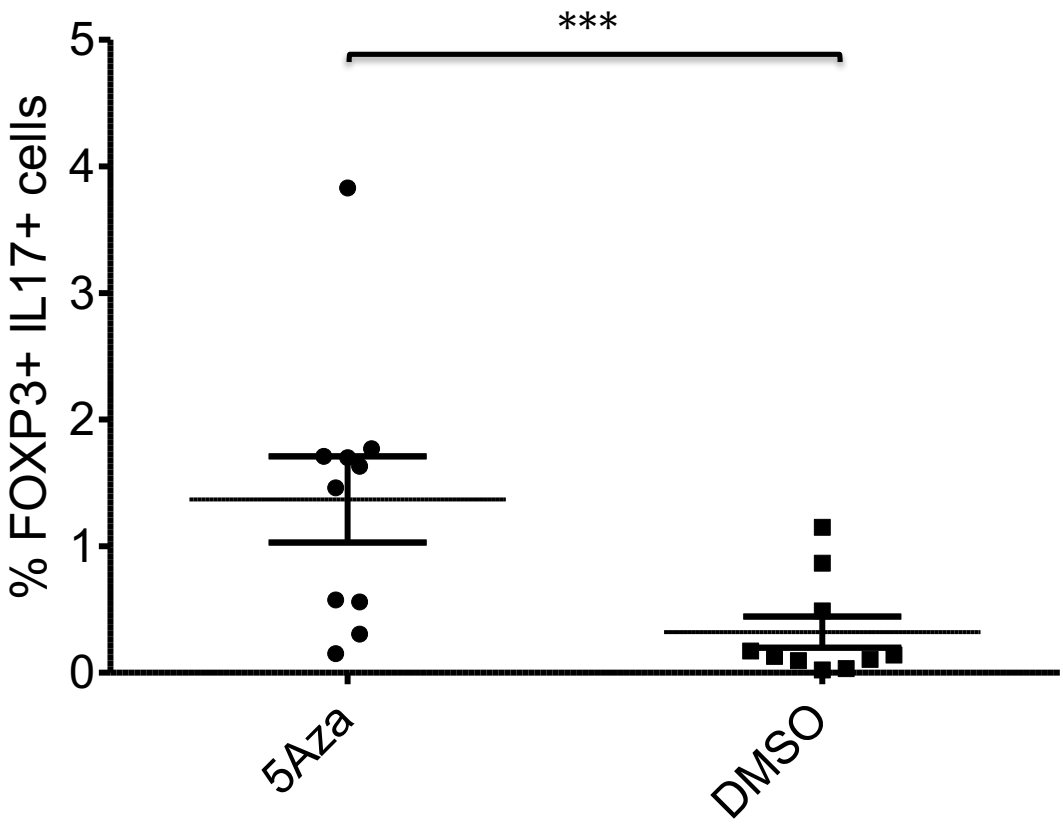


Figure 25. Percentage of FOXP3$^+$IL-17$^+$ cells. This figure represents the data from the 10 cultures mentioned above. In this plot, the percentage of FOXP3+ IL-17$^+$ cells was higher in "5Aza" treated cells compared with "DMSO" treated cells. Raw data were analysed using paired *t* test followed by Mann Whitney's multiple comparison test. Error bars are standard error of the mean. Significance was set at $p < 0.05$. Legend for data p values: **** p<0.0001, *** p<0.001, ** p<0.01, * p<0.05

4.3.2. Functional analysis of T_{con} after 5AzaC treatment.

The following question was investigated in this section:

1. Are TrLCs functional and can they suppress T_{con} cells?

A proliferation assay was performed to establish whether the TrLCs after 5AzaC treatment were able to suppress autologous T_{con}, a characteristic of Treg cells. TrLCs were stained with Violet Proliferation Dye (VPD, BD biosciences) and proliferation was assessed using flow cytometry. The VPD is a fluorescent dye that binds to any cellular proteins containing primary amines and as cells divide, the dye is distributed equally between daughter cells. Co-culture of 5AzaC treated T_{con} from HDs with autologous T_{con} displayed lack of suppressive function (51.7 % cells had divided) as compared with control that were Tregs co-cultured with T_{con} (13.4 % cells had divided) (Figure 26). Figure

8 is a representative example of 3 independent experiments from 3 different donors. The overall percentage of cell proliferation, at the end of the experiment, has increased in T_{con} treated with 5AzaC and T_{con} with stimulation (positive control) as compared with Tregs cultured with T_{con} and T_{con} without stimulation (negative control) (n=3) (31.8 % ±13.44 & 58.75 % ±5.30 *vs* 9.84% ±6.43 & 0.75% ±5.3, *p*=0.0002) (Figure 27).

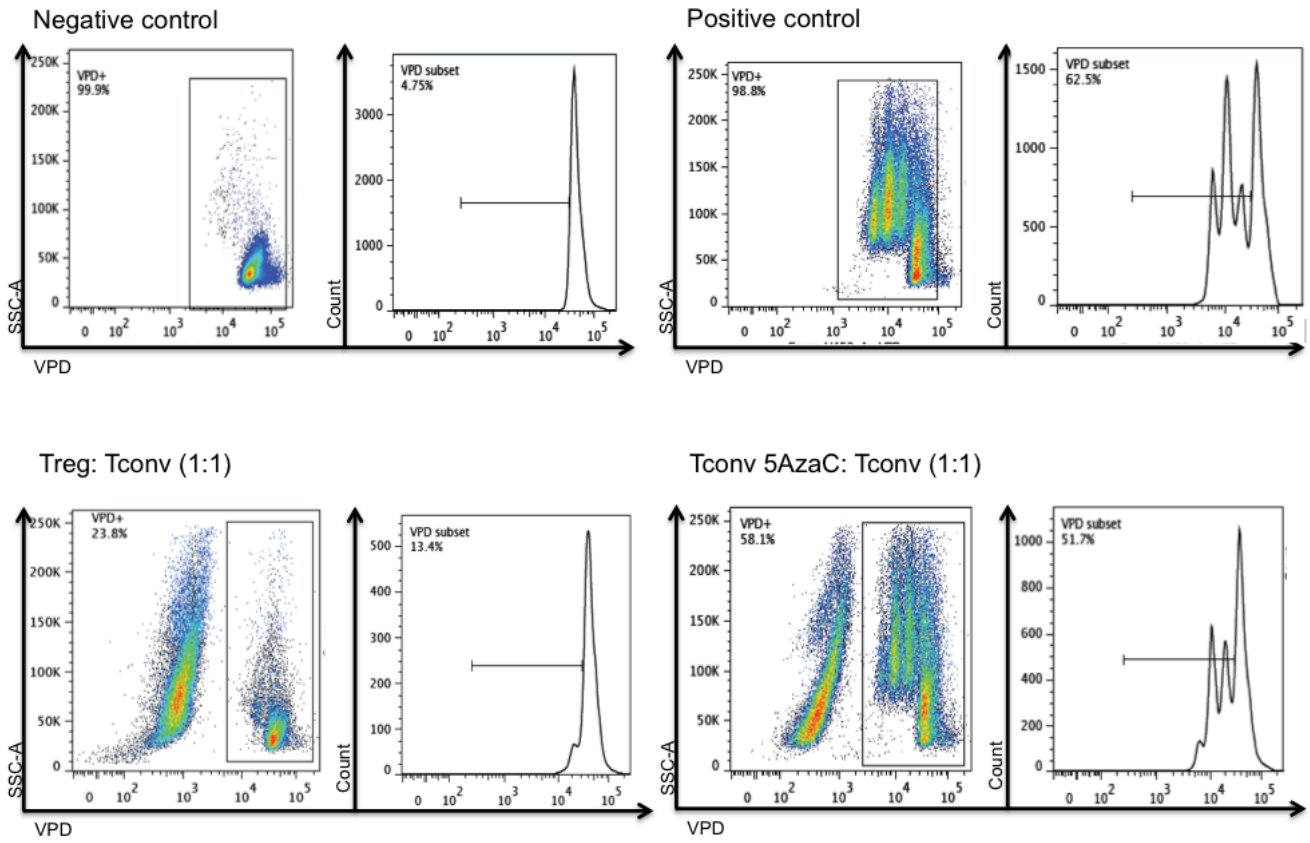


Figure 26. Proliferation assay 5AzaC treated T_{con}. This figure is a representative example of 3 independent experiments using cells isolated from 3 different donors. T_{con} without stimulation (Control -) and Tregs in co-culture with autologous T_{con} with stimulation (Treg:T_{con} 1:1 ratio) displayed less proliferation than T_{con} with stimulation (Control +) and T_{con} stimulated treated with 5AzaC in co-culture with autologous T_{con} (Tcon 5AzaC: T_{con} 1:1 ratio). Autologous T_{con} were stained with a violet fluorescent dye (VPD) that is used to monitor individual cell divisions. Every division is a peak in the graph, from right to left.

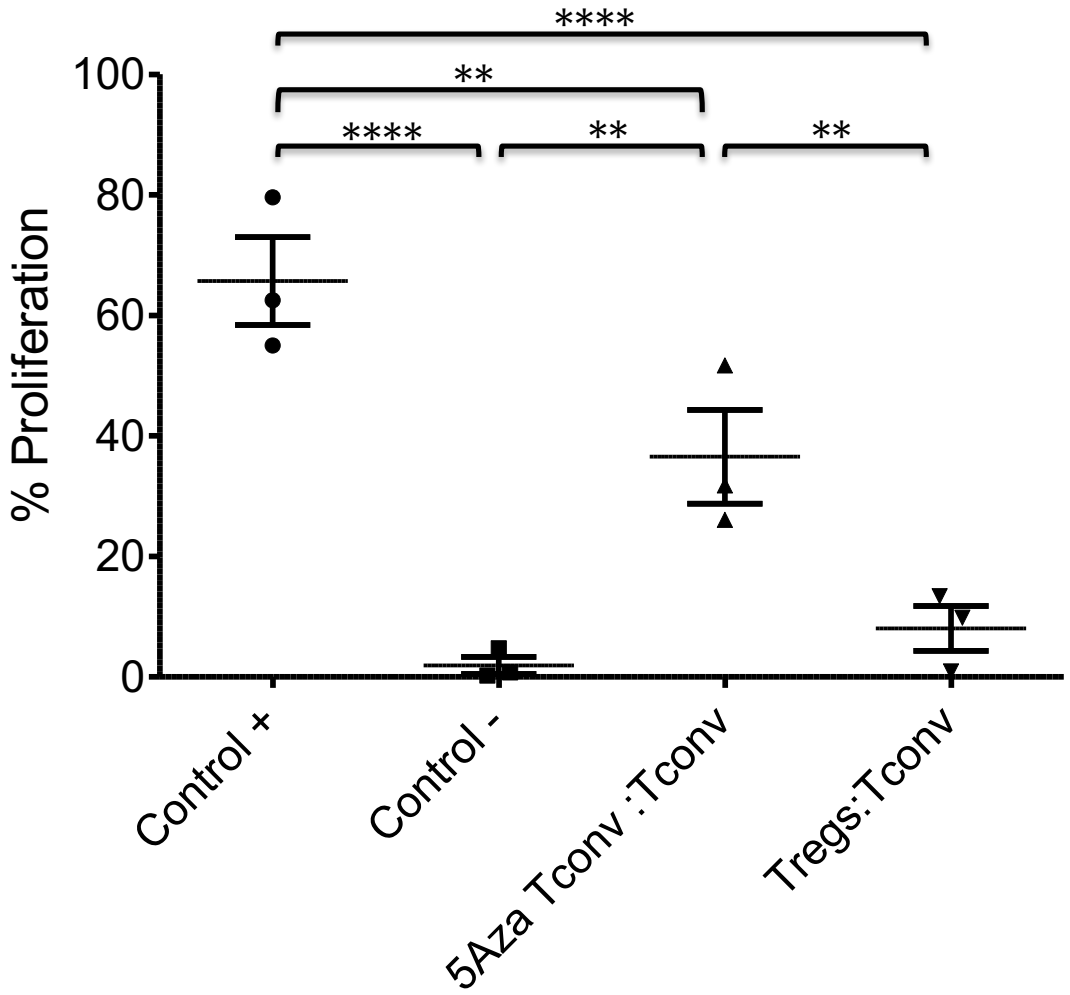


Figure 27. Proliferation assay 5AzaC treated T_{con}. This figure shows the percentage of cell proliferation of 3 independent experiments. The first condition is T_{con} with CD3/CD28 stimulation (Control +). The second is T_{con} without stimulation (Control -). The third condition is T_{con} stimulated with CD3/CD28 and treated with 5AzaC in co-culture with autologous T_{con} (Tcon 5AzaC: T_{con} 1:1 ratio). The fourth is Tregs in co-culture with autologous T_{con} with CD3/CD28 stimulation (Treg:T_{con} 1:1 ratio). Raw data were analysed using one-way ANOVA followed by Bonferroni's multiple comparison test. Error bars are standard error of the mean. Significance was set at $p < 0.05$. Legend for data p values: **** p<0.0001, *** p<0.001, ** p<0.01, * p<0.05.

Results from this section suggested that although TrLCs were able to suppress autologous T_{con}, their suppressive function is significantly lower compared with Tregs in co-culture with autologous T_{con}. The conclusion is that TrLCs are unlikely to be Tregs.

4.3.3. Cytokine concentration analysis

The following question was investigated in this section:

1. How different are TrLCs and Tregs, which are polarised *in-vitro* by IL-1β, IL-6 and IL-2 in terms of cytokine secretion?

The concentration of proinflammatory cytokines in the supernatant was investigated using Luminex and CBA assays. Levels of IFN-γ, IL-10, IL-17A, IL-1β, IL2 and TNF-α were measured using a multiplex array technique. Once the proliferation assay procedure was ended supernatants were taken and analysed. T_{con} co-cultured with autologous Tregs shows no significant difference in the level of IL-10, IL1 β, IL-2, and IL-17A as compared with T_{con} treated with 5AzaC and put in co-culture with autologous T_{con}. Interestingly, the level of IFN-γ increased in T_{con} treated with 5AzaC and put in co-culture with autologous T_{con} as compared with T_{con} co-cultured with autologous Tregs (n=3) (mean 462.3 pg/ml *vs* 407.5 pg/ml) (Figure 28).

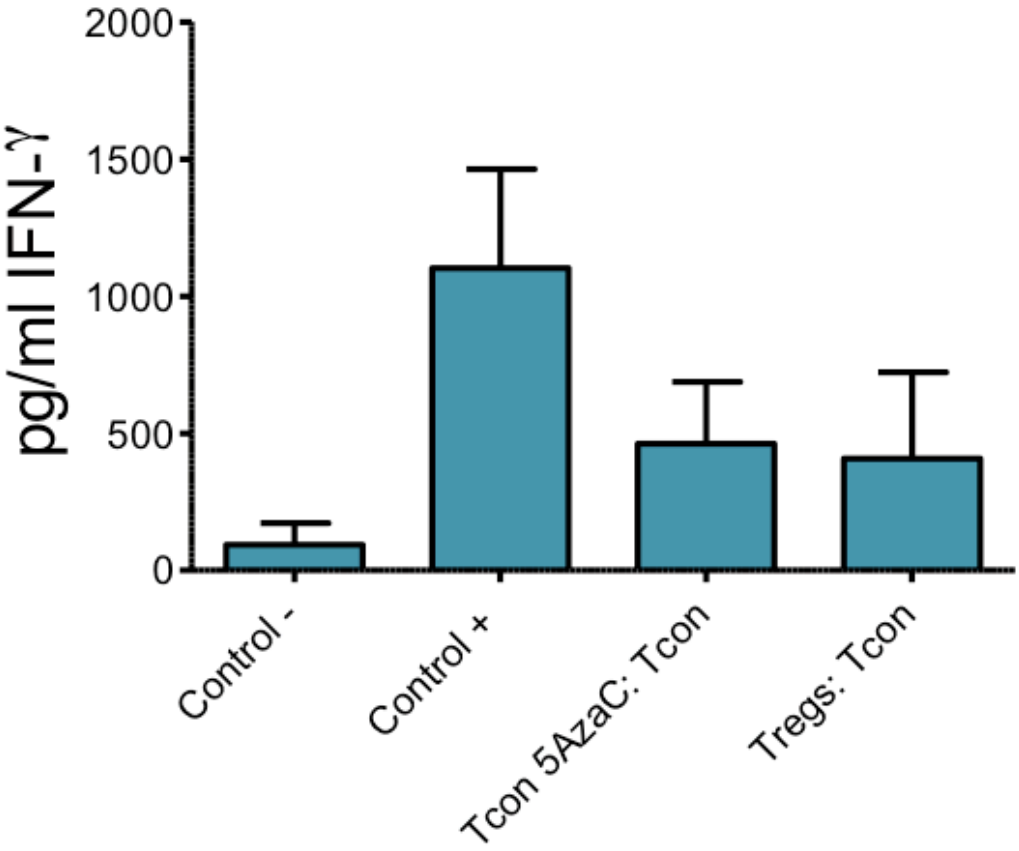


Figure 28. INF-γ measurement. This figure represents the pg/ml of INF-γ detected in the supernatant of the following conditions: T_{con} stimulated (anti-CD3/CD28 expander beads) (Control +), T_{con} not stimulated (Control -), T_{con} stimulated (anti-CD3/CD28 expander beads) and treated with 5AzaC in co-culture with autologous T_{con} (5AzaC T_{con}: T_{con} 1:1 ratio) and T_{con} stimulated and treated with autologous Tregs (Tregs: T_{con} 1:1 ratio). Data were analysed using one-way ANOVA (p=0.145) followed by Bonferroni's multiple comparison test. Error bars are standard error of the mean. Significance was set at $p < 0.05$.

In addition, the level of TNF-α increased in T_{con} treated with 5AzaC and put in co-culture with autologous T_{con} as compared with T_{con} co-cultured with autologous Tregs (n=3) (mean 1084 pg/ml *vs* 563.3 pg/ml) (Figure 29).

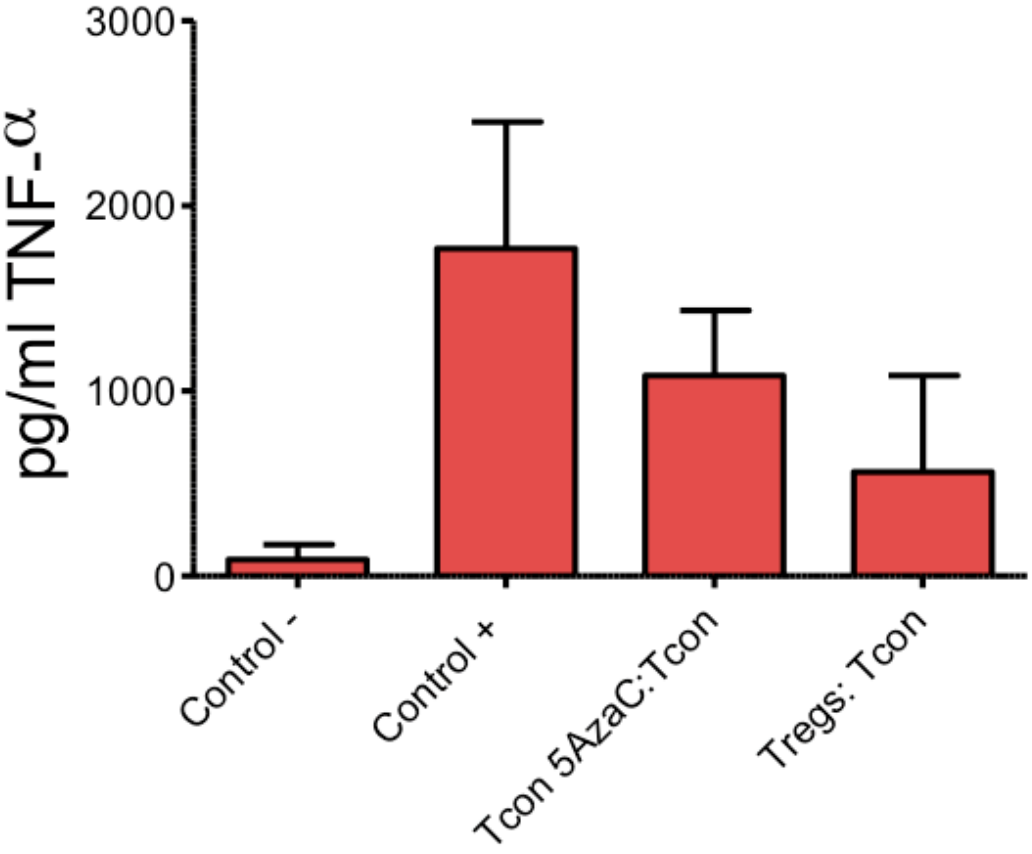


Figure 29. TNF-α measurement. This figure represents the concentration (pg/ml) of TNF-α found in the supernatant of the following conditions: T_{con} stimulated (anti-CD3/CD28 expander beads) (Control +), T_{con} not stimulated (Control -), T_{con} stimulated (anti-CD3/CD28 expander beads) and treated with 5AzaC in co-culture with autologous T_{con} (5AzaC T_{con}: T_{con} 1:1 ratio) and T_{con} stimulated and treated with autologous Tregs (Tregs: T_{con} 1:1 ratio). Data were analysed using one-way ANOVA (*p=0.161*) followed by Bonferroni's multiple comparison test (*p=ns)*. Error bars are standard error of the mean. Significance was set at $p < 0.05$

The results of this section suggest that, although both TrLCs and Tregs reduce the production of TNF-α and IFN-γ (pg/ml) compared with the positive control, secretion of TNF-α and IFN-γ (pg/ml) was higher in TrLCs compare with Tregs.

4.3.4. Tregs: polarisation and functional analysis

Although secretion of IL-17 occurred in TrLCs, assessed by measuring the percentage of IL-17 secreting cells after 5AzaC treatment using flow

cytometry (see section 3.1 of this current Chapter), we wanted to determine whether T_{con} after 5AzaC treatment are the same as IL-17 secreting Tregs.

The following question was investigated in this section:

1. Is the function of TrLCs and Tregs, which are, polarised *in-vitro* by IL-1β, IL-6 and IL-2 the same?

In order to answer this question, we determined whether we were able to polarise Tregs into IL-17 secreting Tregs by culturing Tregs *in-vitro* with IL-1β, IL-6 and IL-2 (see section 2.1.2 of this current Chapter), as shown before[118, 119]. Then, we analysed the functions of TrLCs and the polarised IL-17 secreting Tregs.

A clear increase in the percentage of $FOXP3^+$ $IL\text{-}17^+$ cells was seen in the Tregs stimulated with anti-CD3/CD28 expander beads co-cultured with IL-1β, IL-6 and IL-2 cytokines (3.1 %) as compared with Tregs stimulated with anti CD3/CD28 expander beads (0.56%) from HDs (Figure 30) (see section 2.1.2. for culture protocol).

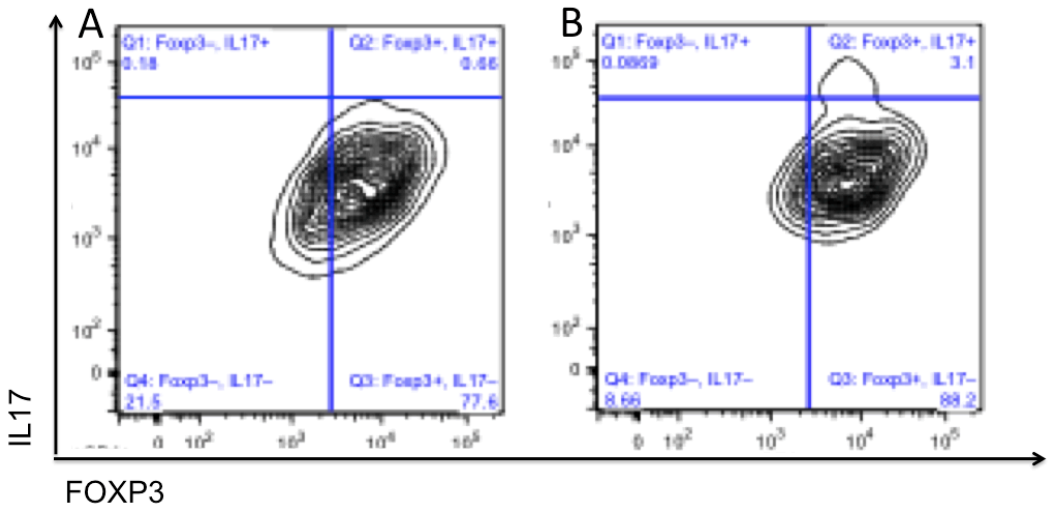


Figure 30. FOXP3$^+$IL-17$^+$ cells. This figure is a representative example of 3 independent experiments using cells isolated from 3 different donors. Cells were gated based on CD25 and CD4 (See Chapter 4 section 3.2. Flow cytometry Fig 4), then on FOXP3 and IL-17. Figure A: Tregs stimulated with anti-CD3/CD28 expander beads. Figure B: Tregs stimulated with anti-CD3/CD28 expander beads and cultured with IL-1 β , IL-6 and IL-2 cytokines.

The data were analysed using one way ANOVA followed by Bonferroni's multiple comparison test, which shows that the overall percentage of *FOXP3*+ IL-17+ cells is increased in the Tregs stimulated with anti-CD3/CD28

expander beads co-cultured in a Th-17 polarising environment (IL-1β, IL-6 and IL-2 cytokines) as compared with Tregs stimulated with anti-CD3/CD28 expander beads and the Tregs at baseline from HDs (n=3) (3.1 % ±6.67 versus 1.16 % ±2.54 & 0.02% ±0.02) (Figure 31). Thus, following *in-vitro* culture of Tregs with IL-1β, IL-6 and IL-2 cytokines, our data demonstrate Tregs are polarised into IL-17 secreting Tregs.

Then we performed a proliferation assay using these IL-17 secreting Tregs whether they were able to suppress T_{con} in order then to be compared with TrLCs proliferation assay. We compared the results with the data from the proliferation assay of TrLCs derived from T_{con} treated with 5AzaC, in order to assess whether TrLCs are still T_{con} or whether they are polarised into IL-17 secreting Tregs.

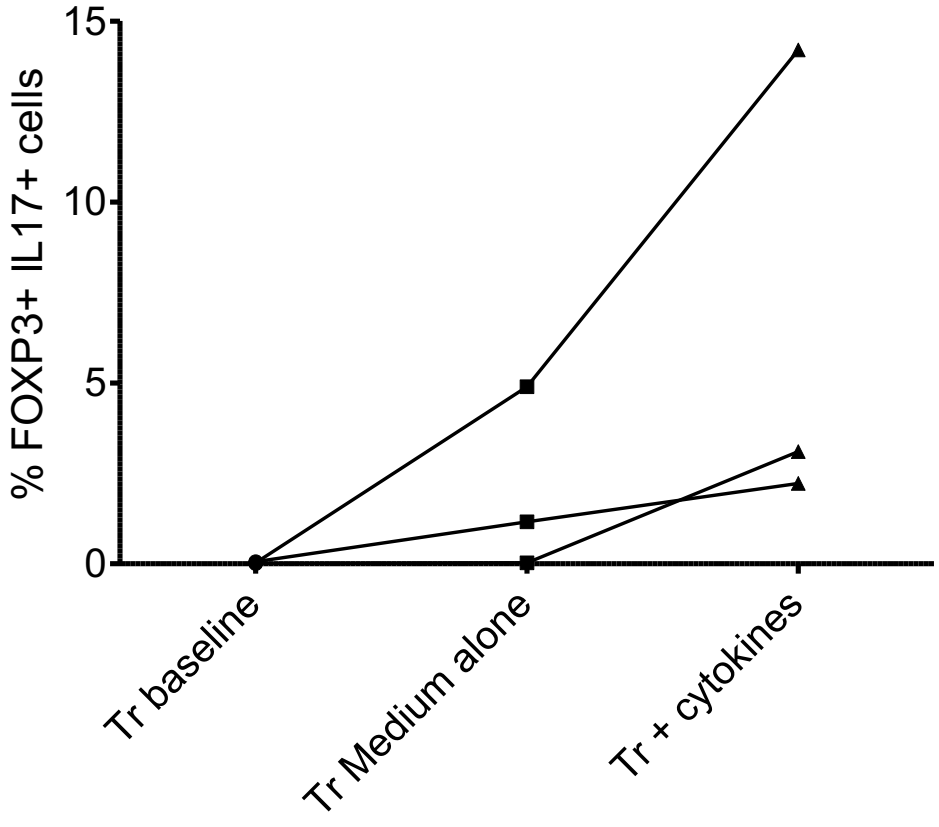


Figure 31. Percentage of FOXP3$^+$ IL-17$^+$ cells. Percentage of FOXP3$^+$ IL-17$^+$ cells for Tregs stimulated with anti-CD3/CD28 expander beads and the addition of with IL-1 β , IL-6 and IL-2 cytokines and Tregs at baseline as compared with stimulated Tregs (without cytokines) (n=3). Data were analysed using one-way ANOVA followed by Bonferroni's multiple comparison test

Co-culture (1:1 ratio) of IL-17 secreting Tregs from HDs with autologous T_{con} demonstrated a suppressive function (1.88 % cells divided) as well as Tregs cultured with autologous T_{con} (1:1) (2.65 % cells divided) (Figure 32).

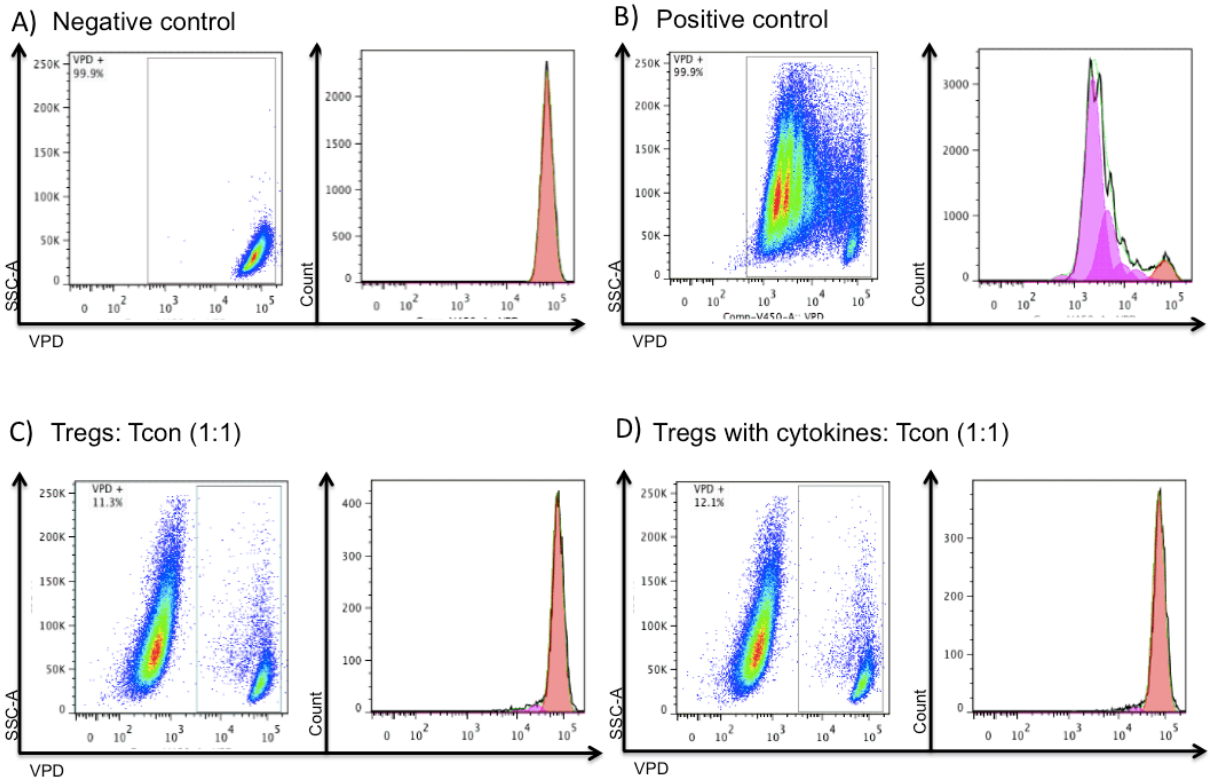


Figure 32. Proliferation assay of Tregs secreting IL-17 cells.

The following cell types were stained with the proliferation dye (VPD) for 3 days in culture (Figure 3) and the percentage of cells that divide during this period was analysed by flow cytometry VPD was used to monitor individual cell divisions. Every division is a peak in the graph. This figure is a representative example of 3 independent experiments of 3 different donors. A) $T_{con,}$ not stimulated (Negative control). B) T_{con} stimulated with anti-CD3/CD28 expander beads (Positive control). C) Tregs in co-culture with autologous T_{con} with stimulation (anti-CD3/CD28 expander beads) (Tregs: T_{con} 1:1). D) Tregs stimulated with anti-CD3/CD28 expander beads and with IL-1 β , IL-6 and IL-2 cytokines (T_{con} with cytokines) in co-culture with autologous T_{con} (T_{con} with cytokines: T_{con}, 1:1).

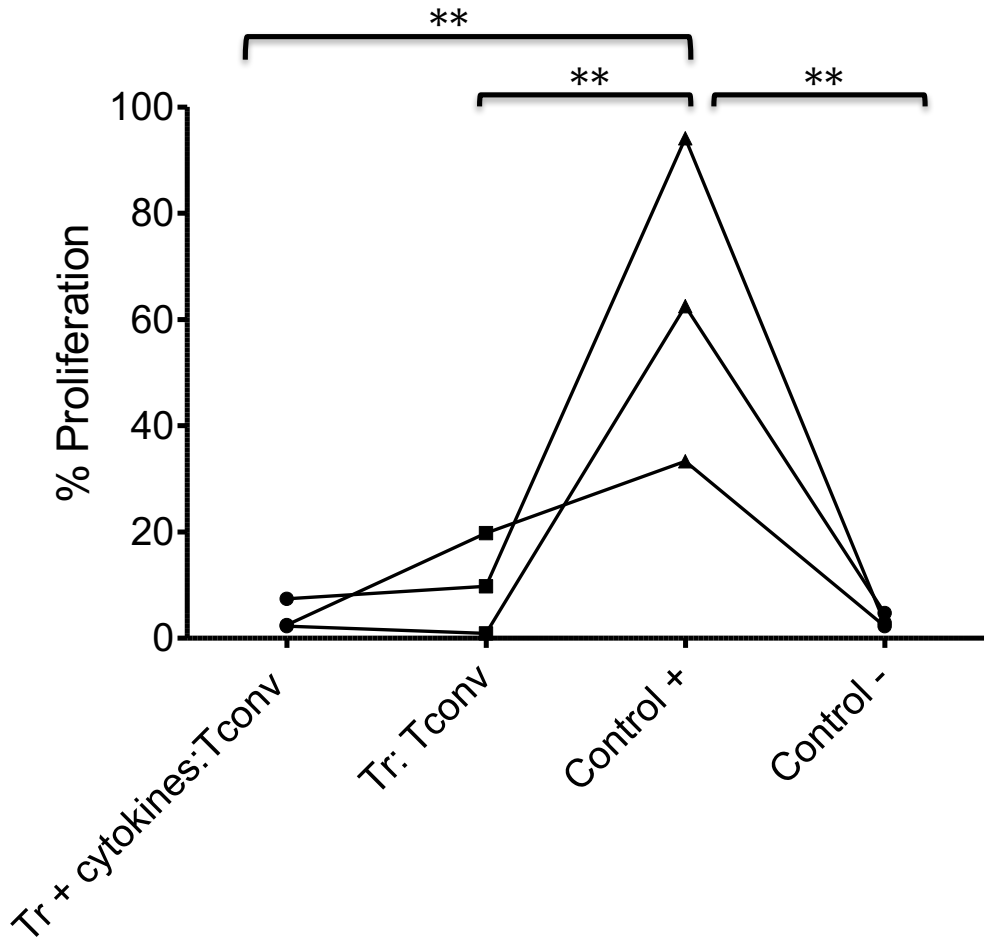


Figure 33. Proliferation assay of IL-17 secreting Tregs. T_{con} stimulated (Control +) and T_{con} stimulated (anti-CD3/CD28 expander beads) and with IL-1β, IL-6 and IL-2 cytokines in co-culture with autologous T_{con} (Tr + cytokines: T_{con}, 1:1) T_{con} stimulated and co-cultured with autologous Tregs (Tregs: T_{con} 1:1 ratio) and T_{con} not stimulated (Control -) (n=3) Legend for data *p* values: **** $p<0.0001$, *** $p<0.001$, ** $p<0.01$, * $p<0.05$

The overall percentage of proliferation decreased in Tregs stimulated with anti-CD3/CD28 expander beads and cultured with a Th-17 polarising environment from HDs with autologous T_{con} and in Tregs cultured with T_{con} as compared with the positive control (n=3) (2.49 % ±2.9 & 9.8 % ±9.44 vs 62.5% ±30.41, $p=0.0047$) (Figure 33).

In figure 34 we compared the suppressive assay from TrLCs with that of IL-17 secreting Tregs. Tregs in co-culture with autologous T_{con} (A) displayed a 2.65% of cell proliferation. While Tregs stimulated with anti-CD3/CD28 expander beads and with IL-1β, IL-6 and IL-2 cytokines in co-culture with autologous T_{con} (B) displayed 1.88 % of cell proliferation, whereas in T_{con}

stimulated treated with 5AzaC in co-culture with autologous T_{con} we can see a 22.7 % of cell proliferation. The graph strongly suggests that TrLCs are unlikely to be IL-17 secreting Tregs in terms of suppressive functions.

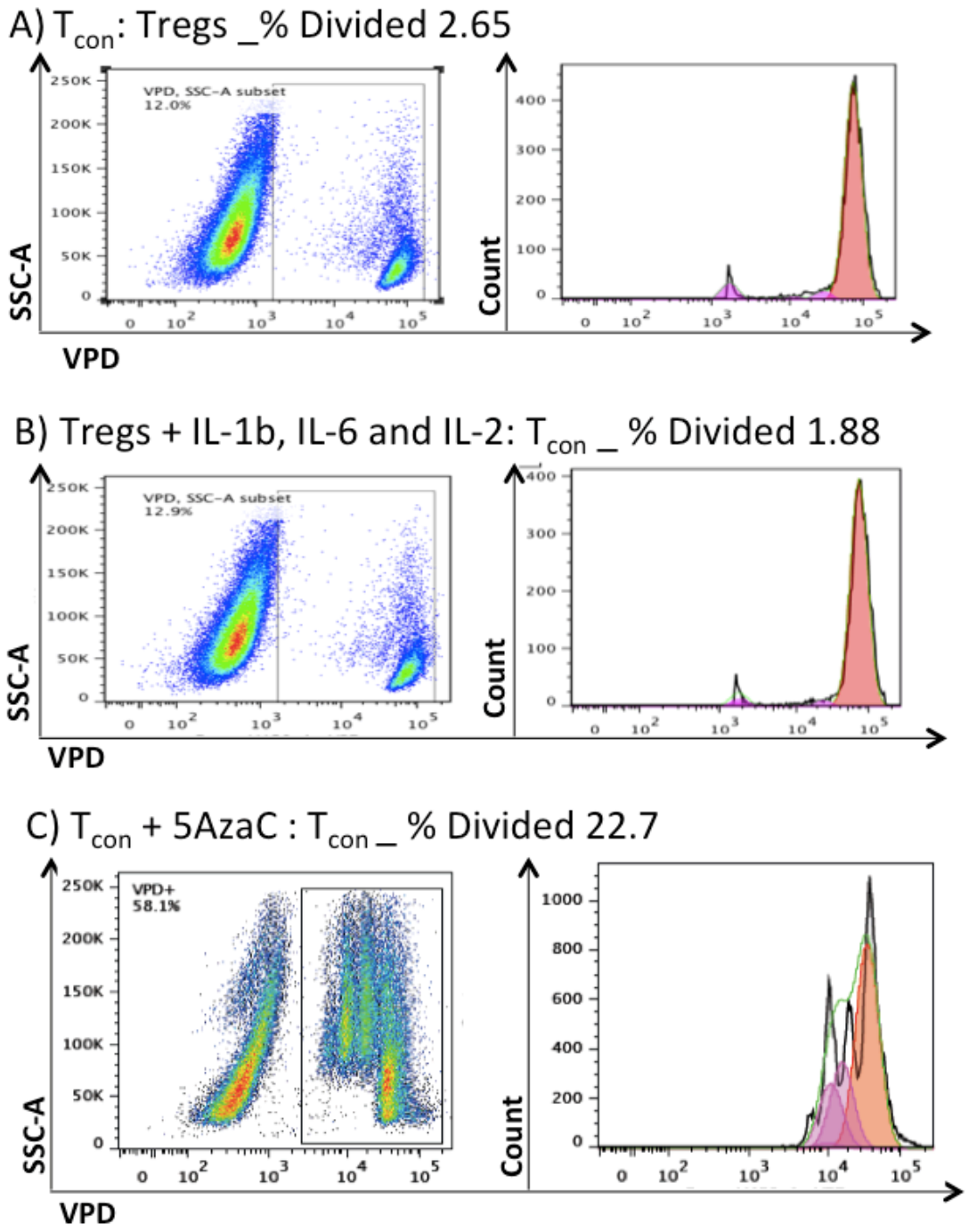


Figure 34. Comparing proliferation assay from Tregs, 5AzaC treated T_{con} and IL-17 secreting Tregs.

The following cell types were stained with the proliferation dye (VPD) for 3 days in culture (Figure 3) and the percentage of cells that divide during this period was analysed by flow cytometry VPD was used to monitor individual cell divisions. Every division is a peak in the graph. Autologous T_{con} were stained with VPD that was used to monitor individual cell divisions. Every division is a peak in the graph. A) Tregs in co-culture with autologous T_{con} with stimulation (anti-CD3/CD28 expander beads) (Tregs: T_{con} 1:1B) Tregs stimulated with anti-CD3/CD28 expander beads and with IL-1β, IL-6 and IL-2 cytokines in co-culture with autologous T_{con} (Tregs with IL-1β, IL-6 and IL-2 cytokines: T_{con}, 1:1) C) T_{con} stimulated treated with 5AzaC in co-culture with autologous T_{con} (Tcon 5AzaC: T_{con} 1:1 ratio).

4.4. Discussion

The aim of the studies described in this Chapter was to investigate the phenotype, function and cytokine profile of T_{con} after *in-vitro* culture in the presence of 5AzaC (TrLCs). We wanted to compare these TrLCs with Tregs, T_{con} and IL-17 secreting Tregs coming from a Th-17 polarising environment (*in-vitro* culture with IL-1β, IL-6 and IL-2) to understand whether the features of this subpopulation were still T_{con} or whether they polarised into a different population.

The first question was whether T_{con} after 5AzaC treatment were able to express FOXP3 and to secrete IL-17. Following *in-vitro* culture, our data demonstrate an increase in secretion of IL-17 and expression of FOXP3 in T_{con} cells following 5AzaC treatment as compared with T_{con}. The next question to be investigated was to analyse the function of these TrLCs and whether they are able to inhibit the proliferation and/or cytokine secretion of T_{con}. The data from proliferation assays suggested that following *in-vitro* culture with 5AzaC, TrLCs have no significant immunosuppressive properties when cultured with autologous T_{con} (1:1) as compared with Tregs cultured with autologous T_{con} (1:1). Both TrLCs and Tregs reduce the production of TNF-α and IFN-γ compared with T_{con} stimulated with anti-CD3/CD28 expander beads (positive control), nevertheless TrLCs showed a decrease in suppressing the secretion of TNF-α and IFN-γ by T_{con} compared with IL-17 secreting Tregs.

The last question was to analyse the difference between T_{con} after 5AzaC treatment and IL-17 secreting Tregs coming from Tregs after *in-vitro* culture with IL-1 β , IL-6 and IL-2 in terms of suppressive functions. Unlike the TrLCs subpopulation, the IL-17 secreting Tregs reduced the percentage of T_{con} which proliferated. Our data suggest that although TrLCs express FOXP3 and secrete IL-17, similar to Tregs and IL-17 secreting Tregs profile, TrLCs appear to be different from them, because TrLCs were not able to suppress T_{con} as showed by IL-17 secreting Tregs and stable Tregs. To take the study further the next Chapter focuses on the methylation status of the genes, which are important for the function and stability of Tregs.

5. Proteome and single-cell mass cytometry, Cytometry by Time of Flight (CyTOF) analysis

5.1. Summary

In high-risk MDS patients, it has been suggested that there is an expansion of Tregs compared with healthy donors[2]. The increase in the number of Tregs affects the immune response against the dysplastic clone and hence may facilitate the progression of the disease. As previously stated, T_{con} express FOXP3 and IL-17 after 5AzaC treatment[4]. In order to investigate whether the "Treg-like" cells (TrLCs) express T_{con} markers or polarise into another population and whether the T_{con} in MDS patients are different from those in healthy donors, we investigated studied their membrane proteome.

5.2. Introduction

5.2.1. Identification of novel components of the cell surface proteome

Membrane proteins are crucial for cellular functions (*e.g.* cell adhesion and ion transport) and also for normal cellular differentiation[114]. Conventional flow cytometry methods are not ideal for this purpose since they only detect known cell surface proteins, which are bound by specific antibodies[107]. Currently, there are no methods that enable us to identify and analyse the complete proteome of a human cell. In order to identify as many proteins as possible in one experiment, it is usually necessary to partially purify a subset of the proteome, *e.g.* an organelle or chromatin-bound, followed by identifying the proteins by mass spectrometry[120]. We wished to identify new components of the cell surface proteome on a large scale in order to study novel protein signature(s) on the cell surface of TrLCs. To purify cell surface proteins, we opted for a Biotinylation capture method, which has been used by others [121]. The proteins are then cleaved into peptides, usually using Trypsin and the proteins present can be identified by LC-MS-MS analysis of the tryptic peptides, based on their spectra (mass-to-charge-ratio)[122].

5.2.2. Identification of the TrLC phenotype by multi-parameter analysis of known proteins.

Our focus, in this part of the Chapter, was to comprehensively characterise and compare the phenotype of T_{con} with TrLCs and identify the potential surface protein signature(s) which could better characterise TrLCs. For this purpose we chose a mass cytometry time of flight (CyTOF) method[123] because it allows multi-parametric single cell analysis of more than 40 proteins at the same time. This novel method is a “deep phenotyping” strategy using multi-parameter mass cytometry. It is a variation of the flow cytometry method in which antibodies are labelled with heavy metal ion tags rather than fluorochromes. This allows the combination of many more antibody specificities in a single sample, without significant spill over between

channels[124]. In this Chapter, we have standardised an immunophenotyping CyTOF panel comprised of 34 antibodies.

5.3. Materials and Methods

5.3.1. Cell surface protein isolation by Biotinylation

The Pierce cell surface protein isolation kit (Thermo Scientific) was used to isolate cell surface proteins[108]. Purified $CD4^+$ cells were centrifuged with 5 ml ice-cold PBS at 220 x G_{max} for 10 minutes, then 60 x 10^6 cells were divided into three conditions (20 x 10^6 cells for each condition): total cell lysate, Biotinylated cells and PBS-treated cells (control) (Figure 12). The steps of the protocol (Figure 13) are: Biotinylation, cell lysis, isolation of labelled proteins and elution of Biotinylated proteins from NeutrAvidin columns.

Biotinylation: The sorted $CD4^+$ T cells were treated using 3 different conditions. The first condition (PBS) was a diluent control for the Biotinylation step, the second condition (Bio) was reaction with the Sulfo-NHS-SS-Biotin compound and the third condition (Total cell lysate) was used as a control for the Biotinylation steps. $60x10^6$ $CD4^+$ T cells were used for the assay, which were divided into three micro centrifuge tubes ($20x10^6$ $CD4^+$ T cells each), one for each of the three different conditions. Cells were centrifuge at 220 x G_{max} for 10 minutes and the pellets were treated in different ways:

6. The pellet of the Total cell lysate (TOT) condition was kept on ice.
7. In the Bio condition 1.5 µg of Sulfo-NHS-SS-Biotin in 1 ml of PBS (Thermo Scientific) was added to the pellet.
8. The PBS condition pellet was resuspended with 1 ml PBS only.

The Bio condition with Sulfo-NHS-SS-Biotin and the PBS condition were placed in an orbital shaker for 30 minutes at 4°C. To stop the reaction, 50µl of Quenching solution (Thermo Scientific: components not divulged by the manufacturer) was added. After 3 washes with 1ml Tris buffered saline (TBS), cells were centrifuged at 300 x G_{max} for 10 minutes. I took 0.50 x 10^6 of $CD4^+$ T cells from Bio and PBS conditions to check the viability by counting cells in the presence of Trypan blue. In addition, a flow cytometry method (Material and Methods 3.3) using Streptavidin e-FluorV450 was applied to check whether the biotin compound bound the surface proteins. Cells treated using the Bio and PBS conditions were centrifuged at 270 x G_{max} for 10 minutes and the pellets were kept on ice.

Cell lysis: The pellets from the three conditions (TOT, Bio and PBS) (Figure 12) were lysed with 50µl of Lysis Buffer (Thermo Scientific: components not divulged by the manufacturer) and placed on ice for 30 minutes. They were sonicated 2 x 10 minutes on medium power in a Bioruptor water bath (Diagenode) and vortexed for 5 seconds. Cells treated according to the three conditions were centrifuged at 300 x G_{max} for 2 minutes at 4°C. The clarified supernatant was the soluble fraction, the pellet the insoluble fraction.

Isolation of labelled proteins: The clarified supernatants of the Bio and PBS conditions were added to two different columns containing a NeutrAvidin-Agarose matrix (previously washed with 100µl of wash buffer and centrifuged at 270 x G_{max} for 10 minutes) and incubated with rolling for 60 minutes at room temperature to let the Biotin bind to Avidin, then centrifuged at 270 x G_{max} for 10 minutes to eliminate unbound proteins as flow through.

Protein elution: Columns were incubated for 5 minutes at 95°C with 50µl of 4x Sample Buffer (1 M Tris-HCl (pH 6.8), 400 mM DTT, 8% (w/v) SDS, 0.4% (w/v) bromophenol blue, 40% (v/v) glycerol) and then centrifuged to elute the proteins bound to Avidin. The samples were then ready to be analysed by gel electrophoresis (see Chapter 3 section 8) and then by Mass Spectrometry (see Chapter 3 section 9).

5.3.2. Phenol-based DNA extraction

Because of the presence of fixation buffer in the cells used for this section's experiments, we opted for a phenol-based DNA isolation protocol proposed by *Bending et al*[125], instead of the genomic DNA isolation method described in the "Materials and Methods" Chapter (see Chapter 3, section 11.1). This protocol aimed to reverse (using sufficient RNAse and Proteinase k) the formaldehyde-induced changes (DNA cross-link) that lead to the impedition of epigenetic analysis. Modifications were brought to the protocol. Cells were incubated with 300ul lysis buffer (10mM Tris-HCL (Life Technologies), 100 mM NaCl (Life Technologies), 50 mM EDTA (Applichem), 0.5% (w/v) SDS (Life Technologies), 0.1mg/ml proteinase K (Roche), pH 8) and 20 ug/ml RNase A (Qiagen) for 24 hours at 60°C on a thermo shaker (Thermo Scientific). Then, the lysis solution was mixed with one volume of

phenol/chloroform/isoamyl alcohol (25:24:1 Sigma- Aldrich). The work was carried out under the chemical fume hood. The solution was centrifuged at 13,000 rpm for 5 minutes at room temperature. The aqueous phase was removed and we kept the non-aqueous phase where the DNA was set. DNA was precipitated by addition of ethanol (Sigma-Aldrich) to a final concentration of 75%. The tube containing the ethanol and the DNA was incubated at -20C for at least 4h. The tube was then centrifuged at 13,000 rpm for 5 minutes. Supernatant was removed and 300 μl of 70% ethanol was added. The tube was centrifuged again at 13,000 rpm for 5 minutes. Supernatant was removed. DNA pellet was air-dried under the hood. DNA was dissolved in TE buffer for at least 24 hours before use in downstream experiments[125].

5.3.3. Single cell mass cytometry or cytometry by time-of-flight (CyTOF)

This novel method is a “deep phenotyping” strategy using multi-parameter mass cytometry to analyse the cellular phenotype at a single cell level using mass cytometry[111] (Figure 35).

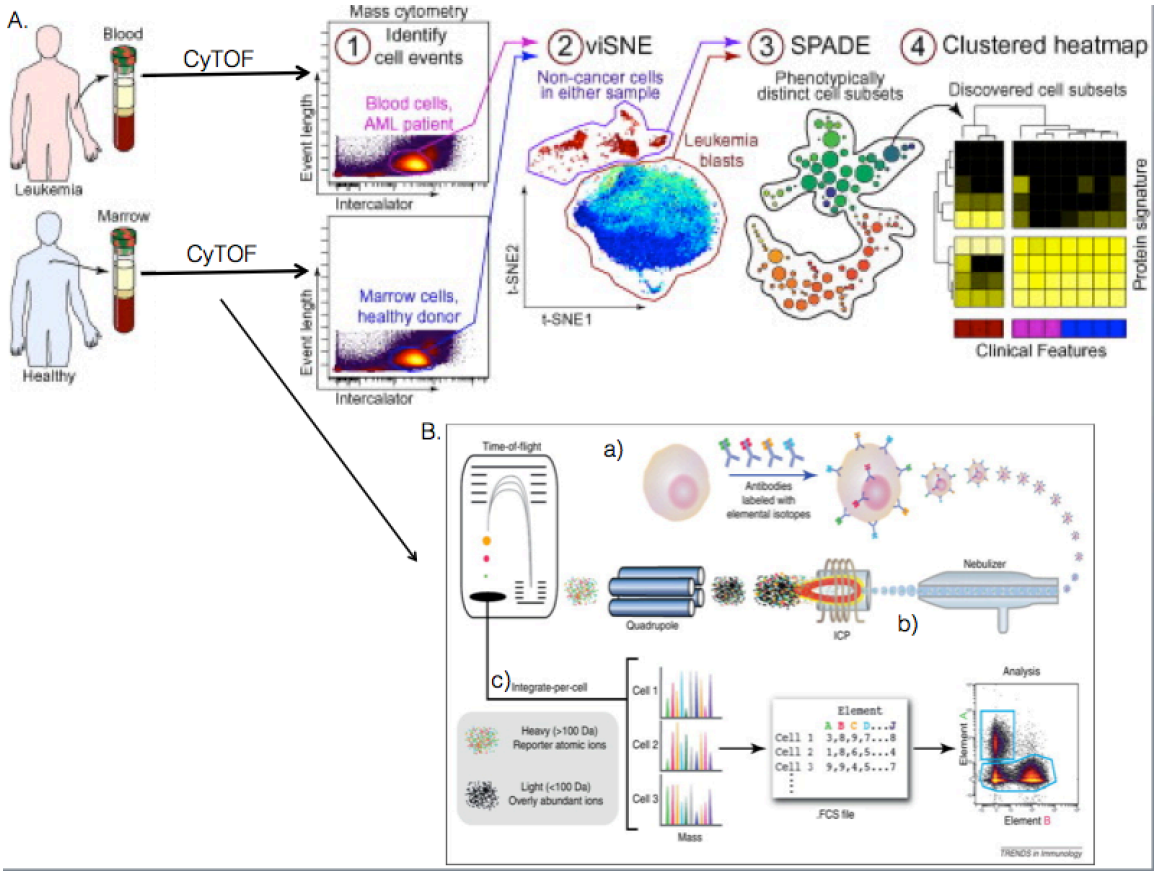


Figure 35. CyTOF workflow. *A. Cells from HD and patients are analysed using a CyTOF method (see B. for more details). Cell events were identified (1).* Initial populations were distinguished using viSNE (2). Cell subsets were revealed using SPADE (3). Cell clusters were then visualised using a heat map (4). *Image adapted from Diggins et al*[126]*. B.* CyTOF machine workflow: *a) a heavy metal isotope is conjugated to the antibody of interest. A panel of up to 40 chosen antibodies are assembled for membrane and intracellular staining. Cells are stained and then passed through a nebulizer. b) Cells are sprayed into an ICP TOF mass spectrometer. c) The individual ions are counted and then the raw data are collected into a flow cytometry file format. Image adapted from Bendall et al*[111]

Antibodies targeting the cellular markers of interest are labelled with antibody metal isotope-conjugate probes rather than fluorochromes. Labelled cells are then introduced in an Inductively Coupled Plasma (ICP) where they are atomized and ionized. The cloud of atomic ions for each single cell moves across a magnetic field towards a detector at a speed proportional to the size of the particle: the lighter the particle, the faster it moves and the lesser the time-of-flight. Compared to fluorescence-based flow cytometry, CyTOF overcomes spectral overlap and cellular auto-fluorescence issues, the latter due to the fact that the rare earth metal isotopes used in CyTOF are not naturally found in biological systems.

5.3.3.1. Cell staining for membrane and intracellular markers

Cells were prepared for analysis by adding a total of 2 µL of Leukocyte Activation Cocktail, with BD GolgiPlug stimulation (LAC) (BD, 550583) per 1ml of cell suspension and incubated for 4 hours at 37^{o}C, 5% (v/v) $CO_{2.}$ The Leukocyte Activation Cocktail is a polyclonal cell activation mixture containing a calcium ionophore (Ionomycin), the phorbol ester PMA (Phorbol 12-Myristate 13-Acetate) and the protein transport inhibitor BD GolgiPlug™ (Brefeldin A). This cocktail is able to elicit a primary cytokine response from T cells. Cytokines are produced and then localised in the rough endoplasmic reticulum of the cells due to the Brefeldin A (a protein transport inhibitor component) that blocks intracellular protein transport processes. The accumulation of cytokine protein levels enhances the detectability of cytokine-producing cells by mass cytometric analysis. During this incubation, the Cell Staining Media (CSM) was prepared using 500 ml low barium PBS (no Ca^{2+}/Mg^{2+}) (Sigma, D8537) plus 2.5% (v/v) foetal calf serum (FCS) and 0.02% (w/v) sodium azide. In addition, the antibody cocktail was prepared using protein Low Bind tubes (Eppendorf) to avoid loss of antibodies by adsorption to the plastic walls of the tubes. Antibodies were kept at 4^{o}C during cocktail preparation. The exact amount of each antibody was added as indicated in the staining panel table (Table 12) for each particular experiment. These volumes were determined by previous titration of the antibodies, as published[127]. Once the cocktails were ready, tubes were placed in a box at 4 ^{o}C until needed. The Viability Stain (Rhodium) was prepared from the stock Rhodium-intercalator solution that was provided by Dr Richard Ellis NIHR GSTFT/ KCL Biomedical Research and kept at -20 ^{o}C. The Rhodium-intercalator solution is a cationic nucleic acid intercalator that allowed us to discriminate viable cells from dead cells. The plasma membrane is impermeable to the Rhodium-intercalator solution, so it only accumulates in dead cells with a compromised membrane. The Rhodium working solution was 1:500 in PBS (no Ca^{2+}/Mg^{2+}). 500 µL of Rhodium working solution is needed per test. The Fc block (preventing non-specific binding) working solution was 1:20 in CSM from the stock solution (Kiovig; Baxter, Human Ig, 100 mg/ml bottle). 10 µL of the working solution was added per test.

After the 4 hours incubation, cells were harvested and put into FACS tubes.
Tubes were centrifuged at 300 x G_{max} for 10 minutes to pellet cells. Tubes were washed once with 2 ml PBS (no Ca^{2+}/Mg^{2+}), centrifuged at 300 x G_{max} for 10 minutes. The supernatant was discarded.
Each cell pellet was resuspended in 500 µL in Rhodium-intercalator working solution and incubated for 15 minutes at RT.
Tubes were washed 2x with 2 ml PBS (no Ca^{2+}/Mg^{2+}), centrifuged at 300 x G_{max} for 10 minutes. The supernatant was then discarded. A total of 10 µL of diluted Fc blocking reagent was added to the cells and incubated for 10 minutes at room temperature.
Straight after the Fc blocking the surface staining antibody cocktail was centrifuged at >10000 x G_{max} for 5 minutes at 4 ^{o}C to bring the contents to the bottom of the tube and the appropriate volume of the cocktail was added to the cells (Table 12) and cells were incubated for 30 minutes at room temperature.

Table 12. Selected antibody markers for membrane and intracellular staining.

Channel	Target	µl	Clone
141	CD3	1	L1cht1
142	CD19	2	H1B19
143	CD56	1	B159
144	CD11b	1	ICRF44
145	CD4	1	RPA-T4
147	CD20	1	2M7
149	CCR4	1	205910
150	CD62L	1	DREG-56
151	CD123	1	6H6
153	CD45RA	1	H1IOU
154	CD45	1	H130
159	CD154	1	24-Mar
162	CD69	1	FN50
166	CD33	1	P67.6
166	CD34	1	581
166	CD15	1	W6D3
168	CD8	1	SK1
169	CD25	2	MA-251
169	CD25	2	2A3
172	CD38	2	HB7
174	HLA-DR	1	L243
175	CD279	1	EH12
176	CD127	1	AO19D5
148	IL-4	2	MP4-25D2
152	TNF-α	1	MAB11
156	IL-6	1	MQ2-13A5
158	IL-2	1	MQ1-17H12
160	Tbet	1	4BIO
164	IL-17a	1	N49-653
165	IFN-γ	1	B27
167	GATA3	1	TWAJ
170	IL-10	3	JES3-9D7
171	FOXP3	2	150D
171	FOXP3	2	259D
171	FOXP3	2	PCH101

This table shows the list of antibodies that were used for CyTOF analysis.

The column “Channel” shows the list of each channel used for every antibody. The column “Target” shows the marker target by the antibody. The column “ µl ” shows the amount of antibody used for one sample. The column “Clone” shows the clones used.

Cells were then centrifuged twice at 300 x G_{max} for 10 minutes and resuspended in 2 ml of CSM each time. The supernatant was discarded and each cell pellet was finally re-suspended in 1 ml of (1x) Fix/Perm solution (eBioscience freshly prepared, 1:3 dilution) and incubated for 45 minutes at 4° C. A total of 2 ml of Permeabilisation wash buffer was added to give a final volume of 3 ml. Each cell pellet was centrifuged at 400 x G_{max} for 8 minutes and the supernatant was discarded. The appropriate volume of the antibody

cocktail was added to the cells (Table 13) and cells were incubated for 30 minutes at RT. Cells were centrifuged 2x with 2 ml of CSM at 300 x G_{max} for 10 minutes and the supernatant was discarded. Cells were then fixed with 500 µL 4% Paraformaldehyde (PFA) solution per test. Cell suspensions were transferred into 1.5 ml tubes ready to be analysed using the CyTOF machine.

5.3.3.2. Data analysis workflow

We followed the published method by Diggins *et al*[126] to analyse our CyTOF dataset. Their method consists of three main components:

a) Distinguish initial populations;
b) Reveal cell subsets;
c) Characterise subset features.

In order to have a comprehensive discovery and characterisation of both cells and populations, this workflow (Table 13) was selected to study and manage the significant amount of data that result from single cell mass cytometry method.

Table 13. Workflow for semi-supervised high dimensional single cell data analysis (Diggins et al[126]).

Analysis step		Traditional	Additional methods[§]	Method here
Data collection	(1) Panel design	Human expert	–	–
	(2) Data collection	Human expert	–	–
Data processing	(3) Cell event parsing	Instrument software	Bead normalization and event parsing [39]	–
	(4) Scale transformation	Human expert	Logicle [47]	–
Distinguishing initial populations	(5) Live single cell gating (6) Focal population gating	Biaxial gating + human expert	No event restriction, AutoGate [61]	viSNE + human expert (Fig. 1)[†]
Revealing cell subsets	(7) Select features	Human expert	Statistical threshold [53]	Human expert[†]
	(8) Reduce dimensions or transform data	N/A	Heat plots [62], SPADE [12], *t*-SNE [63], viSNE [8], ISOMAP [27], LLE [29], PCA in R/flowCore [64]	SPADE[†], viSNE
	(9) Identify clusters of cells	Human expert	SPADE, *k*-medians, R/flowCore, flowSOM [65], Misty Mountain [13], JCM [30], ACCSENSE [66], DensVM [28], AutoGate, *Citrus* [14]	SPADE (Fig. 2)[†], viSNE + human expert (Fig. 1)
	(10) Cluster refinement	Human expert	Citrus, DensVM, R/flowCore	–
Characterizing cell subsets	(11) Feature comparison	Select biaxial single cell views	viSNE, SPADE, heatmaps [25,53], histogram overlays [25,53], violin or box and whiskers plots [64], wanderlust [31], gemstone	Heatmaps (Fig. 3A)[†], viSNE (Fig. 1C), SPADE (Fig. 2C)
	(12) Model populations	N/A	Median [53], JCM, PCA	–
	(13) Learn cell identity	Human expert	–	Human expert[†] (Figs. 1B, 2B, and 3B)
	(14) Statistical testing	Prism, excel	R/flowCore	–

[§] Methods with broad application (e.g. R/flowCore) are listed minimally at select steps based on particular strengths or published applications.
[†] Denotes the primary approach used at each step in the sequential analysis workflow shown here.

Analysis step: these are the steps to follow in order to process and analyse the CyTOF dataset. Column "Traditional", displays the methods that can be used in a particular step (ex. under "analysis step" column, the "Distinguishing initial populations" row, in this step the analyses that have to be done are (5) Live single cell gating and (6). Focal population gating, under the column "traditional" it is suggested that "Biaxal gating + human expert" could be the methods to use. The column "Additional methods" displays the methods that can be used for a particular step (ex. also in the "Distinguishing initial populations" row it is suggested that the "No event restriction, AutoGate" could be used). The column "Method here" contains the methods used in that paper (ex. also in the "Distinguishing initial populations" row they used viSNE + human expert). For the references in this table please see Diggins *et al* [126].

CyTOF data were output in flow cytometry standard (.fcs) file format. In order to avoid sensitivity fluctuations from the CyTOF machine, internal bead controls were added to our samples while staining. The bead controls were monoisotopic metal elements (Ce140, Eu151, Eu153, Ho165 and Lu175). Acquired data were normalised using an algorithm[128] to correct the instrument performance that could change with time. For the data analysis, a web-based package (Cytobank, enabling viSNE and SPADE) designed to facilitate the study and visualization of the dataset was used (Table 13). After the normalisation of the. fcs files, we gated the events using Cytobank as follows: we first gated based on intact cells and single cells (event length versus IR_191 DNA content) (Figure 36, plot 1.), then on single cells (Ir_191 versus Ir_193 DNA content) (Figure 36, plot 2.). Iridium (Ir) intercalator uptake helped mark all cells and it was proportional to nucleic acid content. After that, we excluded the internal bead controls (CD45 versus Bead_140Ce) (Figure 36,

plot 3.) and finally we gated based on the viability of the cells (CD45 versus Viability) (Figure 36, plot 4.) and on $CD3^{+}CD8^{-}$ cells (CD3 *versus* CD8) (Figure 36, plot 5.). Our $CD3^{+}CD8^{-}$ population was ready to be analysed further.

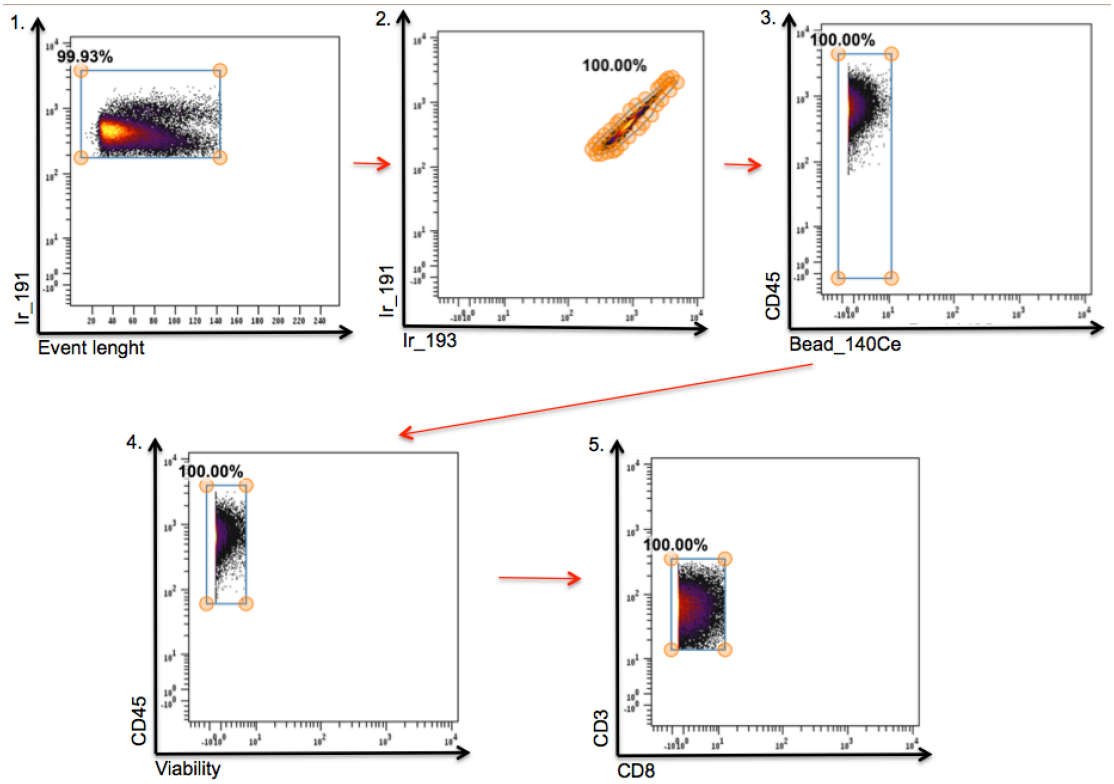


Figure 36. Gating strategy.

Here we show a gating strategy for the $CD3^{+}CD8^{-}$ population. We first gated based on event length versus IR_191 that shows DNA content (plot 1.) to have intact cells, then on Ir_191 versus Ir_193 (plot 2.) to have single cells. After we gated on CD45 *versus* Bead_140Ce (plot 3.) to exclude the internal bead controls. Final gating was based on CD45 *versus* Viability (plot 4.) to exclude dead cells and on CD3 *versus* CD8 (plot 5.) to analyse the final $CD3^{+}CD8^{-}$ population

Then, we wanted to visualise major cell subsets. To do that we used an algorithm called visually identify stochastic neighbour embedding or viSNE to map the high-dimensional data (up to 40 markers analysed in millions of single cells) onto two-dimensional view while conserving high-dimensional structure. In order to run viSNE we selected the most relevant markers (TNF-α, CD45, IL-17a, CD279, CD154, CD62L, HLA_DR, T-bet, IL-6, IL-10, CCR4, IL-4, IFN-γ, CD25, CD69, CD38, IL-2, CD127, CD45RA, FOXP3, GATA3 and CD4) to cluster CD4+ cells. So, we clustered our cells with viSNE using the selected markers. The result of viSNE analysis is called t-distributed

stochastic neighbour embedding or *t*-SNE (Figure 37) that is calculated based on the markers used by viSNE. viSNE is the visualisation of all the markers combined together (*t*-SNE1 and *t*-SNE2) (Figure 38).

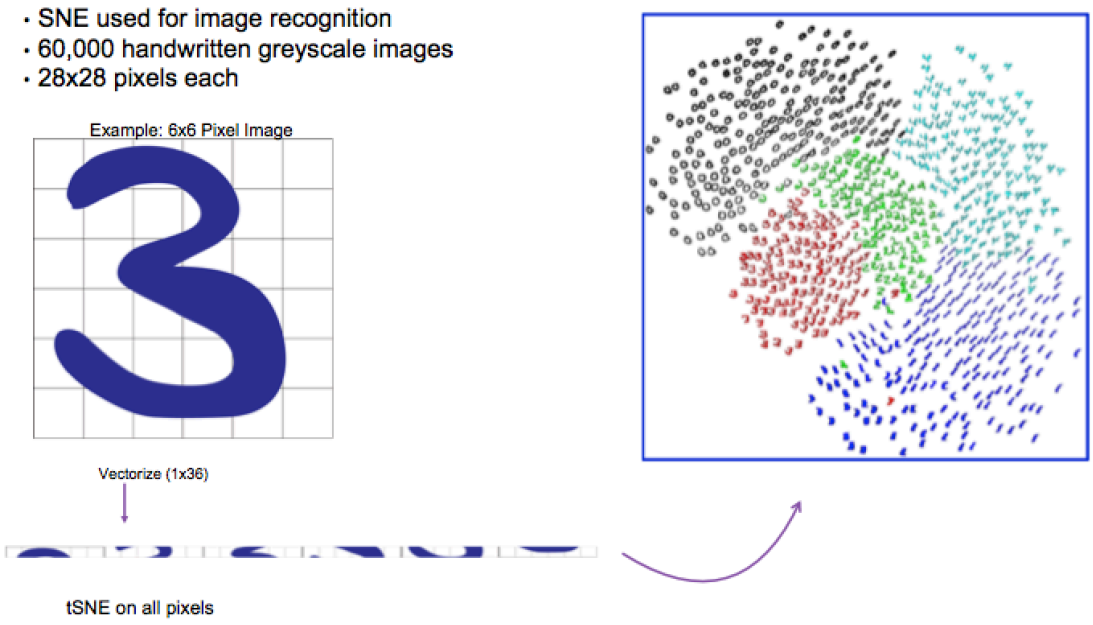


Figure 37. Stochastic Neighbor Embedding (SNE) – Machine Learning to Reduce Dimensionality. ViSNE enables mapping of high-dimensional cytometry data into two dimensions, yet conserving the high-dimensional structure of the data. viSNE uses imagine recognition to vectorise the image into pixels and to plot individual cells in a manner similar to a scatter plot. Figure adapted from Hinton *et al.*

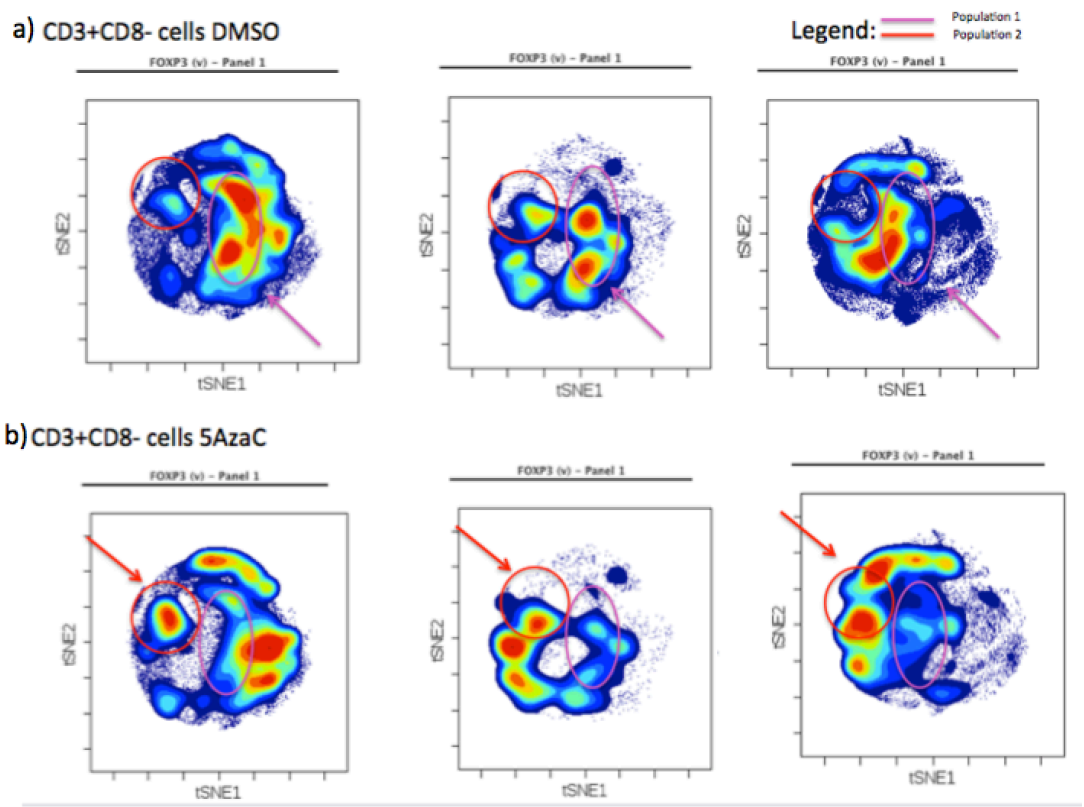


Figure 38. Visualisation of initial populations on viSNE map. Row a) displays 3 biological replicates of CD3+CD8- cells treated with DMSO, the same biological replicates are treated with 5AzaC in row b). Cells are mapped based on their high dimensional phenotypic similarity. viSNE arranges cells along *t*-SNE axes according to FOXP3 expression. In this Figure expression of FOXP3 is shown for each replicate for both conditions (+/- 5AzaC). Cell population density changed in one condition compared to the other. Populations 1 (pink borders) were present only in DMSO treated cells, whereas population 2 (red borders) was present only in 5AzaC treated cells.

At next step, we wanted to identify cell subsets using the spanning-tree progression analysis of density-normalized events (SPADE) based on the t-stochastic neighbour embedding tool (*t*-SNE)[129] (Table 13). SPADE is an algorithm that includes dimensionality reduction. It allowed us to cluster cells into populations and to visualise cells using a two dimension-spanning tree.

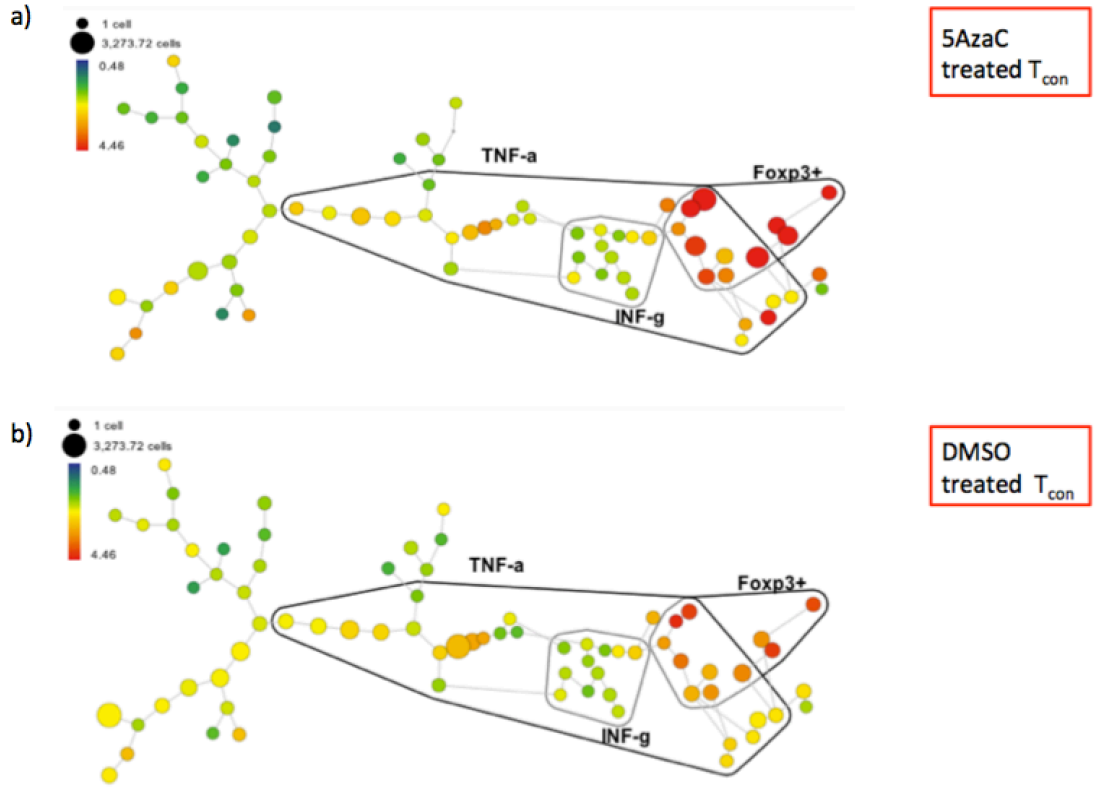


Figure 39. Cell subsets using SPADE analysis. Plots a) and b) show the use of SPADE analysis to reveal cell subset clusters based on FOXP3 expression. The colour of the dots ("nodes") depends of the expression of FOXP3; red colour represents high expression of FOXP3, blue colour represents low expression of FOXP3. Plot a) shows expression of FOXP3, TNF-α and INF-γ by 5AzaC treated T_{con} expressing high levels of FOXP3. Plot b) shows expression of FOXP3, TNF-α and INF-γ on DMSO treated T_{con}. The warmer the colour (shades of red) of the node (cell subsets) the higher is the expression of that particular marker.

The use of SPADE on *t*-SNE was applied to the dataset to discover and to cluster cell subsets (called "nodes") (Figure 39). The algorithms used allowed dimensionality reduction steps that projected multi-dimensional dataset into a lower dimensional space for visualization and further interpretation[126].

After that we exported the files and we used a software package that was developed by our group which scales data based on published scripts[126] to divide the expression of a selected marker (FOXP3 in our case) to high, medium or low based on its distribution across all cell clusters. Specifically, cell clusters that have expression of a given protein that is lower than the first quartile (Q1) of the marker's distribution are marked as "Low" (L), cell clusters with expression values within the interquartile range (IQR) are marked as "Medium" (M) and finally, cell clusters with expression values greater than the

third quartile are marked as “High” (H). The quartiles were estimated based on the scaled data. Transformation of expression values was implemented using the following formula:
log (x/c + sqrt (1 + (x/c) ^2));

where x = the value (intensity value from flow) and c = cofactor (constant per channel; default is 5). So, we applied arcsinh transformation with a cofactor of 5 as suggested by Irish *et al*[126, 130]. Finally, we wanted to characterise further the clusters discovered using heat maps (Figure 45-46-47-48) and statistical analysis.

5.3.4. Statistical analysis

Statistical analysis was performed using Prims version 6 or SPSS version 22. One-way Anova followed by Bonferroni’s multiple comparison tests were used to compare more then 2 sets of non parametric data. T test followed by Mann Whitney’s multiple comparison test were used to compare 2 sets of non-parametric data. Error bars are standard error of the mean. Significance was set at $p < 0.05$.
**** $p<0.0001$, *** $p<0.001$, ** $p<0.01$, * $p<0.05$ are used in figures.

5.4. Results

5.4.1. Cell surface protein identification

The purpose of this part of the study was to identify novel protein signature(s) on the cell surface of TrLCs using Mass Spectrometry analysis of cell surface proteins isolated by a biotinylation capture method. In this method a cell impermeable Sulfo-NHS-SS-Biotin reagent was used which reacts with primary amine groups of cell surface proteins[109]. These proteins were then isolated by binding to an Avidin-Agarose affinity matrix. We wanted to identify the cell surface proteome of Tregs, however, these cells are present at a low frequency in the PB of MDS patients (approximately $0.5x10^6$ in 40ml of PB). Therefore, we choose to optimise the method using $CD4^+$ T cells from HDs because we could isolate large numbers at will and also because Tregs are a subpopulation of $CD4^+$ T cells which should have similar physical characteristics.

First, the potential damage to the $CD4^+$ T cells caused by this method was evaluated using $20x10^6$ $CD4^+$ T cells. I isolated $CD4^+$ T cells from a HD leukocyte cone by negative selection, which were on average 95% ± 0.52 (n=6 independent experiments) pure, as assessed by flow cytometry of $CD4^+$ cells. As explained in section 3.1 this method involves the use of Sulfo-NHS-SS-Biotin, a chemical compound where the NHS ester group reacts with any primary amine group ($-NH_2$) on lysine side chains, producing a covalent bond. The reaction is stopped after 1 h by adding quenching buffer (containing EDTA). Three conditions were processed: untouched cells (TOT), cells labelled with biotin (Bio) and cells incubated with diluent only (PBS). After the Biotinylation step, viability was assessed by manual counting in the presence of Trypan blue and the two conditions Bio and PBS were assessed (Figure 12). The Sulfo-NHS-SS-Biotin compound can bind any primary amine group on lysine side chains and so the integrity of the plasma membrane is crucial to ensure that the reaction only labels cell surface and not intracellular proteins, which would be accessible in dead cells. The viability in the Bio sample was 95% ± 0.58 (n=6 independent experiments), which was considered satisfactory.

Next, we assessed the percentage of cells labelled with Biotin, using flow cytometry (Figure 40). An aliquot of $2.5x10^5$ CD4+ T cells from Bio and PBS conditions were stained with Streptavidin-eFluor450 and analysed by flow cytometry. The gate was set on the lymphocyte population, based on Side Scatter and Forward Scatter characteristics to exclude dead cells and debris. A gate was set based on the negative control (Figure 40-A PBS condition, unlabelled cells (set to include 99.9% of the population)) and then I applied the same gate to the positive labelled cells (Figure 40-B Bio condition, labelled cells). All the cells labelled with biotin (Bio) were positive for Streptavidin. From these data, we concluded that the Biotinylated cells (Figureure 40-B) were tagged with Biotin, consistent with labelling cell surface proteins with Biotin.

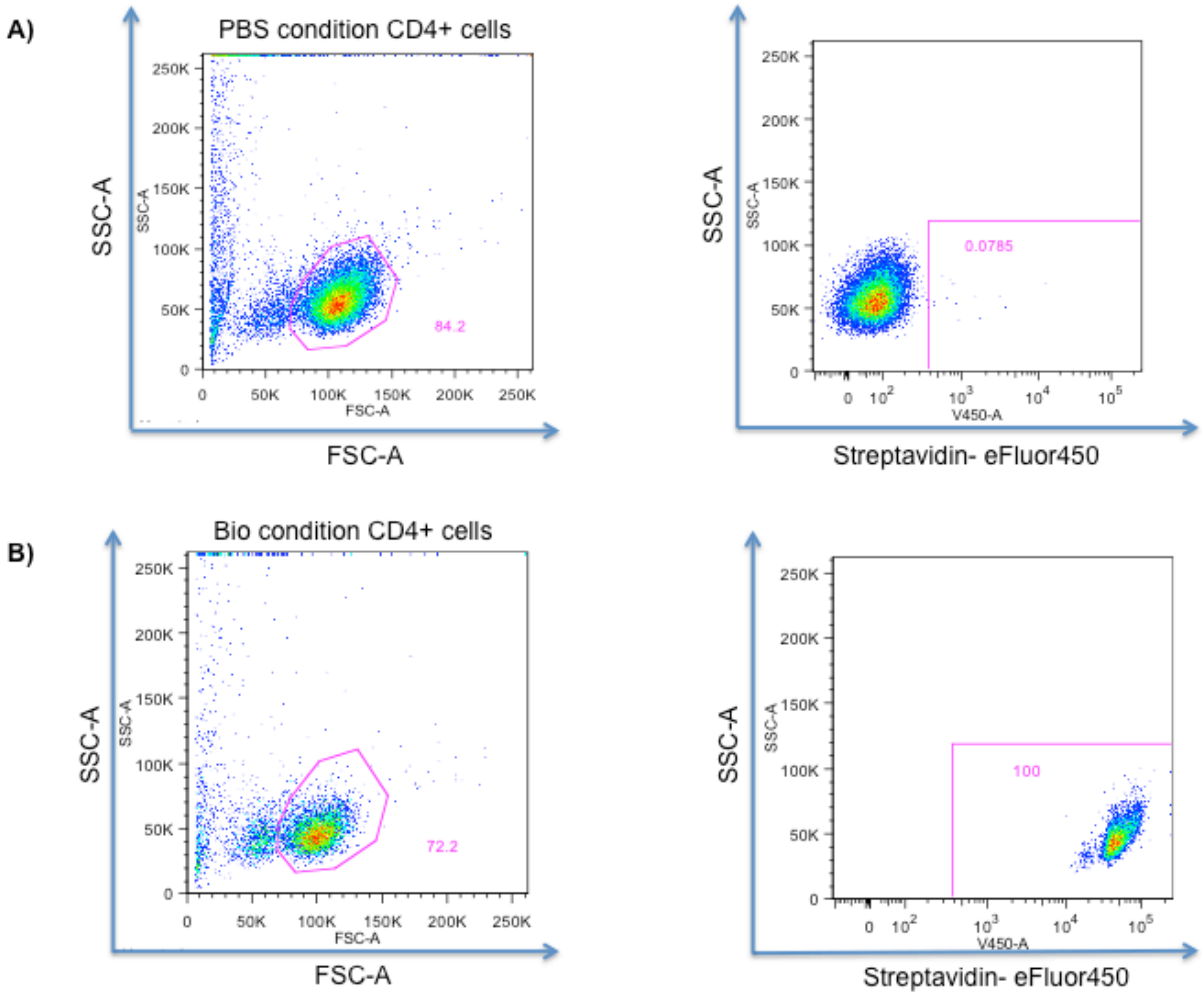


Figure 40. Flow cytometry analysis using Streptavidin-eFluor450.

Flow cytometry was used in order to assess the percentage of cells labelled with Sulfo-NHS-SS-Biotin. The CD4+ T cell population negative for Streptavidin (A) indicate cells not labelled with Biotin, CD4+ T cells population positive for Streptavidin (B) indicate cells labelled with Biotin. The percentage of cells within each gate is shown.

Each of the 3 conditions (total cell, Bio and PBS) was subsequently lysed, using sonication in the presence of a Lysis buffer (containing detergent, protease and phosphatase inhibitors). Then, soluble proteins from Bio and PBS conditions were isolated using a NeutrAvidin matrix and then eluted with SDS-PAGE sample buffer. The presence of an intracellular protein, Histone H3 and a membrane protein, CD44 were investigated by Western blotting to determine whether the method was able to isolate membrane proteins but not intracellular proteins. The samples analysed were: non labelled cells, non labelled cells flow-thorough, Biotinylated protein, Biotinylated protein flow-through and the total cell lysate (Figure 41). The presence of Histone H3 and

CD44 proteins in each sample was assessed by western blotting. Both Histone H3 and CD44 proteins were observed in the total cell lysate sample (Figure 41-E) and in the non-labelled and labelled cell flow-through samples (Figure 41-B and 41-D). Histone H3 and CD44 were not detectable in the sample of non-labelled proteins which were bound to the column (Figure 41-A). Only the CD44 protein was detected in the sample of labelled proteins bound to the column (Figure 41-C). These data are consistent with biotinylation occurring of cell surface and not intracellular proteins.

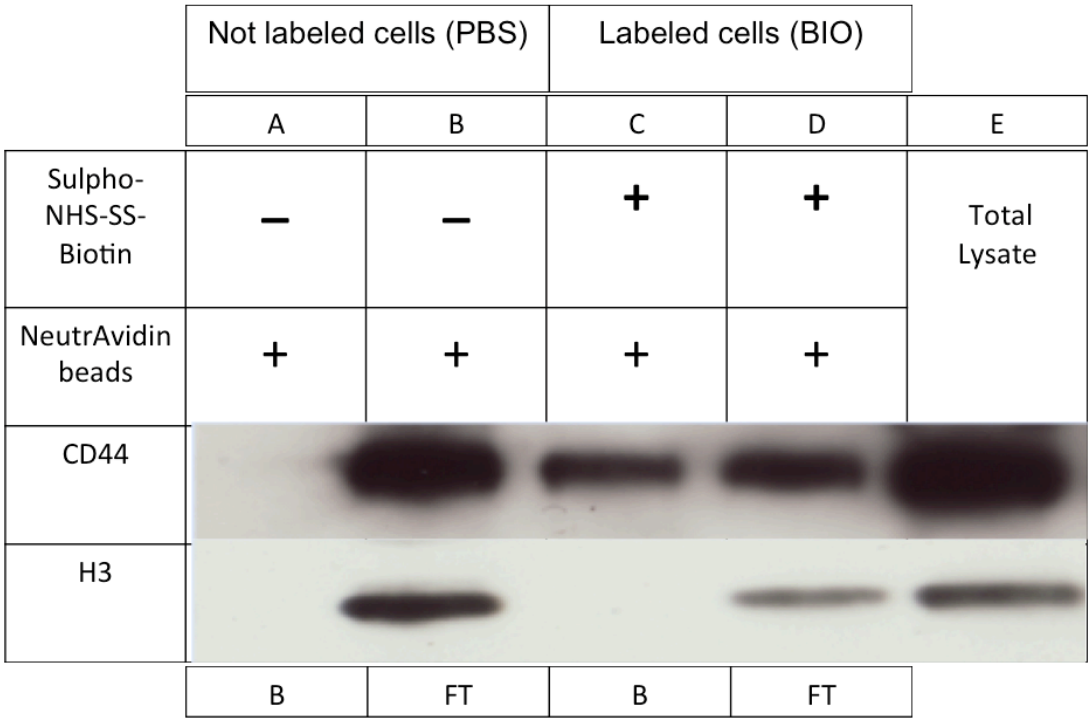


Figure 41. Western blot analysis.Western blot analysis of isolated proteins form Bio, PBS and Total lysate conditions. B: bound to NeutrAvidin beads; FT: flow through – not bound to NeutrAvidin.

According to the flow cytometry results (Figure 40) and Western blot analysis (Figure 41), the majority of cells are biotinylated and membrane proteins and not intracellular proteins were present in the Biotinylated sample captured on NeutrAvidin beads. Therefore, there is evidence that the method was able to isolate cell surface proteins even if the presence of CD44 in the flow-through of biotinylated cells (Figure 41; column C) suggest that either the column with the Avidin matrix was overloaded or some of the CD44 is not biotinylated.

This is possible as there is intracellular as well as cell surface CD44[131] is intracellular. We then proceeded with the experiment.

A total cell lysate sample (TOT Figure 41-E), Biotinylated proteins bound to Avidin (Bio Figure 41-C) and non-Biotinylated proteins bound to Avidin (PBS Figure 41-A) were prepared for Mass Spectrometry as followed (analysed by the Proteomic Laboratory Facility, Institute of Psychiatry, Denmark Hill Campus). Samples were first alkylated using iodoacetamide (IAM) and Trypsinised. After digestion, the peptides were separated using high-pressure liquid chromatography (HPLC) then analysed using an Orbitrap Velos Pro mass spectrometer. A search was carried out for each of the peptides against the sequences of all proteins encoded by genes in the human genome (Mascot software, Matrix Science) and with variable modifications on Lysine due to the residual Biotin compound left attached to peptides containing Lysine (Figure 42).

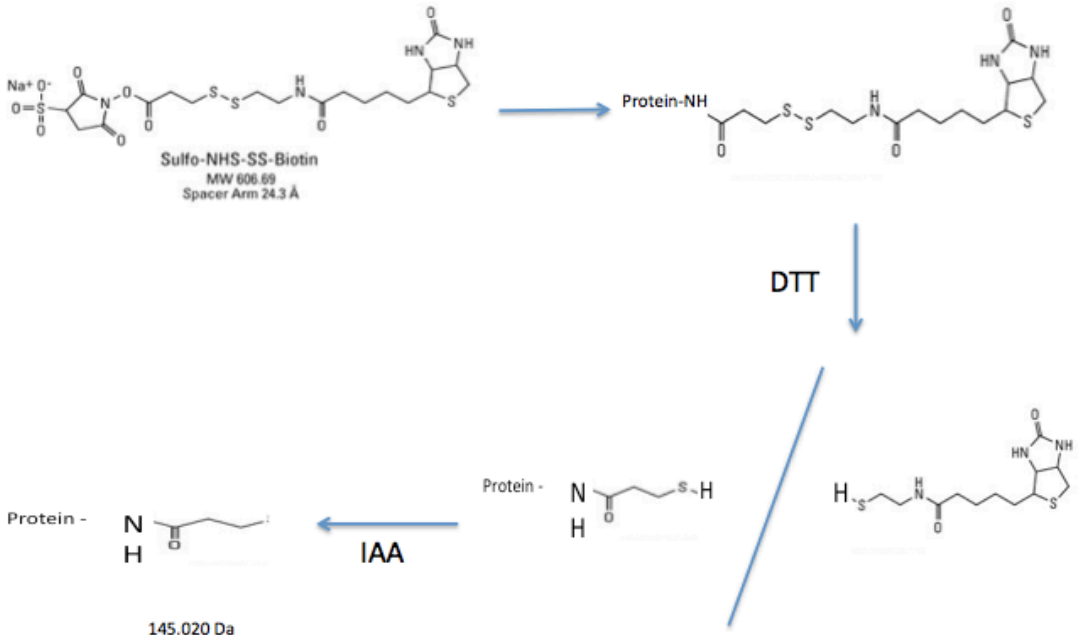


Figure 42. Biotin compound. This figure represents the residual biotin compound left attached to Tryptic peptides. During sample preparation, the sulfhydryl group was first reduced (DTT) and then alkylated (iodoacetamide) to yield a carbamidomethyl group (C_2H_4NO). The loss of one H from the sulfhydryl results in a net gain of C_2H_3NO (57.022 Da). The final modification considered in the MS database search is $C_5H_7NO_2S$, with a molecular weight of 145.020 Da.

From the raw data, for each protein I took into consideration the percentage of total spectra for that protein. This number corresponds to the number of spectra assigned to any given protein divided by the total number of spectra in the sample. Among all the proteins, I filtered those with more than zero percentage of total spectra in at least one of the three conditions (Bio, PBS and Total cell lysate). A total of 902 proteins were identified in the three conditions. A total of 241 proteins were identified in the Bio condition, 111 proteins in the PBS control sample and 850 proteins in the total cell lysate (Figure 43). The list of the proteins can be found in the Supplementary data CD-ROM, folder named “List of proteins”.

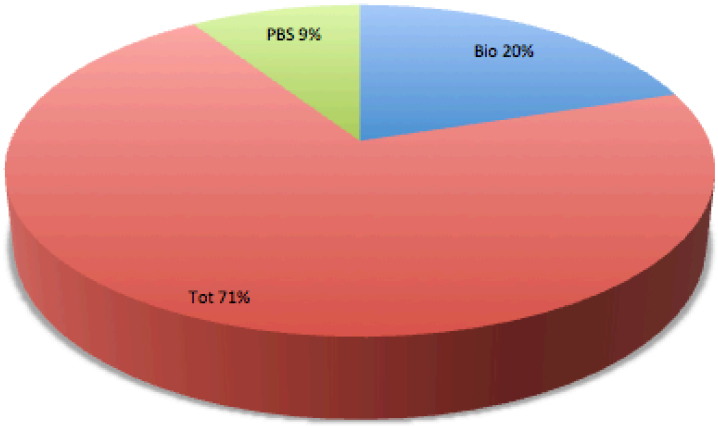


Figure 43. Summary of identified proteins. Proteins in the samples labelled (Bio blue section) with Sulfo-NHS-SS-Biotin, non-labelled (PBS green section) and total cell lysate (Tot red section). A total of 241 proteins (20%) were identified in the Bio condition, 850 (71%) proteins identified in Tot condition and 111 (9%) identified in the PBS condition.

In order to check whether the Biotinylation was able to isolate and enrich the surface proteins, I built two lists: in the first one I calculated and identified those whose percentage of total spectra was at least twice as high in the Bio condition compared with the PBS condition (see Supplementary data CD-ROM, file named “Bio condition compared with PBS condition”); in the second list I calculated and identified those whose percentage of total spectra was at least twice as high in the Bio condition compared with the Total cell lysate condition (see Supplementary data CD-ROM, file named “Bio condition

compared with Total cell lysate condition"). Among these two lists I have then chosen those proteins whose percentage of total spectra was at least twice as high in the Bio condition compared with both PBS and Total cell lysate conditions. In addition, I assessed the location of the identified proteins within the cell (membrane or intracellular) and excluded any contaminating intracellular protein.

A total of 180 proteins in the Bio condition were identified with two-fold or more enrichment compared to the PBS control. 65 proteins in the Bio condition were identified with two-fold or more enrichment compared to the Total cell lysate. The location of the 180 and 65 labelled proteins (Bio condition) was assessed using http://www.uniprot.org/ http://www.genecards.org/ and http://human.med.utoronto.ca/index.php websites. The data from the websites agreed and were based on publications and clear experimental evidence such as Edman sequencing, identification by mass spectrometry, X-ray or NMR structure, good quality protein-protein interaction or detection of the protein by antibodies. 16% of the 180 proteins were identified as membrane proteins, 10% were identified in both membrane and intracellular locations, 66% of proteins were identified in intracellular locations and information was not available for 8% (Figure 44- A). 32% of the 65 proteins were identified on the membrane, 12% were identified in both membrane and intracellular locations, 45% were identified in intracellular locations and no data was available for the remaining 11% (Figure 44- B). The list of the proteins can be found in the Supplementary data.

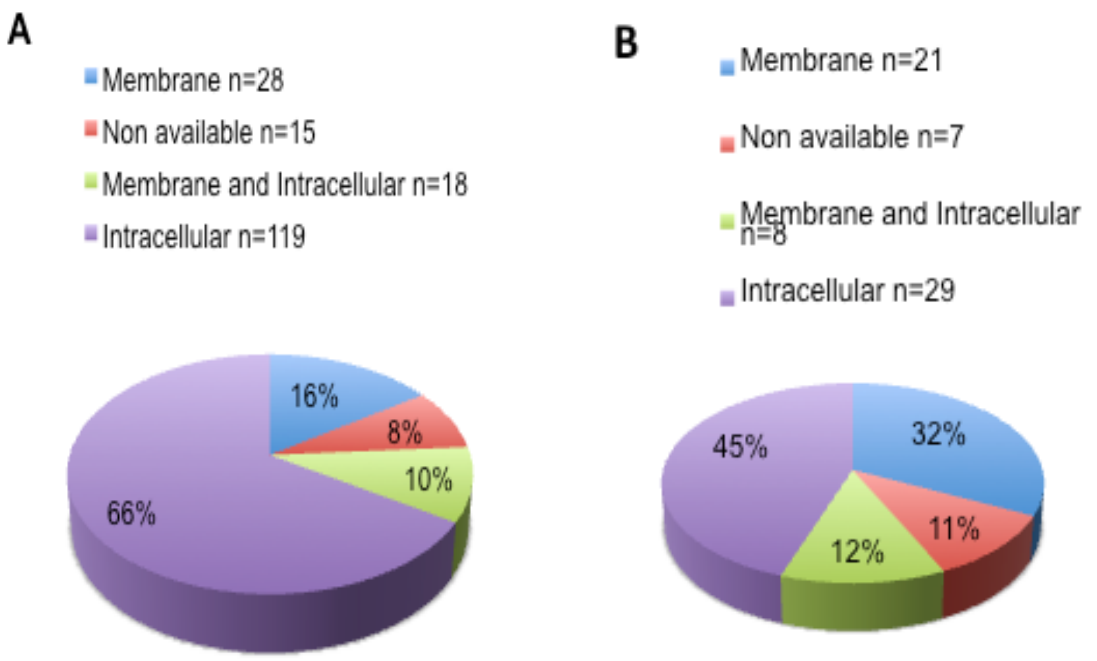


Figure 44. Location of labelled proteins (Bio condition). Location of the labelled proteins (Bio condition) whose percentage of total spectra was at least twice as high in the Bio condition compared to the PBS condition (A) and Total cell lysate (B). (A) Location of the 180 labelled proteins (Bio condition): 28 proteins were identified on the membrane, for 15 proteins the location was not available, 18 proteins were identified in both membrane and intracellular locations and 119 proteins were identified in the intracellular location. (B) Location of the 65 labelled proteins (Bio condition): 21 proteins were identified on the membrane, for 7 proteins the location was not available, 8 proteins were identified in both membrane and intracellular locations and 29 proteins were identified in the intracellular location. Keratin, Albumin and Trypsin were excluded from the list.

After I identified the proteins in the Bio condition with two-fold or more enrichment compared to PSB or Total cell lysate, 55 labelled proteins with two-fold or more enrichment compared to PSB and Total cell lysate were identified. Of these 55 proteins, 19 proteins (34.54%) were identified as membrane proteins or proteins secreted outside the cell membrane, 6 proteins were identified as membrane and intracellular proteins (10.90%), 24 proteins were identified as intracellular proteins (43.63%) and no data were available for the remaining 6 proteins (10.90%) (Table 14).

Table 14. List (Location order) of the 55 proteins identified in the Bio condition.

Identified proteins in the cells labeled with biotin (Bio condition)	Uniprot AC number	Enrichment compared to the PBS condition	Enrichment compared to the Tot condition	Location (http://human.med.utoronto.ca/index.php and http://www.uniprot.org/)
Apolipoprotein L1	O14791	2.7	2.7	Secreted outside the membrane
ATP-binding cassette sub-family A member 3	Q99758	2.7	2.7	Cell membrane
Beta-2-microglobulin	P61769	5.3	5.3	Secreted outside the membrane
CD48 antigen	P09326	2.7	2.7	Cell membrane
Dermcidin	P81605	2.7	2.7	Secreted outside the membrane
HLA class I histocompatibility antigen. B-15 alpha chain	P30464	19	2.6	Membrane, Single-pass type I membrane protein.
HLA class I histocompatibility antigen. B-41 alpha chain	P30479	2.7	2.7	Membrane, Single-pass type I membrane protein.
HLA class I histocompatibility antigen. B-48 alpha chain	P30486	2.7	2.7	Membrane, Single-pass type I membrane protein.
Integrin alpha-L	P20701	5.3	5.3	Membrane, Single-pass type I membrane protein
Integrin beta-1	P05556	2.7	2.7	Membrane, Single-pass type I membrane protein.melanosome
L-xylulose reductase	Q7Z4W1	2.7	2.7	Membrane. Pheripheral membrane protein
Lysozyme C	P61626	2.7	2.7	Secreted outside the membrane
Protein tyrosine phosphatase receptor type C-associated protein	Q14761	8	8	Membrane, Single-pass membrane protein
Receptor-type tyrosine-protein phosphatase C	P08575	28.57	2.22	Cell membrane, Single-pass type I membrane protein
Signaling threshold-regulating transmembrane adapter 1	Q9Y3P8	2.7	2.7	Cell membrane, Single-pass type I membrane protein
Suprabasin	Q6UWP8	2.7	2.7	Secreted outside the cell membrane
T-cell surface glycoprotein CD3 delta chain	P04234	5.3	5.3	Cell membrane, Single-pass type I membrane protein
T-cell surface glycoprotein CD3 epsilon chain	P07766	2.7	2.7	Cell membrane, Single-pass type I membrane protein
T-cell surface glycoprotein CD5	P06127	8	8	Cell membrane, Single-pass type I membrane protein
2.4-dienoyl-CoA reductase. mitochondrial	Q16698	2.7	2.7	Mitochondrion
39S ribosomal protein L12. mitochondrial	P52815	2.7	2.7	Mitochondrion
40S ribosomal protein S14	P62263	5.3	2.52	Nucleus
40S ribosomal protein	P61247	16	3.8	Cytoplasm. nucleus

S3a				
6-phosphogluconolactonase	O95336	2.7	2.7	Cytoplasm
60S ribosomal protein L11	P62913	5.3	2.52	Nucleus
60S ribosomal protein L22	P35268	5.3	5.3	Nucleus
80 kDa MCM3-associated protein	O60318	2.7	2.7	Nucleus
Arf-GAP with dual PH domain-containing protein 1	O75689	2.7	2.7	Nucleus, Cytoplasm
DNA annealing helicase and endonuclease ZRANB3	Q5FWF4	2.7	2.7	Nucleus. Chromosome.
Dynein heavy chain 11. axonemal	Q96DT5	2.7	2.7	Cytoplasm
ELAV-like protein 1	Q15717	2.7	2.7	Cytoplasm
Enoyl-CoA hydratase. mitochondrial	P30084	5.3	2.52	Mitocondria
F-actin-capping protein subunit alpha-1	P52907	8	2.5	Cytoplasm, cytoskeleton
High mobility group protein HMG-I/HMG-Y	P17096	2.7	2.7	Nucleus
Hornerin	Q86YZ3	2.85	8	Cytoplasm
Hypoxanthine-guanine phosphoribosyltransferase	P00492	5.3	5.3	Cytoplasm
Polyubiquitin-B	P0CG47	3.92	3.54	Cytoplasm. nucleus
Protein S100-A11	P31949	2.7	2.7	Cytoplasm nucleus
Putative SCAN domain-containing protein 2	Q9GZW5	2.7	2.7	Nucleus
Putative tropomyosin alpha-3 chain-like protein	A6NL28	2.7	2.7	Cytoplasm, cytoskeleton
Serine/arginine-rich splicing factor 3	P84103	5.3	2.52	Nucleus
Small nuclear ribonucleoprotein Sm D1	P62314	2.7	2.7	Nucleus
Small ubiquitin-related modifier 3	P55854	2.7	2.7	Cytoplasm
Tyrosine-protein kinase Lck	P06239	11	2.61	Cell membrane protein, Cytoplasmic side
Calcium/calmodulin-dependent protein kinase type II subunit beta	Q13554	2.7	2.7	Peripheral membrane protein, cytoplasmic side
GTPase IMAP family member 1	Q8WWP7	8	8	Endoplasmic reticulum membrane, Single-pass type IV membrane protein
Nesprin-1	Q8NF91	2.7	2.7	Nucleus outer membrane, Single-pass type IV membrane protein, cytoplasmic side
Regulator of G-protein signaling 6	P49758	2.7	2.7	Cytoplasm. Membrane, Peripheral membrane protein
Retinitis pigmentosa 1-like 1 protein	Q8IWN7	2.7	2.7	Cytoplasm, cytoskeleton, cilium axoneme. Cell projection
Armadillo repeat-containing protein 8	Q8IUR7	2.7	2.7	Not available
Myosin regulatory light chain 12B	O14950	2.85	2.58	Not available

Phosphoribosyl pyrophosphate synthase-associated protein 2	O60256	8	8	Not available
Protein DDX26B	Q5JSJ4	2.7	2.7	Not available
Protein S100-A4	P26447	2.7	2.7	Not available
Ribose-phosphate pyrophosphokinase 2	P11908	2.7	2.7	Not available

List (Location order) of the 55 proteins identified in the Bio condition with more than two-fold difference in the percentage of total spectra, compared to the PBS and Total cell lysate conditions. 19 proteins (34.54%) were identified as membrane proteins or proteins secreted outside the cell membrane (written in blue), 6 proteins were identified as membrane and intracellular proteins (10.90%) (written in purple), 24 proteins were identified as intracellular proteins (43.63%) (written in red) and no data were available for the remaining 6 proteins (10.90%)

The preliminary data from the MS analysis shows that there is an increase in the percentage of total spectra for 19 membrane proteins in the Bio Sample compared to PBS and Total cell lysate conditions. The presence of 24 intracellular proteins among the list (Table 14) could be due to the ability of the Biotin to tag primary amine groups of proteins also within dead cells or that these proteins are also present on the surface of cells. The purpose of this experiment was to enrich the cell surface proteins and identify them. Therefore, because the Biotinylation method was able to enrich 17 membrane proteins two-fold or more compared with non-Biotin labelled samples these preliminary data suggest that the method can potentially be used to concentrate membrane proteins. However, considering the low number of Treg cells in the samples we wish to analyse, the relatively high number of dead cells in these cultures and the presence of a significant number of intracellular proteins even after purification, we concluded that his method may not be the best choice for the purpose of this project. As a more “targeted” mass spectrometry (CyTOF technology) became available at this time and the possibility of using multidimensional analysis of TrLCs (both surface markers and intracellular cytokines), we have opted to use this technology to better characterise TrLCs.

5.4.2. TrLC phenotype characterisation

In this part of the Chapter we wanted to comprehensively characterise and compare the phenotype of T_{con} and TrLCs. We also had the chance to study PBMCs from HDs compared with PBMCs from MDS patients. We decided to use CyTOF [123], a deep phenotyping strategy method using multi-parameter mass cytometry.

5.4.2.1. PBMCs HDs versus PBMCs MDS patients

For this section 3 biological replicates of PBMCs from HDs were analysed together with 3 samples from MDS patients. All the 3 patients were high-risk MDS patients (see Chapter 2, section 2.1). The idea was to compare and to investigate the markers from both conditions (+/- 5AzaC) from HDs and MDS patient samples and identify potential differences between PMCs from HD and MDS in terms of distinct populations and cytokine profile.

PBMCs were isolated from HDs and MDS patient samples using gradient cell separation (see Chapter 3, section 2.1) and were treated with 5AzaC or with DMSO as follows: culture with 2 μM 5AzaC (Celgene) or 2 μL/ml DMSO as vehicle (Sigma) was carried out in a 48-well cell culture plate (Cellstar) ($1x10^6$ cells each well) with 1ml/well X-Vivo media (Lonza) or a 96-well cell culture plate (Cellstar) ($0.5x10^6$ to $0.25x10^6$ cells each well) with 500ul/well X-Vivo. 5AzaC was dissolved in DMSO and therefore DMSO was used as the control vehicle. In both conditions (5AzaC and DMSO), cells were stimulated with 10 μ L/$1x10^6$ cells anti-CD3/CD28 expander beads (Dynabeads Human T-activator, Invitrogen ratio 1:15). Cultured cells were initially stimulated for 24 hours. 5AzaC or DMSO were added to the cultures on days 2 to 5 and cells were harvested for further analysis on day 6. Because of the abundant stimulation induced by the beads, at day 8, magnetic beads were removed using a magnetic plate and cells were left in culture overnight to rest. At day 9, 2 μ l/ml Leukocyte Activation Cocktail with BD Golgi Plug (BD Pharmingen) was added and incubated for 4 hours according to the manufacturer's instructions at 37°C in the 5% CO_2 Incubator (240i HERACell ThermoScientific). Cells were harvested as follows: the X-Vivo media containing the cells was transferred to a 15ml tube, then centrifuged at 270 x

G_{max} for 10 minutes and the media was removed. The centrifugation step and removal of the media was repeated twice. The cell pellet was finally resuspended in 100 μl of PBS. Cells were then ready to be stained for intracellular and surface proteins (see section 3.3.1 of this current Chapter) and analysed using CyTOF. After the. fcs files were generated, we applied the normalisation and gated cell populations using the Cytobank 2D gating tool (Figure 38). After the gating, we focused on $CD4^+$ cells. To visualise major cell subsets, we used viSNE (see section 3.3.2 of this current Chapter). Then, the use of SPADE on *t*-SNE (that is the result of viSNE) was applied to the dataset to discover and to cluster cell subsets (see section 3.3.2 of this current Chapter). We downloaded the statistics for all markers (TNF-α, CD45, IL-17a, CD279, CD154, CD62L, HLA_DR, T-bet, IL-6, IL-10, CD123, CCR4, IL-4, IFN-γ, CD25, CD69, CD38, IL-2, CD127, CD8, CD45RA, CD3, FOXP3, GATA3, CD11 and CD4). Data were scaled with co-factor of 5 as recommended for CyTOF data. We focused on cells expressing a high level of FOXP3 (identified as explained in the Materials and Methods section) and we generated a heat map of the markers that were chosen to characterise TrLCs (TNF-α, CD45, IL-17a, CD279, CD154, CD62L, HLA_DR, T-bet, IL-6, IL-10, CCR4, IL-4, IFN-γ, CD25, CD69, CD38, IL-2, CD127, CD45RA, FOXP3, GATA3 and CD4) to have a broad idea of the expression of every marker in the datasets (Figures 45-46-47 and 48).

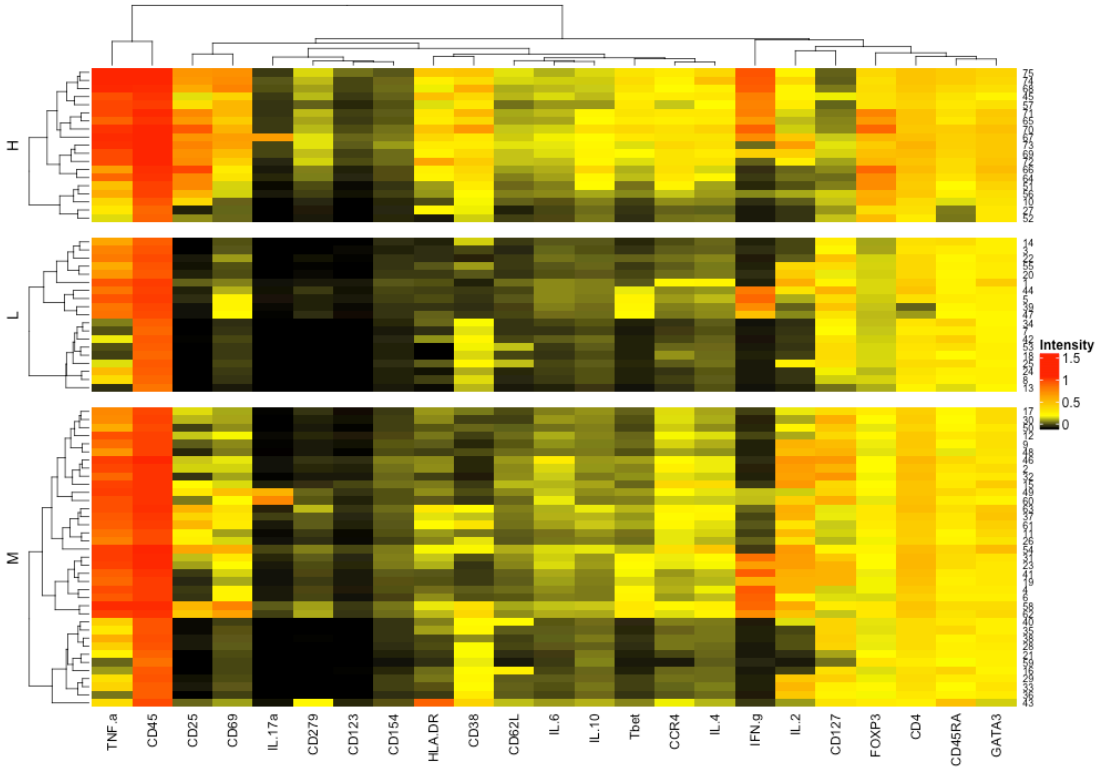


Figure 45. Analysis of PBMCs expressing FOXP3 from HDs treated with 5AzaC. In this heat map, TNF-α, CD45, CD25, CD69, IL-17a, CD279, CD123, CD154, HLA_DR, CD38, CD62L, IL-6, IL-10, T-bet, CCR4, IL-4, IFN-γ, IL-2, CD127, FOXP3, CD4, CD45RA, GATA3 markers were tested in PBMCs from HDs treated with 5AzaC that express FOXP3. The expression level corresponds to the intensity legend. In these 3 plots, cells that expressed high “H”, low “L” and medium “M” FOXP3 are studied.

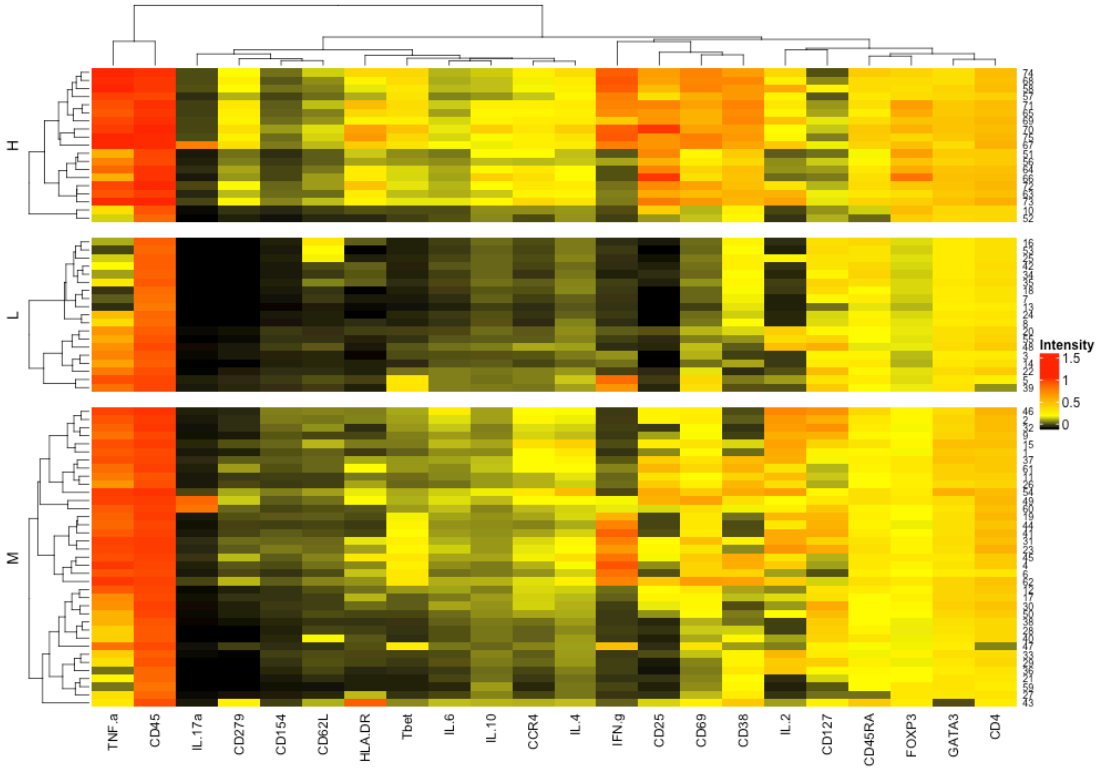


Figure 46. Analysis of PBMCs expressing FOXP3 from HDs treated with DMSO. In this heat map, TNF-α, CD45, IL-17a, CD279, CD154, CD62L, HLA_DR, T-bet, IL-6, IL-10, CCR4, IL-4, IFN-γ, CD25, CD69, CD38, IL-2, CD127, CD45RA, FOXP3, GATA3 and CD4 markers were tested in FOXP3 expressed PBMCs HDs treated with 5AzaC. The expression level corresponds to the intensity legend. In these 3 plots, cells that expressed high “H”, low “L” and medium “M” FOXP3 are studied

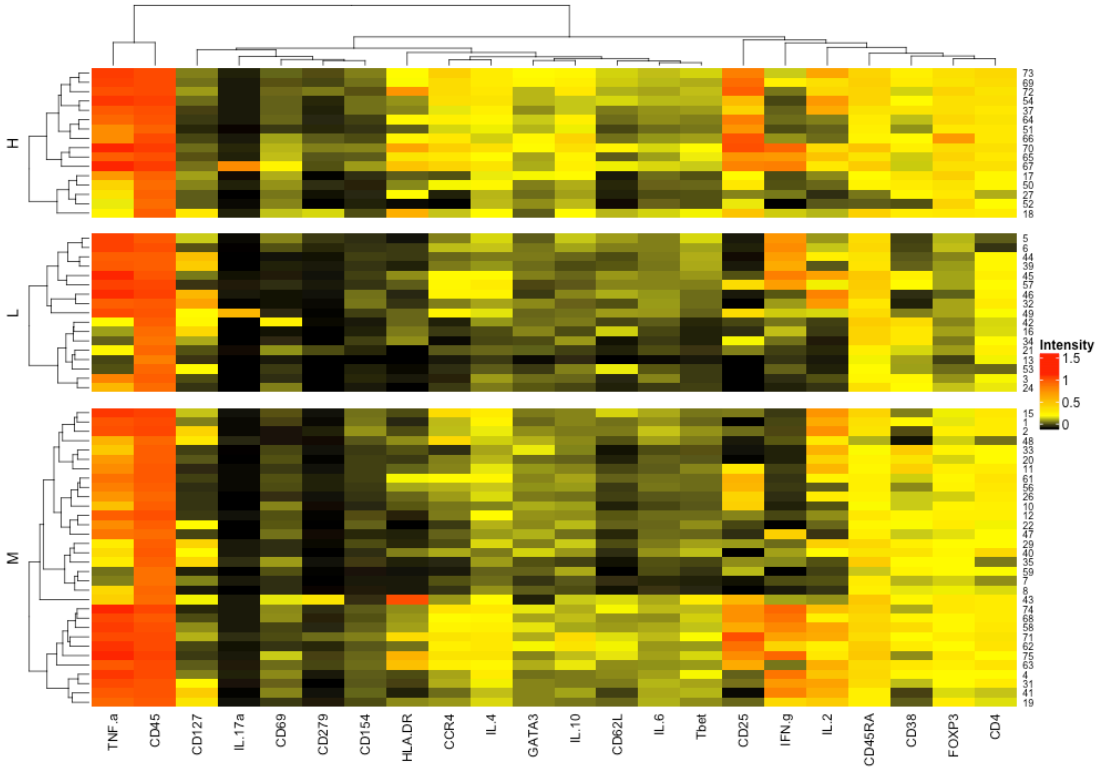


Figure 47. Analysis of PBMCs expressing FOXP3 from MDS patients treated with DMSO. In this heat map, TNF-α, CD45, IL-17a, CD279, CD154, CD62L, HLA_DR, T-bet, IL-6, IL-10, CCR4, IL-4, IFN-γ, CD25, CD69, CD38, IL-2, CD127, CD45RA, FOXP3, GATA3 and CD4 markers were tested in FOXP3 expressed PBMCs HDs treated with 5AzaC. The expression level corresponds to the intensity legend. In these 3 plots, cells that expressed high “H”, low “L” and medium “M” FOXP3 are studied.

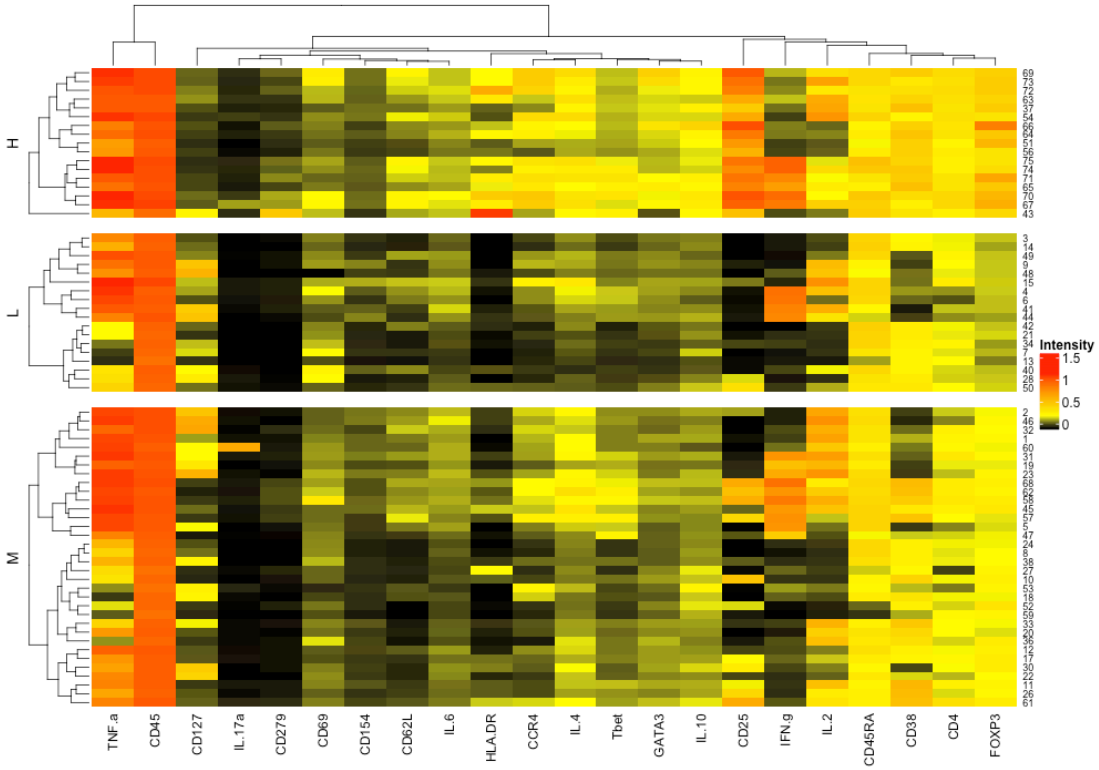


Figure 48. Analysis of PBMCs expressing FOXP3 from MDS patients treated with 5AzaC. In this heat map, TNF-α, CD45, IL-17a, CD279, CD154, CD62L, HLA_DR, T-bet, IL-6, IL-10, CCR4, IL-4, IFN-γ, CD25, CD69, CD38, IL-2, CD127, CD45RA, FOXP3, GATA3 and CD4 markers were tested in FOXP3 expressed PBMCs HDs treated with 5AzaC. The expression level corresponds to the intensity legend. In these 3 plots, cells that expressed high "H", low "L" and medium "M" FOXP3 are studied.

The main question in this part of the Chapter is whether TrLCs closely resemble Tregs or T_{con} in terms of their phenotype, so we decided to focus on the cell clusters that expressed higher FOXP3, because it is a feature of Tregs.

From all the markers listed above, except FOXP3 and CD4 (Figure 49) we focused on the markers that were statistically significant ($p < 0.05$) between the two conditions (+/- 5AzaC).

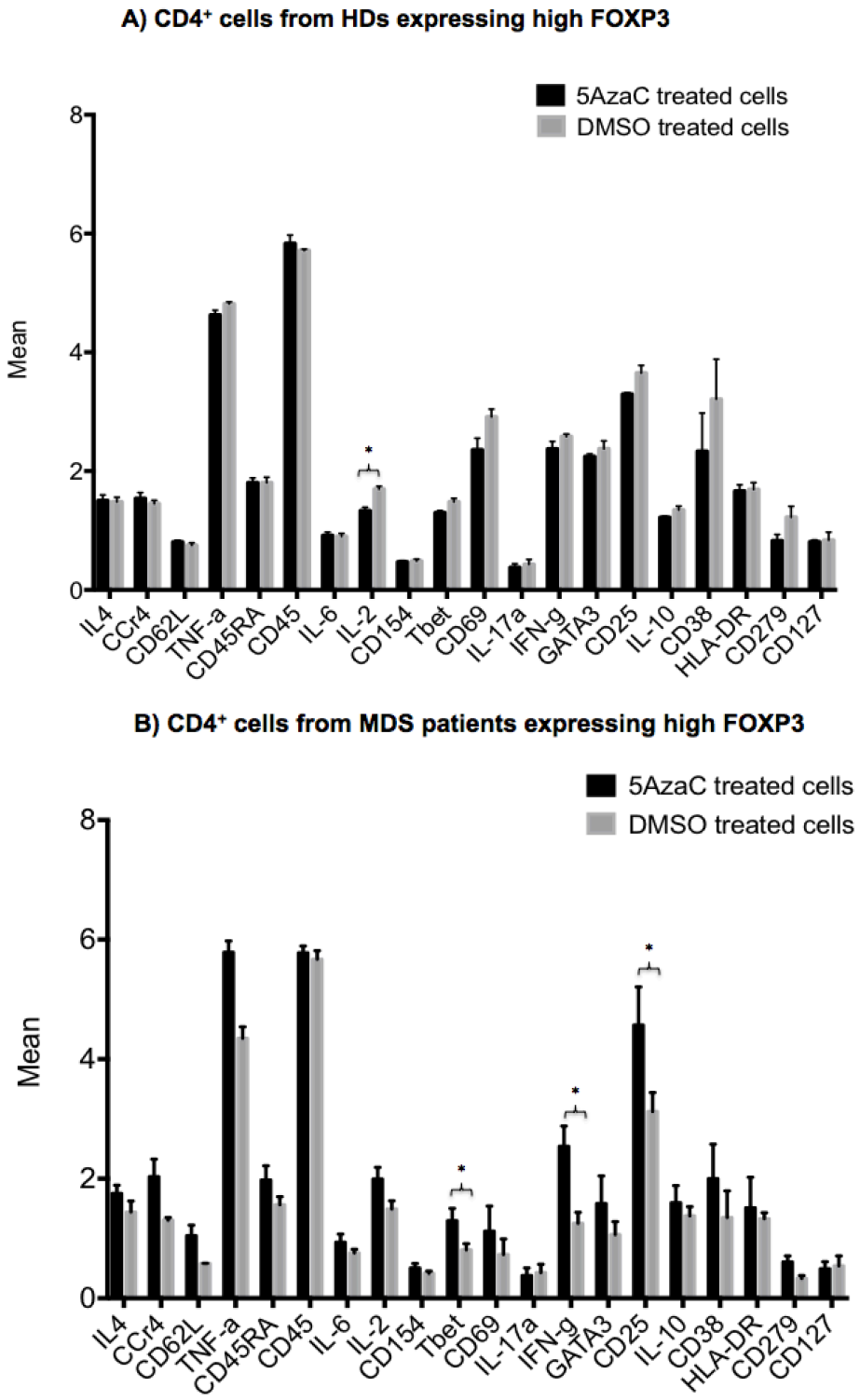


Figure 49. CD4+ cells from HDs and MDS patients: marker analysis.

Plot A) shows the expression of the markers shown in CD4+ cells from HDs with high FOXP3 expression. A total of 26 markers were investigated in cells cultured with 5AzaC and DMSO (diluent control) treated cells. Plot B) shows the expression of the same markers in $CD4^+$ cells from MDS patients with high FOXP3 expression. The average of the 3 biological replicates for each marker is shown. Errors bars are standard error of the mean. * indicate statistically significant differences ($p<0.05$).

For the $CD4^+$ cells from the MDS samples, culturing with 5AzaC causes a statistically significant increase in CD25 (*p*-value 0.0461), T-bet (*p*-value 0.0404) and IFN-γ (*p*-value 0.0198). Whereas for the $CD4^+$ cells from the HDs, culturing with 5AzaC leads to an increase in IL-2 (*p*-value 0.0129).

The increase in CD25 in MDS samples caused by 5AzaC treatment is a feature of Tregs. However, high expression of INF-γ and T-bet in these cells is not typical of Tregs (Figure 50). In contrast, 5AzaC treatment of cells from HDs, reduced the expression of IL-2, which is common for Tregs, but crucial cytokines normally expressed by Tregs *e.g.* IL-10, TGF-β and IL-35 were not present (Figure 51).

These data suggest that $CD4^+$ cells from MDS patients expressing high levels of FOXP3 are polarised towards a T helper profile rather than a Treg profile[38],, compared with $CD4^+$ T cells from HDs expressing high FOXP3.

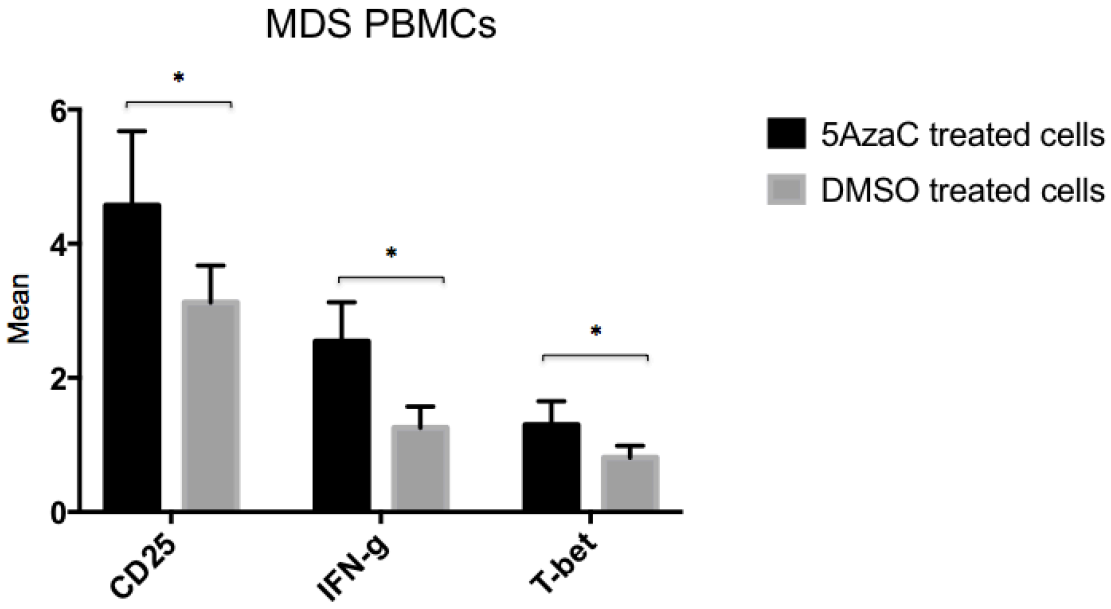


Figure 50. $CD4^+$ T cells expressing high FOXP3 from PBMCs isolated from MDS patients. The mean of cells expressing each marker in cells cultured with and without 5AzaC is shown. A total of 3 markers were investigated: IFN-γ, CD25, and T-bet between 5AzaC treated cells and DMSO treated cells. The average of the 3 biological replicates for each marker is shown. Errors bars are standard error of the mean. * indicates a statistically significant difference (*P*-value < 0.05).

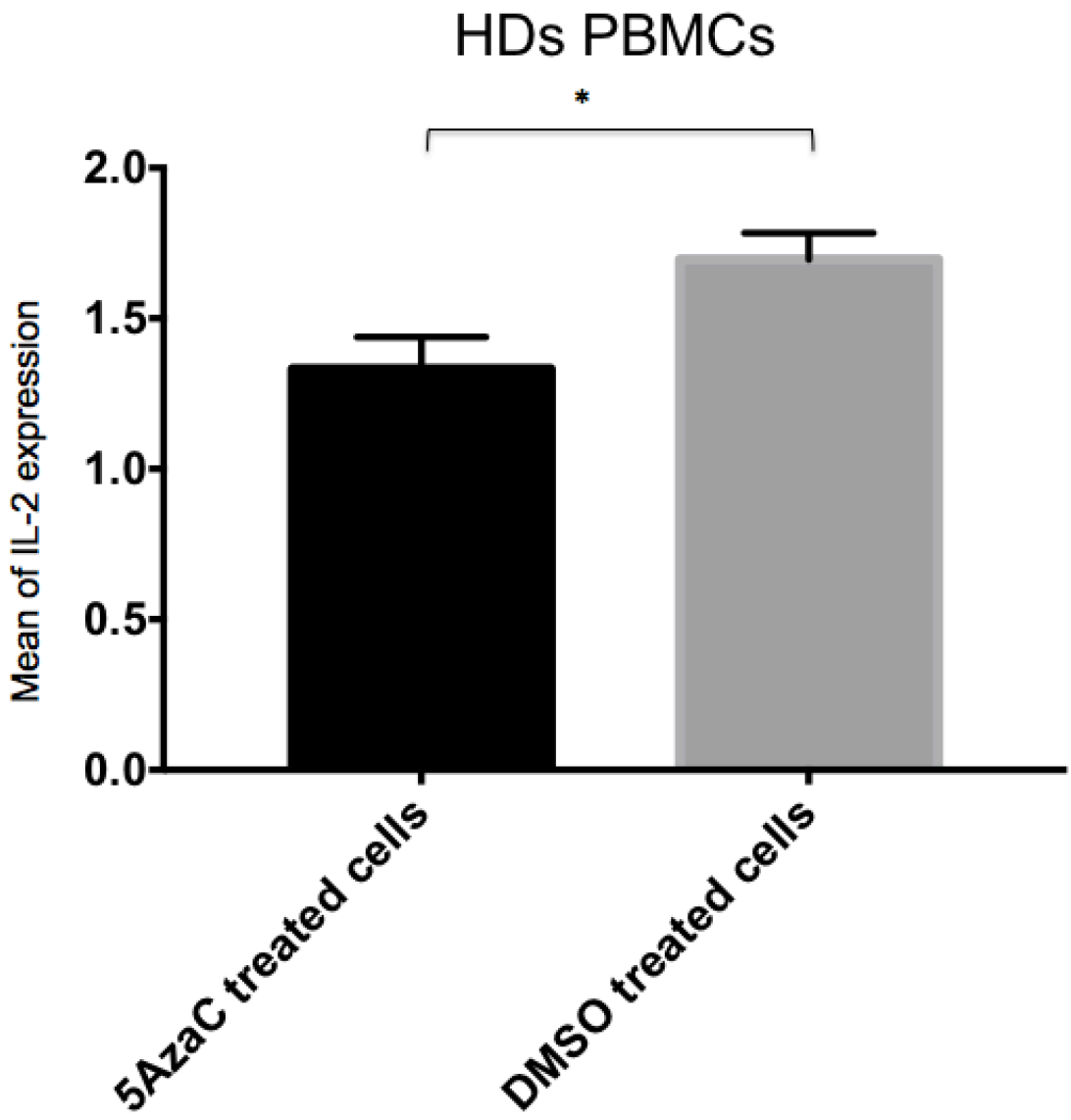


Figure 51. CD4^{+} T cells expressing high FOXP3 from PBMCs isolated from HDs. The mean of cells expressing IL-2 in cells cultured under the two conditions is displayed: 5AzaC treated cells and DMSO treated cells. The graphs are an average of the 3 biological replicates. Errors bars are standard error of the mean. *P*-value < 0.05

5.4.2.2. Profile analysis of T_{con} from HDs (+/- 5AzaC)

The focus of this section is to determine whether TrLCs are closer to Tregs in terms of their phenotype or to another subpopulation, like T inflammatory cells. In order to study that we focused on T_{con} (+/- 5AzaC) that express high levels of FOXP3, a canonical marker for Tregs. We cultured the biological replicate isolates of T_{con} from HDs with 5AzaC and with DMSO as described in section 1.4.2.1 Cells were then ready to be stained for intracellular and surface proteins (section 3.3.1 of this current Chapter) and analysed using

CyTOF. After. fcs file was generated, we applied the normalisation and we gated them using Cytobank 2D. To visualise major cell subsets, we used ViSNE (see section 3.3.2 of this current Chapter). Then, the use of SPADE on *t*-SNE (that is the result of viSNE) was applied to the dataset to discover and to cluster cell subsets (see section 3.3.2 of this current Chapter). We downloaded the statistics data for the markers that were chosen to characterise TrLCs (TNF-α, CD45, IL-17a, CD279, CD154, CD62L, HLA_DR, T-bet, IL-6, IL-10, CCR4, IL-4, IFN-γ, CD25, CD69, CD38, IL-2, CD127, CD45RA, FOXP3, GATA3 and CD4 markers) and we generated a heat map, as described in section 3.3.2 (Figures 52-53). Then, we scaled the dataset to discriminate cells with high/low/medium expression of FOXP3 (Figures 54-55. We then focused on the cells expressing high FOXP3.

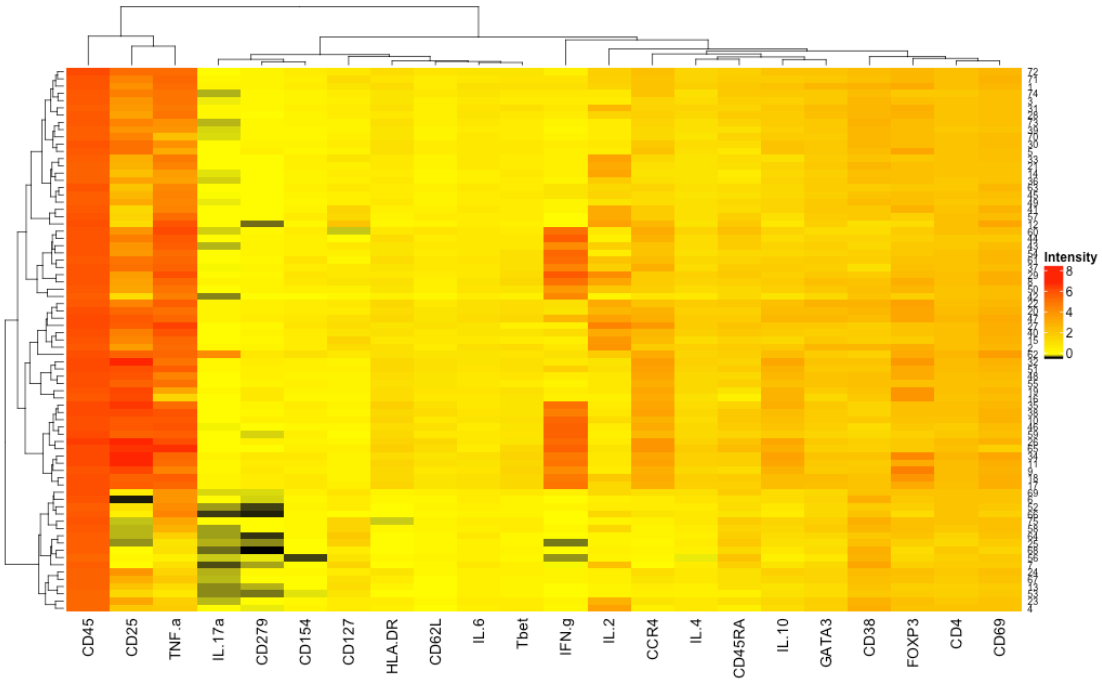


Figure 52. T_{con} from HDs treated with DMSO. In this heat map, TNF-α, CD45, IL-17a, CD279, CD154, CD62L, HLA_DR, T-bet, IL-6, IL-10, CCR4, IL-4, IFN-γ, CD25, CD69, CD38, IL-2, CD127, CD45RA, FOXP3, GATA3 and CD4 markers were analysed in the 3 biological replicates of T_{con} from HDs treated with DMSO. The expression level corresponds to the intensity legend. The dendograms on the left cluster the cells based on the physical distance, whereas those on top of the heat map cluster cells based of signal strength.

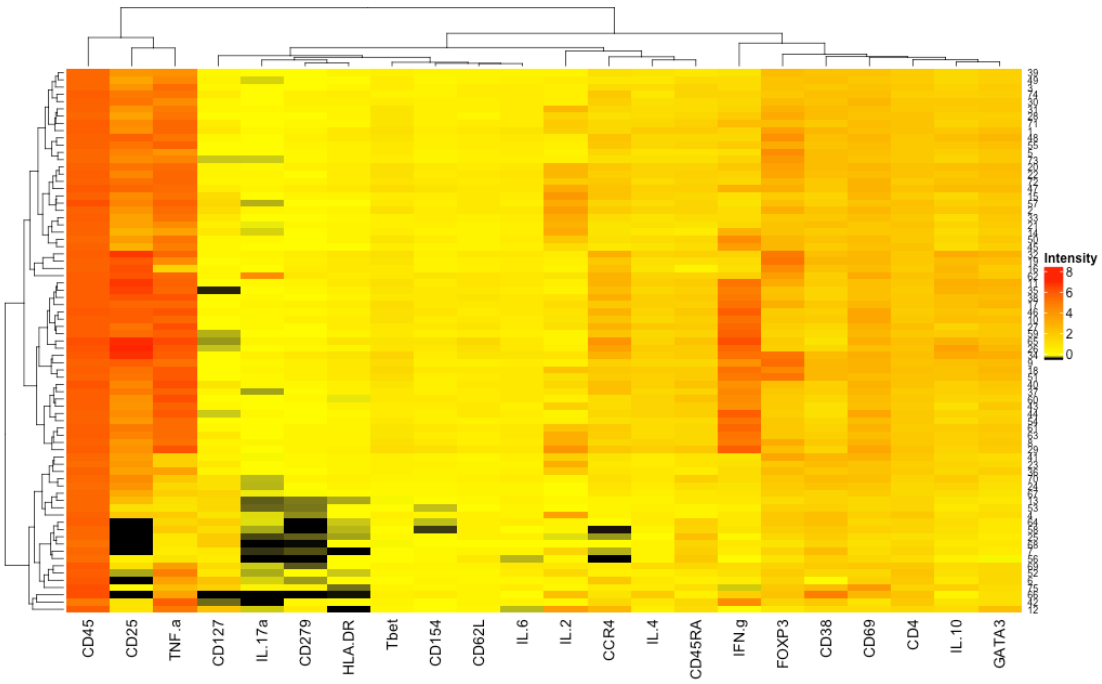


Figure 53. T_{con} from HDs treated with 5AzaC. In this heat map, TNF-α, CD45, IL-17a, CD279, CD154, CD62L, HLA_DR, T-bet, IL-6, IL-10, CCR4, IL-4, IFN-γ, CD25, CD69, CD38, IL-2, CD127, CD45RA, FOXP3, GATA3 and CD4 markers were analysed in the 3 biological replicates of T_{con} from HDs treated with 5AzaC. The expression level corresponds to the intensity legend. The dendograms on the left cluster the cells based on the physical distance, whereas those on top of the heat map cluster cells based of signal strength.

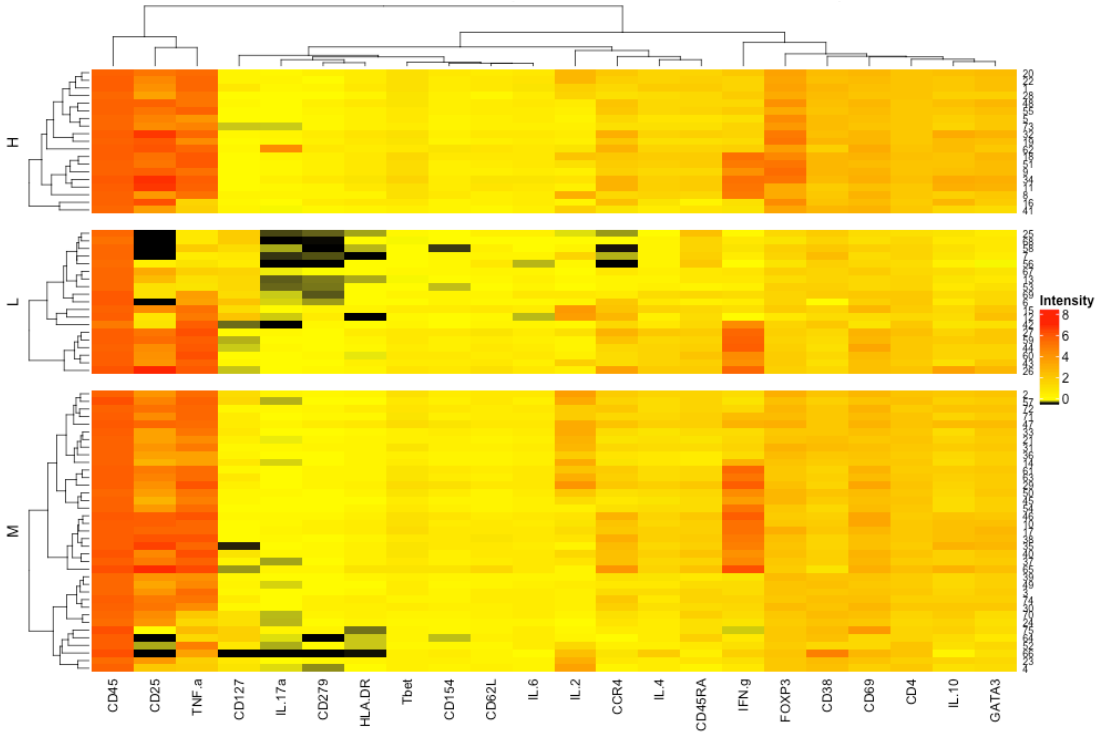


Figure 54. FOXP3 expression clusters of 5AzaC treated T_{con}. The dataset was scaled to discriminate cells with high/low/medium expression of FOXP3. TNF-α, CD45, IL-17a, CD279, CD154, CD62L, HLA_DR, T-bet, IL-6, IL-10, CCR4, IL-4, IFN-γ, CD25, CD69, CD38, IL-2, CD127, CD45RA, FOXP3, GATA3 and CD4 markers were analysed in the 3 biological replicates of T_{con} from HDs treated with 5AzaC. The expression level corresponds to the intensity legend. Cells that express high "H", low "L" and medium "M" FOXP3 are studied.

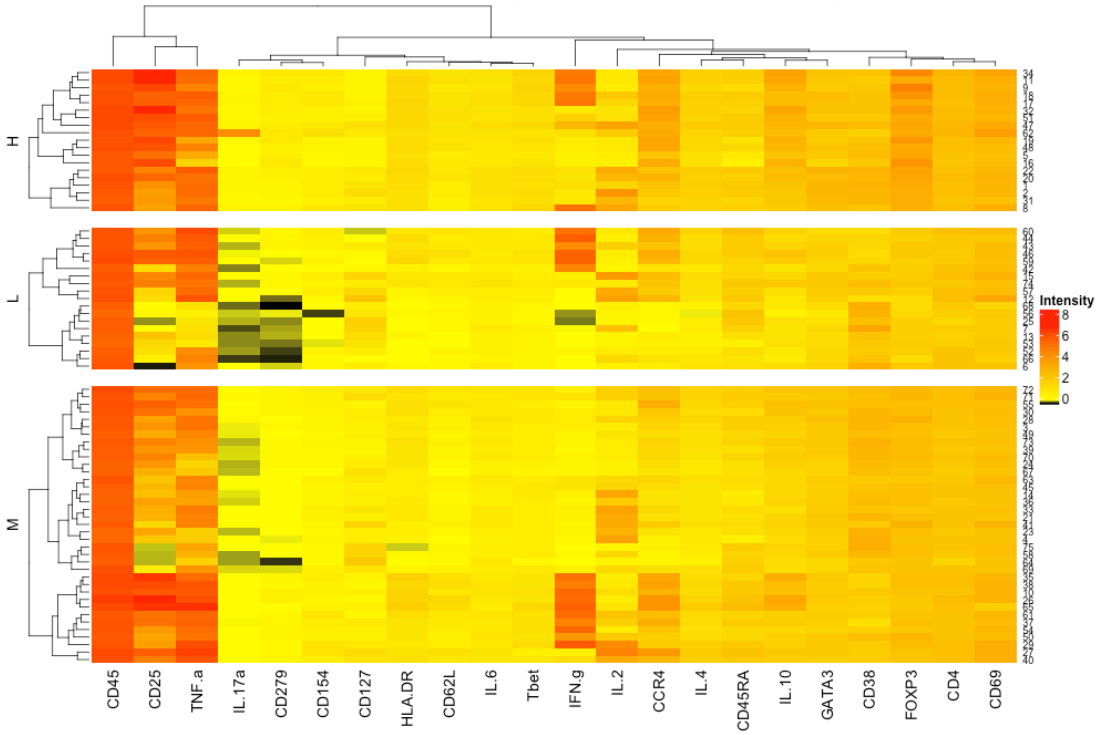


Figure 55. FOXP3 expression clusters of DMSO treated T_{con}.

Dataset was scaled to discriminate cells with high/low/medium expression of FOXP3. TNF-α, CD45, IL-17a, CD279, CD154, CD62L, HLA_DR, T-bet, IL-6, IL-10, CCR4, IL-4, IFN-γ, CD25, CD69, CD38, IL-2, CD127, CD45RA, FOXP3, GATA3 and CD4 markers were analysed in the 3 biological replicates of T_{con} from HDs treated with DMSO. The expression level corresponds to the intensity legend. Cells that express high "H", low "L" and medium "M" FOXP3 are studied.

In order to determine whether TrLCs are closer to Tregs in term of their phenotype or to another subpopulation like T inflammatory cells, we focused on the cluster of T_{con} that express higher FOXP3 and analysed the expression of TNF-α, CD45, IL-17a, CD279, CD154, CD62L, HLA_DR, T-bet, IL-6, IL-10, CCR4, IL-4, IFN-γ, CD25, CD69, CD38, IL-2, CD127, CD45RA, FOXP3, GATA3 and CD4 in these cells. We focused on those that were statistically significantly different ($p < 0.05$) between the 2 conditions (+/- 5AzaC).

5AzaC treated T_{con} expressing high FOXP3 (TrLCs) from HDs expressed low CD127 (*p*-value 0.0279), similar to Tregs, but low IL-10 (*p*-value 0.0129) (Figure 56) compared with the DMSO control. Even though TrLCs express high FOXP3 and low CD127 compared with the DMSO control, the crucial Treg related cytokine (IL-10) is lower than in the control. From these data, we conclude that TrLCs are more likely to be T inflammatory cells rather then Tregs.

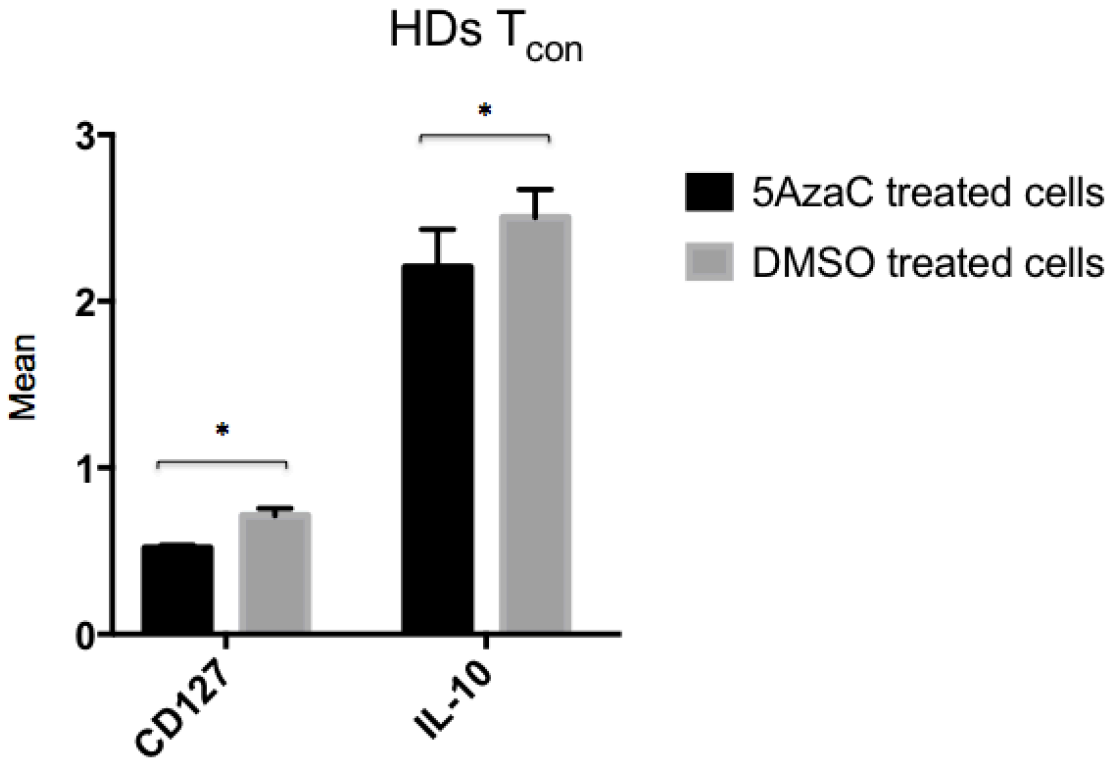


Figure 56. CD4^{+} T cells expressing high FOXP3 from T_{con} isolated from HDs. The mean of cells expressing each marker in cells cultured T_{con} from HDs cultured in the two conditions is displayed. Two statistically significant markers were investigated: CD127 (*p*-value 0.0279) and IL-10 (*p*-value 0.0129) between 5AzaC treated cells and DMSO treated cells. The average of the 3 biological replicates for each marker is shown. Errors bars are standard error of the mean. *P*-value < 0.05

5.5. Discussion

The main aim of this Chapter was to investigate the cell surface proteins expressed on TrLCs and the potential differences between these cells and Tregs. We focused on their surface and intracellular proteins, using mass-spectrometry, both non-targeted (Biotin-Avidin capture/mass spectrometry) and targeted (CyTOF).

First, we focused on identifying components of the cell surface proteome on a large scale. Membrane proteins are crucial for cellular functions (*e.g.* signal transduction, cell adhesion and ion transport) and also for normal cellular differentiation[114]. A cell surface protein Biotinylation and capture method was tested and the data show that the method can be used to isolate membrane proteins. Mass spectrometry analysis (LC-MS-MS) was then used to identify the proteins isolated by this method[122]. Three conditions were processed: Total cell lysate conditions (TOT), cells labelled with biotin (Bio) and cells incubated with diluent only (PBS). The preliminary data from the MS analysis shows that there is an increase in the percentage of the total spectra for 19 membrane proteins in the Bio Sample compared to PBS and TOT samples (Figure 12). The purpose of this experiment was to enrich the cell surface proteins and identify them. The biotinylation method was able to enrich 17 membrane proteins two-fold or more compared with non-biotin labelled samples. Although these preliminary data suggested that the method could have potentially been used to concentrate membrane proteins, we were aware that cultured cells were a mixture of $CD4^+CD25^+$ cells therefore we won't be able to look just at $FOXP3^+$ cells or at specific subsets. In addition, because we wanted to focus just on membrane proteins we used a biotin compound to extract them (section 3.1 of this current Chapter) but we still had some intracellular contamination. The presence of 24 intracellular proteins among the list (Table 14) could be due to the ability of the biotin compound to react with primary amine groups of proteins also within dead cells, or because some of the intracellular proteins have also been shown to be present on the cell surface (see Table 14, purple highlighted proteins). The existence of dead cells could be linked to the protocol and the methods that we were using. This

circumstance makes it very challenging to have a dataset without any intracellular protein contamination.

Meanwhile the single cell mass cytometry or cytometry by time-of-flight [123](CyTOF) became available in our department. This novel method is a deep phenotyping strategy using multi-parameter mass cytometry that we used in a recent study to assess the stability of expanded Tregs[132]. Therfore we continued this project using the CyTOF method (Figure 35) because it allows multi-parametric single cell analysis for more than 40 channels without significant spill over between them[124]. For this section PBMCs from HDs were analysed together with samples from MDS patients. All MDS patients were high-risk MDS. T_{con} from HDs were also analysed to characterise further the TrLCs subset. PBMCs and T_{con} were separately cultured with 5AzaC and DMSO vehicle control, then stained for intracellular and membrane markers and analysed using CyTOF. After the .fcs files were generated, we applied the normalisation and we gated on the $CD4^+$ population for further clustering and downstream analysis. To visualise major cell subsets, we used viSNE (see section 3.3.2 of this current Chapter). Then, the use of SPADE on *t*-SNE (that is the result of viSNE) was applied to the dataset to discover and to cluster cell subsets (see section 3.3.2 of this current Chapter). We downloaded the statistics data for the markers that were chosen to characterise TrLCs. We focused on cells expressing high FOXP3 and we generated a heat map to have a broad idea of every marker expression within the dataset (see section 3.3.2 of this current Chapter). We also analysed the samples further using statistical analysis. First, we wanted to comprehensively characterise $CD4^+$ cells from HDs after 5AzaC treatment focusing on the cells with higher expression of FOXP3.

Interestingly, while in healthy donors TrLCs the main difference between 5AzaC and control was lower expression of IL-10, in MDS patients, however, TrLCs secrete pro-inflammatory cytokines, which suggests that the $CD4^+$ T cells are polarising toward inflammatory T cells. This is in agreement with our published *in-vivo* data of cells isolated from MDS patients who respond to 5AzaC treatment[4] as well as other recently published research suggesting that inhibition of DNA methylation causes an interferon response in cancer[133]. Our findings also reject the hypothesis that 5AzaC expand functional, 'real'

Tregs. In patients with MDS T cell are exposed to a suppressive microenvironment and under check by expanded Tregs[2]. Nonetheless, our data suggest that T cells from high-risk MDS patients could potentially polarise toward inflammatory T cells in response to 5AzaC which may induce immune response against the malignant clone.

6. Quantification of methylated and demethylated*FOXP3 TSDR* and DNA Methylome analysis

6.1. Summary

The drug 5AzaC is a demethylating agent and it was shown to demethylate the *FOXP3* promoter[104], however it is not clear whether 5AzaC has the same effect on the Treg Specific Demethylated Region (*TSDR*) and on the methylation status of gene promoters regulated by FOXP3. In order to understand whether the "Treg-like" cells (TrLCs) were still T_{con} or they have acquired the Treg gene methylation signature, we investigated whether CpG dinucleotides in the *TSDR* are methylated and the methylation status of gene promoters that are regulated by FOXP3.

6.2. Introduction

6.2.1. TSDR analysis

The *TSDR* is contained within a specific intron of the *FOXP3* gene whose CpG dinucleotides are demethylated in nTregs but methylated in the CD3+ T population (Figure 57). It has been proposed that a steady demethylation profile of the *TSDR* is a fundamental feature of stable Tregs[44, 134] (see Chapter 1, section 3.2.1.1). In addition, "CpG islands" (defined as a DNA sequence of around 1000 base pairs (bp) in lenght, that shows an elevated G+C base composition, frequent absence of DNA methylation and little CpG depletion)[135] within the *CD3G/CD3D* intergenic region are unmethylated in T lymphocytes[45]. *Sehouli et al*[45] quantified the percentage of Tregs and $CD3^+$ cells within a tumour using the methylation status of the *TSDR* to identify Tregs and the methylation status of *CD3G/CD3G* to identify $CD3^+$ cells. Because of the importance in my project to identify and quantify Tregs, my purpose was to use techniques such as qPCR to quantify the methylation status of the *TSDR* and *CD3G/CD3D* within Tregs, T_{con} and $CD3^+$ cells. The goal was to apply these techniques to identify and quantify T_{con} and Tregs in samples of $CD3^+$ T cells. However, the inconsistency in the qPCR results (see Chapter 6 section 4.1.3) were such that we decided to switch to amplicon sequencing of bisulfite treated DNA on an Illumina MiSeq instrument[127].

The questions that have been addressed in the first part of this Chapter are:

1. What is the copy number of unmethylated *TSDR* and *CD3G/CD3D* in Tregs, T_{con} and CD3+ cells from HD?
2. What percentage of CpGs of the *TSDR* intron are unmethylated in TrLCs, Tregs and in T_{con} from HD?

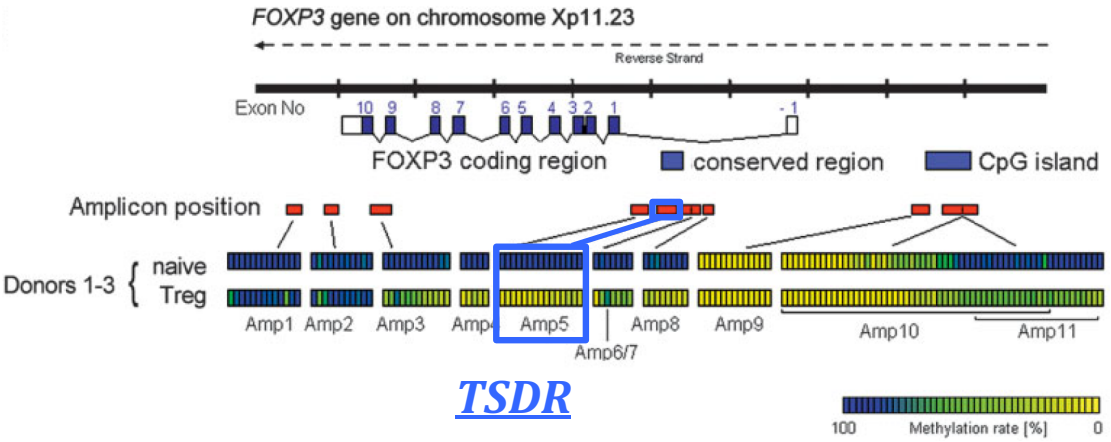


Figure 57. *TSDR* sequence within the *FOXP3* gene. The Figure shows the percentage of *FOXP3* amplicons that are methylated in Tregs *versus* naive T cells. Each box represents methylation of a single CpG according to the colour (yellow=0%, blue=100% methylation). The *TSDR* (Amp 5) from Tregs is less methylated compared with the same region in naive T cells. *Figure adapted from Baron et al 2007*[40]

6.2.2. Genome-wide DNA methylation analysis

In the second part of this Chapter we focused on the methylation state of the promoters of protein-encoding genes throughout the genome of TrLCs, with an emphasis on the genes which are regulated by FOXP3. We wanted to study primarily whether T_{con} are still T_{con} after 5AzaC treatment or if they polarise into another population, such as Tregs. As a well-enstablished result published by many groups, *FOXP3*'s *TSDR* is demethylated in Tregs. As we assessed, it was methylated in TrLCs subpopulation. According to Zhang *et al*[136] the *FOXP3*'s binding sites are demethylated in Tregs as compared with T_{con}. The DNA genome-wide of nTregs and T_{con} HD (+/- 5-AzaC) was investigated, using a methylation analysis (450K Illumina). Our aim was to focus on the list of the *FOXP3* binding sites (Zhang *et al*[136]*)* (see Appendix, Table 20), plus additional interesting genes related to *FOXP3* (see Appendix, Table 20 from gene number 105). Among those genes, we wanted to investigate those that displayed a major difference in term of methylation on T_{con} HD (+/- 5-AzaC).

The questions that we wanted to address in the second part of this Chapter are:

1. What is the methylation state of promoters containing a Foxp3 binding site in T_{con} after 5AzaC treatment?
2. Which gene promoters are most affected by 5AzaC treatment?

3. Are CpG methylation states of these promoters different in T_{con} and Tregs from HD and AML or MDS patients?

6.3. Materials and Methods

General methods which have been used in this Chapter are discussed in Chapter 3. The specific methods used in this Chapter are:

6.3.1. TSDR analysis

6.3.1.1. Annealing temperature

Primers to amplify the *FOXP3-TSDR* and the promoters of *GAPDH* (housekeeping gene) and *CD3G/CD3D* of bisulfite converted and not converted DNA have been published[45, 115] (see Table 9). These primers were synthesized and different annealing temperatures (55°C, 58°C, 61°C and 64°C) were tested. I chose to use genomic DNA (gDNA) isolated from Tcon because these cells are abundant compared to Tregs. The amount of gDNA amplified was measured after each PCR cycle using the SYBR green dye that yields increasing fluorescent signals in direct proportion to the amplicons generated. By plotting fluorescence *versus* cycle number the PCR machine generated an amplification plot that represents the accumulation of product over the duration of the PCR reaction. The best annealing temperature corresponds to a peak in the melt curve, which should be the expected melt temperature (Tm) for the specific qPCR amplified product (amplicon). The peak indicates that the SYBR green is no longer bound to the double strand DNA because of the transition to single strand (sharp decrease in fluorescence). The melt curve analysis at 61° C (Figure 58-B, 58-D, 58-F) was detected at the expected melting temperature for the *FOXP3-TSDR, GAPDH* and *CD3G/CD3D* (86.9°C, 101.8°C and 81°C respectively). Hence, 61°C was deemed to be the optimal annealing temperature, which is in agreement with the previously published study[115].

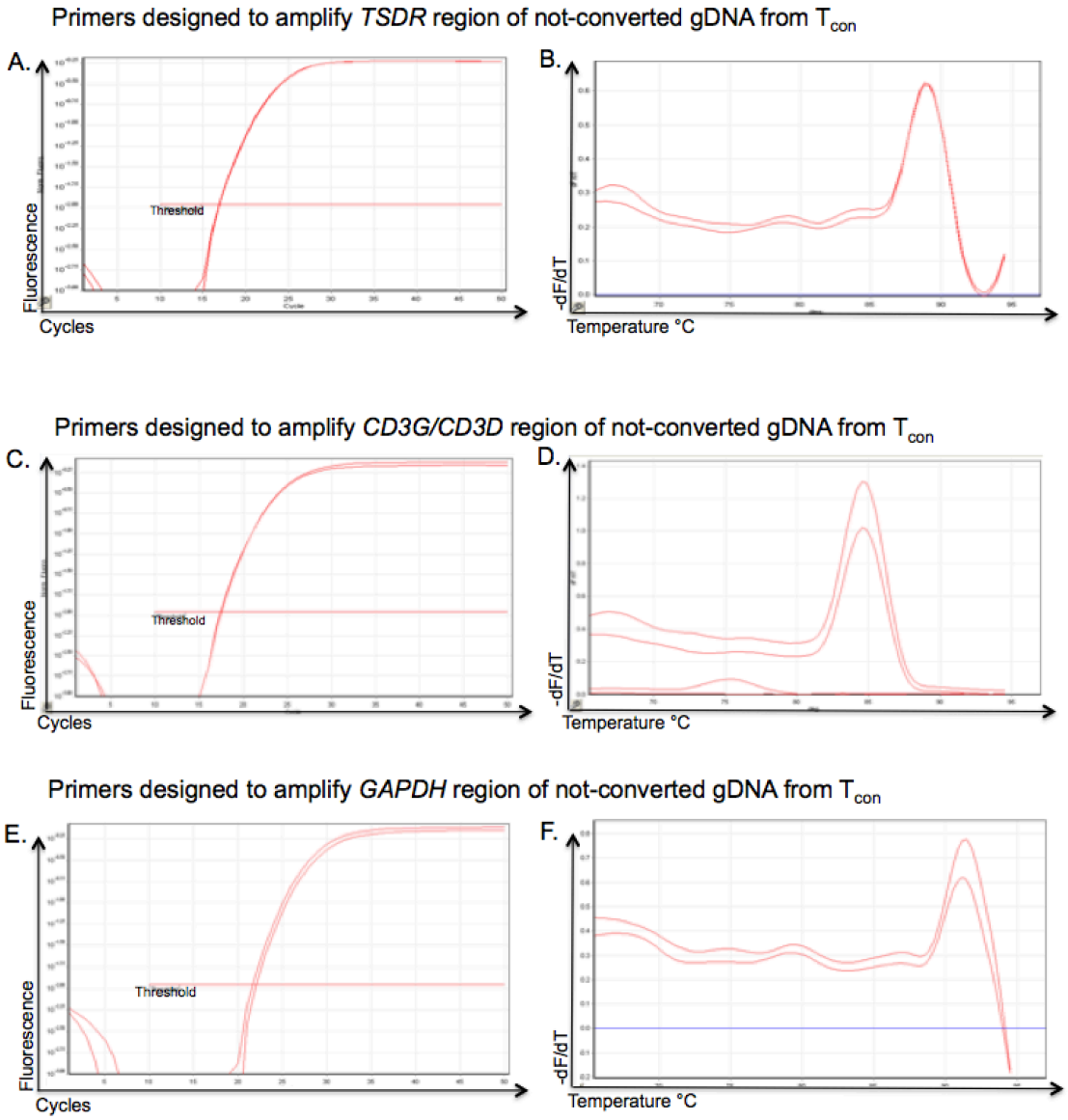


Figure 58. qPCR analysis to identify the most suitable annealing temperature. The fluorescence plotted against the cycles (58-A, 58-C, 58-E) represents the standard curve of the amplification of the T_{con} not-converted genomic DNA with SYBR green (respectively *TSDR*, *CD3G/CD3D* and *GAPDH*). Then the -dF/dT (change in fluorescence/change in temperature) is plotted against temperature (58-B, 58-C, 58-F) to obtain a clear view of the melting dynamics.

6.3.1.2. Quantification of methylated and demethylated TSDR, and GAPDH promoter in gDNA from CD3+ T cells, and the Tregs, CD4+ T_{con} subpopulations

Quantitative PCR was used to quantify methylated and demethylated *TSDR* and *GAPDH* promoter in gDNA from the cell types described below (see Chapter 3, section 12). SYBR green was used to detect PCR products as they accumulate during each PCR cycle. Genomic DNA isolated (see Chapter 3,

section 11.1) from Tregs, T_{con} and $CD3^+$ cells both bisulfite and not-bisulfite converted (see Chapter 3, section 11.3) was used as template. The *GAPDH* promoter region was used as "housekeeping gene" in order to normalise qPCR data. Primers were designed based on publications above mentioned, on bisulfite converted and not-converted sequences. Five different plasmids with *TSDR, CD3* bisulfite converted and non-converted sequences as insert and the *GAPDH* unconverted sequence as insert (see Chapter 3, section 3.13) were used as controls to produce the standard curves. The plasmids were serially diluted in 0.1% (v/v) TE (Life Technologies) + tRNA (Life Technologies) to generate a 5 point standard curve, comprised of $12.5x10^3$, $2.5x10^3$, $0.5x10^3$, 100 and 20 copies/5μl.

qPCR was performed using a Rotor Gene 6000 (Corbett Lifescience). HotStarTaq Master Mix (Qiagen), which contains HotStarTaq DNA Polymerase, SYBR Green dye, PCR Buffer with 3 mM $MgCl_2$, and 400 μM of each dNTP was used for qPCR. qPCR was performed in a final volume of 10μl using HotStarTaq Master Mix (Qiagen); 1μM (final concentration) of bisulfite converted or non-converted *TSDR, CD3* and *GAPDH* specific forward and reverse primers (see Chapter 3, section 3.12.3), 25 ng of bisulfite converted or non-converted gDNA and HyClone molecular biology grade water (GE Healthcare).

6.3.1.3. TSDR analysis by deep amplicon bisulfite sequencing

Genomic DNA was isolated from fresh or frozen cells using the DNeasy Blood & Tissue kit (Qiagen) and quantified with the Quant-iT PicoGreen dsDNA kit (Life Technologies). A total of 80 ng of gDNA was bisulfite converted and purified with the EpiTect DNA Bisulfite kit (Qiagen, Crawley, UK) according to the manufacturer's instructions.

Table 15. *TSDR* primers used.

Name primers	*Sequence*
TSDR_1_bst (fwd)	5'-TCGTCGGCAGCGTCAGATGTGTATAAGAGACAGTGTTTGGGGGTAGAGGATTTAGAGGG-3'
TSDR_1_bst (rev)	5'-GTCTCGTGGGCTCGGAGATGTGTATAAGAGACAGACATCACCTACCACATCCACCAACACCCAT-3')
TSDR_3_bst (fwd)	5'-TCGTCGGCAGCGTCAGATGTGTATAAGAGACAGTGTTTGGGGGTAGAGGATTT-3'
TSDR_3_bst (rev)	5'-GTCTCGTGGGCTCGGAGATGTGTATAAGAGACAGTATCACCCCACCTAAACCAA-3'

List of TSDR primers used. (fwd) means forward and (rev) means reverse.

Bisulfite converted gDNA was amplified with primer pairs using the EpiMark Hot Start Taq DNA Polymerase (New England Biolabs Ltd). The cycling conditions were: 30 seconds denaturation at 95°C and then 38 cycles at 95° C for 30 seconds, 64° C (primers TSDR_1_bst) or 56° C (primers TSDR_3_bst) (Table 15) for 45 seconds and 68°C for 45 seconds (according to the manufacture). A final elongation step of 5 minutes at 68° C. Then, amplicons were purified from a 2% (w/v) agarose gel with QIAquick Gel Extraction Kit (Qiagen). The PCR libraries (DNA fragments) were first purified by using Agencourt AMpure XP beads (Beckman Coulter), then quantified (see Chapter 3, section 11.2). The specificity and the product sizes were determined by agarose gel electrophoresis (see Chapter 3 section 13.4.). Pooled libraries were further processed for sequencing in a batch-wise manner. Each pooled HDs PCR amplicon library was diluted in HyClone molecular biology grade water (GE Healthcare) to 0.2 ng/µl (final concentration). Diluted libraries were then used to prepare the Illumina sequencing libraries through transposon-based Illumina Nextera technology (Illumina, UK) according to the manufacturer's guidelines.

A total of 1.25µl (0.25ng) of each pooled PCR amplicon library (0.2 ng/µl) was transferred to a new 96 well PCR plate. A total of 2.5µl of tagment DNA (TD-

Tagmentation uses a transposase to simultaneously fragment and insert adapters onto DNA) buffer and then 1.25µl of amplicon tandem mix (ATM) was added to each PCR well. PCR libraries were mixed using a multichannel pipette, followed by centrifugation at 280x G_{max} for 1 minute. The PCR plate was incubated first at 55°C (5 minutes) and then at 4°C (2 minutes). Next, a total of 1.25µl of neutralised tagment (NT) buffer was added to each mixture in the PCR plate and rested for 7 minutes at room temperature. A total of 3.75µl of Nextera PCR master mix (NPM) was added to each well of the PCR plate. 1.25µl of index-1 primer and 1.25µl of index-2 primer were also added. These dual indexes allowed multiplexing of 96 samples in independent sequencing experiments utilising Nextera-amplicon methodology. Then, mixtures were mixed using a multichannel pipette, followed by centrifugation at 280x*g* for 1 minute. PCR amplification was performed using GoTaq Hot Start Polymerase (Promega Ltd.) at the following cycling conditions: 3 minutes denaturation at 95°C and then 8 cycles of 95° C for 20 seconds, 55° C for 30 seconds and 72° C for 30 seconds with a final elongation of 5 minutes at 72°C. Barcoded amplicons were evaluated on an agarose gel. Amplified libraries were then purified using Agencourt AMpure XP beads and quantified (see Chapter 3, section 11.2). Purified libraries were sequenced with the MiSeq Reagent Nano Kit (Illumina) according to the manufacturer's guidelines.

6.3.1.4. Infinium Human Methylome assay

The methylation statuses of gene were studied using the HumanMethylation450 BeadChip (Illumina Infinium). The Infinium Human Methylation assay uses beads attached to target-specific DNA probes designed to bind to individual DNA sites in gDNA containing CpGs. They are designed to evaluate the methylation status of up to 14,495 human genes. This technique employs two types of assay: Infinium I and Infinium II to enhance the extent of coverage. In the Infinium I (Figure 59 A) assay two bead types per CpG locus are used. Each probe is designed to match either the protected cytosine (methylated) or the thymine base (unmethylated). In the Infinium II (Figure 59 B) assay only one bead that is designed for the

methylated state, in this case the probe complements the base directly upstream of the query site given a G or A base complementary to either the "methylated" C or "unmethylated" T (see Chapter 3, section 15). A total of 150ng of gDNA from each sample tested was bisulfite converted as described in section 3.9.3. DNA samples were processed using the HumanMethylation450 BeadChip assay and raw data were analysed using R software in the Department of Respiratory Medicine and Allergy, Division of Asthma, Allergy and Lung Biology at King's College London.

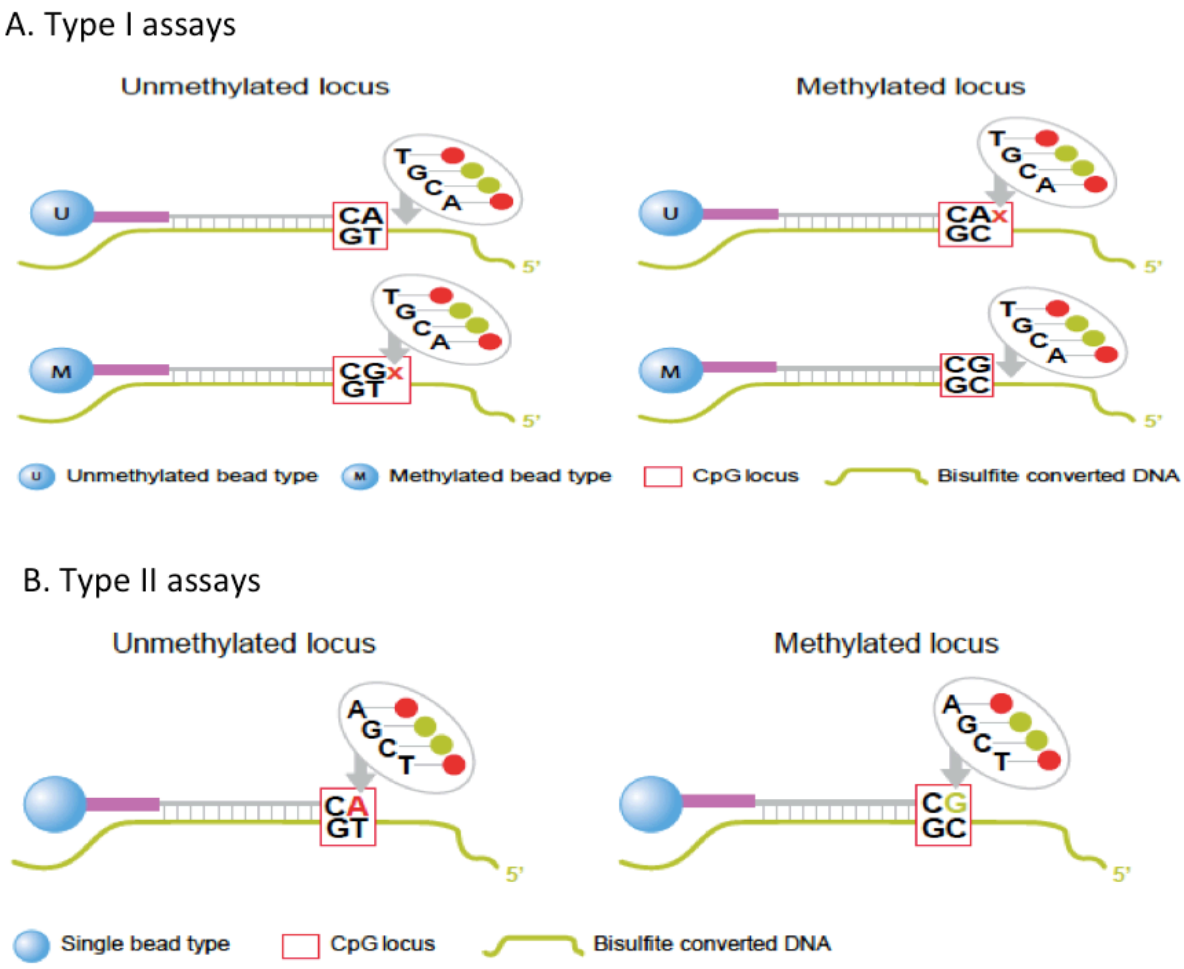


Figure 59. Human Methylation450 BeadChip Array. The methylome status of the promoters of 14,495 genes were investigated using the HumanMethylation450 BeadChip assay. This assay consists of two parts: Infinium I and Infinium II. Each probe is designed to match either the protected cytosine (methylated) or the thymine base (unmethylated). In the Infinium II (Fig. 2 B.) assay only one bead is designed to bind to the sequence containing the methylated base, in this case the probe complements the base directly upstream of the query site given a G or A base complementary to either the "methylated" C or "unmethylated" T.

6.3.2. Phenol-based DNA extraction

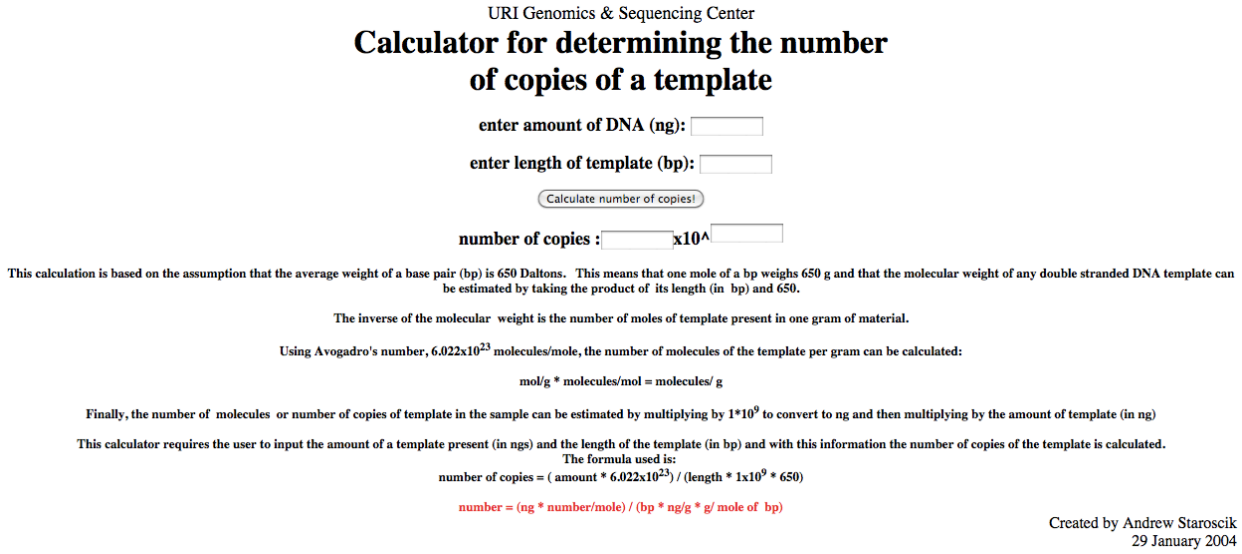
Because of the presence of fixation buffer (see Chapter 3, section 5.2) in the cells used for this section, we opted for a phenol-based DNA isolation protocol proposed by *Bending et al*[125], instead of the genomic DNA isolation described in Chapter 3, section 11.1. This protocol aimed to reverse (using sufficient RNAse and Proteinase k) the formaldehyde-induced changes (DNA cross-link) that impede bisulfite conversion. Modifications of the protocol were as follows: Cells were incubated with 300 µl lysis buffer (10mM Tris-HCL pH 8, 100 mM NaCl (Life Technologies), 50 mM EDTA (Applichem), 0.5% (w/v) SDS (Life Technologies), 0.1mg/ml proteinase K (Roche), pH 8) and 20 µg/ml RNase A (Qiagen) for 24h at 60°C on a thermo shaker (Thermo Scientific). Then, the lysis solution was mixed with one volume of phenol/chloroform/isoamyl alcohol (25:24:1 Sigma- Aldrich). The work was carried out in a chemical fume hood. The solution was centrifuged at 280x G_{max} for 5 minutes at room temperature. The acqueous phase was removed and we kept the non-acqueous phase containing the DNA. DNA was precipitated by addition of ethanol (Sigma-Aldrich) to a final concentration of 75% (v/v). The tube containing the ethanol and the DNA was incubated at -20°C for at least 4h. The tube was then centrifuged at 280x G_{max} for 5 minutes. The supernatant was removed and 300 µl of 70% (v/v) ethanol was added. The tube was centrifuged again at 280x G_{max} for 5 minutes. The supernatant was removed and the DNA pellet was air-dried in a laminar flow hood. The dried DNA was dissolved in TE buffer for at least 24 hours before use in downstream experiments.

6.4. Results

6.4.1. Quantification of methylated and demethylated TSDR and the GAPDH promoter in gDNA from CD3+ T cells, Treg and CD4$^+$ T_{con}.

6.4.1.1. Standard curve using plasmids

The purpose of this section was to use techniques such as qPCR to quantify the methylation status of the *TSDR* and *CD3G/CD3D* within Tregs, T_{con} and CD3 T cells. The goal was to identify and quantify T_{con} and Tregs in samples of CD3$^+$ T cells. In order to do that we first wanted to assess the absolute quantification of the unknown target samples (*TSDR, CD3* and *GAPDH*) using standard curves. Standard curve was generated by diluting a series of known template concentrations (gDNA from T_{con}) to determining the initial start amount of the target template. To build the standard curve, circular plasmids were used instead of genomic DNA isolated from T_{con}. Plasmids not only have a smaller seize then gDNA but also the inserted sequences are more accessible. . We decided to choose 20, 100, 500, 2,500 and 12,500 copy numbers to prepare the standard curve. In order to know how many ng of gDNA corrisponds to 20, 100, 500, 2,500 and 12,500 copy numbers of our standard curve we used the http://cels.uri.edu/gsc/cndna.html website (Figure 60).



URI Genomics & Sequencing Center

Calculator for determining the number of copies of a template

enter amount of DNA (ng):

enter length of template (bp):

Calculate number of copies!

number of copies : x10^

This calculation is based on the assumption that the average weight of a base pair (bp) is 650 Daltons. This means that one mole of a bp weighs 650 g and that the molecular weight of any double stranded DNA template can be estimated by taking the product of its length (in bp) and 650.

The inverse of the molecular weight is the number of moles of template present in one gram of material.

Using Avogadro's number, 6.022×10^{23} molecules/mole, the number of molecules of the template per gram can be calculated:

mol/g * molecules/mol = molecules/ g

Finally, the number of molecules or number of copies of template in the sample can be estimated by multiplying by $1*10^{9}$ to convert to ng and then multiplying by the amount of template (in ng)

This calculator requires the user to input the amount of a template present (in ngs) and the length of the template (in bp) and with this information the number of copies of the template is calculated.
The formula used is:
number of copies = (amount * 6.022×10^{23}) / (length * 1×10^{9} * 650)

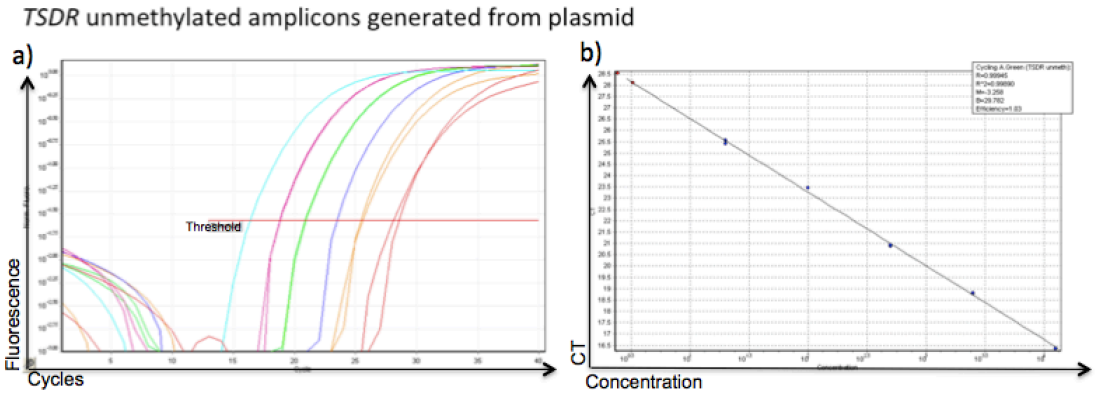
number = (ng * number/mole) / (bp * ng/g * g/ mole of bp)

Created by Andrew Staroscik
29 January 2004

Figure 60. Copy number calculator website.

Using the previously established annealing temperature (see above), we performed a qPCR for each of the plasmids (see below) containing sequences with the appropriate primers (*i.e.* plasmid with *TSDR* unmethylated insert amplified by *TSDR* unmethylated primer) (Figure 61 to 64).

The *GAPDH* insert was amplyfied using the related primer pair and with the addition of T_{con} as “unknown copy number” to check whether the sample was able to fall within the standard curve points (Figure 65). Standard curve points and unknown samples were run at the same time in each experiment.

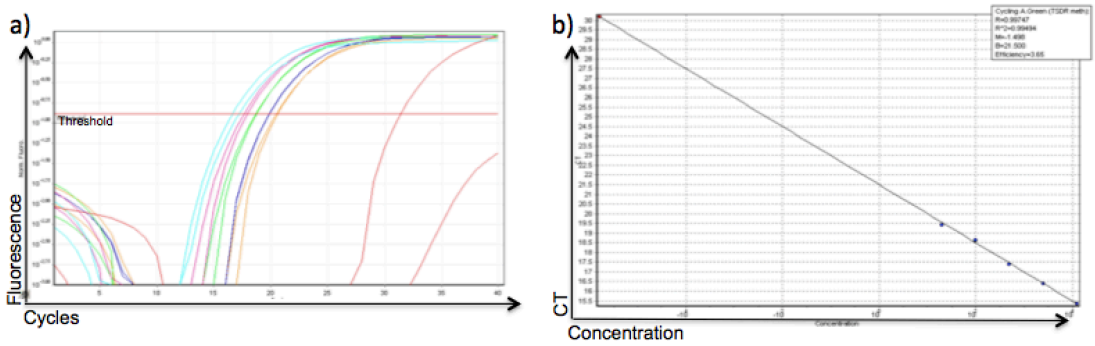


c)

Type	Ct	Given Conc (copies/ reaction)	Calc Conc (copies/ reaction)
Standard	25.58	20	20
Standard	25.42	20	22
Standard	23.45	100	88
Standard	20.87	500	542
Standard	20.93	500	520
Standard	18.77	2,500	2,395
Standard	18.81	2,500	2,338
Standard	16.36	12,500	13,197
NTC	28.11		3
NTC	28.52		2

Figure 61. TSDR unmethylated standard curve. Panel a) shows the amplification curves of the dilution series using known amounts of the *TSDR* plasmid. If the efficiency is 100%, the Ct values of the 10 fold dilution will be 3.3 cycles apart (there is a 2-fold change for each change in Ct). Light blue represents 12,500 copy numbers, pink 2,500, green 500, purple 100, orange 20 and red is water. Panel b) The stanard curve with the Ct plotted against the log of the starting quantity of the template for each dilution. The efficiency of the PCR should be between 90–100% (−3.6 ≥ slope ≥ −3.3). Another important value is the linear standar curve r or R^2 that should be $R^2 > 0.980$ or r > 1- 0.990. In this plot, R is 0.99. Panel c) shows the data from the assay. Second column: the threshold cycle or Ct, is the spot where the reaction curve intersects your threshold line. This shows the number of cycles it took to detect a real signal from each sample. Lower Ct values indicate high amounts of targeted nucleic acid, while higher Ct values mean lower amounts of the target nucleic acid. The third column represents the “given concentration”, the number of copies calculated from the website mentioned above. The fourth column represents the “calculated concentration” where the copy numbers where actually calculated from the machine using the standard curve. For the qPCR to be precise, column 3 and 4 should have the closest values.

TSDR methylated amplicons generated from plasmid

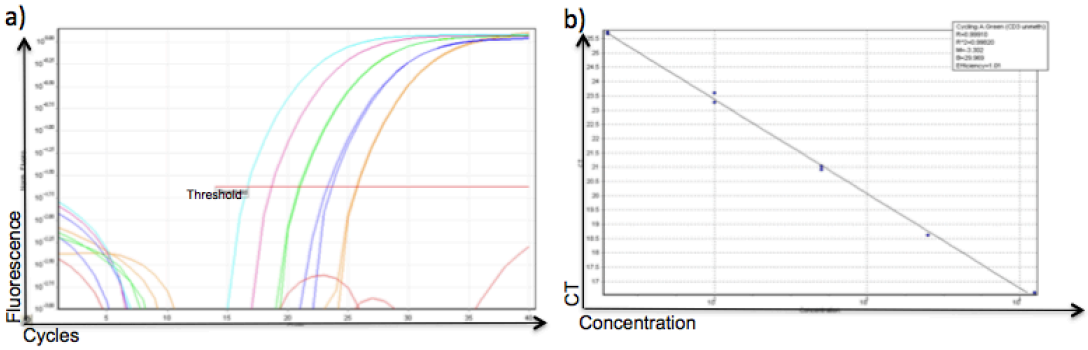


c)

Name	Type	Ct	Given Conc (copies/ reaction)	Calc Conc (copies/ reaction)
20	Standard	19.4	20	25
100	Standard	18.61	100	85
100	Standard	18.65	100	80
500	Standard	17.39	500	559
2500	Standard	16.38	2,500	2,616
12500	Standard	15.36	12,500	12,599
water	NTC	30.18		

Figure 62. TSDR methylated standard curve. Panels (a-c) Are described in Figure 61, but the plasmid containing the *TSDR* methylated sequence is used.

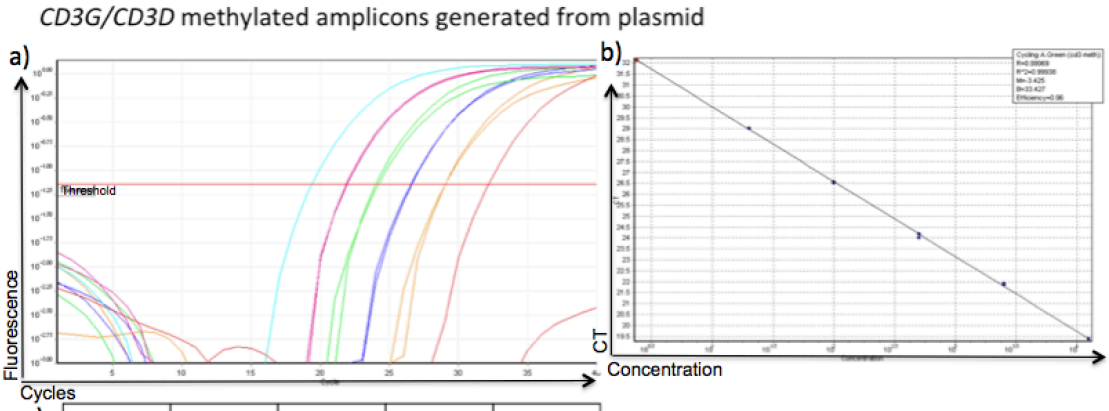
CD3G/CD3D unmethylated amplicons generated from plasmid



c)

Name	Type	Ct	Given Conc (copies/ reaction)	Calc Conc (copies/ reaction)
20	Standard	25.72	20	19
20	Standard	25.65	20	20
100	Standard	23.27	100	107
100	Standard	23.6	100	85
500	Standard	20.91	500	554
500	Standard	21.01	500	515
2500	Standard	18.62	2,500	2,746
12500	Standard	16.6	12,500	11,175
water	NTC			

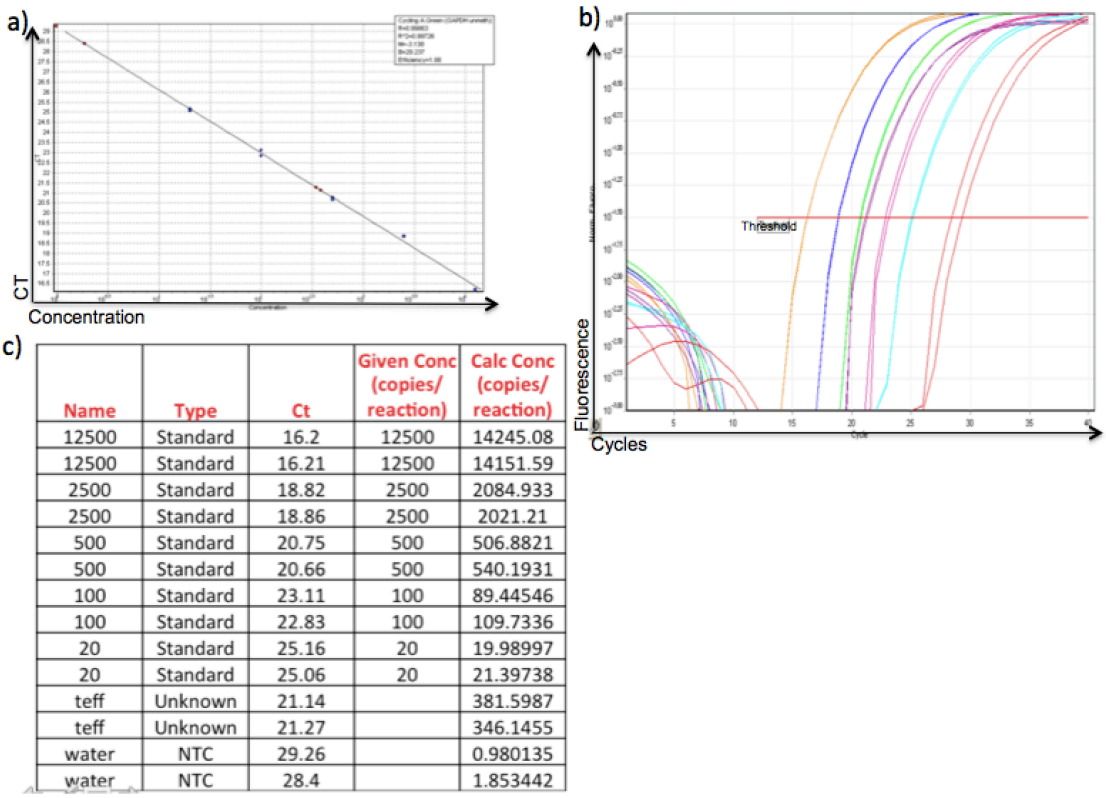
Figure 63. CD3G/CD3D unmethylated standard curve. Panels (a-c) Are described in Figure 61, but the plasmid containing the *TSDR* methylated sequence is used.



c)

Name	Type	Ct	Given Conc (copies/ reaction)	Calc Conc (copies/ reaction)
20	Standard	29.02	20	19
20	Standard	29.02	20	19
100	Standard	26.52	100	104
100	Standard	26.57	100	100
500	Standard	24.18	500	499
500	Standard	24	500	564
2500	Standard	21.84	2,500	2,413
2500	Standard	21.9	2,500	2,324
12500	Standard	19.38	12,500	12,634
water	NTC	32.13		2

Figure 64. CD3G/CD3D methylated standard curve. Panels (a-c) Are described in Figure 61, but the plasmid containing the *TSDR* methylated sequence is used.



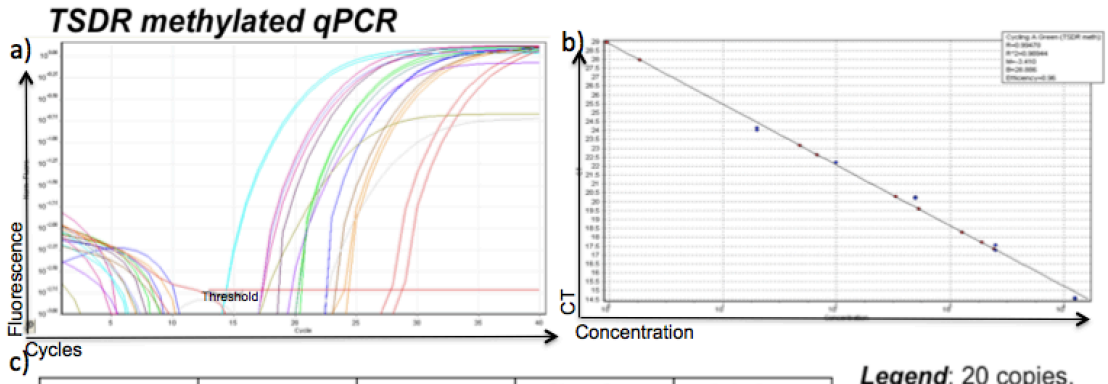
Name	Type	Ct	Given Conc (copies/ reaction)	Calc Conc (copies/ reaction)
12500	Standard	16.2	12500	14245.08
12500	Standard	16.21	12500	14151.59
2500	Standard	18.82	2500	2084.933
2500	Standard	18.86	2500	2021.21
500	Standard	20.75	500	506.8821
500	Standard	20.66	500	540.1931
100	Standard	23.11	100	89.44546
100	Standard	22.83	100	109.7336
20	Standard	25.16	20	19.98997
20	Standard	25.06	20	21.39738
teff	Unknown	21.14		381.5987
teff	Unknown	21.27		346.1455
water	NTC	29.26		0.980135
water	NTC	28.4		1.853442

Figure 65. GAPDH methylated standard curve. Panels (a-c) Are described in Figure 61, but the plasmid containing the *TSDR* methylated sequence is used.

After several attemps we were able to have a reliable standard curve for every plasmid but more importantly every standard curve had the closest value for the “calculated concentration”. We kept a stock of 12,500 copy number of each plasmid at -20°C so a standard curve could be produced for each experiment.

6.4.1.2. Healthy donor run and standard curve unreproducibility

Healthy donors sample were run together with the standard curve (Fig 66-67). Figures 66 and 67 are representative examples of the qPCR outcome.

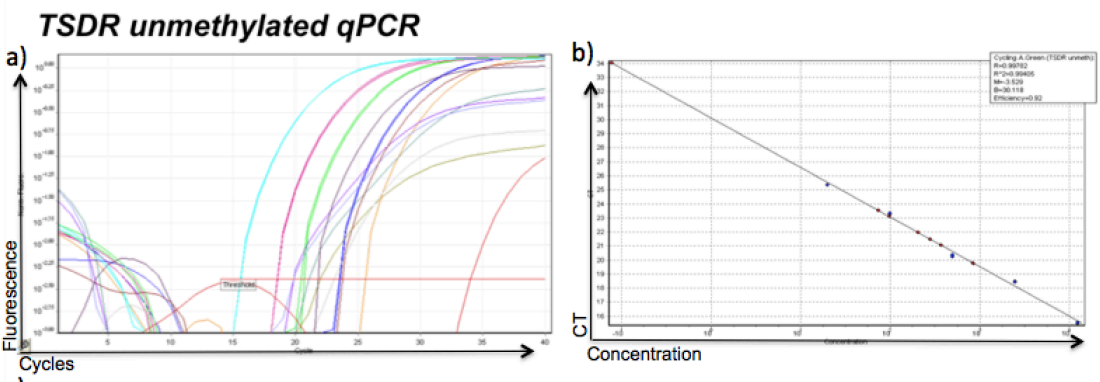


c)

Name	Type	Ct	Given Conc (copies/reaction)	Calc Conc (copies/reaction)
20	Standard	24.14	20	24.61484
20	Standard	24.01	20	26.99692
100	Standard	22.18	100	92.49749
100	Standard	22.18	100	92.49749
500	Standard	20.25	500	342.2127
500	Standard	20.17	500	359.5876
2500	Standard	17.55	2500	2113.685
2500	Standard	17.27	2500	2558.192
12500	Standard	14.52	12500	16355.39
12500	Standard	14.57	12500	15783.16
water	NTC	28.95		0.956778
water	NTC	27.97		1.8542
HD Tregs	Unknown	19.6		529.672
HD Tconv	Unknown	17.71		1900.559
CD3	Unknown	20.27		336.36

Legend: 20 copies, orange; 100 copies, blue; 500 copies, green; 2500 copies magenta; 12500 copies, light blue; water, red; HD Tregs, purple; HD Tconv, brown; CD3, green-brown.

Figure 66. TSDR methylated qPCR.Panel a) shows the amplification curves of the dilution series therefore after how many cycles (X axis) we have an amplification of the product (amplicon). In this plot, R is 0.99. Panel b) shows the standard curve with the Ct plotted against the log of the starting quantity of the template for each dilution. In this plot, R is 0.99. Panel c) shows the data from the assay. First column itemed the names gave to the single sample. Second column shows the Type as “standard” or “NTC” (not template) or “unknown”. The third column shows the threshold cycle or Ct. Fourth column represents the “given concentration”, the number of copy that I’ve calculated from the website mentioned above. The fifth column represents the “calculated concentration” where the copy numbers where actually calculated from the machine using the standard curve. For the qPCR to be precise, column 4 and 5 of the standard curve points should have the closest values.



c)

Name	Type	Ct	Given Conc (copies/ reaction)	Calc Conc (copies/ reaction)
20	Standard	25.33	20	22.77323
100	Standard	23.27	100	87.21211
100	Standard	23.31	100	84.89591
500	Standard	20.24	500	630.3306
500	Standard	20.34	500	587.7861
2500	Standard	18.45	2500	2018.073
2500	Standard	18.42	2500	2066.703
12500	Standard	15.49	12500	13914.61
12500	Standard	15.54	12500	13468.15
water	NTC	34.03		7.77E-02
HD Treg	Unknown	19.76		861.6928
HD Tconv	Unknown	21.96		204.3554
CD3	Unknown	21.06		368.695

Legend: 20 copies, orange; 100 copies, blue; 500 copies, green; 2500 copies magenta; 12500 copies, light blue; water, red; HD Tregs, purple; HD Tconv, brown; CD3, green-brown.

Figure 67. TSDR unmethylated qPCR.Panel a) shows the amplification curves of the dilution series therefore after how many cycles (X axis) we have an amplification of the product (amplicon). In this plot, R is 0.99. Panel b) shows the standard curve with the Ct plotted against the log of the starting quantity of the template for each dilution. In this plot, R is 0.99. Panel c) shows the data from the assay. First column itemed the names gave to the single sample. Second column shows the Type as “standard” or “NTC” (not template) or “unknown”. The third column shows the threshold cycle or Ct. Fourth column represents the “given concentration”, the number of copy that I’ve calculated from the website mentioned above. The fifth column represents the “calculated concentration” where the copy numbers where actually calculated from the machine using the standard curve. For the qPCR to be precise, column 4 and 5 of the standard curve points should have the closest values.

We then calculated the percentage of unmethylated copy number according to *Sehouli et al*[45] using the following equation*:*

TpG/(TpG+CpG)

Where *TpG*: unmethylated Cytosine and *CpG*: methylated Cytosine (Table 16)

Table 16. Calculation

		GAPDH			*CD3G/CD3D*			
	copy num		ratio	%	copy num		ratio	%
	TpG	CpG	TpG/(TpG+CpG)		TpG	CpG	TpG/(TpG+CpG)	
Tregs I	255.21	0.00	1.00	100.00	397.67	1.65	1.00	99.59
Tregs II	497.54	0.00	1.00	100.00	514.46	19.39	0.96	96.37
Tregs III	159.85	0.00	1.00	100.00	147.84	23.88	0.86	86.09
Tconv I	545.52	0.00	1.00	100.00	547.46	4.07	0.99	99.26
Tconv II	591.48	0.00	1.00	100.00	628.11	5.34	0.99	99.16
Tconv III	514.08	0.00	1.00	100.00	790.20	15.61	0.98	98.06

	FOXP3_*TSDR*			
	copy num		ratio	%
	TpG	CpG	TpG/(TpG+CpG)	
Tregs I	150.08	74.27	0.67	66.89
Tregs II	160.16	103.80	0.61	60.67
Tregs III	90.45	77.54	0.54	53.84
Tconv I	24.88	158.94	0.14	13.54
Tconv II	32.64	185.61	0.15	14.96
Tconv III	18.46	185.08	0.09	9.07

This excel sheet is divided into 3 parts: *GAPDH, CD3G/CD3D* and *FOXP3_TSDR*. In the first column, we can find the name of the samples. Column "TpG" displays the copy number of the unmethylated target (*GAPDH* green part, *CD3G/CD3D* blue part and *FOXP3_TSDR* pink part). Column "CpG" displays the copy number of the methylated target. Column "TpG/(TpG+CpG)" displays the unmethylated copy number according to *Sehouli et al* equation. Column "%" is the "TpG/(TpG+CpG)" result multiplied by 100.

We first isolated Tregs and T_{con} (see Chapter 3, section 2) from 3 different female HDs (I, II and III). The *TSDR* location (*FOXP3*) is in the X chromosome therefore we decided to use only female samples. Genomic DNA isolated (see Chapter 3, section 11.1) from Tregs, T_{con} bisulfite converted (see Chapter 3, section 11.3) was used as template. The primers (see Chapter 3, section 12.3) were designed to amplify the following regions of interest: *TSDR, GAPDH* and *CD3G/CD3D*. Primers were designed on bisulfite converted sequences. The *GAPDH* was our housekeeping gene and had to be unmethylated in cells. *CD3G/CD3D* as mentioned before is found unmethylated in the CD3 population, so the percentage of unmethylated CpGs should be around 100% in CD3 population. *TSDR* should be methylated in T_{con} and unmethylated in Tregs, but in this particular case we used all female samples, so the percentage had to be divided by 2 due to the X-chromosome inactivation. The 3 biological replicates (HDs I, II and III) were run together with the standard curve.

We repeated the experiment and we noticed that each standard curve aliquoted was presenting a different Ct value for the same standard curve point (Figure 68). Although we followed the guidelines to freeze and thaw cells (see Chapter 3, section 3), the same values from the aliquoted standard curves did not occur. To reduce any potential error, we have diluted again the plasmid from frozen stock and repeated the experiment. Nevertheless, the

repeated results were still not reproducible and robust enough. In Figure 68, a total of 2 different batches of *TSDR* methylated and unmethylated standard curve were run together. Panel a) represents the same standard curve repeated 3 times, panel b) represents a different standard curve. In “Quantity 500” the mean of the Ct values is 31.78, 31.78 and 31.53 in a); in b) the mean of the Ct values is 22.84. In this case, there was almost 9 Ct values of difference. Several batches of frozen standard curves were run on qPCR. The inconsistency in the Ct values were such that we decided to switch to amplicon sequencing of bisulfite treated DNA on an Illumina MiSeq instrument.

Target Name	Quantity	Ct	Ct Mean	Ct	Ct Mean	Ct	Ct Mean
TSDR methylated	12500	27.20	26.96	26.45	26.72	26.90	26.65
TSDR methylated	12500	26.72	26.96	27.00	26.72	26.41	26.65
TSDR methylated	2500	29.34	29.37	29.76	29.76	28.50	28.69
TSDR methylated	2500	29.40	29.37	29.76	29.76	28.88	28.69
TSDR methylated	500	31.87	31.78	31.78	31.78	31.53	31.53
TSDR methylated	500	31.68	31.78			31.53	31.53
TSDR methylated	100	33.66	33.99	33.63	33.63		
TSDR methylated	100	34.33	33.99				
TSDR unmethylated	12500	24.60	24.55	24.64	24.68	26.56	26.45
TSDR unmethylated	12500	24.50	24.55	24.72	24.68	26.33	26.45
TSDR unmethylated	2500	27.03	27.23	26.84	26.84	29.73	29.15
TSDR unmethylated	2500	27.42	27.23			28.58	29.15
TSDR unmethylated	500	29.59	29.21	28.93	29.02	31.80	31.30
TSDR unmethylated	500	28.83	29.21	29.11	29.02	30.79	31.30

Target Name HDs	Quantity	Ct Mean	Ct
TSDR methylated	12500	17.59125	17.708
TSDR methylated	12500	17.59125	17.474
TSDR methylated	2500	20.56063	20.561
TSDR methylated			
TSDR methylated	500	22.84837	22.857
TSDR methylated	500	22.84837	22.84
TSDR methylated	100	27.38062	25.216
TSDR methylated	100	27.38062	24.957
TSDR methylated	20	25.0865	27.467
TSDR methylated	20	25.0865	27.295
TSDR unmethylated	12500	24.75307	24.827
TSDR unmethylated	12500	24.90187	24.827
TSDR unmethylated	2500	27.95183	27.874
TSDR unmethylated	2500	27.7966	27.874
TSDR unmethylated	500	30.40015	30.4
TSDR unmethylated			
TSDR unmethylated	20	35.1175	35.118
TSDR unmethylated			

Figure 68. Standard curve repetition.The column “Target name” displays the target names. The column “Quantity” shows the number of copy that I’ve calculated from the website http://cels.uri.edu/gsc/cndna.html. The column “Ct” shows the threshold cycle or Ct. The column “Ct Mean” displays the mean of the Ct. a) The same frozen standard curve was run in triplicate. The Ct values were consistent within the 3 replicates. b) Another frozen standard curve. The Ct values were different from those on a).

6.4.2. Percentage of unmethylated CpGs of the TSDR intron in TrLCs, Tregs and in Tcon from HD

The inconsistency of the Ct values in the previously mentioned standard curves run could not be rectified. Therefore, we opted for another method to investigate the FOXP3 Treg-specific demethylated region (*TSDR*). We

decided to use sequencing of bisulfite treated DNA to assess the stability of our Tregs. We studied the methylation status of 15 CpG sites within the *TSDR* by amplicon sequencing of bisulfite treated DNA on an Illumina MiSeq instrument[127]. First, we isolated Tregs and T_{con} from one HD. T_{con} were cultured with 5-Aza-2-deoxycytidine (2 μM 5AzaC or 5Aza, Celgene) or Dimethyl sulfoxide as vehicle (2 μL/ml DMSO, Sigma) in a 48-well cell culture plate (Cellstar) ($1x10^6$ cells each well) with 1ml/well X-Vivo media (Lonza) or a 96-well cell culture plate (Cellstar) ($0.5x10^6$ to $0.25x10^6$ cells each well) with 500ul/well X-Vivo. 5AzaC has been dissolved in DMSO therefore used as control vehicle. In all the conditions, except for the controls, cells were stimulated with 10 μl/$1x10^6$ cells anti-CD3/CD28 expander beads (Dynabeads Human T-activator, Invitrogen ratio 1:15). Cultured cells were initially stimulated for 24 hours. 5AzaC or DMSO were added to the culture on days 2 to 5 and cells were harvested for further analysis on day 6. Because of the abundant stimulation induced by the beads, at day 8, magnetic beads were removed using a magnetic plate and cells were left in culture overnight to rest. At day 9 cells were harvested as follows: the X-Vivo media containing the cells was transferred to a 15ml tube, then centrifuged at 270 x G_{max} for 10 minutes and the media was removed. The centrifugation step and removal of media was repeated twice. The cell pellet was finally resuspended in 100 μl of PBS. Genomic DNA was extracted from the 2 culture conditions, Tregs and Tcon at baseline and 2 additional frozen samples of HD T_{con} treated with 5AzaC using DNeasy blood and tissue kit (Qiagen) following manifacturer's guidelines (see Chapter 3, section 11). Genomic DNA was quantified using Quant-iT PicoGreen dsDNA kit (Life Technologies, Paisley, UK) (see Chapter 3, section 11.2.1). A total of 80 ng of gDNA was bisulfide converted and purified using EpiTect Bisulfite Kit (Qiagen) (see Chapter 3, section 11.3). The A total of 6 conditions were then sequenced as explained in Chapter 6, section 3.1.3. The results from the sequencing are displayed in Table 4. The 15 CpGs of the *TSDR* are displayed in "TSDR-CpG" column. In the following columns, the percentage of methylation in each CpG is displayed. The conditions are: T_{con} stimulated and treated with DMSO ("Tcon treated with DMSO"); Tregs no stimulated no drug added, or called at baseline ("Tregs");

T_{con} at baseline ("Tcon"); T_{con} stimulated and treated with 5AzaC ("Tcon treated with 5AzaC"). According to the results from the sequencing, *TSDR* CpG sites in 5AzaC treated T_{con} from HDs were found to be > 73.21% methylated compared with 6.92% of methylation of Tregs, which confirms that TrLCs are most likely not to be Tregs. (Table 17).

Table 17. Percentage of methylation.

TSDR - CpG	Tcon treated with DMSO	Tregs	Tcon	Tcon treated with 5AzaC	Tcon treated with 5AzaC	Tcon treated with 5AzaC
1	89.66%	8.51%	85.19%	94.47%	92.31%	75.12%
2	97.71%	8.92%	89.30%	95.53%	95.68%	76.96%
3	73.46%	7.62%	79.97%	77.13%	81.84%	58.38%
4	86.63%	7.12%	69.86%	82.04%	78.29%	50.61%
5	97.94%	7.76%	87.41%	85.99%	94.23%	62.69%
6	89.40%	7.91%	85.47%	96.15%	92.03%	74.73%
7	97.97%	8.28%	88.92%	94.09%	90.81%	66.53%
8	90.81%	6.34%	84.34%	95.47%	88.20%	84.04%
9	95.92%	4.85%	88.24%	87.51%	89.03%	76.67%
10	91.72%	4.91%	86.29%	93.51%	91.23%	77.46%
11	96.24%	4.66%	86.87%	90.77%	90.61%	80.17%
12	84.16%	5.39%	83.12%	88.36%	86.36%	80.55%
13	92.04%	4.91%	85.91%	90.57%	91.67%	83.34%
14	93.89%	8.19%	77.07%	92.35%	91.89%	74.08%
15	92.05%	8.41%	87.46%	94.11%	92.48%	76.77%
	91.31%	6.92%	84.36%	90.54%	89.78%	73.21%

The table below displays the percentage of methylation for each CpGs within the TSDR intron. The 15 CpGs of the TSDR are displayed in "TSDR-CpG" column. In the following columns, the percentage of methylation in each CpG is displayed. The conditions are: T_{con} stimulated and treated with DMSO ("Tcon treated with DMSO"); Tregs no stimulated no drug added, or called at baseline ("Tregs"); T_{con} at baseline ("Tcon"); T_{con} stimulated and treated with 5AzaC ("Tcon treated with 5AzaC").

6.4.3. Human Methylation450 BeadChip (Illumina Infinium) array

In this part of the Chapter we wanted to focus on the genome-wide of the TrLCs, with a particular emphasis on the genes that are regulated by *FOXP3*. The purpose was to assess whether the T_{con} after 5AzaC treatement were still T_{con} or they polarised into another population like Tregs. The DNA genome-wide of Tregs and T_{con} from HD (+/- 5AzaC) was investigated, using a methylation analysis (450K Illumina). Our aim was to focus on the list of the *FOXP3* binding sites[136] (see Appendix, Table 20) plus additional interesting genes related to *FOXP3* (see Appendix, Table 20 from gene number 105).

Among those genes, we wanted to investigate the single gene, that was displaying a major difference in term of methylation on T_{con} HD (+/- 5AzaC).
The questions that we wanted to be addressed in this part of the Chapter were:

1. What happen to the *FOXP3* binding sites after 5AzaC treatment on T_{con}?
2. Which gene does 5AzaC treatment affect the most in term of methylation?
3. Are methylation levels different from HD and AML or MDS patient's T_{con} and Tregs?

We first isolated from 2 HDs Tregs and T_{con} (see Chapter 3, section 2.4) using magnetic beads. We also isolated Tregs and T_{con} from a high-risk MDs patient, an MDS patient and a HDs (Figure 69). Tregs and T_{con} from 2 HDs were cultured with 5-Aza-2-deoxycytidine (2 μM 5AzaC or 5Aza, Celgene) or Dimethyl sulfoxide as vehicle (2 μL/ml DMSO, Sigma) in a 48-well cell culture plate (Cellstar) ($1x10^6$ cells each well) with 1ml/well X-Vivo media (Lonza) or a 96-well cell culture plate (Cellstar) ($0.5x10^6$ to $0.25x10^6$ cells each well) with 500ul/well X-Vivo. 5AzaC has been dissolved in DMSO therefore used as control vehicle. Culture conditions were as follow: control (no stimulation, no drugs), with 2μM 5AzaC and with 2μM DMSO. In all the conditions, except for the controls, cells were stimulated with 10 μ l/$1x10^6$ cells anti-CD3/CD28 expander beads (Dynabeads Human T-activator, Invitrogen ratio 1:15). Cultured cells were initially stimulated for 24 hours. 5AzaC or DMSO were added to the culture on days 2 to 5 and cells were harvested for further analysis on day 6. Because of the abundant stimulation induced by the beads, at day 8, magnetic beads were removed using a magnetic plate and cells were left in culture overnight to rest. At day 9, $125x10^5$ cells were taken as control, in order to check the polarisation of T_{con} in TrLC (see Chapter 4 section 3.1). The other cells were harvested as follows: the X-Vivo media containing the cells was transferred to a 15ml tube, then centrifuged at 270 x G_{max} for 10 minutes and the media was removed. The centrifugation step and removal of media was repeated twice. The cell pellet was finally resuspended in 100 μl of PBS. From all the conditions listed in Figure 69, the gDNA was

extracted using DNeasy blood and tissue kit (Qiagen) following manifacturer's guidelines (see Chapter 3, section 11). The gDNA concentration was determined by Nanodrop (ND-1000; Nanodrop) spectrophotometry, measuring the absorbance of the DNA solution at 260nm (see Chapter 3, section 12). Bisulfite conversion and methylome array (see section 3.1 of this current Chapter) were performed on all the samples. The measurement of the gDNA concentration, the bisulfite conversion and the Human Methylation450 bead chip array were carried out in the Department of Respiratory Medicine and Allergy, Division of Asthma, Allergy and Lung Biology at King's College London.

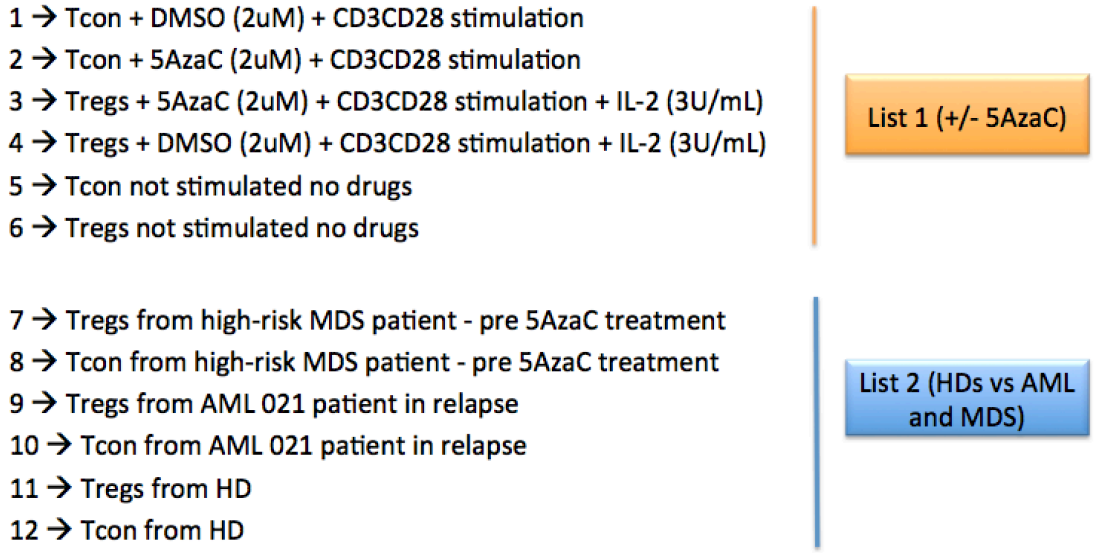
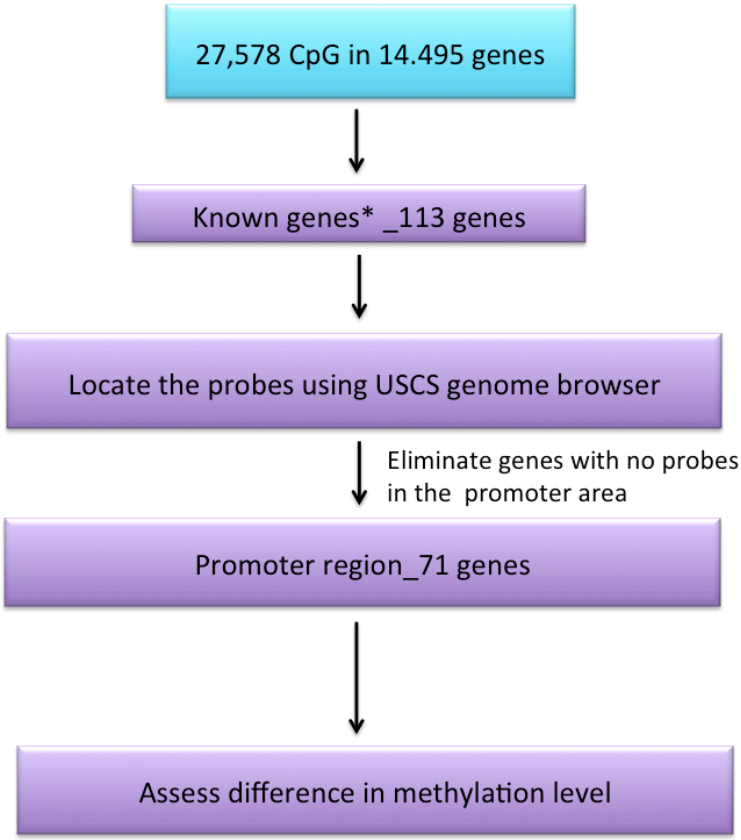


Figure 69. List of Methylome Array conditions. The conditions were divided into two lists: "List 1", only HD's samples from cell culture and "List 2", MDS, AML and HDs sample not cultured. In "List 1" we can find T_{con} stimulated with DMSO or 5AzaC treatment, Tregs stimulated with DMSO or 5AzaC treatment and Tregs and T_{con} at baseline (no stimulated and no drugs added). In "List 2" we can find Tregs and T_{con} from high-risk MDS patient at diagnosis; Tregs and T_{con} from AML patient in relapse (to return to AML; Tregs and T_{con} from HDs.

6.4.3.1. Analysis of methylation status of human genes in Tregs and T_{con}

Among the 14.495 genes analysed through the methylome array we focused on the 113 gene of the list of the *FOXP3* binding sites (Zhang *et al*[136]) (see Appendix, Table 20), plus additional important genes related to *FOXP3* (see Appendix, Table 20 from gene number 105). Because we wanted to focus mainly on *FOXP3* binding sites, only the genes with the probes of the array on

the CpG, within the promoter region (71 genes) were interrogated. Then genes that displayed a major difference in term of methylation between 5AzaC treated cells and not treated cells, in particular on T_{con} (Figure 70) were analysed.



*Zhang Y, Maksimovic J, Naselli G, Qian J, Chopin M, Blewitt ME, *et al.* Genome-wide DNA methylation analysis identifies hypomethylated genes regulated by FOXP3 in human regulatory T cells. *Blood* 2013, **122**(16): 2823-2836. + additional 17 from various papers

Figure 70. Methylome data workflow. The methylome status of 14.495 genes were investigated using the methylome array. We decided to be focused on the 113 genes from the list of Zhang *et al* ("known genes"). Genes that presented probes located within the promoter region were taking in consideration. The "USCS genome browser" (University of California, Santa Cruz) was used to locate the probes. A total of 71 genes displayed probes within the promoter region. The last step was to analyse the methylation level from single gene.

A total of 71 genes displayed probes within the promoter region, the methylation level of these 71 genes was investigated.

The result from the first run of methylome array of T_{con} from HD are displayed in Table 18. "T_{con} 5AzaC" column displays the level of methylation in the corresponded gene in the T_{con} after 5AzaC treatment condition. "T_{con} DMSO" column displays the level of methylation in the corresponded gene in the T_{con}

after DMSO treatment condition. "T_{con}_ctr" column displays the level of methylation in the corresponded gene in the control that is T_{con} at baseline condition. The trend of the methylation level between T_{con} with 5AzaC or DMSO related to the control ("T_{con}_Trend" column) was analysed as followed: methylation levels from the T_{con} with 5AzaC condition divided by the control (T_{con} at baseline) as compared with the T_{con} with DMSO condition divided by the control.

In particular D (Decrease as compared with control), I (Increase as compared with control), (5AzaC vs non)/ (DMSO vs non).

The following abbreviations describe the trend of the methylation level within the conditions:

I/D =Methylation level of 5AzaC > Methylation level of control / Methylation level of DMSO < Methylation level of control

D/I = Methylation level of 5AzaC < Methylation level of control / Methylation level of DMSO > Methylation level of control

DD/D = Methylation level of 5AzaC < Methylation level of control / Methylation level of DMSO < Methylation level of control (Methylation level of 5AzaC < Methylation level of DMSO)

D/DD = Methylation level of 5AzaC < Methylation level of control / Methylation level of DMSO < Methylation level of control (Methylation level of 5AzaC > Methylation level of DMSO)

II/I = Methylation level of 5AzaC > Methylation level of control / Methylation level of 5 DMSO> Methylation level of control (Methylation level of 5AzaC > Methylation level of DMSO)

I/II = Methylation level of 5AzaC > Methylation level of control / Methylation level of 5AzaC > Methylation level of control (Methylation level of 5AzaC < Methylation level of DMSO).

Table 18. Methylation level T_{con} HD.

GeneName	Number of CpG	Tconv 5AzaC	Tconv DMSO	Tconv_ctr	Tconv_Trend
ACSF3	2	0,0543291	0,0492735	0,049719	I/D
ADO	2	0,06365575	0,0611999	0,07163665	D/DD
ANGPT1	1	0,171867	0,137324	0,14752	I/D
APLP2	3	0,028671367	0,025826933	0,038872133	D/DD
ATXN7L1	2	0,07828175	0,06593155	0,0872184	D/DD
AXIN2	2	0,0689924	0,05034495	0,09391465	D/DD
BCL11A	4	0,208812225	0,182515575	0,23523075	D/DD
BCL11B	1	0,14005	0,108278	0,158699	D/DD
BCL9L	4	0,322638	0,28618475	0,36283475	D/DD
CA5A	2	0,826664	0,850936	0,8431555	D/I
CASP10	1	0,120158	0,127749	0,207862	DD/D
CNKSR1	2	0,48504	0,458447	0,5309	D/DD
CNOT3	4	0,065250325	0,0601143	0,0775444	D/DD
CREB1	1	0,037037	0,058952	0,056419	D/I
CRY2	1	0,0183123	0,0242691	0,0151074	I/II
CUTA	5	0,06151856	0,06236486	0,0761458	DD/D
CXCR5	2	0,592048	0,645521	0,6800155	DD/D
DUSP6	2	0,082138	0,0783493	0,1061725	D/DD
EDNRB	2	0,08466545	0,080552	0,11471975	D/DD
EMR3	2	0,5409945	0,5304385	0,59531	D/DD
ETS1	2	0,04937715	0,03893275	0,04290075	I/D
FAM124B	1	0,915959	0,931543	0,922573	D/I
FLOT1	5	0,05463672	0,05157972	0,06786594	D/DD
FOXO1	3	0,085826167	0,101054533	0,099205667	D/I
FOXP3	2	0,7880965	0,7848045	0,7923565	D/DD
GALNT2	1	0,129363	0,137148	0,159861	DD/D
GATA1	2	0,8757455	0,899741	0,884481	D/I
HDAC4	1	0,090294	0,0773123	0,108468	D/DD
HIVEP3	1	0,599344	0,613521	0,648677	DD/D
HORMAD2	1	0,566463	0,519801	0,644264	D/DD
HSD17B8	1	0,0666861	0,0467361	0,0790033	D/DD
IKZF4	2	0,1773305	0,1353505	0,1963825	D/DD
IL2RA	1	0,397256	0,398934	0,438502	DD/D
IRF4	2	0,06020805	0,048219	0,063753	D/DD
ITGAL	1	0,069075	0,058673	0,088984	D/DD
KCNAB3	1	0,694254	0,713163	0,70566	D/I
KCNN4	2	0,1140524	0,1397905	0,1675635	DD/D
KRT72	4	0,631985	0,62941925	0,65788125	D/DD
LEF1	1	0,0423707	0,0432893	0,0648718	DD/D
LOC338799	3	0,690725333	0,710577	0,715468667	DD/D
LRRC32	3	0,500791667	0,482046667	0,511358333	D/DD
MAOB	3	0,080012867	0,076928967	0,094422867	D/DD
MEOX1	1	0,480058	0,571781	0,599616	DD/D
MMP14	2	0,498132	0,447383	0,5111815	D/DD
NET1	1	0,0602373	0,0574668	0,0907496	D/DD
NFATC2	1	0,0422698	0,0223034	0,0319569	I/D
PAOX	2	0,07860525	0,06554645	0,07320305	I/D
PLAGL1	5	0,6050678	0,603775	0,6186922	D/DD
PRDM8	1	0,452216	0,440341	0,580315	D/DD
RGS12	1	0,72578	0,863102	0,617329	I/II
RPTOR	2	0,04342045	0,0476686	0,072888	DD/D
SATB1	2	0,2228019	0,1944965	0,2940421	D/DD
SCARF1	1	0,695473	0,687382	0,695302	I/D
SCNN1A	1	0,78866	0,811854	0,816022	DD/D
SLC1A5	4	0,08449575	0,071960625	0,104081075	D/DD
SMAD3	1	0,0814611	0,0825626	0,109797	DD/D
SNED1	3	0,803129333	0,813051	0,809436667	D/I
ST6GALNAC1	4	0,18696925	0,1547191	0,25885875	D/DD
STAT3	2	0,1358833	0,11893265	0,1512284	D/DD
TGFBR2	3	0,072100633	0,083219933	0,111302533	DD/D
TGIF1	1	0,0796808	0,0438101	0,0889423	D/DD
THBS1	2	0,0780071	0,05958105	0,06973675	I/D
TIGIT	4	0,6385285	0,70028625	0,65640625	D/I
TNFRSF13B	1	0,692583	0,721717	0,677839	I/II
TNFRSF4	1	0,818056	0,841868	0,806943	I/II
TYROBP	1	0,734406	0,74896	0,760027	DD/D
UPP1	1	0,0912593	0,0934535	0,118973	DD/D
VGLL4	1	0,0429398	0,0278697	0,0524685	D/DD
WIPI2	1	0,218626	0,232167	0,278356	DD/D
ZC3H12D	1	0,211407	0,197867	0,210781	I/D
ZHX1	3	0,104248467	0,100964433	0,1227402	D/DD

Name of the genes are listed in first column. “Number of CpG” column displays the number of probes found within the promoter region in that particular gene. “Tcon 5AzaC” column displays the level of

methylation in the corresponded gene in the T_{con} after 5AzaC treatment condition. “Tcon DMSO” column displays the level of methylation in the corresponded gene in the T_{con} after DMSO treatment condition. “Tcon_ctr” column displays the level of methylation in the corresponded gene in the control that is Tcon at baseline condition. “Tcon_Trend” displays the trend of the methylation level between T_{con} with 5AzaC or DMSO related to the control.

The results from Table 18 suggested that different levels of methylation occurred in “Tcon_ctr” as compared with “Tcon 5AzaC”. Also, stimulation with CD3CD28 (“Tcon DMSO”) affected methylation levels.

Out of 71 genes, 8 genes were unmethylated by the 5AzaC treatement (D/I), displaying low level of methylation in T_{con} after 5AzaC treatement as compared with T_{con} after DMSO (Table 19).

Table 19. Unmethylated genes in 5AzaC condition.

Gene Name	Number of CpG	Tconv 5AzaC	Tconv DMSO	Tconv_ctr
CA5A	2	0,826664	0,850936	0,8431555
CREB1	1	0,037037	0,058952	0,056419
FAM124B	1	0,915959	0,931543	0,922573
FOXO1	3	0,085826167	0,101054533	0,099205667
GATA1	2	0,8757455	0,899741	0,884481
KCNAB3	1	0,694254	0,713163	0,70566
SNED1	3	0,803129333	0,813051	0,809436667
TIGIT	4	0,6385285	0,70028625	0,65640625

The name of the genes is listed in first colum. “Number of CpG” column displays the number of probes found within the promoter region in that particular gene. “Tcon 5AzaC” column displays the level of methylation in the corresponded gene in the T_{con} after 5AzaC treatment condition. “Tcon DMSO” column displays the level of methylation in the corresponded gene in the Tcon after DMSO treatment condition. “Tcon_ctr” column displays the level of methylation in the corresponded gene in the control that is T_{con} at baseline condition.

6.4.3.2. Distribution of the FOXP3+ cells within the CD25 ^{high}expressing cells

During the process of preparing samples, we wanted to investigate the distribution of the *FOXP3*+ cells within the CD25 expressing cells. We isolated T_{con}, cultured with 5AzaC and stained for cellular and intracellular protein marker as we did for the first group of samples (see section 4.3of this current Chapter) before analysed them using flow cytometry. $FOXP3^{+}$ cells distribution was spread within the CD25+ cells and not just within the cells that were expressing high level of CD25 (Figure 71). Therefore, the magnetic bead isolation kit that we were using was not ideal. We opted to switch to Cell

Sorting (see Chapter 3, section 4) so that we could have chosen the population that we wanted to be isolated.

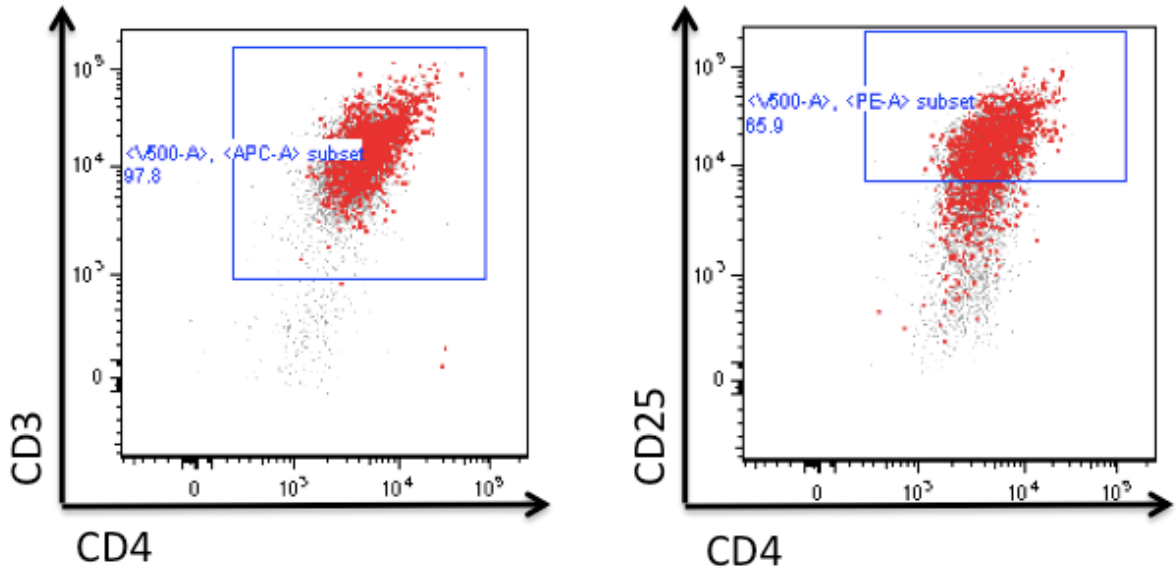


Figure 71. FOXP3$^+$ cells backgating analysis. For parent gating strategy see Chapter 3.6. Red dots represent cells that are *FOXP3*$^+$. Grey dots represent cells that are *FOXP3* $^-$. Based on CD25 and CD4 gating plot, FOXP3+ cells are spread within CD25 high cells (gated in blue) and also CD25 low cells.

6.4.3.3. FOXP3$^+$ cells gDNA quality check

In order to perform the Human Methylation450 bead chip array, gDNA was extracted from *FOXP3*$^+$ CD25$^{high/medium}$ cells. First, *FOXP3*$^+$ CD25$^{high/medium}$ cells were sorted using a Cell Sorting (see Chapter 3, section 4) based on FOXP3 intracellular protein marker and CD25 cellular protein marker. Intracellular staining was performed using 4% paraformaldehyde (see Chapter 3, section 5.2). Because of the potential DNA degradation, following the use of paraformaldehyde, we have checked the DNA quality after the extraction to make sure it has reasonable quality for downstream amplification and sequencing. To improve the quality of extracted DNA, a modified method has also been used which is optimised for pareformaldehyde fixed cells' DNA extraction (see Chapter 6, section 3.2). We performed a phenol-based DNA isolation (see Chapter 5, section 3.2) that was able to undo (using RNAse and Proteinase k) the formaldehyde-induced changes (DNA cross-link) that lead to the imposition of epigenetic analysis in general, but bisulfite conversion in our case. Once the isolation was performed, we proceeded to check the DNA

integrity using the Human DNAOK! Kit (Microzone) (Figure 72). This method uses a multiplex PCR reaction to amplify five different regions of the genome as well as a positive PCR control. If the DNA has good quality, the reaction will produce amplicons from five regions plus the control (100, 200, 300, 400, 500, 600 base pairs “bp”). If the DNA was partially degraded or fragmented, one or more of the amplicons from the genome will be missing. Despite the missing 600 bp band, we have decided to carry on the sequencing process as the majority of the amplicons were present.

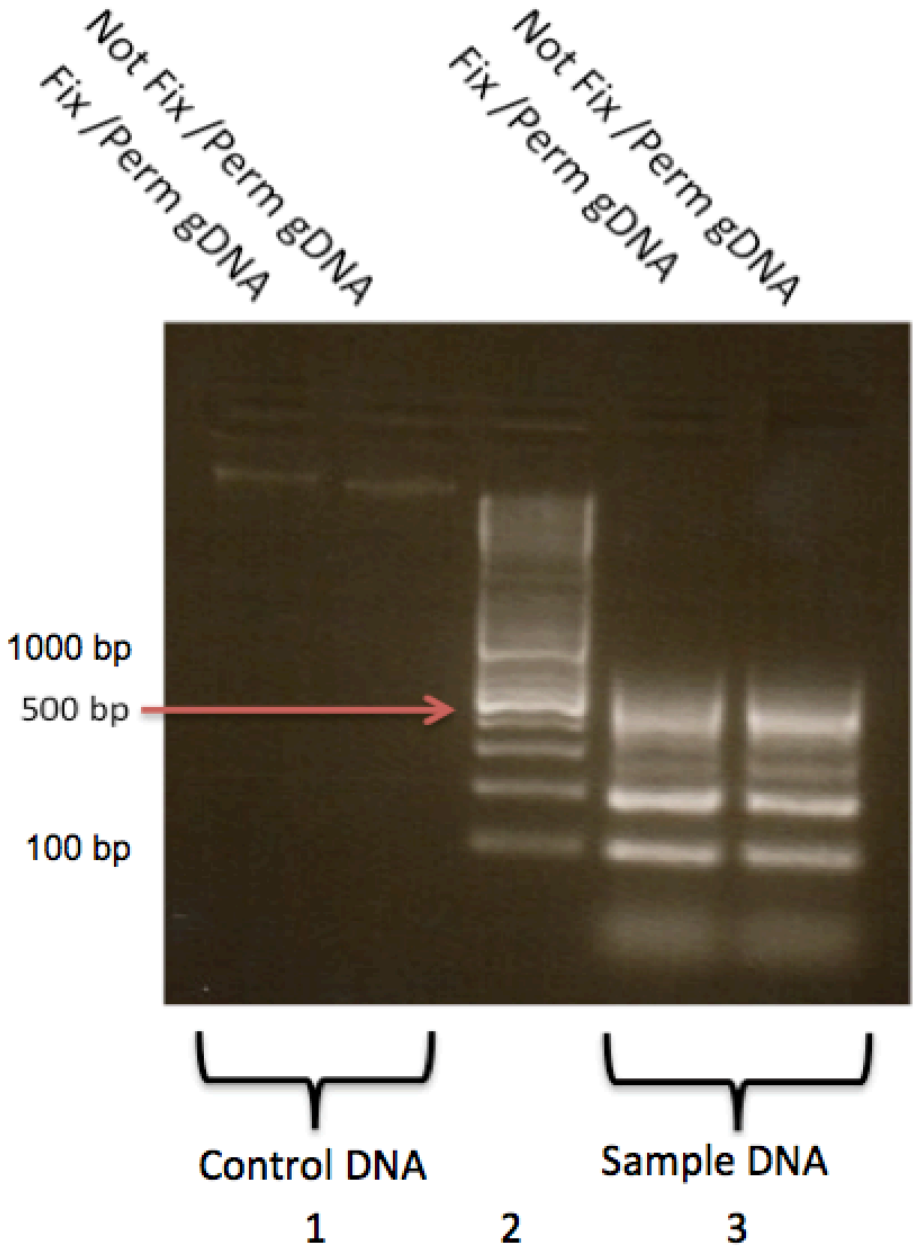


Figure 72. DNA integrity analysis. The figure shows the ethidium bromide-stained agarose gel result. Samples were analysed on a 1.5% (wt/vol) agarose gel. We used 2 conditions: "Fix/Perm gDNA" (cells fixed with 4% paraformaldehyde and then permealised (See Chapter 3.5.2) and "Not Fix/Perm gDNA" (cells at baseline). In the "Control DNA" 2 lanes (1) displayed the conditions without the Human DNAOK! Kit, so we had just one line around at the top of the gel (all gDNA sample) as we expected. Lane 2 was the DNA ladder. In the "Sample DNA" 2 lanes (3) displayed the 2 conditions where the Human DNAOK! Kit was performed.

A total of 3 sets of samples were prepared for Methylome array.
Conditions were:

1. T_{con} stimulated and 5AzaC treated
2. T_{con} stimulated and DMSO treated
3. T_{con} at baseline

6.4.3.4. TIGIT and CREB1 sequencing

Due to a financial budget issue, we opted to use the already prepared 3 set of samples (see section 4.3.3 of this current Chapter) for sequencing. The aim was to validate the first run of the Methylome array data using the 3 set of samples for DNA sequencing. We focused on the 8 genes displayed low level of methylation in T_{con} after 5AzaC treatement as compared with T_{con} after DMSO (Table 19). CAMP Responsive Element binding protein 1 (CREB1) and T cell immunoreceptor with Ig and ITIM domains (TIGIT) were chosen to be sequenced because of their scientific importance on T cells compared with the other 6 genes[137, 138].

We designed using and 2 sets of primers for each gene based on bisulfite converted and not converted DNA sequence (Figure 73 and see Appendix Figures 78 and 79). The Methprimer and Primer3 websites were used as primer design tool.

CREB1	
Meth Fw	3-GTTGTTGTTGTTTGTGGTTCG-5
Meth Rev	5-CGATAATACAAACTCCTCCGTC-3
Unmeth Fw	3-TTGTTGTTGTTTGTGGTTTGG-5
Unmeth Rev	5-CAATAATACAAACTCCTCCATC-3
TIGIT	
Meth Fw	3-TGTGTTTTTCGTGTATAAGTTATCGA-5
Meth Rev	5-CTACGCCCTATAAAAATCCCG-3
Unmeth Fw	3-TGTGTTTTTTGTGTATAAGTTATTGA -5
Unmeth Rev	5-CCTACACCCTATAAAAATCCCAAA-3

Figure 73. CREB1 and TIGIT primers. This is a list of the 8 primers used for the PCR above mentioned. The primers are “Meth”, that means designed on bisulfite converted methylated sequences or “Unmeth” that means designed on bisulfite converted unmethylated sequences. Fw: forward; Rev: reverse.

We bisulfite converted the gDNA from the 3 sets of samples. We generated PCR amplicons using both bisulfite converted and not-converted based primers (Figure 74). Sequencing has been done using Sanger sequence (a service by Genewiz, UK). The PCR product for CREB1 was 162 bp. The PCR product for TIGIT was 157 bp. Figure 18 is an example of the 9 samples.

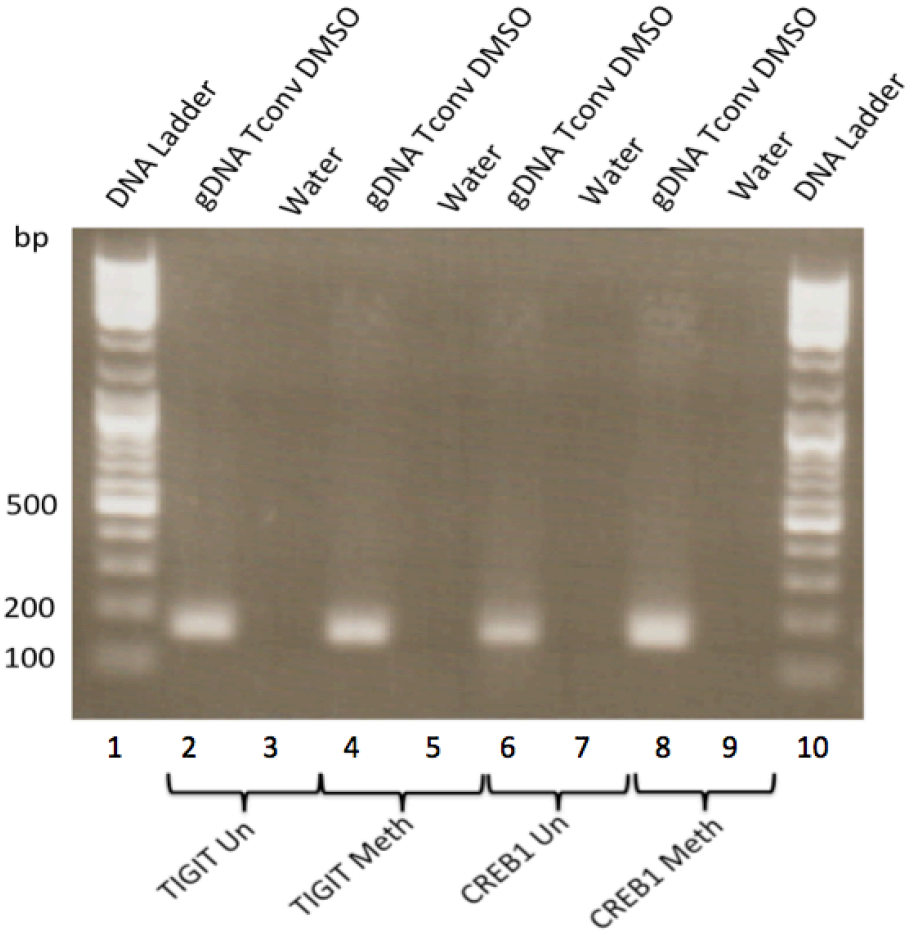


Figure 74. TIGIT and CREB1 PCR. The figure above shows the ethidium bromide-stained agarose gel picture. Samples were run on a 1.9% (w/v) agarose gel on a 95V (current <70mA) for 45 minutes. Lane 1 and 10 represented the DNA ladder. In the lower side of the figure there are the type of amplicon (TIGIT Un (Unmethylated), TIGIT Meth (Methylated), CREB1 Un (Unmethylated) and CREB1 Meth (Methylated) generated and in the upper side the condition where the amplicon was generated (in this example "gDNA T_{con} DMSO" so Tcon treated with DMSO). We also add the Water as control to check whether the primers were contaminated and if there was a non-specific amplification. In lane 2 the product generated using TIGIT unmethylated primers on Tcon treated with DMSO was shown. Lane 3 is the water control. Lane 4 shows the amplicon generated using TIGIT methylated primers on Tcon treated with DMSO was shown. Lane 5 is the water control. Lane 6 shows the amplicon generated using CREB1 unmethylated primers on Tcon treated with DMSO was shown. Lane 7 is the water control. Lane 8 shows the amplicon generated using CREB1 methylated primers on Tcon treated with DMSO was shown. Lane 9 shows the water control.

The chromatogram files from the sequencing company (Genewiz) were aligned to the reference sequences TIGIT and CREB1 (downloaded from the NCBI set and bisulfite converted). However, robust sequencing results after the DNA extraction and bisulfite conversion were not achived by currently available methodology.

6.5. Discussion

tTregs originate *de novo* in the thymus through the recognition of self-antigen[38]. They express high levels of CD25 together with the transcription factor and lineage marker *FOXP3*. The phenotype of Tregs in normal circumstances is stable and the cells are long-lived due to the epigenetic modification of the conserved non-coding sequences (CNS) in the *FOXP3* locus[35, 39]. In particular, CNS1, 2 and 3 are crucial for *FOXP3* expression. CNS1 contains a TGF-β -NFAT response element and has a pivotal role for iTreg cell generation. In the CNS2 (also known as *TSDR* Treg specific demethylation region_ Amp 5 Figure 57)[40] *FOXP3* binds to *CNS2* itself in a CpG DNA methylation dependent manner, that leads to demethylated CpG dinucleotides in stable Tregs but methylated CpGs in naive and Tcon cells. CNS3 appears to control *de novo FOXP3* expression[40, 41]. In this Chapter, we decided to focus on *TSDR* because of its importance on the stability of Tregs.
Also the 5AzaC compound was studied in this Chapter because is a demethylating agent and it was shown to demethylate the *FOXP3* promoter[104], however it is not clear whether 5AzaC has the same effect on the *TSDR* and on the methylation status of downstream genes. In order to understand whether TrLCs were still T_{con} or they have acquired the Treg gene methylation signature, we investigated their *TSDR* status and their methylation status of genes that are regulated by *FOXP3.* For this purpose, we focus on the work of *Sehouli et al*[45], which they were able to design an experiment to quantify the percentage of copy number of Tregs and CD3+ cells within a tumour using the methylation status of the *TSDR* to identify Tregs and the methylation status of *CD3G/CD3G* to identify oTL. Because of the importance in my project to identify and quantify Tregs, my purpose was to acquire and optimise relevant techniques such as qPCR, to quantify the methylation status of the *TSDR* and *CD3G/CD3D* within Tregs, T_{con} and CD3 T cells. The goal was to apply the experiment to identify and quantify among various population within a sample $CD3^+$ T cell population, T_{con} and Tregs. However, the inconsistency in the qPCR results (see section 4.1.3 of this current Chapter) were such that we decided to switch to amplicon sequencing of bisulfite treated DNA on an Illumina MiSeq instrument[127]. According to the

results from this section, the *TSDR* CpG sites in 5AzaC treated T_{con} from HDs were found to be > 73.21% methylated compared with 6.92% of methylation of Tregs, which confirms that TrLCs are most likely not to be Tregs.

Then, we wanted to focus on the genome-wide of the TrLCs, with a particular emphasis on the genes that are regulated by *FOXP3*. The purpose was to assess whether the T_{con} after 5AzaC treatement were still T_{con} or they polarised into another population like Tregs. The DNA genome-wide of Tregs and T_{con} from HD (+/- 5AzaC) was investigated, using a methylation analysis (450K Illumina) following by sequencing. Our aim was to focus on the list of the *FOXP3* binding sites[136] (see Appendix, Table 20) plus additional interesting genes related to *FOXP3* (see appendix, table 20 from gene number 105).

The preliminary methylation results from Table 18 suggested that there is a difference in term of levels of methylation that occurred in "Tcon_ctr" as compared with "Tcon 5AzaC". Also, stimulation with CD3CD28 ("Tcon DMSO") affected methylation levels. Out of 71 genes, 8 genes were unmethylated by the 5AzaC treatement (D/I), displaying low level of methylation in T_{con} after 5AzaC treatement as compared with T_{con} after DMSO (Table 19). Due to a financial budget issue, we were not able to run the Methylome array additional times. We then opted to use the already prepared 3 set of samples (see section 4.3.3 of this current Chapter) for sequencing. The aim was to validate the first run of the Methylome array data using the 3 set of samples for DNA sequencing. We focused on the 8 genes displayed low level of methylation in Tcon after 5AzaC treatement as compared with T_{con} after DMSO (Table 19). CAMP Responsive Element binding protein 1 (CREB1) and T cell immunoreceptor with Ig and ITIM domains (TIGIT) were chosen to be sequenced because of their scientific importance on T cells compared with the other 6 genes[137, 138]. However, consistent sequencing results after the DNA extraction and bisulfite conversion were not achived by currently available methodology.

7. General discussion and further directions

7.1. Background

In majority of malignancies, there are strong evidences to show the role of adaptive immune system in tumour elimination and immune-surveillance.[139] Innate immune responses, which manifests as inflammation (see below), has a strong role in the initiation of adaptive immune responses[140] and tumour rejection. However, chronic inflammation (due to chronic infections or 'sterile' inflammation) could increase the risk of genomic instability and malignant transformation. The balance between "evil" smouldering inflammation and "good" immunesurveillance and the mechanisms which tip the balance toward the so called good inflammation and in favour of adaptive immunity has been the subject of several researches in tumour immunology field[140, 141]. Due to heterogeneity among different malignancies, it is not entirely clear which immune signatures is correlated with cancer protection, nevertheless in some inflammatory diseases like psoriasis there are strong evidences to show that a combination of $CD4^+$ T helper 1 (Th-1) and the M1 phenotype of macrophages protect these patients from skin cancers[140]. Whereas $CD4^+$ T helper 2 (Th-2) and macrophage M2 phenotype do not show any protective effect.[140]

Myelodysplastic Syndrome (MDS) are a heterogeneous group of clonal haematopoietic disorders. They are characterised by ineffective haematopoiesis and are usually associated with genetic instability and immune-dysregulation[2, 142, 143, 144]. MDS are usually considered as part of a group of diseases called bone marrow failure syndromes (BMFs), which consist of an array of disorders ranging from an autoimmune type disease called idiopathic aplastic anaemia (AA) to more pre-/malignant conditions such as high risk MDS.

Cellular immune response in established MDS is multifactorial and follows a stepwise transformation as the disease progresses toward AML (Figure 75).

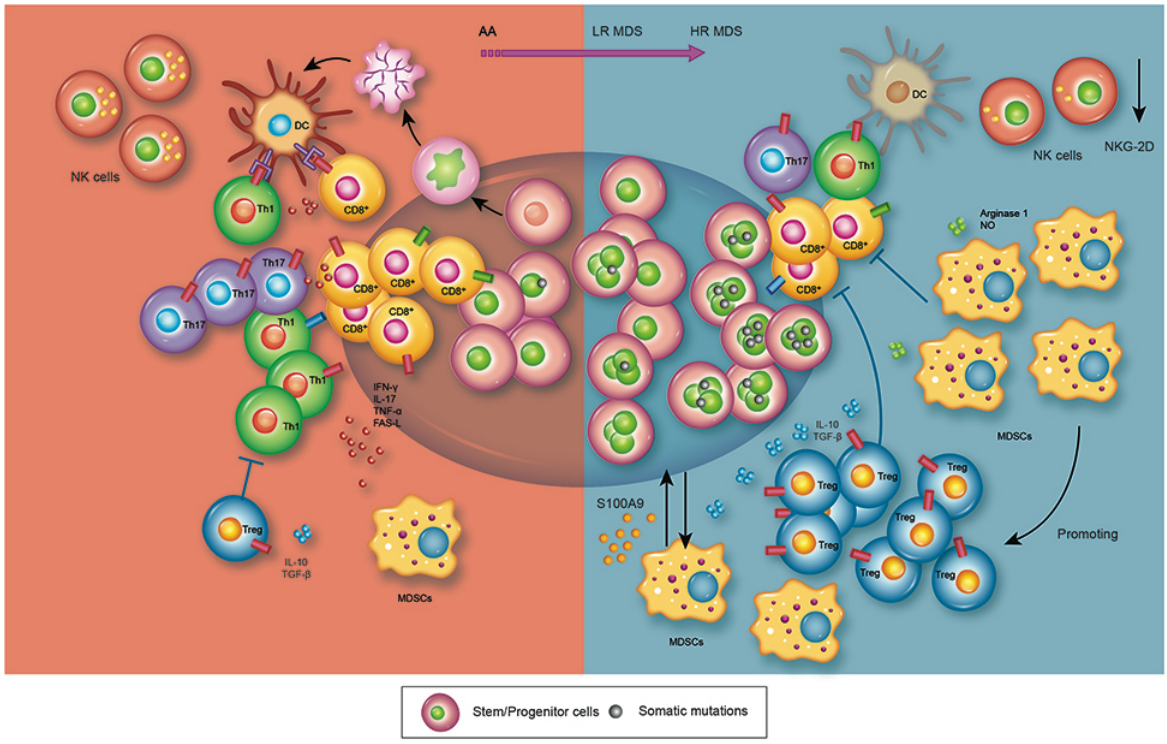


Figure 75. Immune response in MDS. The immune-signature of bone marrow failure syndromes varies and ranging from a pro-inflammatory response in AA and low-risk MDS to a more immunosuppressive environment in high risk MDS. While pro-inflammatory T cells such as Th-1 and Th-17 cells are more prominent in AA and low risk MDS, the suppressive immune cells such as Tregs and MDSCs play the dominant role in high risk MDS.

Previous work by our group has shown profound changes in the adaptive immune system in MDS. Our group was the first to demonstrate a correlation between increased numbers of Tregs in higher risk MDS and risk of progression to AML[2]. We were also the first to identify an increase in the number of IL-17 producing T cells (Th-17) in low risk MDS; the Th-17: Tregs ratio was significantly higher in low risk disease compared with higher risk MDS and correlated significantly with apoptosis[103]. We have shown that treatment with hypomethylating agent (5AzaC) switches Tregs to inflammatory T helpers which correlates with better survival[4]. Moreover, comprehensive mutational profiling has identified the presence of somatic mutations in nearly 80-90% of those with MDS, which may correlate with clinical phenotype, outcome and response to therapeutic agents such as hypomethylating agents[145, 146, 147] .

It is crucial to understand in more details the origin of these cells and their functional properties and whether an increase in FOXP3 expression following

treatment with 5AzaC will actually increase the suppressive properties of T cells and subsequently contribute in disease progression or the 'aberrant' expression of FOXP3 is the result of a more general and non-specific demethylation of genes by 5AzaC.

The CD4 plasticity is not a new concept and using specific conditions, it has been shown that CD4+ T cells could polarise toward Th-1 and Th-2 phenotypes[148, 149]. The regulation of $CD4^+$ T cells is controlled by a combination of extracellular cues, cytosolic signaling and metabolism as well as gene and chromatin regulation (reviewed by DuPage *et al*)[150]. $CD4^+$ T-cell subsets are ranging from pro-inflammatory Th-1 (IFN- γ secreting), Th-2 (IL-4, IL-5, IL-13 secreting), Th-9 (IL-9 secreting), Th-17 (IL-17, IL-22 secreting), T follicular helper (IL-21 secreting), to forkhead box P3 $(FOXP3)^+$ regulatory T cells (Tregs) with immunosuppressive function[150]. However, the $CD4^+$ T cell subsets are not hardwired and show a significant plasticity and are flexible in response to changing environmental cue.[150] Also Tregs were divided into thymically (tTregs) and peripherally induced (pTregs) regulatory T cells[151, 152, 153, 154]. Among CD4+ T cells, Tregs are particularly plastic and could be polarised towards T inflammatory cells (Figure 76) in response to microenvironment[155, 156, 157].

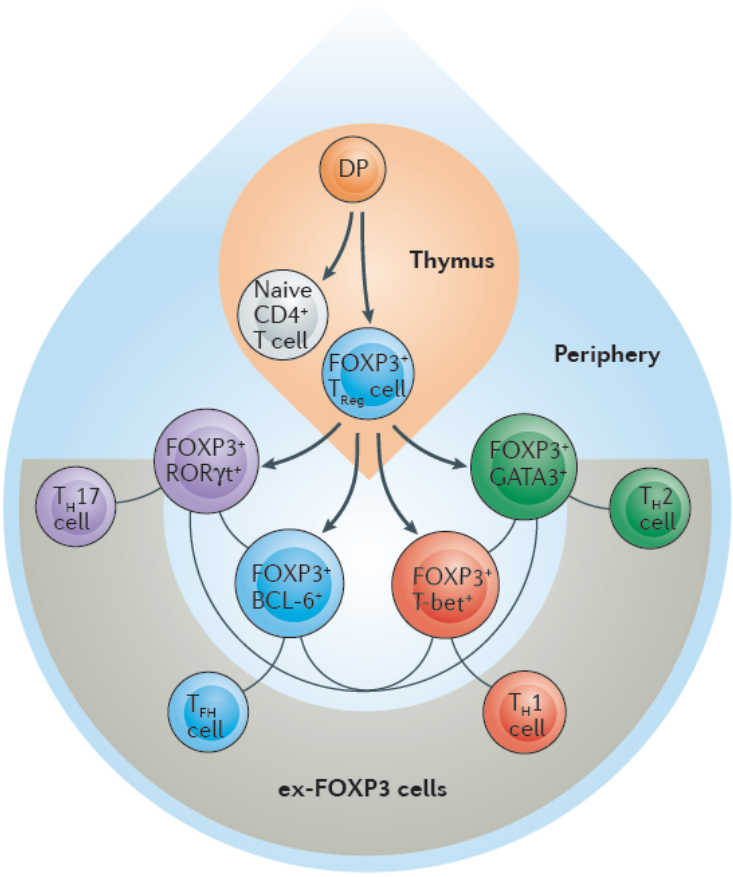


Figure 76. Tregs polarisation into T inflammatory subsets. In the thymus, from the double positive precursor (DP), Tregs diverge from CD4+ T cells during T cell development. Then, in response to environmental cues, the co expression of FOXP3 and the master transcriptor factors of each T helper cell subset (GATA3+, T-bet+, CL-6+, ROR[redacted]+) lead to the different Tregs subsets. The transition between Tregs and T inflammatory cells is likely to be due to different settings like inflammation. The acquisition of inflammatory cytokines and the loss of the FOXP3 signature occurred. Figure adapted from Du Page *et al*[150]

Extracellular cues, like drugs (*e.g.* 5AzaC) or cytokines, can activate different pathways that lead to cell plasticity. For example, the phosphatidylinositol 3-kinase (PI3K) – AKT – mammalian target of rapamycin (mTOR) pathway is required for the functions and polarisation of T helpers cells, but repressed in Tregs. In T helper, the deletion of mTOR complexes inhibits Th-17, Th-1, Th-2 cell polarisation, whereas the blockade promotes Tregs (Figure 77).

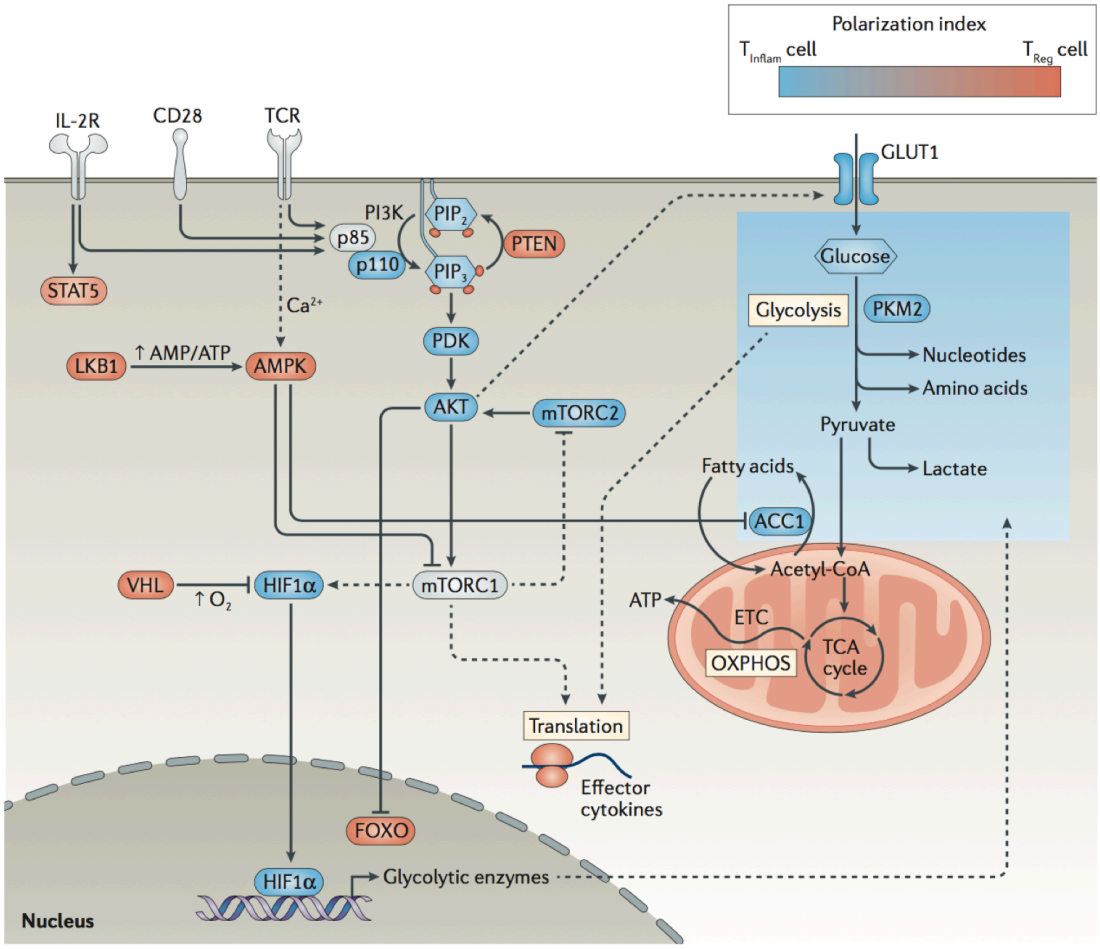


Figure 77. Plasticity of T inflammatory cells versus Tregs. The polarisation index demonstrates process of proteins that support the induction of Tregs (red) or inflammatory T cells. Connections between the phosphatidylinositol 3-kinase (PI3K) – AKT – mammalian target of rapamycin (mTOR) pathway, extracellular signal, gene regulation and metabolic programmes are illustrated in the picture. Figure adapted from Du Page *et al*[150]

Although we have shown that Tregs can be polarised to T inflammatory cells by 5AzaC and it correlates with better survival, nevertheless, the expression of FOXP3 goes higher following therapy. It is known that the increased number of $FOXP3^+$ Tregs in MDS is associated with poorer prognosis and if 5AzaC increases the number of Tregs then it may undermine the beneficial therapeutic effect.

We have shown that following treatment with 5AzaC[104], the absolute number of Tregs is reduced and they not only became non-suppressive but also secrete pro-inflammatory cytokines, such as IL-17 and IFN-γ. There is also an increase in *FOXP3* expression by T_{con} following *in-vitro* culture with 5AzaC, without significant immunosuppressive properties. This subpopulation is known as “Treg-like” cells (TrLCs).

Due to these promising data, we wanted to investigate further the differences between Tregs, T_{con} and TrLCs from HDs and MDS patients in term of phenotype, cytokine secretion and DNA methylation profile and whether TrLCs show any molecular or functional properties of Tregs.

7.2. Findings

The specific aims of this PhD project and summary of findings are summarised:

7.2.1. *The effects of 5AzaC on phenotype, cytokine profile and function of T_{con}.*

The aim of this part was to compare TrLCs with Tregs, T_{con} and IL-17 secreting Tregs coming from a Th-17 polarising environment (*in-vitro* culture with IL-1β, IL-6 and IL-2) to understand whether the features of this subpopulation were still T_{con} or they polarised into another population. To address this, we cultured T_{con} from HDs with and without 5AzaC for 5 days and we checked the phenotype and the cytokine profile using either flow cytometry and Luminex technology. Then, we co-cultured those 5AzaC treated T_{con} with T_{con} and we compare their suppressive function with Tregs and with IL-17 secreting Tregs.

Following the above *in-vitro* cultures, our data demonstrated an increase in secretion of IL-17 and expression of *FOXP3* in T_{con} cells following 5AzaC treatment as compared with untreated T_{con}. In addition, we demonstrated that TrLCs have no significant immunosuppressive properties when culture with autologous T_{con} (1:1) as compared with Tregs cultured with autologous T_{con} (1:1). In term of cytokine suppression both TrLCs and Tregs reduce the production of TNF-α and IFN-γ (pg/ml) compare with the positive control, nevertheless TrLCs was not as good as Tregs to suppress Tcon.

Then we have investigated the differences between T_{con} after 5AzaC treatment and IL-17 secreting Tregs coming from Tregs after *in-vitro* culture with IL-1β, IL-6 and IL-2 in term of suppressive function. Unlike IL-17 secreting Tregs, TrLCs were unable to suppress T_{con} proliferation when co-cultured in 1:1 ratio. Our data suggested that although TrLCs display Tregs

and IL-17 secreting Tregs' phenotypic signatures, they lack suppressive function.

7.2.2. *Phenotypic characterisation of TrLCs*

The aim of this part was to further characterise the phenotype of TrLCs and identifying components of the cell surface proteome, which define TrLCs.

As T_{con} started to express FOXP3 following culture with 5AzaC, which is not common for T_{con} and they are not functional and secrete aberrant cytokines like IL-17 we wanted to further study those TrLCs and their (dis) similarity with Tregs. To address this, we analysed the TrLCs using Mass Spectrometry in order to analyse cell surface proteome on a large scale. Although preliminary data from Mass Spectrometry analysis suggested that the method could have potentially been used to concentrate membrane proteins, we were aware that cultured cells were a mixture of $CD4^+CD25^+$ cells therefore we were not being able to look just at $FOXP3^+$ cells or at specific subsets. In addition, because we wanted to focus just on membrane proteins we used a biotin compound to extract them (see Chapter 5 section 3.1) but we still had some intracellular contaminations. This circumstance makes it very challenging to have a dataset without any intracellular protein contamination.

Meanwhile the single cell mass cytometry or cytometry by time-of-flight [123](CyTOF) became available. This novel method is a deep phenotyping strategy using multi-parameter mass cytometry. Therefore, we have decided to switch to CyTOF method as it allows multi-parametric single cell analysis for more than 40 channels without significant spillover between them[124]. First, we wanted to comprehensively characterise T cells from HDs after 5AzaC treatment focusing on the cells with higher expression of FOXP3.

$CD4^+$ FOXP3hi (as determined by automated clustering) cells from the MDS patients showed a statistically significant increase in CD25, T-bet and IFN-γ following culture with 5AzaC. The increase in CD25 in MDS samples caused by 5AzaC treatment is a feature of Tregs. However, high expression of INF-γ and T-bet in these cells is not typical for Tregs. In contrast, 5AzaC treatment of cells from HDs, reduced the expression of IL-2, which is common for Tregs,

but crucial cytokines normally expressed by Tregs *e.g.* IL-10, TGF-β and IL-35 were not present.

This consideration is very interesting as one of the features of MDS is the lack of effective immune response. Therefore, if 5AzaC treatment would be able to convert high FOXP3 cells into high FOXP3 cells with the inflammatory phenotype that could potentially keep malignant clone under check. The fact that T cells from MDS patients are more prone to polarisation toward T inflammatory cells may suggest a 'priming' role for the microenvironment in MDS, which needs further investigation.

We also focused on characterise T_{con} (+/- 5AzaC) from HDs. As we already shown in Chapter 4, following *in-vitro* culture, our data demonstrated an increase in secretion of IL-17 and expression of *FOXP3* in T_{con} cells following 5AzaC treatment as compared with T_{con} treated with DMSO. In this case, we cultured just T_{con} so the effects were more pronounced and clear compared with PBMCs.

Unfortunately, because of the low cell number, it was impossible to investigate T_{con} in MDS patients. Nevertheless, the dataset from T_{con} from HDs shown that although they were expressing high *FOXP3* and low CD127, similar to Tregs, IL-10 was lower compared with the DMSO control and many important Tregs markers such as CD27 or homing receptors were not different between 5AzaC treated T_{con} and control.

From this dataset we concluded that, even in isolated T_{con}, that is a cleaner system because we don't have interaction with other cells or effects from other cells, they are still presenting some TrLCs features like FOXP3 expression. More important we have also showed by looking at several markers that, not only these T_{con} displayed inflammatory features but also, they don't have crucial cytokines for Tregs profile like IL-10. Datasets from this Chapter strongly suggested that cells with high FOXP3 expression following 5AzaC treatment are not similar to functioning $FOXP3^+$ Tregs.

7.2.3. *Methylation statues of Treg related genes in TrLCs*

The Treg Specific Demethylated Region (*TSDR*) is an evolutionarily conserved non-coding element

contained within a specific intron of the *FOXP3* gene whose CpG dinucleotides are demethylated in nTregs but methylated in the CD3+ T population. It has been proposed that a steady demethylation profile of the *TSDR* is a fundamental feature of stable Tregs[44, 134] (see Chapter 1, section 3.2.1.1). In order to understand whether TrLCs were still T_{con} or they have acquired the Tregs gene methylation signature, we investigate their *TSDR* status. After many attempts with the qPCR methods and the inconsistency in the results (see Chapter 6 section 4.1.3) we decided to switch to amplicon sequencing of bisulfite treated DNA on an Illumina MiSeq instrument[127]. According to the results from this section, the *TSDR* CpG sites in 5AzaC treated T_{con} from HDs were found to be > 73.21% methylated compared with 6.92% of methylation of Tregs. From this data, we can conclude that TrLCs are more likely to be not Tregs.

7.3. Conclusions and future directions

Altogether the results of this thesis suggested that T cells subsets are able to adapt their functions to changing environment. As we showed with our data, 5AzaC treatment can potentially increase FOXP3 expression in T_{con}.

According to the suppressive assay, TrLCs are not functional; therefore, they are less likely to be Tregs. Even though TrLCs displayed high *FOXP3* expression following 5AzaC treatment, they are not stable Tregs, and therefore FOXP3 marker is not an indication for Tregs. 5AzaC cannot hypomethylate TSDR and therefore these cells are less likely to maintain their FOXP3 expression or show stable suppressive function. More importantly the *TSDR*, that is unmethylated in stable Tregs, was found to be methylated in TrLCs after 5AzaC treatment. In addition, mass-cytometry and automated clustering identifies a population of T_{con}, which showed some characteristics of Tregs but lacked several crucial markers like IL-10.

The aim of this thesis was to develop and deepen the knowledge on “Treg-like” cells coming from 5AzaC treated T_{con}. Through a methodical and quantitative analysis, we assessed that the TrLCs are less like to be Tregs. Even though they expressed some Tregs features like high FOXP3 expression, 5AzaC treated T_{con} polarised towards a T inflammatory cells

profile rather than a Tregs profile. These observations can help to direct future researches in the field.

A consistent theme throughout the thesis work was the emphasis on studying the dynamics of biological processes on 5AzaC treated T_{con} from HDs. As suggested by the results from Chapter 4 and 5, a future direction would be to expand the study of the deep phenotyping of $CD4^+$ cells from both low and high-risk MDS in larger cohort, and to investigate the effect of microenvironment in priming of T cells and their response to 5AzaC.

The data assessed in Chapter 6 suggested another interesting aspect to be investigated, which is to compare gene expression profile in MDS versus healthy donors to identify relevant pathways.

A fundamental issue to address is whether or not TrLCs could potentially target malignant clone in MDS. Further investigation is needed to prove the mechanism and the behavior of TrLCs in malignant clones' rejection in mice models.

Overall, these proposed investigations would provide important information concerning the study of TrLCs *in vitro* and *in vivo* (mice models) on MDS patients. This Ph.D. thesis provides a foundation upon which these other works can be built. The empirical nature of the topic explored, and its potential relevance to clinical application, will hopefully expedite a deeper knowledge on TrLCs in MDS patients and a possible use of this cell subset in cancer therapies.

9. References

1. Greenberg, P.L. *et al.* Revised international prognostic scoring system for myelodysplastic syndromes. *Blood* **120**, 2454-2465 (2012).

2. Kordasti, S.Y. *et al.* CD4+CD25high Foxp3+ regulatory T cells in myelodysplastic syndrome (MDS). *Blood* **110**, 847-850 (2007).

3. Raj, K. & Mufti, G.J. Azacytidine (Vidaza(R)) in the treatment of myelodysplastic syndromes. *Ther Clin Risk Manag* **2**, 377-388 (2006).

4. Costantini, B. *et al.* The effects of 5-azacytidine on the function and number of regulatory T cells and T-effectors in myelodysplastic syndrome. *Haematologica* **98**, 1196-1205 (2013).

5. Golub, E.S. The immune response: an overview. *Methods in cell biology* **37**, 1-5 (1993).

6. Parkin, J. & Cohen, B. An overview of the immune system. *Lancet* **357**, 1777-1789 (2001).

7. Abbas, A.K., Lichtman, A.H. & Pillai, S. *Cellular and molecular immunology*, 7th edn. Elsevier/Saunders: Philadelphia, 2012.

8. Akira, S., Uematsu, S. & Takeuchi, O. Pathogen recognition and innate immunity. *Cell* **124**, 783-801 (2006).

9. Akira, S. Pathogen recognition by innate immunity and its signaling. *Proceedings of the Japan Academy. Series B, Physical and biological sciences* **85**, 143-156 (2009).

10. Jounai, N., Kobiyama, K., Takeshita, F. & Ishii, K.J. Recognition of damage-associated molecular patterns related to nucleic acids during inflammation and vaccination. *Frontiers in cellular and infection microbiology* **2**, 168 (2012).

11. Litvack, M.L. & Palaniyar, N. Review: Soluble innate immune pattern-recognition proteins for clearing dying cells and cellular components: implications on exacerbating or resolving inflammation. *Innate immunity* **16**, 191-200 (2010).

12. Bonilla, F.A. & Oettgen, H.C. Adaptive immunity. *The Journal of allergy and clinical immunology* **125**, S33-40 (2010).

13. Iwasaki, A. & Medzhitov, R. Toll-like receptor control of the adaptive immune responses. *Nature immunology* **5**, 987-995 (2004).

14. Simpson, E. Function of the MHC. *Immunology. Supplement* **1**, 27-30 (1988).

15. Hamilos, D.L. Antigen presenting cells. *Immunologic research* **8**, 98-117 (1989).

16. Holling, T.M., Schooten, E. & van Den Elsen, P.J. Function and regulation of MHC class II molecules in T-lymphocytes: of mice and men. *Human immunology* **65**, 282-290 (2004).

17. Sharma, P., Wagner, K., Wolchok, J.D. & Allison, J.P. Novel cancer immunotherapy agents with survival benefit: recent successes and next steps. *Nature reviews. Cancer* **11**, 805-812 (2011).

18. Miller, J.F. The Thymus and the Development of Immunologic Responsiveness. *Science* **144**, 1544-1551 (1964).

19. Miller, J.F. Immunological function of the thymus. *Lancet* **2**, 748-749 (1961).

20. Miller, J.F. Analysis of the thymus influence in leukaemogenesis. *Nature* **191**, 248-249 (1961).

21. Miller, J.F. & Osoba, D. Current concepts of the immunological function of the thymus. *Physiol Rev* **47**, 437-520 (1967).

22. Gershon, R.K. & Kondo, K. Infectious immunological tolerance. *Immunology* **21**, 903-914 (1971).

23. Sakaguchi, S., Sakaguchi, N., Asano, M., Itoh, M. & Toda, M. Immunologic self-tolerance maintained by activated T cells expressing IL-2 receptor alpha-chains (CD25). Breakdown of a single mechanism of self-tolerance causes various autoimmune diseases. *Journal of immunology* **155**, 1151-1164 (1995).

24. Sakaguchi, S., Setoguchi, R., Yagi, H. & Nomura, T. Naturally arising Foxp3-expressing CD25+CD4+ regulatory T cells in self-tolerance and autoimmune disease. *Current topics in microbiology and immunology* **305**, 51-66 (2006).

25. Brunkow, M.E. *et al.* Disruption of a new forkhead/winged-helix protein, scurfin, results in the fatal lymphoproliferative disorder of the scurfy mouse. *Nat Genet* **27**, 68-73 (2001).

26. Bennett, C.L. *et al.* The immune dysregulation, polyendocrinopathy, enteropathy, X-linked syndrome (IPEX) is caused by mutations of FOXP3. *Nat Genet* **27**, 20-21 (2001).

27. Khattri, R., Cox, T., Yasayko, S.A. & Ramsdell, F. An essential role for Scurfin in CD4+CD25+ T regulatory cells. *Nature immunology* **4**, 337-342 (2003).

28. Hori, S., Nomura, T. & Sakaguchi, S. Control of regulatory T cell development by the transcription factor Foxp3. *Science* **299**, 1057-1061 (2003).

29. Fontenot, J.D., Gavin, M.A. & Rudensky, A.Y. Foxp3 programs the development and function of CD4+CD25+ regulatory T cells. *Nature immunology* **4**, 330-336 (2003).

30. Sakaguchi, S., Wing, K. & Miyara, M. Regulatory T cells - a brief history and perspective. *European journal of immunology* **37 Suppl 1**, S116-123 (2007).

31. Yamagiwa, S., Gray, J.D., Hashimoto, S. & Horwitz, D.A. A role for TGF-beta in the generation and expansion of CD4+CD25+ regulatory T cells from human peripheral blood. *Journal of immunology* **166**, 7282-7289 (2001).

32. Shevach, E.M. From vanilla to 28 flavors: multiple varieties of T regulatory cells. *Immunity* **25**, 195-201 (2006).

33. Shevach, E.M. & Thornton, A.M. tTregs, pTregs, and iTregs: similarities and differences. *Immunological reviews* **259**, 88-102 (2014).

34. Povoleri, G.A. *et al.* Thymic versus induced regulatory T cells - who regulates the regulators? *Frontiers in immunology* **4**, 169 (2013).

35. Sakaguchi, S., Vignali, D.A., Rudensky, A.Y., Niec, R.E. & Waldmann, H. The plasticity and stability of regulatory T cells. *Nature reviews. Immunology* **13**, 461-467 (2013).

36. Mills, K.H. Regulatory T cells: friend or foe in immunity to infection? *Nature reviews. Immunology* **4**, 841-855 (2004).

37. Abbas, A.K. *et al.* Regulatory T cells: recommendations to simplify the nomenclature. *Nature immunology* **14**, 307-308 (2013).

38. Vignali, D.A., Collison, L.W. & Workman, C.J. How regulatory T cells work. *Nature reviews. Immunology* **8**, 523-532 (2008).

39. Bos, P.D. & Rudensky, A.Y. Treg cells in cancer: a case of multiple personality disorder. *Science translational medicine* **4**, 164fs144 (2012).

40. Baron, U. *et al.* DNA demethylation in the human FOXP3 locus discriminates regulatory T cells from activated FOXP3(+) conventional T cells. *Eur J Immunol* **37**, 2378-2389 (2007).

41. Zheng, Y. *et al.* Role of conserved non-coding DNA elements in the Foxp3 gene in regulatory T-cell fate. *Nature* **463**, 808-812 (2010).

42. Miyara, M. *et al.* Functional delineation and differentiation dynamics of human CD4+ T cells expressing the FoxP3 transcription factor. *Immunity* **30**, 899-911 (2009).

43. Tatura, R. *et al.* Quantification of regulatory T cells in septic patients by real-time PCR-based methylation assay and flow cytometry. *PloS one* **7**, e49962 (2012).

44. Floess, S. *et al.* Epigenetic control of the foxp3 locus in regulatory T cells. *PLoS biology* **5**, e38 (2007).

45. Sehouli, J. *et al.* Epigenetic quantification of tumor-infiltrating T-lymphocytes. *Epigenetics : official journal of the DNA Methylation Society* **6**, 236-246 (2011).

46. Polansky, J.K. *et al.* DNA methylation controls Foxp3 gene expression. *European journal of immunology* **38**, 1654-1663 (2008).

47. Ohkura, N., Kitagawa, Y. & Sakaguchi, S. Development and maintenance of regulatory T cells. *Immunity* **38**, 414-423 (2013).

48. Sawant, D.V. & Vignali, D.A. Once a Treg, always a Treg? *Immunol Rev* **259**, 173-191 (2014).

49. Piccirillo, C.A., d'Hennezel, E., Sgouroudis, E. & Yurchenko, E. CD4+Foxp3+ regulatory T cells in the control of autoimmunity: in vivo veritas. *Current opinion in immunology* **20**, 655-662 (2008).

50. Chatenoud, L. & Bach, J.F. Adaptive human regulatory T cells: myth or reality? *The Journal of clinical investigation* **116**, 2325-2327 (2006).

51. Janson, P.C. *et al.* FOXP3 promoter demethylation reveals the committed Treg population in humans. *PloS one* **3**, e1612 (2008).

52. Yu, N. *et al.* CD4(+)CD25 (+)CD127 (low/-) T cells: a more specific Treg population in human peripheral blood. *Inflammation* **35**, 1773-1780 (2012).

53. Liu, W. *et al.* CD127 expression inversely correlates with FoxP3 and suppressive function of human CD4+ T reg cells. *The Journal of experimental medicine* **203**, 1701-1711 (2006).

54. Ustun, C., Miller, J.S., Munn, D.H., Weisdorf, D.J. & Blazar, B.R. Regulatory T cells in acute myelogenous leukemia: is it time for immunomodulation? *Blood* **118**, 5084-5095 (2011).

55. Gondek, D.C., Lu, L.F., Quezada, S.A., Sakaguchi, S. & Noelle, R.J. Cutting edge: contact-mediated suppression by CD4+CD25+ regulatory cells involves a granzyme B-dependent, perforin-

independent mechanism. *Journal of immunology* **174**, 1783-1786 (2005).

56. Bopp, T. *et al.* Cyclic adenosine monophosphate is a key component of regulatory T cell-mediated suppression. *The Journal of experimental medicine* **204**, 1303-1310 (2007).

57. Hubert, P., Jacobs, N., Caberg, J.H., Boniver, J. & Delvenne, P. The cross-talk between dendritic and regulatory T cells: good or evil? *Journal of leukocyte biology* **82**, 781-794 (2007).

58. Oderup, C., Cederbom, L., Makowska, A., Cilio, C.M. & Ivars, F. Cytotoxic T lymphocyte antigen-4-dependent down-modulation of costimulatory molecules on dendritic cells in CD4+ CD25+ regulatory T-cell-mediated suppression. *Immunology* **118**, 240-249 (2006).

59. Huang, C.T. *et al.* Role of LAG-3 in regulatory T cells. *Immunity* **21**, 503-513 (2004).

60. Hori, S. Lineage stability and phenotypic plasticity of Foxp3(+) regulatory T cells. *Immunological reviews* **259**, 159-172 (2014).

61. Hori, S. Stability of regulatory T-cell lineage. *Advances in immunology* **112**, 1-24 (2011).

62. Pandiyan, P. & Zhu, J. Origin and functions of pro-inflammatory cytokine producing Foxp3(+) regulatory T cells. *Cytokine* **76**, 13-24 (2015).

63. Zhou, L. *et al.* TGF-beta-induced Foxp3 inhibits T(H)17 cell differentiation by antagonizing RORgammat function. *Nature* **453**, 236-240 (2008).

64. Gagliani, N. *et al.* Th-17 cells transdifferentiate into regulatory T cells during resolution of inflammation. *Nature* **523**, 221-225 (2015).

65. Curiel, T.J. *et al.* Specific recruitment of regulatory T cells in ovarian carcinoma fosters immune privilege and predicts reduced survival. *Nature medicine* **10**, 942-949 (2004).

66. Leong, P.P. *et al.* Phenotyping of lymphocytes expressing regulatory and effector markers in infiltrating ductal carcinoma of the breast. *Immunology letters* **102**, 229-236 (2006).

67. Beyer, M. *et al.* Comparative approach to define increased regulatory T cells in different cancer subtypes by combined assessment of CD127 and FOXP3. *Clinical & developmental immunology* **2011**, 734036 (2011).

68. Schaefer, C. *et al.* Characteristics of CD4+CD25+ regulatory T cells in the peripheral circulation of patients with head and neck cancer. *British journal of cancer* **92**, 913-920 (2005).

69. Javia, L.R. & Rosenberg, S.A. CD4+CD25+ suppressor lymphocytes in the circulation of patients immunized against melanoma antigens. *Journal of immunotherapy* **26**, 85-93 (2003).

70. Liyanage, U.K. *et al.* Prevalence of regulatory T cells is increased in peripheral blood and tumor microenvironment of patients with pancreas or breast adenocarcinoma. *Journal of immunology* **169**, 2756-2761 (2002).

71. Ormandy, L.A. *et al.* Increased populations of regulatory T cells in peripheral blood of patients with hepatocellular carcinoma. *Cancer research* **65**, 2457-2464 (2005).

72. Roncador, G. *et al.* FOXP3, a selective marker for a subset of adult T-cell leukaemia/lymphoma. *Leukemia : official journal of the Leukemia Society of America, Leukemia Research Fund, U.K* **19**, 2247-2253 (2005).

73. Baraka, A. & Salem, H.M. Clinical significance of T-regulatory cells in B-cell non-Hodgkin's lymphoma. *The Egyptian journal of immunology / Egyptian Association of Immunologists* **18**, 23-30 (2011).

74. Banerjee, A., Vasanthakumar, A. & Grigoriadis, G. Modulating T regulatory cells in cancer: how close are we? *Immunology and cell biology* **91**, 340-349 (2013).

75. Gallimore, A.M. & Simon, A.K. Positive and negative influences of regulatory T cells on tumour immunity. *Oncogene* **27**, 5886-5893 (2008).

76. Marshall, N.A. *et al.* Immunosuppressive regulatory T cells are abundant in the reactive lymphocytes of Hodgkin lymphoma. *Blood* **103**, 1755-1762 (2004).

77. Kottke, T. *et al.* Treg depletion-enhanced IL-2 treatment facilitates therapy of established tumors using systemically delivered oncolytic virus. *Molecular therapy : the journal of the American Society of Gene Therapy* **16**, 1217-1226 (2008).

78. Ghiringhelli, F. *et al.* CD4+CD25+ regulatory T cells inhibit natural killer cell functions in a transforming growth factor-beta-dependent manner. *The Journal of experimental medicine* **202**, 1075-1085 (2005).

79. Ruter, J. *et al.* Altering regulatory T cell function in cancer immunotherapy: a novel means to boost the efficacy of cancer vaccines. *Frontiers in bioscience* **14**, 1761-1770 (2009).

80. Mufti, G.J. *et al.* Diagnosis and classification of myelodysplastic syndrome: International Working Group on Morphology of myelodysplastic syndrome (IWGM-MDS) consensus proposals for the definition and enumeration of myeloblasts and ring sideroblasts. *Haematologica* **93**, 1712-1717 (2008).

81. Munn, D.H. *et al.* GCN2 kinase in T cells mediates proliferative arrest and anergy induction in response to indoleamine 2,3-dioxygenase. *Immunity* **22**, 633-642 (2005).

82. Ben-Shoshan, J., Maysel-Auslender, S., Mor, A., Keren, G. & George, J. Hypoxia controls CD4+CD25+ regulatory T-cell homeostasis via hypoxia-inducible factor-1alpha. *European journal of immunology* **38**, 2412-2418 (2008).

83. Mufti, G.J. Pathobiology, classification, and diagnosis of myelodysplastic syndrome. *Best practice & research. Clinical haematology* **17**, 543-557 (2004).

84. Ghariani, I., Braham, N., Hassine, M. & Kortas, M. [Myelodysplastic syndrome classification]. *Annales de biologie clinique* **71**, 139-144 (2013).

85. Vardiman, J.W. *et al.* The 2008 revision of the World Health Organization (WHO) classification of myeloid neoplasms and acute leukemia: rationale and important changes. *Blood* **114**, 937-951 (2009).

86. Raza, A. & Galili, N. The genetic basis of phenotypic heterogeneity in myelodysplastic syndromes. *Nature reviews. Cancer* **12**, 849-859 (2012).

87. Greenberg, P. *et al.* International scoring system for evaluating prognosis in myelodysplastic syndromes. *Blood* **89**, 2079-2088 (1997).

88. Seiter, K. Myelodysplasia: new approaches. *Current treatment options in oncology* **14**, 156-169 (2013).

89. Lim, Z.Y. *et al.* Low IPSS score and bone marrow hypocellularity in MDS patients predict hematological responses to antithymocyte globulin. *Leukemia* **21**, 1436-1441 (2007).

90. Guo, G. *et al.* Synthesis and Antiproliferative Activities of 5-Azacytidine Analogues in Human Leukemia Cells. *Molecules* **13**, 1487-1500 (2008).

91. Sekeres, M.A. Lenalidomide in MDS: 4th time's a charm. *Blood* **118**, 3757-3758 (2011).

92. Giagounidis, A.A. *et al.* Long-term transfusion independence in del(5q) MDS patients who discontinue lenalidomide. *Leukemia* **26**, 855-858 (2012).

93. Sorm, F., Piskala, A., Cihak, A. & Vesely, J. 5-Azacytidine, a new, highly effective cancerostatic. *Experientia* **20**, 202-203 (1964).

94. Fenaux, P. Inhibitors of DNA methylation: beyond myelodysplastic syndromes. *Nat Clin Pract Oncol* **2 Suppl 1**, S36-44 (2005).

95. Jones, P.A. & Taylor, S.M. Cellular differentiation, cytidine analogs and DNA methylation. *Cell* **20**, 85-93 (1980).

96. Robertson, K.D. DNA methylation, methyltransferases, and cancer. *Oncogene* **20**, 3139-3155 (2001).

97. Tate, P.H. & Bird, A.P. Effects of DNA methylation on DNA-binding proteins and gene expression. *Curr Opin Genet Dev* **3**, 226-231 (1993).

98. Bird, A.P. DNA methylation and the frequency of CpG in animal DNA. *Nucleic Acids Res* **8**, 1499-1504 (1980).

99. Lyko, F. & Brown, R. DNA methyltransferase inhibitors and the development of epigenetic cancer therapies. *J Natl Cancer Inst* **97**, 1498-1506 (2005).

100. Wang, W. *et al.* Analysis of methylation-sensitive transcriptome identifies GADD45a as a frequently methylated gene in breast cancer. *Oncogene* **24**, 2705-2714 (2005).

101. Thakur, S. *et al.* ING1 and 5-azacytidine act synergistically to block breast cancer cell growth. *PloS one* **7**, e43671 (2012).

102. Aggarwal, S. *et al.* Role of immune responses in the pathogenesis of low-risk MDS and high-risk MDS: implications for immunotherapy. *British journal of haematology* **153**, 568-581 (2011).

103. Kordasti, S.Y. *et al.* IL-17-producing CD4(+) T cells, pro-inflammatory cytokines and apoptosis are increased in low risk myelodysplastic syndrome. *British journal of haematology* **145**, 64-72 (2009).

104. Costantini, B. *et al.* The effects of 5-azacytidine on the function and number of regulatory T-cells and T-effectors in myelodysplastic syndrome. *Haematologica* **98**, 1196-1205 (2013).

105. Lin, Z. *et al.* In vivo antigen-driven plasmablast enrichment in combination with antigen-specific cell sorting to facilitate the isolation of rare monoclonal antibodies from human B cells. *Nature protocols* **9**, 1563-1577 (2014).

106. Yokoyama, W.M., Thompson, M.L. & Ehrhardt, R.O. Cryopreservation and thawing of cells. *Current protocols in immunology / edited by John E. Coligan ... [et al.]* **Appendix 3**, 3G (2012).

107. Craig, F.E. & Foon, K.A. Flow cytometric immunophenotyping for hematologic neoplasms. *Blood* **111**, 3941-3967 (2008).

108. Macher BA, Y.T. Proteins at membrane surfaces-a review of approaches. *Mol Biosyst. 2007 Oct;3(10):705-13.*

109. Macher, B.A. & Yen, T.Y. Proteins at membrane surfaces-a review of approaches. *Molecular bioSystems* **3**, 705-713 (2007).

110. Rosa Viner, T.Z., Scott Peterman, and Vlad Zabrouskov,. Advantages of the LTQ Orbitrap for Protein Identification in Complex Digests

. *Thermo Fisher Scientific, San Jose, CA, USA*.

111. Bendall, S.C. *et al.* Single-cell mass cytometry of differential immune and drug responses across a human hematopoietic continuum. *Science* **332**, 687-696 (2011).

112. Cashion, A.K., Umberger, R.A., Goodwin, S.B. & Sutter, T.R. Collection and storage of human blood and adipose for genomic analysis of clinical samples. *Research in nursing & health* **34**, 408-418 (2011).

113. Zhang, Y. *et al.* DNA methylation analysis by bisulfite conversion, cloning, and sequencing of individual clones. *Methods in molecular biology* **507**, 177-187 (2009).

114. Lodish, H., Berk, A., Zipursky, S.L. et al. Molecular Cell Biology. **4th** (2000).

115. Veerapathran, A. *et al.* Human regulatory T cells against minor histocompatibility antigens: ex vivo expansion for prevention of graft-versus-host disease. *Blood* (2013).

116. Westermann, J. *et al.* Simultaneous cytokine analysis by cytometric bead array for the detection of leukaemia-reactive T cells in patients with chronic myeloid leukaemia. *British journal of haematology* **132**, 32-35 (2006).

117. Touleimat, N. & Tost, J. Complete pipeline for Infinium((R)) Human Methylation 450K BeadChip data processing using subset quantile normalization for accurate DNA methylation estimation. *Epigenomics* **4**, 325-341 (2012).

118. Beriou, G. *et al.* IL-17-producing human peripheral regulatory T cells retain suppressive function. *Blood* **113**, 4240-4249 (2009).

119. Afzali, B. *et al.* CD161 expression characterizes a subpopulation of human regulatory T cells that produces IL-17 in a STAT3-dependent manner. *European journal of immunology* **43**, 2043-2054 (2013).

120. Orr, S.J. *et al.* Proteomic and protein interaction network analysis of human T lymphocytes during cell-cycle entry. *Molecular systems biology* **8**, 573 (2012).

121. Janes, M.R. & Rommel, C. Next-generation flow cytometry. *Nature biotechnology* **29**, 602-604 (2011).

122. Gingras, A.C., Gstaiger, M., Raught, B. & Aebersold, R. Analysis of protein complexes using mass spectrometry. *Nature reviews. Molecular cell biology* **8**, 645-654 (2007).

123. Bandura, D.R. *et al.* Mass cytometry: technique for real time single cell multitarget immunoassay based on inductively coupled plasma time-of-flight mass spectrometry. *Anal Chem* **81**, 6813-6822 (2009).

124. Bendall, S.C. & Nolan, G.P. From single cells to deep phenotypes in cancer. *Nature biotechnology* **30**, 639-647 (2012).

125. Bending, D. *et al.* Hypomethylation at the regulatory T cell-specific demethylated region in CD25hi T cells is decoupled from FOXP3 expression at the inflamed site in childhood arthritis. *Journal of immunology* **193**, 2699-2708 (2014).

126. Diggins, K.E., Ferrell, P.B., Jr. & Irish, J.M. Methods for discovery and characterization of cell subsets in high dimensional mass cytometry data. *Methods* **82**, 55-63 (2015).

127. Kordasti, S. *et al.* Deep-phenotyping of Tregs identifies an immune signature for idiopathic aplastic anemia and predicts response to treatment. *Blood* (2016).

128. Finck, R. *et al.* Normalization of mass cytometry data with bead standards. *Cytometry A* **83**, 483-494 (2013).

129. Qiu, P. *et al.* Extracting a cellular hierarchy from high-dimensional cytometry data with SPADE. *Nature biotechnology* **29**, 886-891 (2011).

130. Irish, J.M. & Doxie, D.B. High-dimensional single-cell cancer biology. *Current topics in microbiology and immunology* **377**, 1-21 (2014).

131. Zoller, M. CD44: can a cancer-initiating cell profit from an abundantly expressed molecule? *Nature reviews. Cancer* **11**, 254-267 (2011).

132. Kordasti, S. *et al.* Deep phenotyping of Tregs identifies an immune signature for idiopathic aplastic anemia and predicts response to treatment. *Blood* **128**, 1193-1205 (2016).

133. Chiappinelli, K.B. *et al.* Inhibiting DNA Methylation Causes an Interferon Response in Cancer via dsRNA Including Endogenous Retroviruses. *Cell* **164**, 1073 (2016).

134. Sakaguchi, S. *et al.* Foxp3+ CD25+ CD4+ natural regulatory T cells in dominant self-tolerance and autoimmune disease. *Immunological reviews* **212**, 8-27 (2006).

135. Illingworth, R.S. & Bird, A.P. CpG islands--'a rough guide'. *FEBS Lett* **583**, 1713-1720 (2009).

136. Zhang, Y. *et al.* Genome-wide DNA methylation analysis identifies hypomethylated genes regulated by FOXP3 in human regulatory T cells. *Blood* **122**, 2823-2836 (2013).

137. Wang, Y.W., Chen, X., Ma, R. & Gao, P. Understanding the CREB1-miRNA feedback loop in human malignancies. *Tumour Biol* (2016).

138. Kourepini, E. *et al.* TIGIT Enhances Antigen-Specific Th-2 Recall Responses and Allergic Disease. *Journal of immunology* **196**, 3570-3580 (2016).

139. Dunn, G.P., Old, L.J. & Schreiber, R.D. The immunobiology of cancer immunosurveillance and immunoediting. *Immunity* **21**, 137-148 (2004).

140. Mantovani, A., Allavena, P., Sica, A. & Balkwill, F. Cancer-related inflammation. *Nature* **454**, 436-444 (2008).

141. Elinav, E. *et al.* Inflammation-induced cancer: crosstalk between tumours, immune cells and microorganisms. *Nat Rev Cancer* **13**, 759-771 (2013).

142. Mian, S.A. *et al.* SF3B1 mutant MDS-initiating cells may arise from the haematopoietic stem cell compartment. *Nat Commun* **6**, 10004 (2015).

143. Smith, A.E. *et al.* Next-generation sequencing of the TET2 gene in 355 MDS and CMML patients reveals low-abundance mutant clones with early origins, but indicates no definite prognostic value. *Blood* **116**, 3923-3932 (2010).

144. Ingram, W. *et al.* The JAK2 V617F mutation identifies a subgroup of MDS patients with isolated deletion 5q and a proliferative bone marrow. *Leukemia* **20**, 1319-1321 (2006).

145. Mian, S.A. *et al.* Spliceosome mutations exhibit specific associations with epigenetic modifiers and proto-oncogenes mutated in myelodysplastic syndrome. *Haematologica* **98**, 1058-1066 (2013).

146. Kulasekararaj, A.G., Mohamedali, A.M. & Mufti, G.J. Recent advances in understanding the molecular pathogenesis of myelodysplastic syndromes. *Br J Haematol* **162**, 587-605 (2013).

147. Traina, F. *et al.* Impact of molecular mutations on treatment response to DNMT inhibitors in myelodysplasia and related neoplasms. *Leukemia* **28**, 78-87 (2014).

148. Mosmann, T.R., Cherwinski, H., Bond, M.W., Giedlin, M.A. & Coffman, R.L. Two types of murine helper T cell clone. I. Definition according to profiles of lymphokine activities and secreted proteins. *Journal of immunology* **136**, 2348-2357 (1986).

149. Del Prete, G.F. *et al.* Purified protein derivative of Mycobacterium tuberculosis and excretory-secretory antigen(s) of Toxocara canis expand in vitro human T cells with stable and opposite (type 1 T helper or type 2 T helper) profile of cytokine production. *The Journal of clinical investigation* **88**, 346-350 (1991).

150. DuPage, M. & Bluestone, J.A. Harnessing the plasticity of CD4(+) T cells to treat immune-mediated disease. *Nature reviews. Immunology* **16**, 149-163 (2016).

151. Crotty, S. T follicular helper cell differentiation, function, and roles in disease. *Immunity* **41**, 529-542 (2014).

152. Schmitt, E., Klein, M. & Bopp, T. Th9 cells, new players in adaptive immunity. *Trends in immunology* **35**, 61-68 (2014).

153. Burkett, P.R., Meyer zu Horste, G. & Kuchroo, V.K. Pouring fuel on the fire: Th-17 cells, the environment, and autoimmunity. *The Journal of clinical investigation* **125**, 2211-2219 (2015).

154. Sakaguchi, S. Naturally arising Foxp3-expressing CD25+CD4+ regulatory T cells in immunological tolerance to self and non-self. *Nature immunology* **6**, 345-352 (2005).

155. Zhou, L., Chong, M.M. & Littman, D.R. Plasticity of CD4+ T cell lineage differentiation. *Immunity* **30**, 646-655 (2009).

156. O'Shea, J.J. & Paul, W.E. Mechanisms underlying lineage commitment and plasticity of helper CD4+ T cells. *Science* **327**, 1098-1102 (2010).

157. Bluestone, J.A., Mackay, C.R., O'Shea, J.J. & Stockinger, B. The functional plasticity of T cell subsets. *Nature reviews. Immunology* **9**, 811-816 (2009).

10. Appendix

In this table are listed the binding site genes of FOXP3 base on Zhan *et al*. Also, from gene number 105 we included some genes related to our project.

Table 20. Zhang et al list of FOXP3 binding sites and interesting genes

	HGNC symbol	Full name	Chromosome
1	HIVEP3	Human immunodeficiency virus type 1 enhancer binding protein 3	chr1
2	TNFRSF9	Tumor necrosis factor receptor superfamily, member 9	chr1
3	AIM2	Absent in melanoma 2	chr1
4	PYHIN1	Pyrin and HIN domain family, member 1	chr1
5	RUNX3	Runt-related transcription factor 3	chr1
6	PRKCZ	Protein kinase C, ζ	chr1
7	VPS13D	Vacuolar protein sorting 13 homolog D (*Saccharomyces cerevisiae*)	chr1
8	TNFRSF4	Tumor necrosis factor receptor superfamily, member 4	chr1
9	CD160	CD160 molecule	chr1
10	GALNT5	UDP-*N*-acetyl-α-D-galactosamine: polypeptide *N*-Acetylgalactosaminyltransferase 5 (GalNAc-T5)	chr2
11	CASP10	Caspase 10, apoptosis-related cysteine peptidase	chr2
12	HDAC4	Histone deacetylase 4	chr2
13	FAM124B	Family with sequence similarity 124B	chr2
14	SP140	SP140 nuclear body protein	chr2
15	SNED1	Sushi, nidogen, and EGF-like domains 1	chr2
16	BCL11A	B-cell CLL/lymphoma 11A (zinc finger protein)	chr2
17	CD8A	CD8a molecule	chr2
18	TIGIT	T-cell immunoreceptor with Ig and ITIM domains	chr3
19	TGFBR2	Transforming growth factor, β receptor II (70/80 kDa)	chr3
20	VGLL4	Vestigial like 4 (Drosophila)	chr3
21	CD47	CD47 molecule	chr3
22	PRDM8	PR domain containing 8	chr4
23	PRDM8	PR domain containing 8	chr4
24	HPGDS	Hematopoietic prostaglandin D synthase	chr4
25	RGS12	Regulator of G-protein signaling 12	chr4
26	NDNF	Neuron-derived neurotrophic factor	chr4
27	CUTA	cutA divalent cation tolerance homolog (*Escherichia coli*)	chr6
28	TNF	Tumor necrosis factor	chr6
29	ZC3H12D	Zinc finger CCCH-type containing 12D	chr6
30	RPS6KA2	Ribosomal protein S6 kinase, 90 kDa, polypeptide 2	chr6
31	FLOT1	Flotillin 1	chr6
32	ZBTB12	Zinc finger and BTB domain containing 12	chr6

33	C6orf222	Chromosome 6 open reading frame 222	chr6
34	HSD17B8	Hydroxysteroid (17- β) dehydrogenase 8	chr6
35	TAGAP	T-cell activation RhoGTPase activating protein	chr6
36	PLAGL1	Pleiomorphic adenoma gene-like 1	chr6
37	TAP1	Transporter 1, ATP-binding cassette, subfamily B (MDR/TAP)	chr6
38	TAP2	Transporter 2, ATP-binding cassette, subfamily B (MDR/TAP)	chr6
39	AIF1	Allograft inflammatory factor 1	chr6
40	ATXN7L1	Ataxin 7-like 1	chr7
41	GIMAP7	GTPase, IMAP family member 7	chr7
42	UPP1	Uridine phosphorylase 1	chr7
43	WIPI2	WD repeat domain, phosphoinositide interacting 2	chr7
44	GNA12	Guanine nucleotide binding protein (G protein) α 12	chr7
45	ZHX1	Zinc fingers and homeoboxes 1	chr8
46	ANGPT1	Angiopoietin 1	chr8
47	PLEC	Plectin	chr8
48	EIF2C2	Eukaryotic translation initiation factor 2C, 2	chr8
49	PAOX	Polyamine oxidase (exo-N4-amino)	chr10
50	NET1	Neuroepithelial cell transforming 1	chr10
51	ADO	2-aminoethanethiol (cysteamine) dioxygenase	chr10
52	FBXO18	F-box protein, helicase, 18	chr10
53	CXCR5	Chemokine (C-X-C motif) receptor 5	chr11
54	CD248	CD248 molecule, endosialin	chr11
55	LRRC32	Leucine-rich repeat containing 32	chr11
56	APLP2	Amyloid β (A4) precursor-like protein 2	chr11
57	BCL9L	B-cell CLL/lymphoma 9-like	chr11
58	CRY2	Cryptochrome 2 (photolyase-like)	chr11
59	ACER3	Alkaline ceramidase 3	chr11
60	DUSP6	Dual-specificity phosphatase 6	chr12
61	IKZF4	IKAROS family zinc finger 4 (Eos)	chr12
62	KRT72	Keratin 72	chr12
63	NCOR2	Nuclear receptor corepressor 2	chr12
64	C12orf42	Chromosome 12 open reading frame 42	chr12
65	LOC338799	Uncharacterized LOC338799	chr12
66	NCOR2	Nuclear receptor corepressor 2	chr12
67	SCNN1A	Sodium channel, nonvoltage-gated 1 α subunit	chr12
68	EDNRB	Endothelin receptor type B	chr13
69	TFDP1	Transcription factor Dp-1	chr13
70	TC2N	Tandem C2 domains, nuclear	chr14
71	BCL11B	B-cell CLL/lymphoma 11B (zinc finger protein)	chr14
72	MMP14	Matrix metallopeptidase 14 (membrane-inserted)	chr14
73	APBA2	Amyloid β (A4) precursor protein-binding, family A, member 2	chr15
74	SMAD3	SMAD family member 3	chr15

75	THBS1	Thrombospondin 1	chr15
76	LOC91450	Uncharacterized LOC91450	chr15
77	ANKRD11	Ankyrin repeat domain 11	chr16
78	ITGAL	Integrin, α L (antigen CD11A (p180), lymphocyte function-associated antigen 1; α polypeptide)	chr16
79	ANKRD11	Ankyrin repeat domain 11	chr16
80	ACSF3	acyl-CoA synthetase family member 3	chr16
81	CA5A	Carbonic anhydrase VA, mitochondrial	chr16
82	MIR21	microRNA 21	chr17
83	KSR1	Kinase suppressor of ras 1	chr17
84	KCNAB3	Potassium voltage-gated channel, shaker-related subfamily, β member 3	chr17
85	VMP1	Vacuole membrane protein 1	chr17
86	RPTOR	Regulatory associated protein of MTOR, complex 1	chr17
87	ST6GALNAC1	ST6 (α -*N*-acetyl-neuraminyl-2,3- β -galactosyl-1,3) -*N*-acetylgalactosaminide α -2,6-sialyltransferase 1	chr17
88	ZPBP2	Zona pellucida binding protein 2	chr17
89	MEOX1	Mesenchyme homeobox 1	chr17
90	SCARF1	Scavenger receptor class F, member 1	chr17
91	SEPT9	Septin 9	chr17
92	AXIN2	Axin 2	chr17
93	SEPT9	Septin 9	chr17
94	TNFRSF13B	Tumor necrosis factor receptor superfamily, member 13B	chr17
95	LAMA3	Laminin, α 3	chr18
96	TGIF1	TGFB-induced factor homeobox 1	chr18
97	SLC1A5	Solute carrier family 1 (neutral amino acid transporter), member 5	chr19
98	EMR3	egf-like module containing, mucin-like, hormone receptor-like 3	chr19
99	TYROBP	TYRO protein tyrosine kinase binding protein	chr19
100	GNG8	Guanine nucleotide binding protein (G protein), γ 8	chr19
101	KCNN4	Potassium intermediate/small conductance calcium-activated channel, subfamily N, member 4	chr19
102	HORMAD2	HORMA domain containing 2	chr22
103	LOC286467	Family with sequence similarity 195, member A pseudogene	chrX
104	MAOB	Monoamine oxidase B	chrX
105	CTLA4	cytotoxic T-lymphocyte-associated protein 4 [Homo sapiens (human)]	Chr2
106	Satb1	SATB homeobox 1 [Homo sapiens (human)]	Chr3
107	Lef1	lymphoid enhancer-binding factor 1 [Homo sapiens (human)]	Chr4
108	IRF4	interferon regulatory factor 4 [Homo sapiens (human)]	Chr6

109	IL2Ra	interleukin 2 receptors, alpha [Homo sapiens (human)]	Chr10
110	IFNg	interferon, gamma [Homo sapiens (human)]	Chr12
111	Foxo1	forkhead box O1 [Homo sapiens (human)]	Chr13
112	IL2Ra	interleukin 2 receptors, alpha [Homo sapiens (human)]	Chr10
113	Gata1	GATA binding protein 1 (globin transcription factor 1) [Homo sapiens (human)]	ChrX

CREB1

Chromosome:GRCh37:2:208393261:208469355:1

Exon 1

3-

TGTTTCCGTGCGCGGCCGCTGCGCACTCGGCACTGGGCGGCGCTGGCTGGCTCCC
CTGGCTGCGGCTCCTCAGTCGGCGCGGCGGCTGCTGCTGCCTGTGGCCCGGGCGGC
TGGGAGAAGCGGAGTGTTGGTGAGTGACGCGGCGGAGGTGTAGTTTGACGCGGT
GTGTTACGTGGGGGAGAGAATAAAACTCCAGCGAGATCCGGGCCGTGAACGAAAG
CAGTGACGGAGGAGCTTGTACCACCG- 5

Exon 1 _ After Bisulfite conversion

3-

TGTTTTCGTGCGCGGTCGTTGCGTATTCGGTATTGGGCGGCGTTGGTTGGTTTTTT
GGTTGCGGTTTTTTAGTCGGCGCGGCGGTTGTTGTTTGTGGTTCG***GGCGGTTGG***
GAGAAGCGGAGTGTTGGTGAGTGACGCGGCGGAGGTGTAGTTTGACGCGGTGT
GTTACGTGGGGGAGAGAATAAAATTTTAGCGAGATTCGGGTCGTGAACGAAAGT
AGTGACGGAGGAGTTTGTATTATCG-5

Meth Fw	3-GTTGTTGTTGTTTGTGGTTCG-5
Meth Rev	5-CGATAATACAAACTCCTCCGTC-3
Unmeth Fw	3-TTGTTGTTGTTTGTGGTTTGG-5
Unmeth Rev	5-CAATAATACAAACTCCTCCATC-3

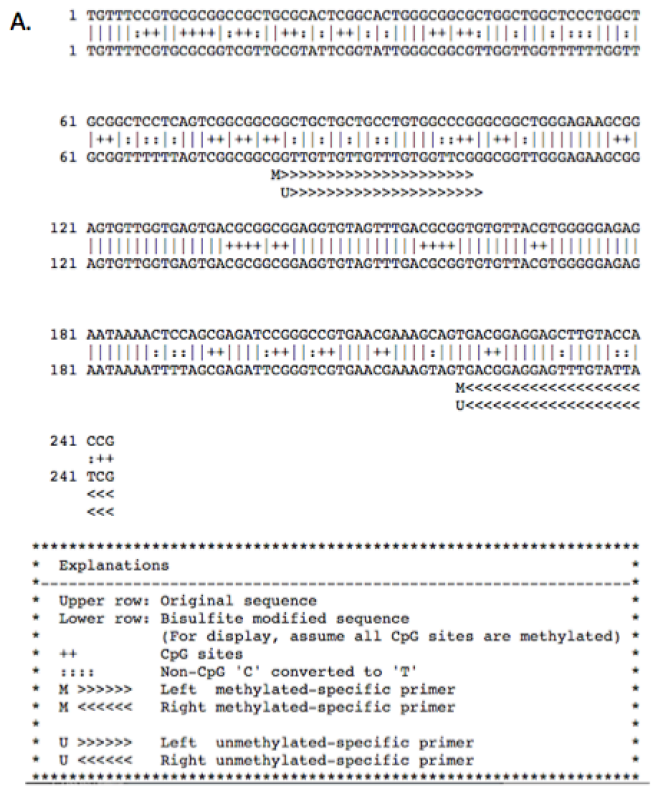


Figure 78. CREB1 primers. The CREB1 primers were designed as follow: We chose the promoter region based on the CpG island and the TATAA box, according to The Methprimer and Primer3 websites. The sequence was then bisulfite converted (assuming that all the CpG were methylated), the CG remained CG and the C became T. Our target sequence was highlighted in bold and in italic. The primers were designed based on the converted sequence (4 primers, 2 based on Methylated sequence, 2 based on Unmethylated sequence). A. According to the legend at the bottom of the figure, the first line is the sequence not-converted and above there is the sequence bisulfite converted. We can see where the primers are attached M >>>>>> (Methylated primer forward); U >>>>> (Unmethylated primer forward); M<<<<<<<< (Methylated primer reverse); U<<<<<<< (Unmethylated primers reverse).

TIGIT

Chromosome:GRchr3:114289102-114310288

Exon 1

3 -

CAGGATGGAGAGTGGGGAGCTTGGAGGAGAGAGCACGACCCCCTGCTGCTGCCG
CAGGATGTTGCCCTTGATTCTAGGCAGAGACAGGAGGCATCAGACAGCTGTGACAG
CCATGGAGCTCCCCTACCACTTCTGAGCCAGAGGGAAGACTTTGGAGAAGCAGAA
GCCCAAAGACACTGCTGGGAGATTGGTCTGTGCTCTGGGAGAACCCTAGGTTGTGT
TTCCCGTGTACAAGCCACCGATCTTGTGGAAGGTACC
ACCACTCCCAGCCCCGCTTGGCTGAGGGCTGCGGCCACAGGTTTTCAGGACCGT
GCTTGTGGTTGGAGGCTGTGGACTCAAGTGCGGCTGGCCCGGGACTTTCACAGGG
CGCAGGGCGGGCTA- 5

Exon 1 _ After Bisulfite conversion

3-

CAGGATGGAGAGTGGGGAGCTTGGAGGAGAGAGCACGACCCCCTGCTGCTGCC
GCAGGATGTTGCCCTTGATTCTAGGCAGAGACAGGAGGCATCAGACAGCTGTGAC
AGCCATGGAGCTCCCCTACCACTTCTGAGCCAGAGGGAAGACTTTGGAGAAGCA
GAAGCCCAAAGACACTGCTGGGAGATTGGTCTGTGCTCTGGGAGAACCCTAGGT
TGTGTTTCCCGTGTACAAGCCACCGATCTTGTGGAAGGTACC
ACCACTCCCAGCCCCGCTTGGCTGAGGGCTGCGGCCACAGGTTTTCAGGACC
GTGCTTGTGGTTGGAGGCTGTGGACTCAAGTGCGGCTGGCCCGGGACTTTCACA
GGGCGCAGGGCGGGCTA
-5

A.

```
  1 CAGGATGGAGAGTGGGGAGCTTGGAGGAGAGAGCACGACCCCCTGCTGCTGCCGCAGGAT
    ||||||||||||||||||||||||||||||||||||||||||||||||||||||||||||||
  1 TAGGATGGAGAGTGGGGAGTTTGGAGGAGAGAGTACGATTTTTTGTTGTTGTCGTAGGAT

 61 GTTGCCCTTGATTCTAGGCAGAGACAGGAGGCATCAGACAGCTGTGACAGCCATGGAGCT
    ||||:::|||||:||||:|||||:||||||:||:|||:||:|||||:||::||||||:|
 61 GTTGTTTTTGATTTTAGGTAGAGATAGGAGGTATTAGATAGTTGTGATAGTTATGGAGTT

121 CCCCTACCACTTCTGAGCCAGAGGGAAGACTTTGGAGAAGCAGAAGCCCAAAGACACTGC
    ::::||::|:||:|||||::|||||||||||:|||||||||||:|||||:::|||||:|:|:
121 TTTTTATTATTTTTGAGTTAGAGGGAAGATTTTGGAGAAGTAGAAGTTTAAAGATATTGT

181 TGGGAGATTGGTCTGTGCTCTGGGAGAACCCTAGGTTGTGTTTCCCGTGTACAAGCCACC
    |||||||||||||:||||:|:||||||||:::|||||||||||||::++||||:|||::|:+
181 TGGGAGATTGGTTTGTGTTTTGGGAGAATTTTAGGTTGTGTTTTTCGTGTATAAGTTATC
                                        M>>>>>>>>>>>>>>>>>>>>>>>>
                                        U>>>>>>>>>>>>>>>>>>>>>>>>

241 GATCTTGTGGAAGGTACCACCACTCCCAGCCCCGCTTGGCTGAGGGCTGCGGGCCCACAGG
    +||:|||||||||||||||::|::|:|:::||:::++:|||||:|||||||:||++||::|:|||
241 GATTTTGTGGAAGGTATTATTATTTTTAGTTTCGTTTGGTTGAGGGTTGCGGGTTATAGG
    >>
    >>

301 TTTTCAGGACCGTGCTTGTGGTTGGAGGCTGTGGACTCAAGTGCGGCTGGCCCGGGACTT
    ||||:||||:++||:|||||||||||||||:||||||:|:|||||++|:|||::++|||:||
301 TTTTTAGGATCGTGTTTGTGGTTGGAGGTTGTGGATTTAAGTGCGGTTGGTTCGGGATTT
                                                      M<<<<<<<<
                                                    U<<<<<<<<<<

361 TCACAGGGCGCAGGGCGGGCTA
    |:|:||||++:||||++||:||
361 TTATAGGGCGTAGGGCGGGTTA
    <<<<<<<<<<<<        M
    <<<<<<<<<<<<<<
```

Meth Fw	3-TGTGTTTTTCGTGTATAAGTTATCGA-5
Meth Rev	5-CTACGCCCTATAAAAATCCCG-3
Unmeth Fw	3-TGTGTTTTTTGTGTATAAGTTATTGA -5
Unmeth Rev	5-CCTACACCCTATAAAAATCCCAAA-3

Figure 79. TIGIT primers. The TIGIT primers were designed as described in Figure 78.

Aknowledgment

Doing a PhD is not an individual experience; rather it takes place in a social context and includes several people, whom I would like to thank sincerely.

First of all, to my beloved Marco, for the moral support and precious love, who was always standing by me in my hard times during this work.

To my first supervisor Shahram and my second supervisor Shaun for their unwareing patience and mentorship throughout this project. Their enthusiasm and dedication to Science led me to find my own path and I will always be grateful for that.

To Memo, Toni and Simona for being there, always.

To the people from the Rayne Institute, for their valuable help and support during these 4 years, especially Kiki, Giulia, Aytug, Mina, Sun, Marta, Tushar, Francesco G, Chlodagh, Monera, Manar, Farzin and Linda. Also, to the collegues from the lab Benedetta, Thomas, Nathalie, Samia and Tom.

To a strong woman, bright scientist and my sister-in-arms Annie. You encouraged me to belive in myself and you will always be dear to my heart. (Ain’t nobody got time for that!)

Dulcis in fundo, to the ones who became my family, my London squad: Rebecca, Benedetta, Cristina, Federica, Loris, Shyam, Jenny, Sonia, Gianluca, Roberto, Matteo, Fran, Gemma, Pilar, Chloe and Gemma. Thanks for the laughs, the hugs when I was down, the parties, the beers at the pub, the craziness, the afternoon walks and the endless chats. Thank you for walking with me when I needed support, ahead of me when I needed guidance and behind me when I needed someone to watch my back.